

STUDENT  
BOOK  
ON

BLACK  
HOLES

Edited by  
Stefan Vandoren



Riccardo Borsato



# Contents

<b>1</b>	<b>Preface and Introduction</b>	<b>11</b>
<b>2</b>	<b>Black Hole Solutions and Penrose Diagrams</b>	<b>15</b>
2.1	The Schwarzschild Solutions . . . . .	16
2.1.1	Minkowski Space . . . . .	16
2.1.2	(Anti-) de Sitter Space . . . . .	22
2.2	The Reissner-Nordström Solutions . . . . .	29
2.2.1	Maxwell Fields and Gravity . . . . .	30
2.2.2	Minkowski Space . . . . .	31
2.2.3	Charged Black Holes in Anti de Sitter and de Sitter Space . . . . .	34
2.3	The Kerr Solution . . . . .	38
2.3.1	Rotating Black Holes . . . . .	38
2.3.2	Rotating Charged Black Holes . . . . .	41
2.3.3	The Ergosphere . . . . .	43
2.4	Rindler Space . . . . .	45
2.4.1	Rindler Coordinates . . . . .	45
2.4.2	Rindler Horizon . . . . .	47

2.4.3	Black Holes and Rindler Space . . . . .	49
2.5	Black Branes in AdS . . . . .	51
2.5.1	Schwarzschild Black Branes in Minkowski Spacetime . . . . .	51
2.5.2	Schwarzschild Black Branes in AdS . . . . .	52
2.5.3	Reissner-Nordström Black Branes in AdS . . . . .	55
2.5.4	Hyperbolic Black Holes in AdS . . . . .	57
<b>3</b>	<b>Black hole formation</b>	<b>59</b>
3.1	Birkhoff's Theorem . . . . .	59
3.2	The Tolman-Oppenheimer-Volkoff Equation . . . . .	68
3.2.1	Derivation of the Tolman-Oppenheimer-Volkoff Equation . . . . .	69
3.2.2	Physical Solutions of the Tolman-Oppenheimer-Volkoff Equation . .	73
3.2.3	Realistic Stellar Models . . . . .	76
3.3	Gravitational Collapse . . . . .	77
3.3.1	Infalling Spherical Shell of Dust . . . . .	78
3.3.2	Realistic Gravitational Collapse . . . . .	82
3.3.3	Consequences . . . . .	83
3.4	Singularity Theorems . . . . .	84
3.4.1	Conjugate Points and Definition of Singularity . . . . .	85
3.4.2	Energy Conditions . . . . .	88
3.4.3	The Schwarzschild Example . . . . .	89
3.4.4	Trapped Surfaces . . . . .	91
3.4.5	The Theorem . . . . .	93

3.5	Cosmic Censorship . . . . .	94
3.5.1	Arguments for the Validity of the Weak Cosmic Censorship Conjecture	95
3.5.2	Overspinning a Kerr Black Hole . . . . .	95
3.5.3	Supercharging a Reissner-Nordström Black Hole . . . . .	97
3.5.4	Censorship Violation in the Non-Homogeneous Dust Cloud . . . . .	98
<b>4</b>	<b>No-hair Theorems</b>	<b>101</b>
4.1	Bekenstein's Method . . . . .	102
4.1.1	Scalar Fields . . . . .	103
4.1.2	Massive Vector Fields . . . . .	105
4.1.3	A Complex Scalar Field Minimally Coupled with Electromagnetism	108
4.1.4	Different Couplings to Scalar Field Functions . . . . .	110
4.2	No-hair theorem for Spinor Fields . . . . .	114
4.3	Hairy Black Hole Solutions . . . . .	122
4.3.1	BBM(B) Model . . . . .	123
4.3.2	Nielsen-Olesen Vortex . . . . .	125
4.3.3	Final remarks . . . . .	128
4.4	No-hair theorems and Hairy Black Holes for $\Lambda \neq 0$ . . . . .	128
4.4.1	A Black Hole with a Scalar Field in both the dS and AdS Case . .	128
4.4.2	Boundary Conditions . . . . .	129
4.4.3	Potential with Minimum at Finite $\phi$ . . . . .	131
4.4.4	Scalar field in a Convex Potential which Approaches its Minimum at $\phi \rightarrow \infty$ . . . . .	133

4.4.5	Example of a Hairy black hole Coupled to a Scalar Field in AdS . . . . .	134
4.4.6	Final Remarks . . . . .	136
<b>5</b>	<b>The Laws of Black Hole Mechanics</b>	<b>137</b>
5.1	Zeroth Law: Surface Gravity . . . . .	137
5.1.1	Null-Hypersurfaces and Killing Horizons . . . . .	138
5.1.2	Killing Horizons and Event Horizons . . . . .	139
5.1.3	Zeroth Law . . . . .	140
5.1.4	Surface Gravity of the Schwarzschild Solution . . . . .	142
5.2	First Law of Black Hole Mechanics . . . . .	143
5.2.1	Mass in GR . . . . .	144
5.2.2	Mass of an Axisymmetric Black Hole . . . . .	147
5.2.3	The First Law . . . . .	148
5.2.4	The First law for the Kerr-Newman Black Hole . . . . .	148
5.2.5	Physical Interpretations . . . . .	149
5.3	The Second Law: the Area Theorem . . . . .	151
5.3.1	Causality . . . . .	152
5.3.2	Horizons . . . . .	154
5.3.3	Hawking's Area Theorem . . . . .	155
5.3.4	Penrose Process . . . . .	156
5.4	The Third Law of Black Hole Mechanics . . . . .	157
5.4.1	Extremal Black Holes Cannot Be Formed Continuously . . . . .	158
5.4.2	Formalisation of the Third Law . . . . .	161

5.4.3	Surface Gravity Cannot Become Zero by Hawking Radiation . . . . .	163
5.5	Black Holes and Entropy . . . . .	164
5.5.1	Relating Black Hole Physics to Thermodynamics . . . . .	164
5.5.2	The Relation Between Entropy and Information . . . . .	166
5.5.3	Estimating the Black Hole Entropy . . . . .	169
5.5.4	The Generalized Second Law of Black Hole Thermodynamics . . . . .	170
5.6	Temperature and Euclidean Gravity . . . . .	171
5.6.1	Surface Gravity as Black Hole Temperature . . . . .	171
5.6.2	Black hole mechanics and Thermodynamics: Zeroth and Third Law	173
5.6.3	Introducing Temperature in Quantum Field Theory . . . . .	173
5.6.4	Euclidean Gravity: Schwarzschild Solution . . . . .	175
5.6.5	Euclidean Gravity: Reissner-Nordström Solution . . . . .	176
<b>6</b>	<b>Perturbations of Black Hole Geometries</b>	<b>179</b>
6.1	Quasinormal Modes of a Schwarzschild Black Hole . . . . .	181
6.1.1	Normal Modes and Quasinormal Modes . . . . .	181
6.1.2	Perturbing a Schwarzschild Black Hole . . . . .	181
6.1.3	Perturbations and Their Effective Potentials . . . . .	183
6.1.4	Quasinormal Modes as an Eigenvalue Problem . . . . .	185
6.1.5	Boundary Conditions . . . . .	185
6.1.6	The Mashhoon Method and Approximation With the Pöschl-Teller Potential . . . . .	186
6.1.7	Numerical Results . . . . .	189

6.2	Quasinormal Modes in AdS . . . . .	191
6.2.1	Scalar Field Perturbations in AdS . . . . .	192
6.2.2	Pure AdS . . . . .	193
6.2.3	BTZ Black Hole . . . . .	194
6.2.4	Schwarzschild AdS . . . . .	194
6.3	Breitenlohner Freedman Bound . . . . .	196
6.3.1	Stability Bound in Minkowski Space . . . . .	196
6.3.2	Stability Bound in AdS Space . . . . .	197
6.3.3	Another Derivation of the BF Bound . . . . .	198
6.4	Quasinormal Modes in Astrophysics . . . . .	200
6.4.1	Quasinormal Modes of Astrophysical Black Holes . . . . .	200
6.4.2	Important Quantities for Detection . . . . .	202
6.4.3	Detectability of Fundamental Modes . . . . .	203
6.4.4	A Black hole Versus a Boson Star . . . . .	204
<b>7</b>	<b>Hawking Radiation</b>	<b>207</b>
7.1	Recap: Quantization of a Scalar Field in Quantum Field Theory . . . . .	208
7.2	Quantum Field Theory in Schwarzschild Spacetime . . . . .	212
7.2.1	Review of Relevant Metrics . . . . .	213
7.2.2	Evaluation of Action . . . . .	214
7.2.3	Solutions to Field Equations . . . . .	216
7.2.4	Ambiguity of The Vacuum . . . . .	218
7.3	The Unruh Effect . . . . .	219

7.3.1	Rindler space Revisited . . . . .	220
7.3.2	The Effect . . . . .	221
7.3.3	Unruh Temperature . . . . .	223
7.4	Hawking radiation . . . . .	225
7.4.1	The Unruh effect in extended Schwarzschild spacetime . . . . .	225
7.4.2	The Hawking Effect for a Collapse to a Schwarzschild Black Hole .	227
7.4.3	The Hawking effect for a Collapse to a Kerr(-Newman) Black Hole .	233
7.4.4	Physical aspects of Black hole emission . . . . .	234
7.4.5	Evolution of black holes . . . . .	237
7.5	Information Loss Paradox . . . . .	238
7.5.1	The Paradox . . . . .	238
7.5.2	Information Comes Out With the Radiation . . . . .	240
7.5.3	Information Stays in the Black Hole . . . . .	241
7.5.4	Information Goes Somewhere Else . . . . .	242
7.5.5	Outlook . . . . .	243
<b>A</b>		<b>245</b>
A.1	Varying the Einstein-Hilbert Action . . . . .	245
A.2	Properties of the Metric Tensor in Asymptotically Flat Black Hole Exterior.	246
A.3	Tetrads and Spinors in Curved Spacetime . . . . .	247
A.4	Surface Gravity of the Reissner-Nordström and Kerr Solutions . . . . .	252
A.4.1	Reissner-Nordström Solution . . . . .	252
A.4.2	Kerr Solution . . . . .	254

A.5 Euclidean Gravity: Kerr Solution . . . . .	255
A.6 The Reason for Quantum Field Theory . . . . .	258
A.7 Evaluation of Action in Curved Spacetime . . . . .	260

# Chapter 1

## Preface and Introduction

This is a book on black holes written by the students that participated in the Student Seminar of the Master Program Theoretical Physics at Utrecht University, during the first semester of the academic year 2013-2014. At the start of the Seminar, I composed a list of topics and organized them into chapters and sections that served as a lay-out of this book. Groups of four to six students were composed, and each group wrote a corresponding chapter. Presentations of each chapter were given during the Seminar meetings. Groups were also asked to give feedback on chapters written by other groups, and to correct possible mistakes. I have given further feedback and suggestions for improvement such that the text got better iteration after iteration. All the teams were further assisted by Riccardo Borsato, who moreover did a fantastic job in collecting all the files and putting it all together in book format. Many thanks to him.

I am proud to present the authors of the book to the reader, and how the teams were composed:

- Chapter 2: Pim Borman, Patrick Hooijer, Guido van Miert, Annelies Veen
- Chapter 3: Nikki Bisschop, Michaël Dagnelie, Stefano Lucat, Otto Rottier, Drian van der Woude
- Chapter 4: Alexandros Aerakis, Bram van Dijk, Babis Lazaridis Patsalias, Bruno Rodrigues, Angelos Tzetzias
- Chapter 5: Rob Klabbers, Daniel Medina Rincon, Nick Plantz, Tycho Sikkenk, Ben Werkhoven, Erik van der Wurff

- Chapter 6: Sjaak van Diepen, Tara Drwenski, Hamish Forbes, Roeland Koelewijn, Mengxi Ren
- Chapter 7: Yassir Awwad, Flore Kunst, Bart de Leeuw, Xuewen Liu, Jorgos Papadomanolakis, Yvette Welling

The main topic of the book is black hole physics, and the text requires knowledge on General Relativity as a start. It is therefore ideal reading material for other students or beginning researchers. At the time of writing, we are approaching the 100th anniversary of the Schwarzschild black hole solution written down in 1916. Many things have happened in the past century, and black hole physics remains a central field of study in theoretical physics and astronomy.

This book is not meant to give a historical overview of all developments that have happened in the last century. It is rather a selection of topics that are suitable for theoretical physics students, starting from black hole solutions of Einsteins equations and no-hair theorems, black hole formation and gravitational collapse, to topics on thermodynamics of black holes, quasi-normal modes and Hawking radiation. In a number of chapters, we also treat spacetimes with a cosmological constant, and pay particular attention to black holes in asymptotically anti-de Sitter spacetime (AdS). The relevance and motivation for this comes from the AdS/CFT correspondence that grew out of string theory, and by the fact that thermodynamical ensembles for black holes are more conveniently studied in AdS.

Pretty much all of the material presented here can be found somewhere in the literature. In many places, it was hard to avoid doing something different than the excellent textbooks and reviews that are already available. However, I have tried as much as possible to make the students present their own line of arguments, and made them solve some exercises that were not obvious to copy from the textbooks. Therefore, in many places this book contains more details or worked out derivations which you will not find in other textbooks or reviews. This can be very useful for other students or beginning researchers. In other places, our treatment here leaves still room for improvement, and we refer to other work for a more elaborated and updated discussion.

Originally, I had planned to include a few more topics, such as greybody factors, phase transitions of black holes in AdS, and black hole complementarity. This would bring the book to the level of current research topics. Because of the limited time span of the Student Seminar (about four months), this was a too ambitious plan. For the same reason, a number of figures used in the book are copied from elsewhere in the literature, with references given. Perhaps a newly improved and extended version of the book will be made in the near future

with new figures made, new chapters added, and corrected mistakes. But I hope for now you will enjoy reading this version as well.

Many thanks to all the students for their contribution and hard work. Due to their enthusiasm, motivation and engagement, this adventurous project turned out to be very successful, beyond my original expectation. I hope you enjoyed it as much as I did, and wish this book will also serve as a nice souvenir, useful for your future careers.

*Stefan Vandoren, Utrecht, January 30, 2014*

## Some notations and conventions used throughout this book

- The spacetime dimension will be 4 unless noted otherwise.
- Schwarzschild coordinates are taken in the order  $x^\mu = (t, r, \theta, \phi)$ .
- The signature of the metric in these coordinates is chosen to be  $(-, +, +, +)$ .
- The length and mass units are redefined such that the speed of light in vacuum,  $c = 1$  and the gravitational constant,  $G = 1$ .
- The factor in front of the cosmological constant is chosen such that the Hilbert-Einstein action is  $\int \sqrt{-g}(R - \Lambda + \mathcal{L}_{\text{matter}})$  and thus the resulting Einstein equation equals

$$R_{\mu\nu} - \frac{1}{2}Rg_{\mu\nu} + \frac{1}{2}\Lambda g_{\mu\nu} = T_{\mu\nu} \quad (1.0.1)$$

(see Appendix A),(A.1)).

# Chapter 2

## Black Hole Solutions and Penrose Diagrams

Historically black holes were theorized before they were discovered empirically. Already in 1916, just one year after Einstein presented his theory of general relativity, Schwarzschild published an exact solution to Einstein's equations. This solution describes the gravitational field produced by a spherically symmetric, non-rotating, uncharged body. It turned out that this solution has two features which are intimately related to each other, the event horizon and the singularity. Once an object passes the event horizon it is doomed to end up in the singularity located at the center. This of course explains why we refer to this solution as a Schwarzschild black hole. Later on the Reissner-Nordström and Kerr solutions were found, describing the gravitational field of a charged and rotating body, respectively. In this chapter we will analyze these three solutions in detail. We will introduce the most important objects like the event horizon, singularities and Penrose diagrams in the context of the Schwarzschild solution. Then we will also discuss these notions for the Reissner-Nordström and Kerr solutions. Furthermore we will quickly introduce Einstein's equations with a cosmological constant, and see whether they still allow for black hole solutions. Finally we try to generalize the notion of a black hole to a black brane.

Section 2.1 covers the Schwarzschild solution, Section 2.2 the Reissner-Nordström solutions, and Section 2.3 covers the Kerr solution and the Kerr-Newman solution. Then in Section 2.4 we introduce Rindler space, i.e. the spacetime coordinates of an uniformly accelerated observer in Minkowski spacetime. Rindler space does not contain a physical singularity, but approximates the spacetime structure of a black hole near the event horizon. Section 2.5 will touch upon black branes, extensions of black holes solutions which are of importance

to string theory and in particular the AdS/CFT correspondence.

## 2.1 The Schwarzschild Solutions

The Schwarzschild solution is the simplest non-trivial solution to Einstein's equation and is therefore extremely well suited to introduce some important concepts as the event horizon, geodesics and Penrose diagrams. Note that in this section we will not derive the Schwarzschild metric, but only state the metric. In the second part of this section we will introduce de Sitter and anti-de Sitter space, in order to study black holes when Einstein's equations are modified by a cosmological constant.

### 2.1.1 Minkowski Space

<sup>1</sup>The Schwarzschild solution describes the simplest category of the black holes, *i.e.* with only mass and no rotation nor charge. The metric is given by

$$ds^2 = - \left(1 - \frac{2M}{r}\right) dt^2 + \left(1 - \frac{2M}{r}\right)^{-1} dr^2 + r^2 d\Omega^2, \text{ where } d\Omega^2 = d\theta^2 + \sin^2(\theta)d\phi^2. \quad (2.1.1)$$

Note that for  $r \rightarrow \infty$  we obtain the Minkowski metric, which justifies the title of this subsection. The Schwarzschild solution has some interesting properties. This exact and static solution to Einstein's equation is according to Birkhoff's theorem the most general solution given the assumptions:

- vacuum energy distribution *i.e.*  $T^{\mu\nu} = 0$ ,
- spherically symmetric metric,
- and negative or zero cosmological constant.

Birkhoff's theorem can be found in Section 3.1. Of importance to us now, is that Birkhoff's theorem states that all spherical symmetric vacuum solutions to Einstein's equation are static.

---

<sup>1</sup>This subsection is based entirely on [1].

### Singularities and the event horizon

Characteristic for a black hole is the singularity located at  $r = 0$ . However since we have not yet defined what we mean by a singularity this is somewhat vague. One may be tempted to define a singularity as a point in spacetime where some components of the metric tensor blow up. Note that such a definition not only incorporates the point  $r = 0$  but also the sphere of radius  $r = 2M$ . Since a singularity should correspond to something physical, it should not depend on your choice of coordinates whether we call a point a singularity, this rules out the proposed definition. In the following we will refer to these points as coordinate singularities. We define a physical singularity as a point in spacetime where a scalar quantity which measures the gravitational field blows up. For example, we find for the Schwarzschild metric that  $R^{\mu\nu\rho\sigma}R_{\mu\nu\rho\sigma} = \frac{48M^2}{r^6}$  [1], marking  $r = 0$  as a genuine singularity. Note that  $R = 0$  for the Schwarzschild metric, and it is thus by no means sufficient to consider only the Ricci scalar. We lack the theoretical tools to answer any questions on the  $r = 0$  singularity with certainty. Due to the small scale combined with high density, quantum gravity effects should play an important role at the origin.

Despite the fact that the sphere located at  $r = 2M$  does not exhibit a singularity, which still has to be shown, it does define the event horizon. The event horizon is defined as the set of spatial coordinates for which  $g_{00} = 0$ <sup>2</sup>. The event horizon is a 2-dimensional surface at  $r = 2M$  that separates  $r > 2M$  from  $r < 2M$ , where hitting the singularity is inevitable. Before we deduce that, note first that an observer far away from the black hole, i.e.  $r > 2M$ , cannot see anything reaching this event horizon, because the light cone closes up as  $r \rightarrow 2M$ :

$$\text{radial light rays} \Rightarrow ds^2 = 0 \Rightarrow \frac{dr}{dt} = \pm \left( 1 - \frac{2M}{r} \right). \quad (2.1.2)$$

Even though the light cone closes up, both light and matter can reach  $r = 2M$  in finite lifetime. When the observer reaches  $r = 2M$  he does not experience anything strange, even though his fate has been sealed and  $g_{rr}$  blows up to infinity. The easiest way to prove that the event horizon is just a coordinate singularity, is not by computing the values of all possible curvature tensor contractions at that point, but by changing the coordinate system to another one that does not entail this singularity.

First let us introduce the tortoise coordinates which solve the differential equation of the light cone (2.1.2) for  $r \geq 2M$ :

$$r^* = r + 2M \ln \left( \frac{r}{2M} - 1 \right). \quad (2.1.3)$$

---

<sup>2</sup>For more information on the coordinate independent way of defining horizons, see [1, p. 238]

$$ds^2 = \left(1 - \frac{2M}{r}\right) (-dt^2 + dr^{*2}) + r^2 d\Omega^2. \quad (2.1.4)$$

In these coordinates the light cone does not close up and no metric components tend to infinity for  $r \rightarrow 2M$ , therefore we conclude that  $r = 2M$  does not correspond to a physical singularity. Infalling and outgoing radial light rays travel along constant Eddington-Finkelstein coordinates:

$$v = t + r^*, \quad (2.1.5)$$

$$u = t - r^*. \quad (2.1.6)$$

In terms of Eddington-Finkelstein coordinates the metric reads

$$ds^2 = - \left(1 - \frac{2M}{r}\right) dv^2 + 2drdv + r^2 d\Omega^2. \quad (2.1.7)$$

In terms of these coordinates the condition for radial null curves is satisfied if

$$\frac{dv}{dr} = \begin{cases} 0 & \text{infalling null curve} \\ 2\left(1 - \frac{2M}{r}\right)^{-1} & \text{outgoing null curve} \end{cases} \quad (2.1.8)$$

From this we immediately read off that  $dv/dr \leq 0$  for  $r < 2M$ , hence for  $r < 2M$  all future directed paths are in the direction of decreasing  $r$ , see figure 2.1. So indeed  $r = 2M$  shields the inside of the black hole from the inside, and is therefore named the event horizon.

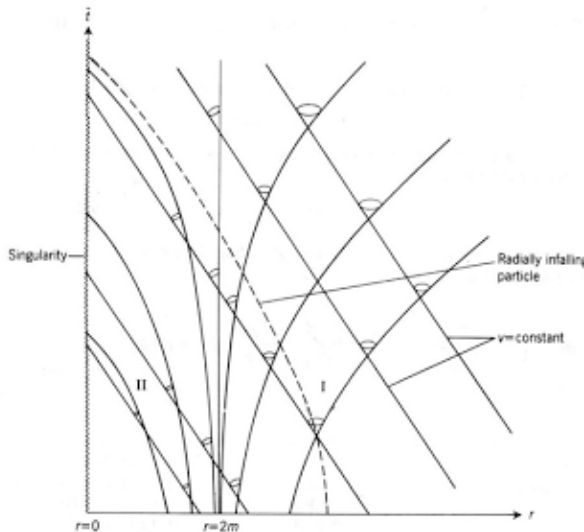


Figure 2.1: Radial null rays in Schwarzschild solution in Eddington-Finkelstein coordinates. Taken from [2]

### Kruskal Szekeres

The most useful coordinates to describe the Schwarzschild black hole are the Kruskal-Szekeres coordinates <sup>3</sup>:

$$R = \left| \frac{r}{2M} - 1 \right|^{\frac{1}{2}} e^{\frac{r}{4M}} \cosh \left( \frac{t}{4M} \right) \text{ and } T = \left| \frac{r}{2M} - 1 \right|^{\frac{1}{2}} e^{\frac{r}{4M}} \sinh \left( \frac{t}{4M} \right) \text{ for } r > 2M, \quad (2.1.9)$$

$$R = \left| 1 - \frac{r}{2M} \right|^{\frac{1}{2}} e^{\frac{r}{4M}} \sinh \left( \frac{t}{4M} \right) \text{ and } T = \left| 1 - \frac{r}{2M} \right|^{\frac{1}{2}} e^{\frac{r}{4M}} \cosh \left( \frac{t}{4M} \right) \text{ for } r < 2M. \quad (2.1.10)$$

In these coordinates the metric changes to

$$ds^2 = \frac{32M^3}{r} e^{-\frac{r}{2M}} (dR^2 - dT^2) + r^2 d\Omega^2, \quad (2.1.11)$$

where we have implicitly defined  $r$  from  $T^2 - R^2 = (1 - r/2M)e^{r/2M}$ . In terms of these coordinates radial null curves obey  $T = \pm R + \text{constant}$ . Furthermore we note that the event horizon is located at  $T = \pm R$ . This follows from the condition  $ds^2 \leq 0$  for time-like and light-like curves. This causal structure can be seen in figure 2.2. The coordinate transformation from  $r, t$  to  $T, R$  only describes regions I and II in figure 2.2. In principle we should allow for all values of  $T$  and  $R$  that do not hit the singularity at  $r = 0$ . Since the singularity corresponds to  $T^2 = R^2 + 1$ , we should really require  $T^2 < R^2 + 1$ , and  $-\infty < R < \infty$ . With these conditions the  $T$  and  $R$  coordinate also cover regions III and IV. Note that the transformation (2.1.9) only applies to regions I and II, and one should thus not think of the other regions as corresponding to complex  $t$ . This only indicates that our original coordinates cover just a patch of the whole spacetime.

In the maximally extended spacetime described, we can thus distinguish four different regions. Region I corresponds to  $r > 2M$ . Region II corresponds to the black hole, since once in there you cannot escape. Region III corresponds to a parallel universe, and is causally disconnected from region I, our universe. Finally, region IV corresponds to a white hole, a region of spacetime from which signals can reach all other points in spacetime, but not the other way round.

### Geodesics

We concluded that the singularity is the destiny for all time-like paths inside the event horizon. But what about outside the horizon? Can we escape the gravitational pull?

---

<sup>3</sup>The reasoning behind these coordinates can be found in [1].

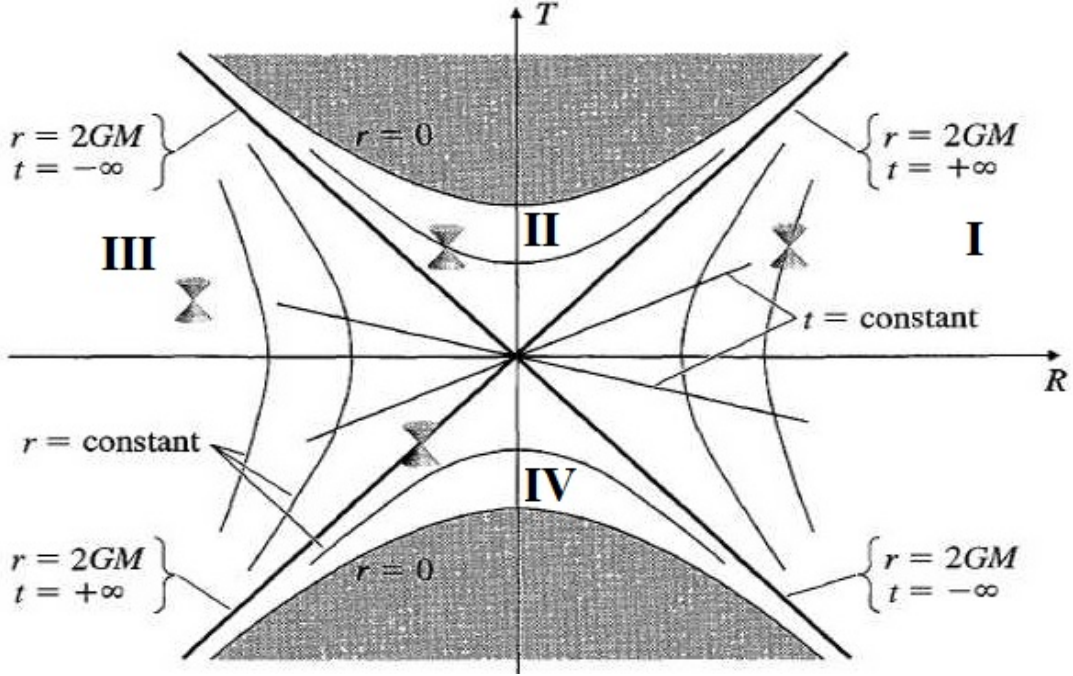


Figure 2.2: Schwarzschild solution in Kruskal coordinates. Edited and extracted from [1]

Yes, we can. The event horizon marks the point of no return. Any time-like path could accelerate away from the event horizon before it reaches it. But if the observer does not have any access to rocket boosters what then? The answer is inside the geodesic equation:

$$\frac{d^2x^\mu}{d\tau^2} = -\Gamma_{\nu\lambda}^\mu \frac{dx^\nu}{d\tau} \frac{dx^\lambda}{d\tau}. \quad (2.1.12)$$

At first sight, this leads to four coupled differential equations, which are seemingly impossible to solve. However symmetry reduces the problem to just one differential equation. Since the metric is spherically symmetric and independent of time, we find two Killing vectors  $K_t^\mu = (1, 0, 0, 0)$  and  $K_\phi^\mu = (0, 0, 0, 1)$ . The by using Killing's equations

$$K_\mu \frac{dx^\mu}{d\tau} = \text{constant}, \quad (2.1.13)$$

one finds that angular momentum  $L$  and energy  $E$  are conserved. Therefore we may reduce the geodesic equation to a problem of classical mechanics, since one has to solve:

$$\frac{1}{2} \left( \frac{dr}{d\tau} \right)^2 + V(r) = \frac{1}{2} E^2 \quad (2.1.14)$$

$$\text{with } V(r) = \frac{1}{2} \left( \epsilon - \frac{L^2}{r^2} \right) \left( 1 - \frac{2M}{r} \right), \quad (2.1.15)$$

$$E = \left( 1 - \frac{2M}{r} \right) \frac{dt}{d\tau}, \quad (2.1.16)$$

$$\text{and } L = r^2 \frac{d\phi}{d\tau}. \quad (2.1.17)$$

Where we have set  $\theta = \frac{\pi}{2}$  due to conservation of angular momentum (see [1]),  $E, L$  and  $\epsilon$  are constants along the path. Here  $\epsilon$  being 1 for time-like, -1 for space-like and 0 for null geodesics. From figure 2.3 we conclude that a freely falling observer starting at a finite distance from the black hole without any spatial velocity,  $L = 0$  is doomed to pass the event horizon and perish consequentially in the singularity. Of course we should not only look

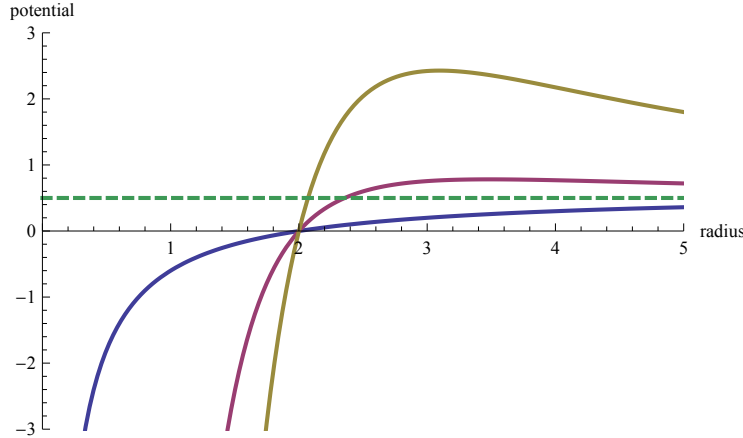


Figure 2.3: Effective potential experienced by time-like geodesics in Schwarzschild metric of  $M = 1$  for  $L = 0, 6, 12$  illustrated by blue, red and yellow respectively. The green dashed line is added for reference. It is the effective potential of  $M = 0$  and  $L = 0$ , i.e. radial time-like geodesic in Minkowski space.

at this very special case  $L = 0$ . Therefore we search for the roots of the derivative of the effective potential and find a second order equation:  $\epsilon \frac{M}{r^2} - \frac{L^2}{r^3} + \frac{3ML^2}{r^4} = 0$ . We deduce that time-like particles have two extremal points if  $L > 12M^2$  namely  $r_{\pm} = \frac{L^2}{2M}(1 \pm \sqrt{L^2 - 12M^2})$  which are a minimum and a maximum respectively. Null geodesics, i.e. light, have an unstable stationary orbit at  $r = 3M$  if  $L > 0$ .

### Penrose diagrams

We end this section with the introduction of Penrose diagrams. Penrose diagrams are diagrams that map the entire spacetime structure onto a compact part of the 2 dimensional space, thus suppressing a few dimensions, such that  $ds^2 = 0$  entails that  $da = \pm db$  where  $a$  and  $b$  are the coordinates of the Image space. This last requirement ensures that null geodesics are depicted by lines at  $\pm 45^\circ$ . This makes Penrose diagrams especially suited to show the causal structure of the spacetime at hand. We will first demonstrate this with an

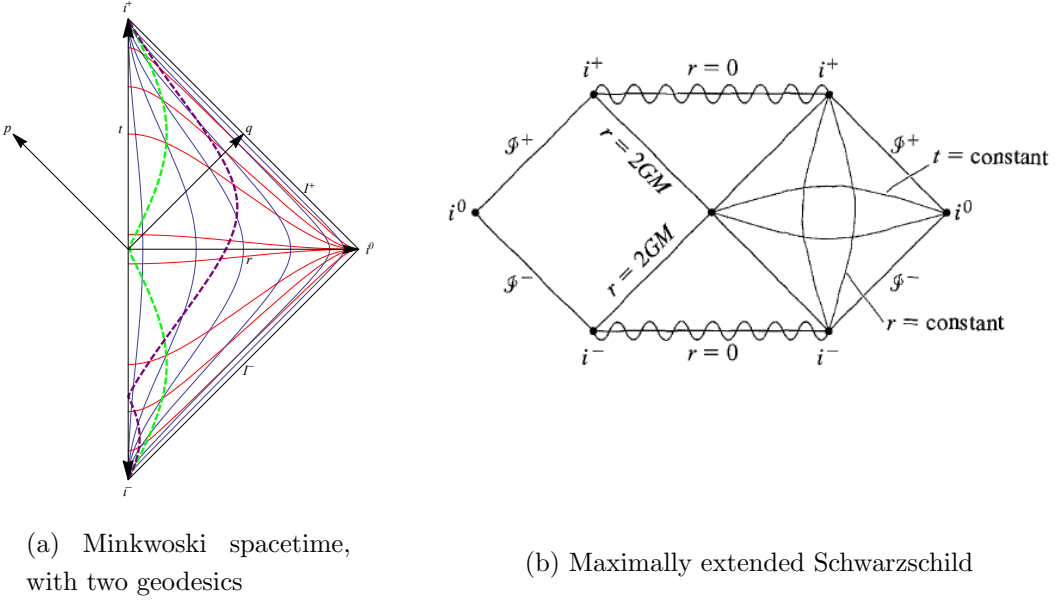


Figure 2.4: Penrose Diagrams

easy example, see figure 2.4(a). To obtain the Penrose diagram for Minkowski space, one simply takes the compactified radial increasing light coordinate  $q = \arctan(t + r)$  and the compactified radial decreasing light coordinate  $p = \arctan(t - r)$ . The arctan ensure that infinities get mapped to finite points  $\pm\frac{\pi}{2}$ . Similarly the Schwarzschild Penrose diagram, see Figure 2.4(b), is obtained by taking the arctanh of the Kruskal coordinates describing the light rays. The symbols in both diagrams are defined as:

$$\begin{aligned} i^+ &= \text{future time-like infinity}, \\ i^0 &= \text{spatial infinity}, \\ i^- &= \text{past time-like infinity}, \\ \mathcal{I}^+ &= \text{future null infinity}, \\ \mathcal{I}^- &= \text{past null infinity}. \end{aligned}$$

### 2.1.2 (Anti-) de Sitter Space

If one extends Einstein-Hilbert action by adding a cosmological constant  $\Lambda$  to the Ricci scalar then one obtains

$$S = \int dx^4 \sqrt{-g} [R - \Lambda] . \quad (2.1.18)$$

The equations of motion are

$$R_{\mu\nu} - \frac{1}{2}Rg_{\mu\nu} + \frac{1}{2}\Lambda g_{\mu\nu} = T_{\mu\nu}. \quad (2.1.19)$$

For the derivation see appendix A.1. Minkowski spacetime is no longer a solution to Einstein's equation in vacuum, i.e. the cosmological constant changes the background of the spacetime. There are several ways to interpret this cosmological constant. Putting the cosmological constant on the right hand side of Einstein's equation gives rise to the interpretation of the cosmological constant as a universal yet constant matter distribution with either an attractive or a repulsive force for  $\Lambda < 0$  and  $\Lambda > 0$  respectively. Due to the matter, these spaces will have nonzero curvature. They are called de Sitter space ( $dS_4$ ) and anti-de Sitter space ( $AdS_4$ ).  $dS_4$  has a positive constant curvature corresponding to  $\Lambda > 0$  and  $AdS_4$  has a negative constant curvature corresponding to  $\Lambda < 0$ . We can embed  $dS_4$  and  $AdS_4$  in the higher dimensional space  $\mathbb{R}^5$  with Minkowski metric. For  $dS_4$  this embedding is defined as

$$-x_0^2 + \sum_{i=1}^4(x_i)^2 = a^2 \quad \text{with } a^2 > 0. \quad (2.1.20)$$

For  $AdS_4$  this embedding is defined as

$$-x_0^2 + \sum_{i=1}^3(x_i)^2 - x_4^2 = a^2 \quad \text{with } a^2 < 0. \quad (2.1.21)$$

From this we see that the spatial part of  $dS_4$  is spherical and the spatial part of  $AdS_4$  is hyperbolic. An explicit coordinate representation is given below.

The Minkowski metric on  $\mathbb{R}^5$  induces the following metric on  $AdS_4$

Coordinates on  $dS_4$ :

$$\begin{aligned} x_0 &= \sqrt{a^2 - r^2} \sinh(t/a), \\ x_1 &= r \cos(\theta), \\ x_2 &= r \sin(\theta) \sin(\phi), \\ x_3 &= r \sin(\theta) \cos(\phi), \\ x_4 &= \sqrt{a^2 - r^2} \cosh(t/a). \end{aligned}$$

Coordinates on  $AdS_4$ :

$$\begin{aligned} x_0 &= \sqrt{a^2 + r^2} \sin(t/a), \\ x_1 &= r \cos(\theta), \\ x_2 &= r \sin(\theta) \sin(\phi), \\ x_3 &= r \sin(\theta) \cos(\phi), \\ x_4 &= \sqrt{a^2 + r^2} \cos(t/a). \end{aligned}$$

$$ds^2 = -dx_0^2 + \sum_{i=1}^4 dx_i^2 = -\left(1 - \frac{\Lambda r^2}{6}\right) dt^2 + \left(1 - \frac{\Lambda r^2}{6}\right)^{-1} dr^2 + r^2 d\Omega^2, \quad (2.1.22)$$

where  $\Lambda = \frac{6}{a^2}$ .  $AdS_4$  and  $dS_4$  are, like Minkowski spacetime, maximally symmetric<sup>4</sup> and thus the curvature tensor simplifies to  $R_{\rho\mu\sigma\nu} = \frac{R}{12}(g_{\rho\sigma}g_{\mu\nu} - g_{\rho\nu}g_{\mu\sigma})$ . It follows that  $R = \frac{12}{a^2} = 2\Lambda$ .

Lastly note that  $dS_4$  and  $AdS_4$  can be thought of as conformal rescaling of the Minkowski metric, this will be used in Section 2.5. The so called Poincaré patch, which covers half of  $AdS_4$ , is  $ds^2 = \frac{1}{x^2}(-dt^2 + dx^2 + dy^2 + dz^2)$ .

### Properties of $dS_4$ and $AdS_4$

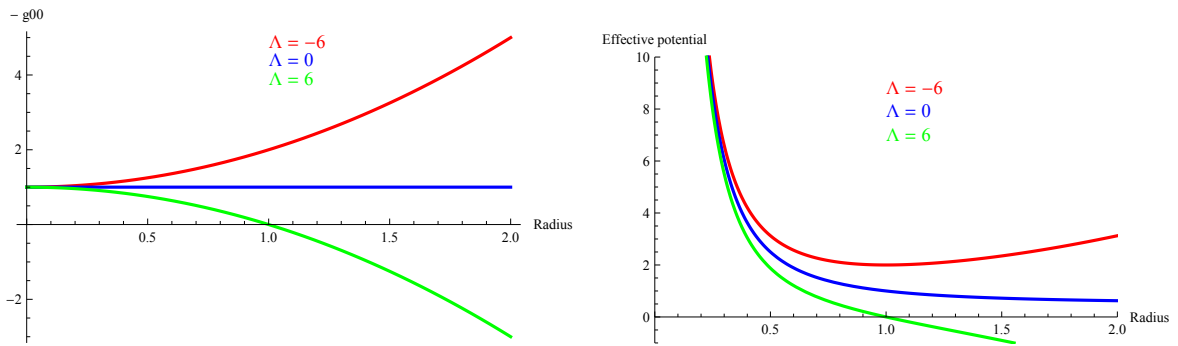


Figure 2.5: Characteristic function of the metric and effective potential for time-like particles for  $M = 0$  and  $L = 1$ .

Unlike  $AdS_4$  or Minkowski spacetime,  $dS_4$  has a horizon,  $g_{00} = 0$ . The light cone closes up at  $r = \sqrt{\frac{6}{\Lambda}}$  analogous to the Schwarzschild case. A radial light ray passing through the origin is described by  $r(t) = \sqrt{\frac{6}{\Lambda}} |\tanh(\sqrt{\frac{\Lambda}{6}} t)|$ . From this formula we deduce that light reaches the boundary at infinite coordinate time.

Consider a radial geodesic with  $E = 1$  (i.e. the initial radial proper velocity is  $\Lambda R^2$ , with  $R$  the starting radial distance). The geodesic equation (2.1.12) gives us that  $\frac{dr}{d\tau} = \sqrt{\Lambda r}$ , thus  $r(\tau) = Re^{\sqrt{\Lambda}\tau}$ . At  $\tau = -\frac{\log(\sqrt{\Lambda}R)}{\sqrt{\Lambda}}$  the time-like geodesic reaches the horizon. Note how this proper time diverges for  $R \rightarrow 0$ , i.e. the horizon cannot be reached by time-like geodesics starting at the origin. This type of event horizon is called a cosmological event horizon. We will elaborate more on this feature of  $dS_4$  when discussing the Penrose diagram.

A property of  $AdS_4$  space is the presence of closed time-like curves. For example the curve

<sup>4</sup>Reminder: Maximally symmetric means that a spacetime structure has a maximal amount of isometries, i.e. distance preserving functions. In four space-time dimension this is 10: 4 translations + 3 boosts + 3 rotations.

parameterized by  $x_0(t) = a \sin(t)$  and  $x_4(t) = a \cos(t)$  is a closed time-like curve that clearly satisfies the defining equation of  $AdS_4$ , (2.1.21). The presence of closed time-like curves conflicts with our fundamental assumptions about physics like causality and therefore  $AdS_4$  is considered unphysical. Another feature is that light rays reach spatial infinity in finite time. The differential equation

$$\frac{dr}{dt} = \pm(1 - \frac{\Lambda}{6}r^2)$$

is now solved by

$$r(t) = |\tan(\sqrt{-\frac{\Lambda}{6}}t)|/\sqrt{-\frac{\Lambda}{6}}.$$

We used the boundary condition  $r(0) = 0$  and have  $r\left(\frac{\pi}{2\sqrt{-\frac{\Lambda}{6}}}\right) = \infty$ . One can heuristically interpret this result as if the curvature force of the cosmological constant contracts spacetime so quickly that light rays seem to go quicker and quicker the farther they are away from the origin.

### Penrose Diagram for $dS_4$

We used static coordinates to represent de Sitter space. To obtain the Penrose diagram we need a whole bunch of other coordinates. Let us start with the global coordinates in the embedding dimension, which satisfy the defining equation quite naturally:

$$X^0 = a \sinh\left(\frac{\tau}{a}\right), \quad (2.1.23)$$

$$X^\alpha = a\omega^\alpha \cosh\left(\frac{\tau}{a}\right) \text{ for } \alpha=1, \dots, d=4, \quad (2.1.24)$$

$$\text{thus } ds^2 = -d\tau^2 + a^2 \cosh^2\left(\frac{\tau}{a}\right) d\Omega_3^2. \quad (2.1.25)$$

where  $\omega^\alpha$  parameterizes the  $S^{d-1}$  sphere of unit radius. Thus in our case  $\omega^1 = \cos(\theta_1)$ ,  $\omega^2 = \sin(\theta_1) \cos(\theta_2)$ ,  $\omega^3 = \sin(\theta_1) \sin(\theta_2) \cos(\theta_3)$ ,  $\omega^4 = \sin(\theta_1) \sin(\theta_2) \sin(\theta_3)$  and  $d\Omega^2 = d\theta_1^2 + \sin^2(\theta_1)d\theta_2^2 + \sin^2(\theta_1)\sin^2(\theta_2)d\theta_3^2$ . Applying the transformation  $\tan(T/a) = \tanh(\tau/a)$  we obtain:  $ds^2 = \sec^2\left(\frac{T}{a}\right) (-dT^2 + a^2 d\Omega_{d-1}^2)$ . The maximally extended Kruskal coordinates are then:

$$U = \tan\frac{1}{2}\left(\frac{T}{a} + \theta_1 - \frac{\pi}{2}\right), \quad (2.1.26)$$

$$V = \tan\frac{1}{2}\left(\frac{T}{a} + \theta_1 + \frac{\pi}{2}\right), \quad (2.1.27)$$

$$\text{thus } ds^2 = \frac{a^2}{(1 - UV)^2} (-4dUdV + (1 + UV)^2 d\Omega_2^2). \quad (2.1.28)$$

The full story can be read in [3] and [4].

Taking the arctan we obtain the following Penrose Diagram, see Figure 2.6. Note that in the picture the denoted future event horizon is the cosmological horizon we mentioned earlier. Furthermore there is a particle horizon in the picture . A particle horizon is a time reversed cosmological horizon, i.e. events outside of the particle horizon can never influence observer O. Lastly note in the picture  $l = a$  and  $0 \leq \theta_1 < \pi$  and moreover  $\theta_1 = \pi$  denotes the same spacetime points as  $\theta_1 = 0$ . We are going to give a more general

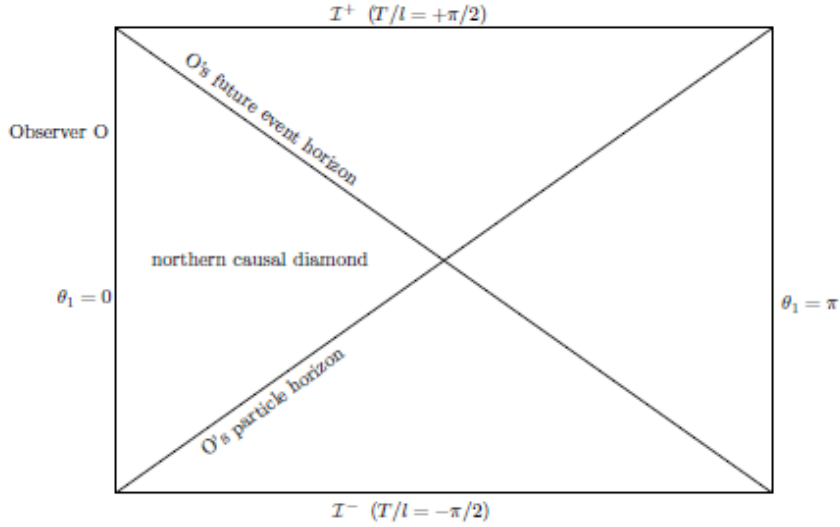


Figure 2.6: de Sitter Penrose diagram

explanation of particle and cosmological horizons, based on [4] and [1]. Consider the past light cone of a future time infinity,  $i^+$ . All the events in this light cone are events that could be seen by an observer on the worldline that ends in this  $i^+$ . In Minkowski space this past light cone encompasses the whole spacetime. In de Sitter space however this past light cone does not encompass everything. There is a region that is never observable by the world line. The boundary between the regions that are observable and that are not is the cosmological event horizon, *i.e.* the future event horizon. Consider the future light of a past time infinity,  $i^-$ . All the events in this light cone are events that could be causally interfered with by an observer on the worldline. In Minkowski spacetime this future light cone encompasses all of spacetime. Yet in de Sitter spacetime this future light cone does not encompass everything. There is a region that is never causally connected to the world line in the past direction. The boundary between the regions that are causally connected, is the particle event horizon, *i.e.* the past event horizon.

### Penrose Diagram for $AdS_4$

$AdS_4$  cannot be conformally compactified to make a Penrose diagram without introducing singularities [5]. One can compactify the  $r$  direction using once again the arctan of the  $r$  coordinate. The spacelike surface  $r = \infty$  is the conformal boundary of light. Due to the null geodesics behavior we deduced before,  $i^0$  is a surface now, instead of a point. Time-like geodesics starting at  $r = 0$  have the strange behavior of all being attracted back to the origin which they will reach at the same time. All of this information is captured in the Penrose diagram, see Figure 2.7.

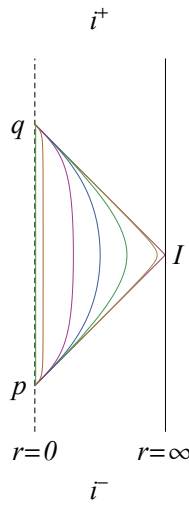


Figure 2.7: anti-de Sitter Penrose diagram. The colored lines are time-like geodesics through the point  $p$ , while the most right one describes a light ray.

### Schwarzschild (Anti-)de Sitter

Can we generalize Birkhoff's Theorem to non zero cosmological constants? Yes, the procedure of adding a cosmological constant to Birkhoff's Theorem can be found in Section 3.1. The main result is that the metric of the Schwarzschild (anti-)de Sitter spacetime, ( $SdS$  and  $SAdS$ ), is given by:

$$ds^2 = - \left( 1 - \frac{2M}{r} - \frac{\Lambda r^2}{6} \right) dt^2 + \left( 1 - \frac{2M}{r} - \frac{\Lambda r^2}{6} \right)^{-1} dr^2 + r^2 d\Omega^2. \quad (2.1.29)$$

Remember that  $\Lambda > 0$  and  $\Lambda < 0$  for  $dS_4$  and  $AdS_4$  space respectively. Note also that in the case of  $\Lambda \rightarrow 0$ , we obtain back the original Schwarzschild solution. On the other hand if  $M \rightarrow 0$  then we obtain  $(A)dS_4$ .  $SdS$  is also known as Kotler spacetime in the literature.

### Properties of Schwarzschild de Sitter Metric

The Schwarzschild metric has one horizon just as  $dS_4$ . The number of horizons in  $SdS$  depends on the relation between  $\Lambda$  and  $M$ . If  $\frac{9}{2}M^2 < \Lambda$  then there are two solutions, namely horizons at  $r_{\pm} = \frac{R}{\sqrt{\Lambda}} \left( 1 \pm \sqrt{1 - \frac{9M^2\Lambda}{R^3}} \right)$ , with  $R = \cos(\frac{1}{3}\cos^{-1}(9M^2\Lambda))$  [6]. The first one is the event horizon and the other one the already encountered cosmological horizon of  $dS_4$ . The singularity is called naked if there is no horizon, *i.e.* if  $\frac{9}{2}M^2 > \Lambda$ . The effective potential can be found in figure 2.8. Obtaining the Penrose diagram of  $SdS$  is roughly

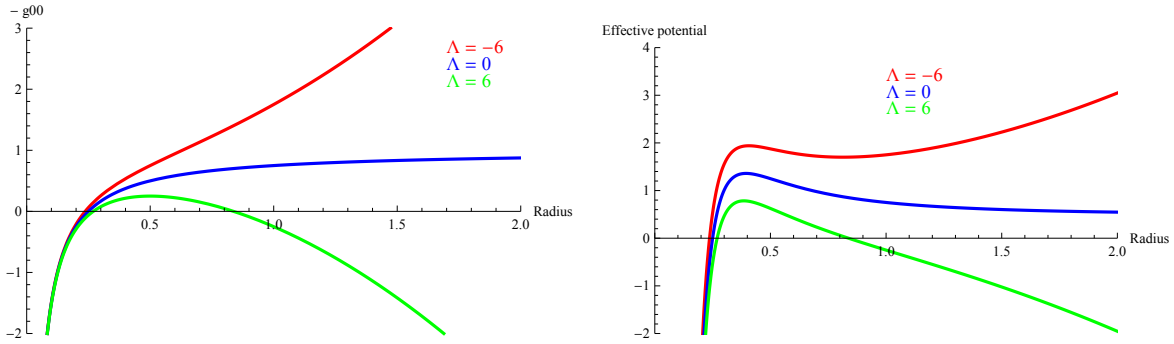


Figure 2.8: Characteristic function of the metric and effective potential for time-like particles for  $M = \frac{1}{8}$  and  $L = 1$

a matter of pasting together the Penrose diagrams of  $dS_4$  and Schwarzschild, see Figure 2.9. The copies of  $dS_4$  are not causally connected. Time and space are exchanged because

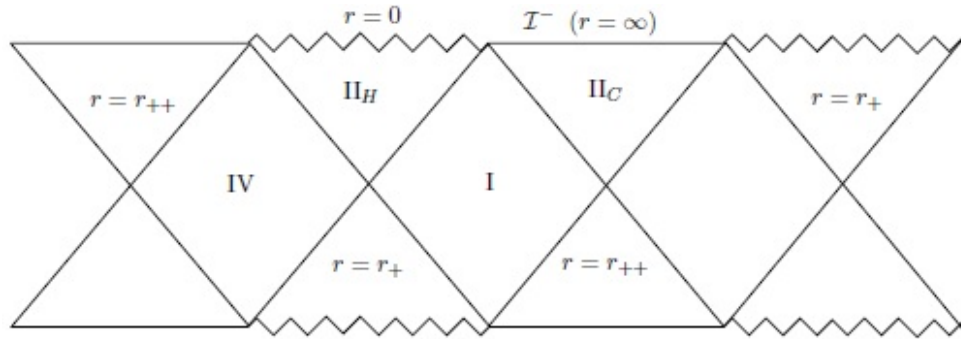


Figure 2.9: Penrose diagram of Schwarzschild de Sitter space time

the time and  $r$  component metric change sign when going through an event horizon. The diagram can be extended infinitely long to the left and the right as one can glue several

solutions to each other. These regions have then the same topological features. More information on  $SdS$  can be found in *e.g.* [3, 7, 6].

### Properties of Schwarzschild anti-de Sitter Metric

The addition of  $-\Lambda r^2$  to  $-g_{00}$  does not lead to extra horizons because  $\Lambda < 0$  and  $V$  was already greater than zero for large  $r$ . If  $L^2 > 11\frac{1}{4}M^2$  [8] there is a stable point in the effective potential. The Penrose diagram is given in figure 2.10. Note that the square sections of the Schwarzschild Penrose diagram are replaced by diamonds with conformal boundaries at both sides. This is due to the fact that all time-like paths get attracted back to the origin and light rays hit the boundary in finite time as we saw before. More information on  $SAdS$  can be found in *e.g.* [5, 7, 6].

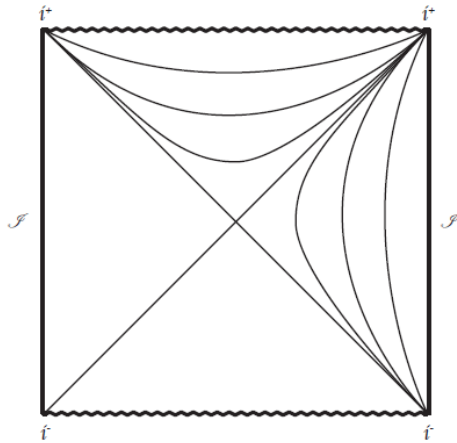


Figure 2.10: Penrose diagram of Schwarzschild anti de Sitter space time

## 2.2 The Reissner-Nordström Solutions

Having seen in Section 2.1.1 the solution for a black hole with only mass, we will now add a constant electric charge.

This solution known as the Reissner-Nordström solution can be found by starting with the same shape of the metric,  $ds^2 = -Adt^2 + Bdr^2 + r^2(d\theta^2 + \sin^2\theta d\phi^2)$ , in Schwarzschild coordinates, but now taking into account a static electric field, denoted by  $\mathcal{E}$ <sup>5</sup>, in the radial

---

<sup>5</sup>To avoid confusion with energy which will be denoted by  $E$ .

direction. This means we will have to combine the Maxwell fields with gravity, which gives a few changes to the non-relativistic equations.

### 2.2.1 Maxwell Fields and Gravity

Based on the conventions we defined in the previous chapter, we add the appropriate Maxwell fields to the action :

$$S = \int d^4x \sqrt{-g} \left( (R - \Lambda) - \frac{1}{4} g^{\mu\alpha} g^{\nu\beta} F_{\mu\nu} F_{\alpha\beta} \right). \quad (2.2.1)$$

Through easy calculations this then leads to the following defining relations

- The Bianchi Identities stay the same when taking into account covariant derivatives.<sup>6</sup> Thus the equations are

$$\partial_\gamma F_{\alpha\beta} + \partial_\alpha F_{\beta\gamma} + \partial_\beta F_{\gamma\alpha} = 0, \quad (2.2.2)$$

in which,

$$F_{\mu\nu} = \partial_\mu A_\nu - \partial_\nu A_\mu. \quad (2.2.3)$$

The formula in (2.2.2) stays true because the connection terms cancel out against each other.

- The inhomogenous Maxwell equations now read

$$D_\mu F_\nu^\mu = g^{\alpha\beta} D_\alpha F_{\beta\nu} = -J_\nu, \text{ or} \quad (2.2.4)$$

$$\partial_\mu (\sqrt{-g} F^{\mu\nu}) = -\sqrt{-g} J^\nu \quad (2.2.5)$$

leading to the conservation law

$$\partial_\mu (\sqrt{-g} J^\mu) = 0. \quad (2.2.6)$$

The first can be found by varying  $A_\mu$  and the second follows directly from the asymmetric properties of  $F_{\mu\nu}$  ( $F_{\mu\nu} = -F_{\nu\mu}$ ).

- Finally the energy momentum distribution follows from the Langragian:

$$T_{\mu\nu} = -F_{\mu\alpha} F_\nu^\alpha + \left( \frac{1}{4} F_{\alpha\beta} F^{\alpha\beta} - J_\alpha A^\alpha \right) g_{\mu\nu} \quad (2.2.7)$$

---

<sup>6</sup>One can read this in any general relativity book, and it can be easily derived explicitly via calculation.

From these relations one can easily derive that

$$F_{rt} = \mathcal{E} = \frac{Q\sqrt{AB}}{r^2},$$

and if one uses these equations to also derive the line element one will again find that

$$A = \frac{1}{B},$$

thus that

$$\mathcal{E} = \frac{Q}{r^2}. \quad (2.2.8)$$

## 2.2.2 Minkowski Space

To find the line-element one can again follow Birkhoffs theorem<sup>7</sup> but now with this new element added. This is still possible as Birkhoffs theorem only requires that the black hole has to be static and symmetric. One will then find

$$ds^2 = - \left(1 - \frac{2M}{r} + \frac{Q^2}{r^2}\right) dt^2 + \left(1 - \frac{2M}{r} + \frac{Q^2}{r^2}\right)^{-1} dr^2 + r^2(d\theta^2 + \sin^2 \theta d\phi^2) \quad (2.2.9)$$

as the line element for the Reissner-Nordström black hole in Minkowski background.

As was done for the Schwarzschild black hole in Section 2.1.1 we will look at  $g_{rr} = \infty$  and show that the solutions do not represent physical singularities but rather event horizons of the Reissner-Nordström black hole. However here we have very different cases depending on our mass and charge. These three distinct options are  $M^2 < Q^2$ ,  $M^2 = Q^2$  and  $M^2 > Q^2$ . The first one is physically considered impossible<sup>8</sup>. The second one is a so called extremal black hole with only one horizon. The last one has two horizons, as  $g_{rr} = \infty$  then implies

$$r_{\pm} = M \pm \sqrt{M^2 - Q^2}. \quad (2.2.10)$$

This last situation is the one we will consider in the rest of this chapter.

**Kruskal-Szekeres Coordinates.** In order to define the Kruskal-Szekeres coordinates we will first need the so-called tortoise coordinate, as was defined in (2.1.3), in this metric

$$r_* = r + \frac{1}{2\kappa_+} \log \left| \frac{r - r_+}{r_+} \right| + \frac{1}{2\kappa_-} \log \left| \frac{r - r_-}{r_-} \right|, \quad (2.2.11)$$

---

<sup>7</sup>See Section 3.1.

<sup>8</sup>In this situation one would only have a naked singularity at  $r = 0$  which is not allowed by the cosmic censorship conjecture. For more see Section 3.5.

with:

$$\kappa_{\pm} = \frac{r_{\pm} - r_{\mp}}{2r_{\pm}^2}, \quad (2.2.12)$$

the surface gravity<sup>9</sup> of the black hole. Afterwards we define  $v = t + r_*$  and  $u = t - r_*$ , the so called Eddington-Finkelstein coordinates as seen before in (2.1.5). We can then define the Kruskal coordinates as:  $U^{\pm} = -e^{-\kappa_{\pm} u}$  and  $V^{\pm} = \pm e^{\kappa_{\pm} v}$ .

Then we get

$$ds^2 = -\frac{r_+ r_-}{\kappa_{\pm}^2} \frac{e^{2|\kappa_{\pm}|r}}{r^2} \left( \pm \frac{r - r_{\mp}}{r_{\mp}} \right)^{1+|\kappa_{\pm}|} dU^{\pm} dV^{\pm} + r^2 d\Omega. \quad (2.2.13)$$

Note that the coordinate combinations  $U^+, V^+$  and  $U^-, V^-$  correspond to two distinct regions. In the positive region we have  $u, v$  as defined before and we can look at this for  $r > r_-$ , in so called outgoing Eddington Finkelstein coordinates.

In the second negative region we will use so called ingoing Eddington-Finkelstein coordinates which implies  $u = v - 2r_*$ , to have the region containing  $r < r_+$ .

This then gives us these two Kruskal diagrams.

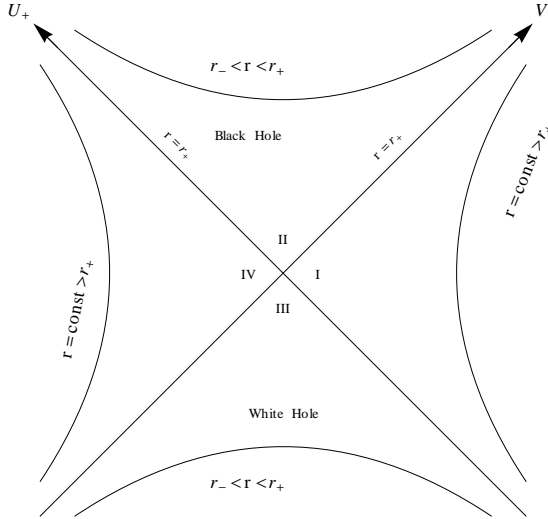


Figure 2.11: Kruskal diagram starting from outgoing Eddington Finkelstein coordinates

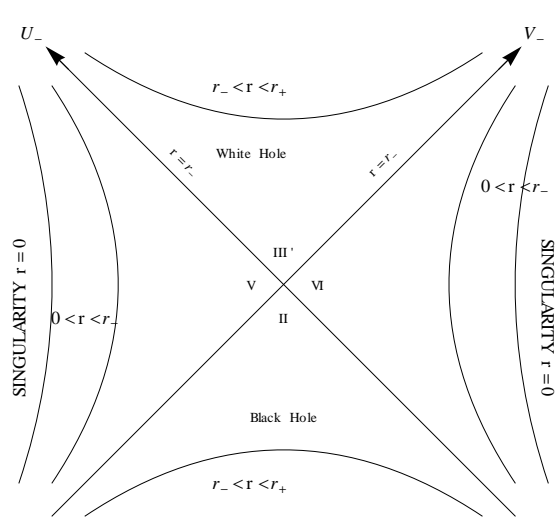


Figure 2.12: Kruskal diagram started from ingoing Eddington Finkelstein coordinates

Now in figure 2.11 sector II is coupled to the sectors, I, III and IV in the past time direction. Now by using time reversal principles we expect region III' (see figure 2.12) to be coupled in the forward direction to a region I', II', IV'.

And actually there is no physical reason for it not to be connected, as the black and white

---

<sup>9</sup>See Section 5.1.

hole will make communication with our universe impossible from these areas. This will thus give the same sort of regions as in the first diagram, which then again will couple to the second diagram shifted and so on and so forth. We can thus create infinitely many regions in this way.

Another thing to note is that there is indeed only one real singularity at  $r = 0$  and it is something we run into in both region V and VI. This is a so-called curvature singularity.

**Geodesics** Using the same equation for the geodesics as given in the previous section, we get four differential equations of which one is canceled out by noting that  $\theta = \frac{\pi}{2}$  is still allowed due to conservation of angular momentum.

$$0 = \frac{d}{d\tau} \left( \log \frac{d\phi}{d\tau} + \log r^2 \right), \quad (2.2.14)$$

$$0 = \frac{d}{d\tau} \left( \log \frac{dt}{d\tau} + \log \left( 1 - \frac{2M}{r} + \frac{Q^2}{r^2} \right) \right), \quad (2.2.15)$$

$$\frac{d^2r}{d\tau^2} = \frac{Q^2 - Mr}{r^3} g_{rr} \left( \frac{dr}{d\tau} \right)^2 - \frac{r}{g_{rr}} \left( \frac{d\phi}{d\tau} \right)^2 - \frac{Q^2 - Mr}{r^3 g_{rr}} \left( \frac{dt}{d\tau} \right)^2. \quad (2.2.16)$$

Then by using the Killing vector, as given in (2.1.13), and metric compatibility equations this can be reduced to:

$$E^2 = \left( \frac{dr}{d\tau} \right)^2 + V(r), \quad (2.2.17)$$

$$E = \left( 1 - \frac{2M}{r} + \frac{Q^2}{r^2} \right) \left( \frac{dt}{d\tau} \right), \quad (2.2.18)$$

$$V(r) = \left( \frac{L^2}{r^2} + \epsilon \right) \left( 1 - \frac{2M}{r} + \frac{Q^2}{r^2} \right), \quad (2.2.19)$$

$$L = r^2 \frac{d\phi}{d\tau}, \quad (2.2.20)$$

with  $\epsilon$  being 1 for timelike, -1 for spacelike and 0 for null geodesics and  $E$  as the energy, as defined in the previous chapter. Now note that for radial falling observers  $L = 0$ , we get

$$\frac{dr}{dt} = \pm \left( 1 - \frac{2M}{r} + \frac{Q^2}{r^2} \right) \frac{1}{E} \sqrt{E^2 - \epsilon \left( 1 - \frac{2M}{r} + \frac{Q^2}{r^2} \right)}, \quad (2.2.21)$$

as the associated differential equation.

### The Penrose-Carter diagrams

By doing a conformal transformation, as explained in chapter 2.1, we can go from Kruskal coordinates to Penrose coordinates. Note that, in order to do that, we have infinitely many regions, as said before. Thus there are infinitely many sets of Kruskal coordinates that are coupled per region to each other.

While the conformal transformation has spatial and timelike infinities transformed into a point, it cannot cover all the Kruskal coordinates. In other words, while the transformation creates a finite worldsheet for each region that exist, it cannot and should not address the amount of possible regions.

The Penrose diagram is therefore infinitely large. Yet since it is repetitive we will only show one of the parts.

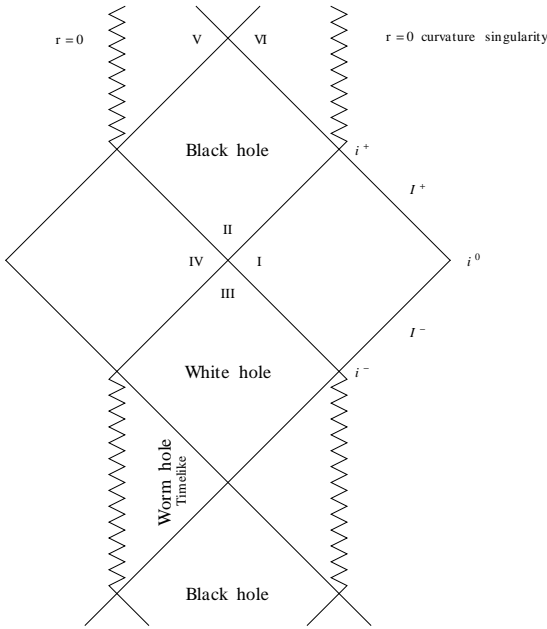


Figure 2.13: Penrose diagram of Reissner-Nordström black hole in Minkowski coordinates

### 2.2.3 Charged Black Holes in Anti de Sitter and de Sitter Space

For both Anti de Sitter and de Sitter spacetime the line element is

$$ds^2 = - \left( 1 - \frac{2M}{r} + \frac{Q^2}{r^2} - \frac{\Lambda}{6} r^2 \right) dt^2 + \left( 1 - \frac{2M}{r} + \frac{Q^2}{r^2} - \frac{\Lambda}{6} r^2 \right)^{-1} + r^2(d\theta^2 + \sin^2 \theta d\phi^2). \quad (2.2.22)$$

Here the difference lies in the sign of the cosmological constant. For (Anti) de Sitter this is positive (negative).

Now it is convenient to make everything dimensionless. Thus we choose  $(t, r) \rightarrow (t/M, r/M)$ ,  $y \equiv \frac{1}{6}\Lambda M^2$  and  $\epsilon \equiv \frac{Q}{M}$ . Then we can use

$$-g_{tt} = 1 - \frac{2}{r} + \frac{\epsilon^2}{r^2} - yr^2 \quad (2.2.23)$$

to find the event horizons, as these are defined by  $g_{rr} = \infty$  which in this case is the same as  $g_{tt} = 0$ .

Thus for given constants this yields

$$y = \frac{r_h^2 - 2r_h + \epsilon^2}{r_h^4}, \quad (2.2.24)$$

which, if we try to solve for  $r_h$ , gives us a fourth order polynomial. This polynomial would usually have four solutions, but there could be negative or complex solutions which are non-physical. In order to only find the proper solutions one needs to give some constraints on the constant. First of all we assume again that  $Q^2 < M^2$  thus that  $0 < \epsilon^2 < 1$ . Furthermore we only consider something a horizon if  $r \geq 0$ .

For de Sitter space this implies that there are 3 horizons called  $r_- < r_+ < r_c$  with the first two black hole horizons and the other cosmological horizon, as was defined in Section 2.1. Note that in order for this to have a physical solution we also need to put a bound on  $y$  with respect to  $\epsilon$  as follows

$$\frac{\frac{3}{2}\left(1 - \left(1 - \frac{8\epsilon^2}{9}\right)^{\frac{1}{2}}\right) - \epsilon^2}{\left(\frac{3}{2}\left(1 - \left(1 - \frac{8\epsilon^2}{9}\right)^{\frac{1}{2}}\right)\right)^4} < y < \frac{\frac{3}{2}\left(1 + \left(1 - \frac{8\epsilon^2}{9}\right)^{\frac{1}{2}}\right) - \epsilon^2}{\left(\frac{3}{2}\left(1 + \left(1 - \frac{8\epsilon^2}{9}\right)^{\frac{1}{2}}\right)\right)^4}. \quad (2.2.25)$$

For more on this we refer to [9].

For Anti de Sitter space there are only two horizons,  $b_- < b_+$ . In this case there is no cosmological horizon. But in order for these  $r$  to have physical solutions we get the same bounds on  $y$  with respect to the  $\epsilon$ . As the solutions are quite terrible to look at we will not define them here. And we leave it up to the reader to use a numerical solving program to construct them.

**Geodesics** The geodesic equations for the freefalling observers are given by nearly the same equations as the case  $\Lambda = 0$ ,

$$0 = \frac{d}{d\tau} \left( \log \frac{d\phi}{d\tau} + \log r^2 \right) \quad (2.2.26)$$

$$0 = \frac{d}{d\tau} \left( \log \frac{dt}{d\tau} + \log \left(1 - \frac{2M}{r} + \frac{Q^2}{r^2} - \frac{\Lambda}{6}r^2\right) \right) \quad (2.2.27)$$

$$\frac{d^2r}{d\tau^2} = \frac{Q^2 - Mr + \frac{r^4\Lambda}{6}}{r^3} g_{rr} \left( \frac{dr}{d\tau} \right)^2 - \frac{r}{g_{rr}} \left( \frac{d\phi}{d\tau} \right)^2 - \frac{Q^2 - Mr + \frac{r^4\Lambda}{6}}{r^3 g_{rr}} \left( \frac{dt}{d\tau} \right)^2. \quad (2.2.28)$$

Note that, as these are nearly the same equations, we can again rewrite them as:

$$E^2 = \left( \frac{dr}{d\tau} \right)^2 + V(r) \quad (2.2.29)$$

$$E = (1 - \frac{2M}{r} + \frac{Q^2}{r^2} - \frac{\Lambda}{6}r^2)(\frac{dt}{d\tau}) \quad (2.2.30)$$

$$V(r) = (\frac{L^2}{r^2} + \epsilon)(1 - \frac{2M}{r} + \frac{Q^2}{r^2} - \frac{\Lambda}{6}r^2) \quad (2.2.31)$$

$$L = r^2 \frac{d\phi}{d\tau} \quad (2.2.32)$$

Hence we get similar differential equations, which have just become harder to solve because of the  $r^2$  term. Now for the radial freefalling observer we get the same type of solution with only this  $\frac{\Lambda}{6}r^2$  term added in the factor in front and the one for the  $\epsilon$  term, thus:

$$\frac{dr}{dt} = \pm(1 - \frac{2M}{r} + \frac{Q^2}{r^2} + \frac{\Lambda}{6}r^2)\frac{1}{E}\sqrt{E^2 - \epsilon(1 - \frac{2M}{r} + \frac{Q^2}{r^2} + \frac{\Lambda}{6}r^2)} \quad (2.2.33)$$

As done for the Schwarzschild black hole we can plot the potential and the metric, this is done in figure 2.14. The old Schwarzschild metric was also showed to make the comparison easier. Here one can clearly see the extra horizon of the Reissner-Nordström black hole.

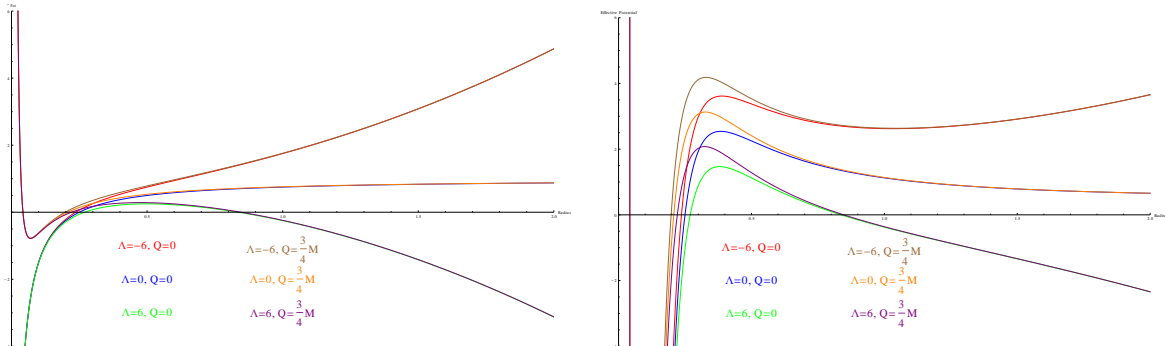


Figure 2.14: Characteristic function of the metric and effective potential for time-like particles for  $M = \frac{1}{8}$  and  $L = 1$

**The Penrose-Carter diagrams** The Penrose diagrams are a bit more complicated in this case. In de Sitter space we need to take into account the extra horizon as well as the singularity at zero.

Just as in the Minkowski space this diagram repeats in the vertical direction onto infinity.

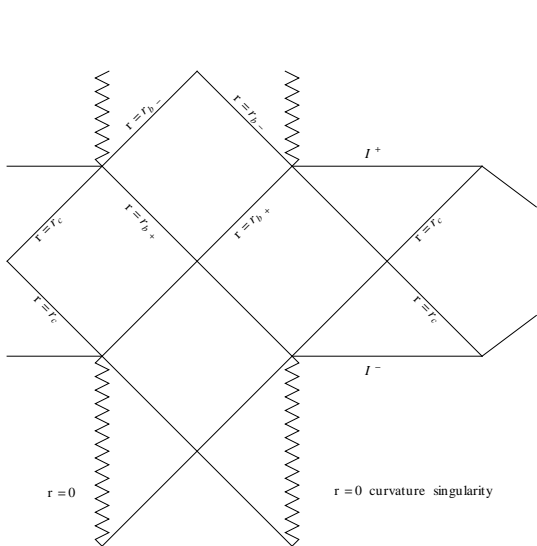


Figure 2.15: Penrose diagram of Reissner-Nordström black hole in de Sitter background

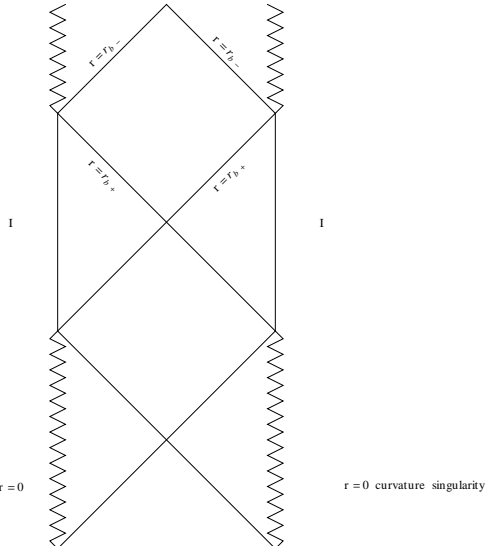


Figure 2.16: Penrose diagram of Reissner-Nordström black hole in Anti de Sitter Background

The new part is that this now also happens in the horizontal (aka space) direction. At the cosmological horizon it couples to the next diagram.

Now in a similar way in Anti de Sitter space we have the  $I$  ( $r = \infty$ ) as a space like infinity that is represented by a time like surface. As this is a vertical time like line we can no longer speak of future and past on this line, and, as is known, the time like infinities are disconnected. Where first we had a future and past spacelike infinity these have now becomes inseparable.

In this section we have expanded on the previous section by now adding a constant electric charge to our black hole. This took us from the Schwarzschild to the Reissner-Nordström solution. In order to be able to talk about a charged black hole we have first looked at the Maxwell fields in a relativistic situation. We then discussed the extra event horizons that will occur and how this will be translated into Kruskal-Szekeres coordinates for a Minkowski space background. The geodesics and the associated effective potentials as well as the Penrose-Carter diagrams were discussed for both Minkowski, de Sitter and Anti de Sitter backgrounds. Finally we have also spent some time on how the non-zero cosmological constant changes the line-element and restricts our bounds on the charge and mass of the black hole further.

## 2.3 The Kerr Solution

### 2.3.1 Rotating Black Holes

So far we have only considered spherically symmetric vacuum solutions of the Einstein equations, which is the geometry outside of a non-rotating black hole. However, we know from astrophysical observations that stars rotate, thus breaking the spherical symmetry.

When a body is rotating sufficiently slowly that only deviations of the first order in the angular momentum are of significance, the body is not rotationally distorted, since centripetal accelerations are of second order in angular momentum.<sup>10</sup> The exterior geometry of spacetime does change because general relativity predicts that curvature is produced by both the distribution of mass-energy and its kinetic energy. The metric outside of a slowly rotating body is

$$ds^2 = ds_{\text{Schwarzschild}}^2 - \frac{4J}{r} \sin^2 \theta d\phi dt + \mathcal{O}(J^2). \quad (2.3.1)$$

This is an excellent approximation for almost any celestial body, but for bodies with a high density or a high mass, this approximation is inadequate.

Physicists and mathematicians looked for an exact vacuum solution for a rotating body for many years, and the solution was discovered by Kerr in 1963[10], 48 years after the derivation of the Einstein field equations. The Kerr solution, as written by Kerr, is given by

$$\begin{aligned} ds^2 = & - \left( 1 - \frac{2Mr}{r^2 + a^2 \cos^2 \theta} \right) (du + a \sin^2 \theta d\phi)^2 \\ & + 2(du + a \sin^2 \theta d\phi)(dr + a \sin^2 \theta d\phi) \\ & + (r^2 + a^2 \cos^2 \theta)(d\theta^2 + \sin^2 \theta d\phi^2), \end{aligned} \quad (2.3.2)$$

where  $a = J/M$  and the metric is written in advanced Eddington-Finkelstein coordinates ( $u = t - r - 2M \ln |\frac{r}{2M} - 1|$ ).

The most commonly used form of the Kerr solution, however, uses Boyd-Lindquist coordinates, which can be derived in two steps. First make the substitution  $u = t + r$ , then

---

<sup>10</sup>For a particle rotating in a circle around a body, its acceleration  $\ddot{x}$  is equal to  $\ddot{x} = R \left( \frac{d\theta}{dt} \right)^2$ , where  $\theta$  is the angle and  $R$  the radius of the circle. Thus, if  $\dot{\theta}^2$  is negligible, the body is not distorted.

make the following coordinate transformation

$$\begin{aligned} t &= t_{BL} + 2M \int \frac{r dr}{r^2 - 2Mr + a^2}; \quad r = r_{BL}; \\ \phi &= -\phi_{BL} - a \int \frac{dr}{r^2 - 2Mr - a^2}; \quad \theta = \theta_{BL}. \end{aligned} \quad (2.3.3)$$

The Kerr solution in Boyer-Lindquist coordinates are (after dropping the BL subscript)

$$\begin{aligned} ds^2 &= - \left( 1 - \frac{2Mr}{\rho^2} \right) dt^2 - \frac{4Mar \sin^2 \theta}{\rho^2} d\phi dt + \frac{\rho^2}{\Delta} dr^2 \\ &\quad + \rho^2 d\theta^2 + \left( r^2 + a^2 + \frac{2Mra^2 \sin^2 \theta}{\rho^2} \right) \sin^2 \theta d\phi^2, \end{aligned} \quad (2.3.4)$$

where  $a = J/M$ ,  $\rho^2 = r^2 + a^2 \cos^2 \theta$  and  $\Delta = r^2 - 2Mr + a^2$ . This form is often favoured because it contains only one off-diagonal term, which makes it useful for analysing the different properties of this metric: **Limit  $a \rightarrow 0$** . When setting the rotation to zero, we notice that  $\rho \rightarrow r$  and  $\Delta \rightarrow r^2 - 2Mr$ , and thus (2.3.4) reduces to (2.1.1): the Schwarzschild metric in Minkowski space. **Limit  $M \rightarrow 0$** . When setting the mass to zero, while keeping  $a$  finite, (2.3.4) reduces to:

$$ds^2 = -dt^2 + \frac{r^2 + a^2 \cos^2 \theta}{r^2 + a^2} dr^2 + (r^2 + a^2 \cos^2 \theta) d\theta^2 + (r^2 + a^2) \sin^2 \theta d\phi^2 \quad (2.3.5)$$

With easy (but tedious) calculations, one can show that this describes flat Minkowski space in oblate spheroidal coordinates plus a time dimension, see figure 2.17 ; these coordinates are given by

$$x = \sqrt{r^2 + a^2} \sin \theta \cos \phi; \quad y = \sqrt{r^2 + a^2} \sin \theta \sin \phi; \quad z = r \cos \theta. \quad (2.3.6)$$

**Limit  $r \rightarrow \infty$** . In the limit  $r \rightarrow \infty$ , the metric reduces to

$$\begin{aligned} ds^2 &= - \left( 1 - \frac{2M}{r} \right) dt^2 + \left( 1 + \frac{2M}{r} \right)^{-1} dr^2 + r^2(d\theta^2 + \sin^2 \theta d\phi^2) \\ &\quad - \frac{4Ma \sin^2 \theta}{r} d\phi dt + \mathcal{O}\left(\frac{1}{r^2}\right), \end{aligned} \quad (2.3.7)$$

which is equal to (2.3.1), the approximation of a slowly rotating black hole. **Reverting time and rotation**. The metric is invariant under the simultaneous transformation of both  $t' = -t$  and  $\phi' = -\phi$ . This is to be expected, because a rotating object going backwards in time rotates in the opposite direction. The metric has singularities when  $r^2 + a^2 \sin^2 \theta = 0$ , that is,  $r = 0$  and  $\theta = \pi/2$ , or when  $\Delta = r^2 - 2mr + a^2 = 0$ , that is,  $r = r_{\pm} = m \pm \sqrt{m^2 - a^2}$ . To investigate the nature of these singularities we use the same

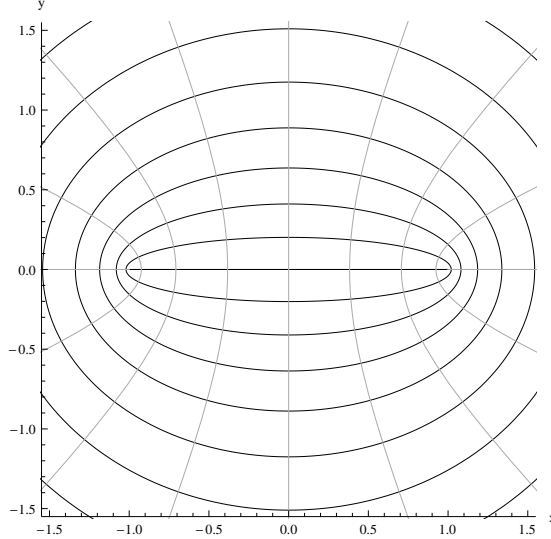


Figure 2.17: Lines of constant  $r$  (black ovals) and constant  $\theta$  (gray hyperboloids) in oblate spheroidal coordinates as given in (2.3.6) when  $\phi = 0$

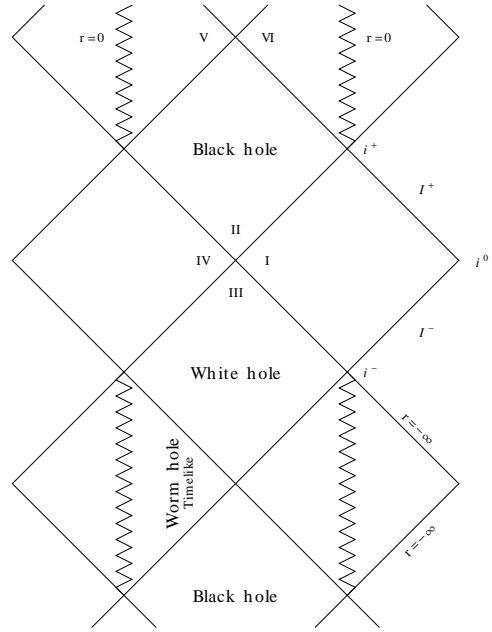


Figure 2.18: Penrose diagram of the Kerr solution

tactic as in the previous sections, namely we transform the metric and see if we can remove these singularities. We do this by transforming to the Kerr coordinates  $(u_+, r, \theta, \phi_+)$ , where

$$du_+ = dt + (r^2 + a^2)\Delta^{-1}dr; \quad d\phi_+ = d\phi + a\Delta^{-1}dr. \quad (2.3.8)$$

The metric then transforms to:

$$\begin{aligned} ds^2 = & - \left( 1 - \frac{2Mr}{\rho^2} \right) du_+^2 + 2drdu_+ - 4a\rho^2 Mr \sin^2 \theta d\phi_+ du_+ \\ & - 2a \sin^2 \theta drd\phi_+ + \rho^2 d\theta^2 + ((r^2 + a^2)^2 - \Delta a^2 \sin^2 \theta) \frac{\sin^2 \theta}{\rho^2} d\phi_+^2. \end{aligned} \quad (2.3.9)$$

In these coordinates the metric is not singular at  $r_{\pm}$ , and thus these surfaces are coordinate singularities. However, just like in the Reissner-Nordström case, this transformation does not cover the full spacetime globally. The coordinate patch can be extended however by using a slightly modified version of (2.3.8), using the coordinates  $(u_-, r, \theta, \phi_-)$ :

$$du_- = dt - (r^2 + a^2)\Delta^{-1}dr; \quad d\phi_- = d\phi - a\Delta^{-1}dr \quad (2.3.10)$$

The metric takes the form of (2.3.9), but with  $u_+$  replaced by  $-u_-$  and  $\phi_+$  replaced by  $-\phi_-$ . The full metric can then be described with a combination of these two metrics, and can be used to draw the Penrose diagram of the Kerr solution, see figure 2.18. This diagram shows many similarities to the Penrose diagram of the Reissner-Nordström solution, except

that there is a region past the  $r = 0$  singularity, where negative values of  $r$  are possible. This is because this singularity has the shape of a ring in the equatorial plane, which an observer can pass through. The regions I (where  $r > r_+$ ) are the regions outside of the black hole, and are asymptotically flat. The regions II (where  $r_- < r < r_+$ ) are between the two event horizons, and the regions III (where  $r < r_-$ , and can be negative) contain the ring singularity at  $r = 0$ . The geodesics of the Kerr solution are tricky to calculate, mainly because of the off-diagonal term in (2.3.4). We note that the metric (2.3.4) has no terms with  $t$  and  $\phi$  in it, and thus  $(1, 0, 0, 0)$  and  $(0, 0, 0, 1)$  are Killing vectors. The corresponding conserved quantities are

$$E = \left(1 - \frac{2Mr}{\rho^2}\right) \frac{dt}{d\tau} + \frac{2Mar \sin^2 \theta}{\rho^2} \frac{d\phi}{d\tau} \quad (2.3.11)$$

$$L = \left(r^2 + a^2 + \frac{2Mra^2 \sin^2 \theta}{\rho^2}\right) \sin^2 \theta \frac{dt}{d\tau} - \frac{2Mar \sin^2 \theta}{\rho^2} \frac{d\phi}{d\tau}. \quad (2.3.12)$$

A relatively simple geodesic to calculate is a particle with energy  $E$  infalling radially in the equatorial plane from infinity. This means there is no angular momentum, thus (2.3.12) with  $L = 0$  reduces to

$$\frac{d\phi}{dt} = \frac{(a^2 + r^2)\rho^2}{2aMr} + a \sin^2 \theta \quad (2.3.13)$$

which is zero only if  $a = 0$ . Even though the particle has no angular momentum when we release it, it gains angular momentum from the black hole. This phenomenon is called frame dragging. The quantity  $d\phi/dr$  can be calculated as function of  $r$  by filling in (2.3.11) and (2.3.13) in (2.3.4), the result is plotted in figure 2.19. In this figure we see that the particle, according to an observer at infinity, eventually rotates around the black hole close to the surface of the outer horizon  $r_+$ . There are also solutions for rotating black holes in de Sitter and anti-de Sitter spaces, this is however outside of the scope of this chapter.

### 2.3.2 Rotating Charged Black Holes

A rotating black hole can also be charged. In 1965, two years after Kerr published his solution, Newman found the solution for a rotating charged black hole [11]. His solution is very similar to Kerr's solution (2.3.4), but with  $2mr$  replaced by  $2mr - Q^2$ .

$$\begin{aligned} ds^2 = & - \left(1 - \frac{2Mr - Q^2}{\rho^2}\right) dt^2 - \frac{2a(2Mr - Q^2) \sin^2 \theta}{\rho^2} d\phi dt + \frac{\rho^2}{\Delta} dr^2 \\ & + \rho^2 d\theta^2 + \left(r^2 + a^2 + \frac{(2Mr - Q^2)a^2 \sin^2 \theta}{\rho^2}\right) \sin^2 \theta d\phi^2 \end{aligned} \quad (2.3.14)$$

where  $a = J/M$ ,  $\rho^2 = r^2 + a^2 \cos^2 \theta$ ,  $\Delta = r^2 + a^2 - 2Mr + Q^2$  and  $Q$  is the charge of the black hole. This solution has most of the properties of the non-charged case, with the

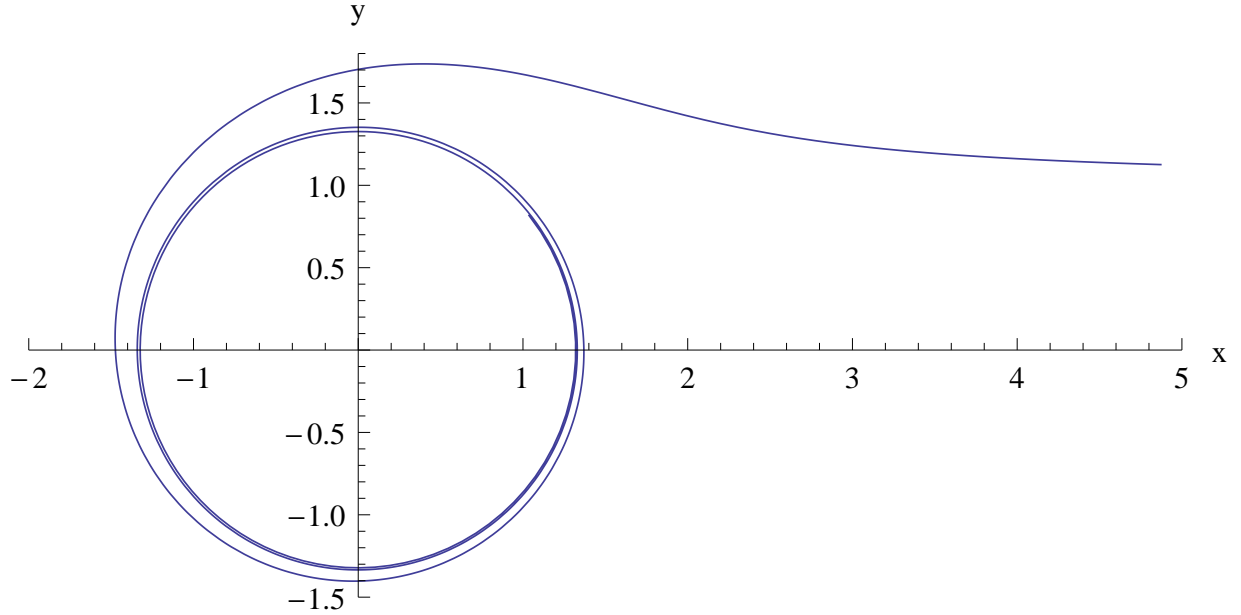


Figure 2.19: The geodesic of a particle infalling radially in a rotating black hole, according to an observer at infinity, with  $m = 1$ ,  $a = 0.95$  and  $E = 1$ .

exception that when  $a \rightarrow 0$ , the metric reduces to the Reissner-Nordström solution (2.2.9), rather than the Schwarzschild metric (2.1.1). The singularities of this solution are at  $r = 0$  and  $\Delta = r^2 - 2Mr + a^2 + Q^2 = 0$ , that is,  $r_{\pm} = M \pm \sqrt{M^2 - a^2 - Q^2}$ . When we transform to the Kerr coordinates  $(u_+, r, \theta, \phi_+)$ , the metric becomes

$$\begin{aligned} ds^2 = & - \left( 1 - \frac{2Mr - Q^2}{\rho^2} \right) du_+^2 + 2drdu_+ - 2a\rho^2(2Mr - Q^2)\sin^2\theta d\phi_+du_+ \\ & - 2a\sin^2\theta drd\phi_+ + \rho^2d\theta^2 + ((r^2 + a^2)^2 - \Delta a^2\sin^2\theta) \frac{\sin^2\theta}{\rho^2} d\phi_+^2, \end{aligned} \quad (2.3.15)$$

and a similar expression for  $(u_-, r, \theta, \phi_-)$ . From here we can see that the Penrose diagram of the Kerr-Newman solution is equivalent to that of the Kerr solution, but with its horizons moved to  $r_{\pm} = M \pm \sqrt{a^2 - M^2 - Q^2}$ . A charged black hole has an electromagnetic potential given by

$$A_\mu = \left( \frac{Q}{r}, 0, 0, -\frac{aQM}{r}\sin^2\theta \right). \quad (2.3.16)$$

Note that the metric does not contain a magnetic field in the  $r$  and  $\theta$  directions only if the black hole does not rotate ( $a = 0$ ) or if the black hole has no charge ( $Q = 0$ ).

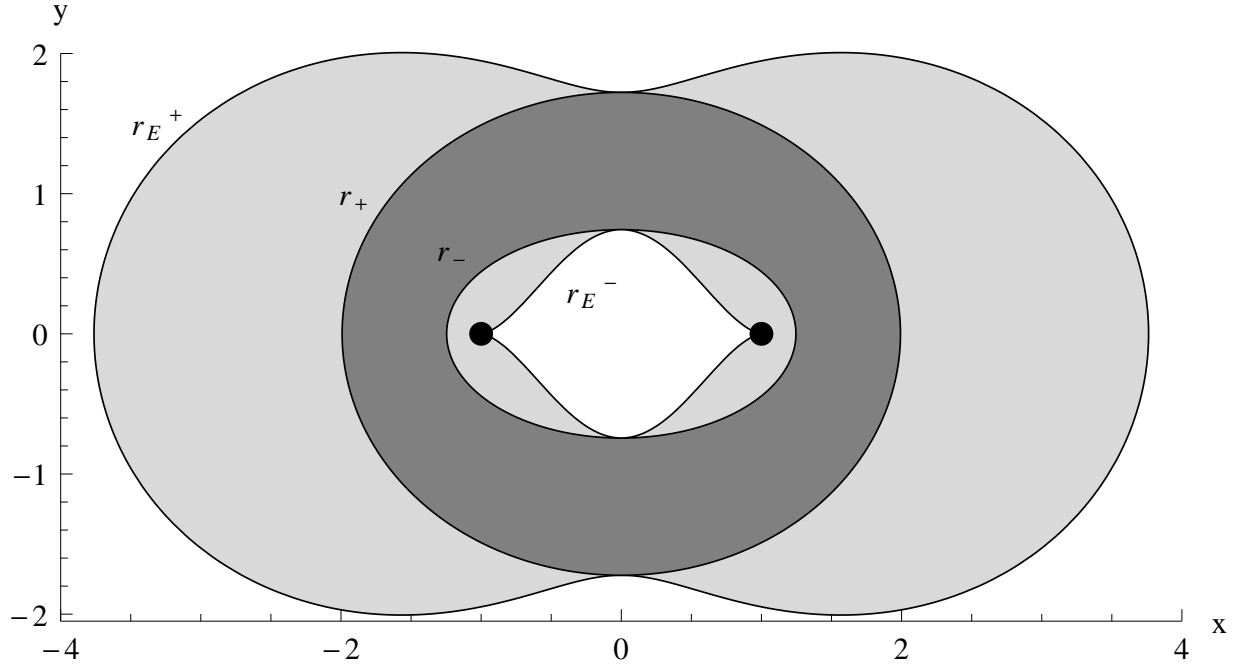


Figure 2.20: The horizons  $r_{\pm} = M \pm \sqrt{M^2 - a^2}$  and edges of the ergosphere  $r_E^{\pm} = M \pm \sqrt{M^2 - a^2 \cos^2 \theta}$  in oblate spheroidal coordinates (2.3.6) for  $m = 1$ ,  $a = 0.95m$  and  $\phi = 0$ . The gray area is the ergosphere, and the dark gray area is the space between the horizons. The points are the locations of the ring singularity at  $r = 0$  and  $\theta = \pi/2$ .

### 2.3.3 The Ergosphere

Suppose an astronaut has a rocket ship and wants to stay stationary near a rotating black hole with respect to an observer at infinity, that is, his position is  $X(t) = (t, r_0, \theta_0, \phi_0)$  and his tangent vector is  $T = (1, 0, 0, 0)$ . His trajectory should be timelike ( $T_\mu T^\mu < 0$ ), but  $T_\mu T^\mu = g_{\mu\nu} T^\nu T^\mu = g_{tt} = -(1 - \frac{2Mr}{r^2 + a^2 \cos^2 \theta})$ , which is positive for  $r_E^- < r < r_E^+$  with

$$r_E^{\pm} = M \pm \sqrt{M^2 - a^2 \cos^2 \theta} \quad (2.3.17)$$

If we compare this with the horizons of the rotating black hole,  $r_{\pm} = M \pm \sqrt{M^2 - a^2}$ , we see that  $r_E^+ \geq r_+ \geq r_- \geq r_E^- \geq 0$ . So there is a region outside the outer horizon where it is impossible to stand still in Boyer-Linquist coordinates, this region is called the ergosphere. More interesting phenomena occur in the ergosphere, for example, it is impossible for an observer to rotate around a black hole in the opposite orientation while in the ergosphere. Assume a light ray is in the equatorial plane  $\theta = \pi/2$  and moves in the  $\phi$  direction (so  $dr = 0$ ). Plugging this into the metric (2.3.4) we get that:

$$\left( r^2 + a^2 + \frac{2Ma^2}{r} \right) \left( \frac{d\phi}{dt} \right)^2 - \frac{4Ma}{r} \left( \frac{d\phi}{dt} \right) - \left( 1 - \frac{2M}{r} \right) = 0, \quad (2.3.18)$$

which has the solutions

$$\frac{d\phi}{dt} = \frac{2aM}{r(r^2 + a^2(1 + 2M/r))} \pm \frac{\sqrt{a^2 - 2Mr + r^2}}{(r^2 + a^2(1 + 2M/r))}. \quad (2.3.19)$$

Filling in  $r_E^+ = 2M$ , the “-” solution equals 0, so  $\frac{d\phi}{dt}$  can never be negative in the ergosphere. This means that in the ergosphere not even light can travel in the opposite direction of the rotation. Another interesting property of the ergosphere is that it allows us to extract energy from a black hole through a mechanism called the Penrose Process. In 1971, Penrose derived [12] that if a particle with mass-energy  $p_a$  is dropped into the ergosphere, and it decays into two particles  $p_a = p_b + p_c$  such that the mass energy of one of them is negative,  $p_b < 0$ , particle  $c$  then leaves the ergosphere to infinity with more mass-energy than the original particle,  $p_c > p_a$ , while particle  $b$  falls into the black hole, and thus energy has been extracted from the black hole. To see if it is possible to have a negative energy solution, we use (2.3.11) and look at the case  $E = 0$ , which results in

$$\left(\frac{d\phi}{dt}\right)_{E=0} = \frac{2Mr - \rho^2}{2aMr \sin^2 \theta}. \quad (2.3.20)$$

If our particles are traveling at the speed of light, we can fill this in (2.3.18) for a particle moving in the  $\phi$  direction in the equatorial plane, we get that

$$\frac{(1 - 2M/r)(a^2 + r^2(1 + 2M/r))}{4a^2M^2} = 0, \quad (2.3.21)$$

which again has solution  $r = 2M$ , the edge of the ergosphere. We conclude that negative energies can occur in the ergosphere, and thus the Penrose process could in principle happen. In this section we studied the properties of the rotating black hole, known as the Kerr solution. We have rewritten the original solution as given by Kerr in Boyer-Lindquist coordinates, and looked at the singularities of the metric. By transforming the metric again, we concluded that the metric consists of one curvature singularity and two horizons, just as in the Reissner-Nordström solution. We also studied the geodesic of a radially infalling observer, with as result that a radially infalling observer, according to an observer at infinity, circles the black hole just outside the outer horizon till infinity. Then we looked at the solution for a charged rotating black hole: the Kerr-Newman solution. Lastly, we studied the ergosphere, a place with many interesting properties like a frame-dragging effect so big that even light cannot rotate in the opposite direction of the black hole; and the Penrose process where energy is extracted from the rotating black hole.

## 2.4 Rindler Space

Rindler space, named after Wolfgang Rindler, describes a portion of Minkowski space as seen by a uniformly accelerating observer, which we will refer to as a Rindler observer. In the first part, we will show how to construct this coordinate chart. In this new coordinate chart the metric exhibits a coordinate singularity, which is related to a horizon with respect to the Rindler observers, this will be the subject of the second part. We conclude this section, by showing how Rindler space can be used to study the Schwarzschild metric.

### 2.4.1 Rindler Coordinates

For simplicity we consider two-dimensional Minkowski spacetime. We consider an observer, which undergoes uniform acceleration. This implies that  $a_\mu a^\mu = \alpha^2$ , where  $a_\mu$  denotes the proper acceleration, and  $\alpha$  is a real constant. Since Minkowski spacetime is flat, all the Christoffel symbols vanish, and hence the equation reads

$$\left( \frac{d^2x}{d\tau^2} \right)^2 - \left( \frac{d^2t}{d\tau^2} \right)^2 = \alpha^2. \quad (2.4.1)$$

This equation allows for several solutions, for example parabolic motion. However if we demand  $\tau$  to be the observer's proper time, then also the following equation has to be satisfied

$$\left( \frac{dx}{d\tau} \right)^2 - \left( \frac{dt}{d\tau} \right)^2 = -1. \quad (2.4.2)$$

It is easily seen that the above two equations are solved by taking

$$x(\tau) = \cosh(\alpha\tau) \frac{1}{\alpha} - \frac{1}{\alpha}, \quad (2.4.3)$$

$$t(\tau) = \sinh(\alpha\tau) \frac{1}{\alpha}. \quad (2.4.4)$$

This describes a particle which at  $t = \tau = 0$ , is at  $x = 0$  and has then zero velocity. This world-line is pictured by the black solid line in figure 2.21 Next we would like to find the proper coordinates corresponding to this observer. First we will outline the general procedure, after which we will apply this to the Rindler observer. In the following we will make use of several coordinate frames, for clarity we will first state these. First of all there is the inertial frame which is described by the coordinates  $(t, x)$ , we call this the laboratory frame. Then there is the proper frame, namely the coordinate system used by the Rindler observer, with coordinates  $(\tau, \xi)$ . Very important in the derivation below will be the set of comoving coordinate frames. For each instant  $\tau$  we define the comoving coordinate frame

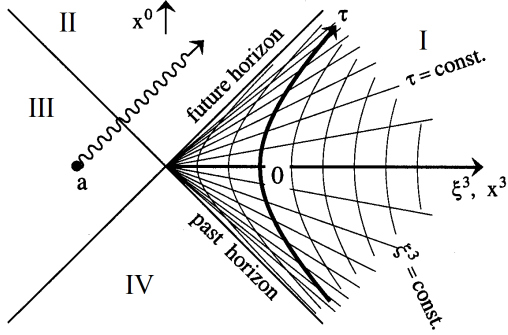


Figure 2.21: Rindler space. The solid line corresponds to the worldline of the Rindler observer. The future and past horizon cross at the point  $(0, -1/\alpha)$ . Figure edited and extracted from [13].

as the inertial frame with velocity  $u^\mu(\tau)$  relative to the laboratory frame, and whose origin coincides with  $x^\mu(\tau)$ . We denote the comoving coordinates at time  $\tau$  by  $(t_\tau, x_\tau)$ .

Note that the following relation between the comoving coordinates  $(t_\tau, x_\tau)$  and the proper coordinates  $(\tau, \xi)$  has to be satisfied:

$$\begin{aligned} x_\tau^0(\tau, \xi) &= 0 \\ x_\tau^1(\tau, \xi) &= \xi. \end{aligned} \tag{2.4.5}$$

Since we have now related the proper coordinates to the comoving coordinates at time  $\tau$ , we need to find the relation between the coordinates  $(x_\tau^0, x_\tau^1)$  and  $(x, t)$ . The comoving coordinate frame at time  $\tau$  moves with a velocity  $u^\mu(\tau) = dx^\mu/d\tau$ , therefore we find

$$\begin{pmatrix} x^0(x_\tau^0, x_\tau^1) \\ x^1(x_\tau^0, x_\tau^1) \end{pmatrix} = \begin{pmatrix} x^0(\tau) \\ x^1(\tau) \end{pmatrix} + \begin{pmatrix} u^0(\tau) & u^1(\tau) \\ u^1(\tau) & u^0(\tau) \end{pmatrix} \begin{pmatrix} x_\tau^0 \\ x_\tau^1 \end{pmatrix} \tag{2.4.6}$$

Combining equations (2.4.5) and (2.4.6), we find the following relation between the proper coordinates  $(\tau, \xi)$  and the inertial coordinates  $(t, x)$ :

$$t(\tau, \xi) = x^0(\tau) + \frac{dx^1(\tau)}{d\tau} \xi \tag{2.4.7}$$

$$x(\tau, \xi) = x^1(\tau) + \frac{dx^0(\tau)}{d\tau} \xi. \tag{2.4.8}$$

If we now apply this to the worldline given by equation (2.4.3), we find

$$x(\tau, \xi) = \cosh(\alpha\tau)(\xi + 1/\alpha) - 1/\alpha \tag{2.4.9}$$

$$t(\tau, \xi) = \sinh(\alpha\tau)(\xi + 1/\alpha). \tag{2.4.10}$$

For future use we also state the inverse relations

$$\tau(t, x) = \sqrt{(x + 1/\alpha)^2 - t^2} - 1/\alpha \quad (2.4.11)$$

$$\xi(t, x) = \operatorname{arctanh}\left(\frac{t}{x + 1/\alpha}\right). \quad (2.4.12)$$

If we express the metric in terms of these new coordinates we find

$$ds^2 = dx^2 - dt^2 \quad (2.4.13)$$

$$\begin{aligned} &= \alpha^2 \sinh^2(\alpha\tau)(\xi + \frac{1}{\alpha})^2 d\tau^2 + \cosh^2(\alpha\tau)d\xi^2 \\ &\quad + 2\cosh(\alpha\tau)\sinh(\alpha\tau)(\xi + \frac{1}{\alpha})d\tau d\xi - \cosh^2(\alpha\tau)(\xi + \frac{1}{\alpha})^2 d\tau^2 \\ &\quad - \sinh^2(\alpha\tau)d\xi^2 - 2\cosh(\alpha\tau)(\xi + \frac{1}{\alpha})\sinh(\alpha\tau)d\tau d\xi \\ &= -\alpha^2(\xi + \frac{1}{\alpha})^2 d\tau^2 + d\xi^2. \end{aligned} \quad (2.4.14)$$

We notice that the proper distance between the different  $\xi$  points remains constant. Since we are free to change variables we introduce  $z = \xi + 1/\alpha$ , then the metric changes to

$$ds^2 = -\alpha^2 z^2 d\tau^2 + dz^2. \quad (2.4.15)$$

As a final check, we investigate how a Rindler observer experiences his own acceleration. For this we will need the Christoffel symbols. The only nonvanishing Christoffel symbols are given by  $\Gamma_{\tau\tau}^z = \alpha^2 z$ ,  $\Gamma_{\tau z}^\tau = \Gamma_{\xi z}^\tau = 1/z$ . The wordline of a Rindler observer expressed in the coordinates  $\tau, z$  reads  $(\tau(t), z(t)) = (t/\alpha z, z_0)$ . It easily follows that the acceleration in the  $z$  direction is given by

$$a^z = u^\mu D_\mu u^z = u^\tau (\partial_\tau u^z + \Gamma_{\tau\tau}^z u^\tau) = 1/z. \quad (2.4.16)$$

The acceleration in the  $\tau$  direction vanishes since

$$a^\tau = u^\mu D_\mu u^\tau = u^\tau (\partial_\tau u^\tau + \Gamma_{\tau\xi}^\tau u^\xi) = 0. \quad (2.4.17)$$

Hence a Rindler observer experiences an acceleration in the  $z$  direction with a magnitude inversely proportional to the distance to the horizon.

## 2.4.2 Rindler Horizon

When one studies the Rindler metric given by equation (2.4.14), one immediately notices that this exhibits a singularity at  $\xi = -\frac{1}{\alpha}$ . This singularity is intimately related to the

Rindler horizon. To study the singularity we divide the Minkowski spacetime in four regions, I, II, III, and IV, as seen in figure 2.21. Note that the Rindler chart only describes region I. We are interested in how events in regions II, III, and IV can influence region I. Since for any timelike or lightlike curve  $\gamma$ , we have  $|\frac{dt}{dx}| \geq 1$ , we immediately see that events from region III are never connected to region I by any timelike or lightlike curve, and vice versa, so these two regions are causally unrelated. Next we consider region IV; since any Rindler wordline will approach the light cone, we can always find a timelike curve which connects an event in region I to this wordline. When we consider region II instead, the situation is completely opposite: we can always find a timelike curve, which connects any Rindler wordline, to any event in region II. These observations lead us to define the future horizon  $H_{\text{future}} = \{(t, x) | t = (x + 1/\alpha) \geq 0\}$ , and the past horizon  $H_{\text{past}} = \{(t, x) | -t = (x + 1/\alpha) \geq 0\}$ . We note that the union of these horizons actually corresponds to the coordinate  $\xi = -\frac{1}{\alpha}$ .

Just as an observer outside the Schwarzschild black hole never sees something entering the

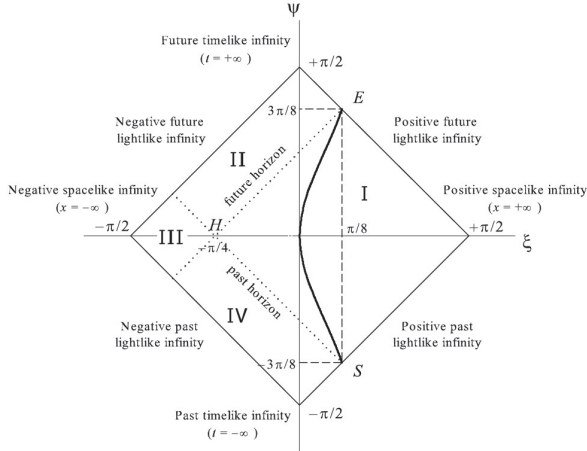


Figure 2.22: Penrose diagram for Rindler space, Rindler space is covered by region I. The Bold line shows the trajectory of a Rindler observer. Figure extracted from [14].

black hole, the Rindler observer will never see something entering or leaving Rindler space. This is due to the fact that in his coordinate system the object that approaches the future horizon will slow down to zero velocity, and anything which enters via the past horizon will start at zero velocity in his coordinate system. This we can elucidate by considering a simple geodesic, which describes a static inertial observer in Minkowski space:

$$\tau(t) = \operatorname{arctanh}(at) \quad (2.4.18)$$

$$\xi(t) = \sqrt{\left(\frac{1}{\alpha}\right)^2 - t^2} - \frac{1}{\alpha}, \quad (2.4.19)$$

where  $\tau$  is the proper time.  $-\frac{1}{\alpha} \leq \tau \leq \frac{1}{\alpha}$ , and  $\lim_{t \rightarrow \pm\frac{1}{\alpha}} \tau(t) = \pm\infty$ , hence the Rindler observer will never actually see this real static observer entering or leaving the Rindler space. To conclude we show the Carter Penrose diagram for Minkowski space, with Rindler space embedded, see figure 2.22. Note that the Penrose diagram for Minkowski space is obtained from the relation  $\Psi \pm \xi = \arctan(x \pm t)$ . Note that  $\Xi$  can also become negative, this is due to the fact that we are not working in spherical coordinates. The embedding of Rindler space is easily found, since the Rindler horizon defines a light-cone.

### 2.4.3 Black Holes and Rindler Space

It turns out that Rindler space can be used to study black holes. Near the horizon we can approximate the Schwarzschild and Reissner-Nordström metric by the Rindler metric. To prove this, we suppose we are given a metric

$$ds^2 = -f(r)dt^2 + \frac{1}{f(r)}dr^2 + r^2d\Omega^2, \quad (2.4.20)$$

where  $f$  is a real valued function with a zero at  $r = r_0$ . Now if we write  $f(r) = f(r_0 + \xi) \approx f'(r_0)\xi$ , then this metric reads

$$ds^2 = -f'(r_0)\xi dt^2 + \frac{1}{f'(r_0)\xi}d\xi^2 + (r_0 + \xi)^2d\Omega^2. \quad (2.4.21)$$

Note that we implicitly assumed that  $f'(r_0) \neq 0$ , and have changed coordinates to  $r = r_0 + \xi$ . We like to approximate the metric near  $\theta = \phi = 0$ , therefore we introduce the coordinates  $x$  and  $y$ . They are given by  $x = r \sin(\theta) \cos(\phi)$  and  $y = r \sin(\theta) \sin(\phi)$ . We may now write  $r^2d\Omega^2 \approx dx^2 + dy^2$ . Note that this approximation is only valid for  $\xi$ ,  $x$ , and  $y$  small. Our next step is to make sure that all our spatial variables actually measure proper distance. For this we switch to the coordinate  $z = \int_0^\xi ds = 2\sqrt{\frac{\xi}{f'(r_0)}}$ . Expressing the metric in terms of  $t, z, x$ , and  $y$  we obtain

$$ds^2 = -(f'(r_0))^2 \frac{z^2}{4} dt^2 + dx^2 + dy^2 + dz^2. \quad (2.4.22)$$

If we now compare this with equation (2.4.15) we see that the metric is approximated by the Rindler metric. Note that the acceleration at the point  $r$  is given by  $1/z(r) = \sqrt{f'(r_0)/(r - r_0)}/2$ . We apply this to the Schwarzschild metric with  $f(r) = 1 - 2M/r$ . Note that  $r_0 = 2M$ , and  $f'(r_0) = 1/2M$ . Therefore we find that in order to stay at fixed  $r$  near the horizon, you have to undergo an acceleration of magnitude  $1/\sqrt{8M(r - 2M)}$ . In the argument above we assumed  $f'(r_0) \neq 0$ , now suppose we find ourselves in the case

$f'(r_0) = 0 \neq f''(r_0)$ . This corresponds to an extremal Reissner-Nordström black hole. This can be seen from the following. For a Reissner-Nordström black hole  $f$  is given by

$$f(r) = 1 - \frac{2M}{r} + \frac{Q^2}{r^2} \quad (2.4.23)$$

$$= \frac{r^2 - 2Mr + Q^2}{r^2} \quad (2.4.24)$$

$$= \frac{(r - r_-)(r - r_+)}{r^2}. \quad (2.4.25)$$

As a result we find that  $f'(r_-) = (r_- - r_+)/r_-^2$  and  $f'(r_+) = (r_+ - r_-)/r_+^2$ . Hence for the extremal case, with  $r_+ = r_-$  the first derivative is zero. Therefore we need to take into account the second derivative, which is given by  $f''(r_+) = 2/r_+^2$  for an extremal Reissner-Nordström black hole.

Having seen where these geometries can arise, we now move on to further investigate this metric. Using  $f(r) \approx f''(r_0)\xi^2$ , with  $\xi = r - r_0$  we find

$$ds^2 = -\frac{1}{2}f''(r_0)\xi^2 dt^2 + \frac{2}{f''(r_0)\xi^2} d\xi^2 + (r_0 + \xi)^2 d\Omega^2. \quad (2.4.26)$$

Now instead of approximating  $(r_0 + \xi)^2 d\Omega^2$  by  $dx^2 + dy^2$ , we just use  $(r_0 + \xi)^2 d\Omega^2 \approx r_0^2 d\Omega^2$ . Therefore we end up with

$$ds^2 = -\frac{1}{2}f''(r_0)\xi^2 dt^2 + \frac{2}{f''(r_0)\xi^2} d\xi^2 + r_0^2 d\Omega^2. \quad (2.4.27)$$

The last part of the metric, which corresponds to the angular coordinates, describes  $S^2$ . The first part is recognized as the  $AdS_2$  metric in terms of Poincaré coordinates. As a result we find that the near-horizon geometry of an extremal Reissner-Nordström black hole is described by the direct product of  $S^2$  and  $AdS_2$ . Since we know the precise form of the function  $f$  we can easily compute the corresponding radii. The radius of  $S^2$  is simply given by  $r_+ = M$ . To find the radius  $a$  of  $AdS_2$  we use that the  $AdS_2$  metric is also given by

$$ds^2 = -\frac{\xi^2}{a^2} dt^2 + \frac{a^2}{\xi^2} d\xi^2, \quad (2.4.28)$$

hence we find  $a = r_+ = M$ . In this section we introduced Rindler space, and have shown how one can obtain the coordinate system corresponding to a non inertial observer. Furthermore we have discussed the Rindler horizon, which clearly shows that an horizon is always defined with respect to an observer, or coordinate system. We finished our discussion by showing how Rindler space can be used to study the spacetime of a black hole near the event horizon.

## 2.5 Black Branes in AdS

Black brane solutions are an extension of black hole solutions. They are interesting if one wants to study string theory, but via the AdS/CFT correspondence[15] they can also tell us something about strongly correlated condensed matter systems. Just as black holes, the black branes can be thermal and have a horizon[16].

The idea of how to construct a black brane is to replace the spherical  $\mathbb{S}^2$  part in the metric by  $\mathbb{R}^2$ . We will focus on Schwarzschild and Reissner-Nordström black branes in AdS, using the method described in [17]. Of course it is not obvious that such a replacement results in a solution of the Einstein equations and describes a physical object, an object in the universe that could be created by imploding matter. Evidence suggests (see Section 3.5) that naked singularities cannot be created from imploding matter. There will always be one or more horizons. For example if we try to solve the Einstein equations for a Schwarzschild Minkowski black brane, we find a metric that has a physical singularity at  $r = 0$  but no horizon. The cosmic censorship conjecture tells us it cannot exist. However in AdS there are black branes with horizons. The motivation for looking at black branes is that they have a planar horizon which can be linked to certain strongly coupled quantum field theories. Here the topology of the horizon becomes important. The Schwarzschild black hole has a spherical horizon whereas the compactification of the planar horizon is a torus.

In the following subsections we will discuss some properties of different kinds of black branes.

### 2.5.1 Schwarzschild Black Branes in Minkowski Spacetime

The metric we will be working with in this section has the general form

$$ds^2 = -A(r)dt^2 + \frac{1}{A(r)}dr^2 + r^2(dx^2 + dy^2). \quad (2.5.1)$$

This follows from assuming that the solution has planar symmetry. Following exactly the same reasoning as in the next section on Birkhoff's theorem we can derive that the solution is static and of the above form, and solves Einstein's equations in vacuum with zero cosmological constant. The appearance of the term  $r^2(dx^2 + dy^2)$  tells us that we are looking for a translational symmetric planar solution (*i.e.* a brane).  $\Lambda = 0$  means the background is Minkowski space and  $T_{\mu\nu} = 0$  means there is no electromagnetic field or any other kind of energy. Together with the absence of other fields in the action and the assumed form of

the metric this makes the solution analogous to the conventional Schwarzschild black hole. By varying the Einstein-Hilbert action and plugging in the assumed metric we get

$$R_{tt} - \frac{1}{2}g_{tt}R = -A \left( \frac{\dot{A}}{r} + \frac{A}{r^2} \right) = 0 , \quad (2.5.2)$$

$$R_{rr} - \frac{1}{2}g_{rr}R = \frac{1}{A} \left( \frac{\dot{A}}{r} + \frac{A}{r^2} \right) = 0 , \quad (2.5.3)$$

$$R_{xx} - \frac{1}{2}g_{xx}R = R_{yy} - \frac{1}{2}g_{yy}R = r^2 \left( \frac{\ddot{A}}{2} + \frac{\dot{A}}{r} \right) = 0 . \quad (2.5.4)$$

From the first two equations we see that  $A + r\dot{A} = 0$  and differentiating this gives a solution to the third equation. Therefore the solution reads

$$A(r) = \frac{b}{r}.$$

The metric then reads

$$ds^2 = -\frac{b}{r}dt^2 + \frac{r}{b}dr^2 + r^2(dx^2 + dy^2) . \quad (2.5.5)$$

This metric has no horizon but a naked singularity at  $r = 0$ . When we add a negative cosmological constant the solution will have a horizon and will be asymptotically Anti-de Sitter. This is explored in the next subsection.

## 2.5.2 Schwarzschild Black Branes in AdS

To find the solution of Einstein's equations in vacuum with negative cosmological constant we again assume the general form of equation (2.5.1). Plugging this into the Einstein equations gives the following differential equations:

$$R_{tt} - \frac{1}{2}g_{tt}R + \frac{1}{2}g_{tt}\Lambda = -A \left( \frac{\dot{A}}{r} + \frac{A}{r^2} + \frac{1}{2}\Lambda \right) = 0 \quad (2.5.6)$$

$$R_{rr} - \frac{1}{2}g_{rr}R + \frac{1}{2}g_{rr}\Lambda = -\frac{1}{A} \left( \frac{\dot{A}}{r} + \frac{A}{r^2} + \frac{1}{2}\Lambda \right) = 0 \quad (2.5.7)$$

$$R_{xx} - \frac{1}{2}g_{xx}R + \frac{1}{2}g_{xx}\Lambda = r^2 \left( \frac{\ddot{A}}{2} + \frac{\dot{A}}{r} + \frac{1}{2}\Lambda \right) = 0 . \quad (2.5.8)$$

Multiplying equation (2.5.7) by  $r^2$  and differentiating, results in equation (2.5.8) which is therefore not independent. The homogeneous solution of equation (2.5.7) is  $A_{hom}(r) = \frac{b}{r}$

with  $b$  a constant and a particular solution of the inhomogeneous differential equation is  $A_{part}(r) = -\frac{\Lambda r^2}{6}$ . The full solution reads:

$$A(r) = \frac{b}{r} - \frac{\Lambda r^2}{6}.$$

In analogy with the conventional Schwarzschild solution, where we can take the Newtonian limit, we relate  $b$  to the mass by  $b = -2M$ . The Schwarzschild AdS black brane metric then takes the form:

$$ds^2 = - \left( \frac{-2M}{r} - \frac{\Lambda r^2}{6} \right) dt^2 + \frac{1}{\frac{-2M}{r} - \frac{\Lambda r^2}{6}} dr^2 + r^2(dx^2 + dy^2).$$

This metric has a physical singularity at  $r = 0$  and a horizon at  $2M + \frac{\Lambda r^3}{6} = 0$ . This last equation only has a positive solution for  $\Lambda < 0$ :

$$r_h = \left( \frac{-12M}{\Lambda} \right)^{\frac{1}{3}}.$$

If we take the limit  $M \rightarrow 0$ , absorb the cosmological constant in the coordinates, and make a substitution  $r \rightarrow -1/r$  we get AdS space in planar coordinates:

$$ds^2 = \frac{1}{r^2} [-dt^2 + dr^2 + dx^2 + dy^2] .$$

In de Sitter space, with  $\Lambda > 0$ , there is again no horizon and thus a naked singularity. Evidence suggests that we live in a universe with a very small positive  $\Lambda$ , therefore this black brane can not be created if the cosmic censorship conjecture holds. However, motivated by the AdS/CFT correspondence, it is still very interesting to study solutions with negative cosmological constant. The horizon of a black brane is an infinite plane. This translates via the AdS/CFT correspondence into a quantum field theory propagating on a Minkowski background. It is beyond the scope of this book to get into the details of this statement, but it is the main motivation for studying black branes.

For massless particles we have  $ds^2 = 0$ . For this specific metric this means

$$\frac{-2M}{r} - \frac{\Lambda r^2}{6} = \frac{1}{\frac{-2M}{r} - \frac{\Lambda r^2}{6}} \dot{r}^2 + r^2 (\dot{x}^2 + \dot{y}^2) ,$$

with  $\dot{r}$  differentiation with respect to  $t$ . At constant  $r$  we have

$$\dot{x}^2 + \dot{y}^2 = \frac{-2M}{r^3} - \frac{\Lambda}{6} .$$

From this we conclude that light rays can move in the  $xy$ -plane provided that  $r > r_h$ . Inside the black brane light rays will inevitably fall in the singularity.

Let us now look at the geodesic equations of this space. The variational approach is the easiest way to do this. We have to minimize the path length

$$l = \int ds = \int \sqrt{-g_{\mu\nu}\dot{x}^\mu\dot{x}^\nu} d\tau = \int L d\tau ,$$

where the dot now means differentiation with respect to proper time. The equations of motion of the Lagrangian  $L$  determine the geodesic equations:

$$L = \left[ -A(r)\dot{t}^2 + \frac{1}{A(r)}\dot{r}^2 + r^2(\dot{x}^2 + \dot{y}^2) \right]^{1/2} .$$

Together with the definition of proper time,  $g_{\mu\nu}\dot{x}^\mu\dot{x}^\nu = -1$ , the Euler-Langrange equations for  $t$ ,  $x$ , and  $y$  give the following conserved quantities:

$$A\dot{t} = E \quad r^2\dot{x} = L_x \quad r^2\dot{y} = L_y .$$

The geodesic equation for  $r$  reads

$$\ddot{r} - \frac{A'}{2A}\dot{r}^2 + \frac{A'A}{2}\dot{t}^2 - Ar(\dot{x}^2 + \dot{y}^2) = 0$$

where the prime means differentiation with respect to  $r$ . Instead of solving the latter equation we can use the definition of proper time, to write

$$-1 = -\left(\frac{-2M}{r} - \frac{\Lambda r^2}{6}\right)\dot{t}^2 + \frac{1}{\frac{-2M}{r} - \frac{\Lambda r^2}{6}}\dot{r}^2 + r^2(\dot{x}^2 + \dot{y}^2) .$$

In terms of the conserved quantities this becomes

$$\dot{r}^2 - \frac{2ML^2}{r^3} - \frac{2M}{r} - \frac{\Lambda r^2}{6} \equiv \dot{r}^2 + V(r) = E^2 + \frac{L^2\Lambda}{6} .$$

The form of the effective potential  $V(r)$  is independent of its parameters and is plotted in figure 2.23. We see that, unlike in the conventional Schwarzschild black hole, there is no stationary point and the potential blows up near infinity. This last property is characteristic for all asymptotic AdS spaces. A particle will always fall into the black brane despite its initial conditions. The Penrose diagram for a Schwarzschild black brane in AdS is the same as for a black hole in AdS. By making the substitution  $r \rightarrow 1/w$  we see that the metric is conformally related to

$$ds^2 = -\left(\frac{-\Lambda}{6} - 2Mw^3\right)dt^2 + \frac{1}{\frac{-\Lambda}{6} - 2Mw^3}dw^2 + dx^2 + dy^2 .$$

This metric is regular at  $w = 0$  so after compactification we get the Penrose diagram shown in figure 2.10 again.

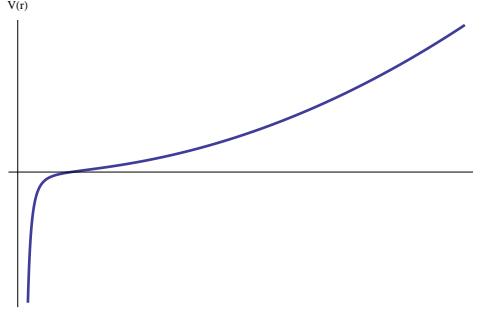


Figure 2.23: Effective radial potential of the Schwarzschild black brane

### 2.5.3 Reissner-Nordström Black Branes in AdS

The black brane found above can also carry an electric charge. Then we have to solve the Einstein equations with a non-zero energy momentum tensor. The energy momentum tensor reads

$$T_{\mu\nu} = F_{\mu\alpha}F_{\nu\beta}g^{\alpha\beta} - \frac{1}{4}g_{\mu\nu}F^2. \quad (2.5.9)$$

There is no magnetic field, so  $A_0 \neq 0$  and  $A_i = 0$  for  $i = 1, 2, 3$ . Furthermore, because of the supposed form of the metric in equation (2.5.1),  $A_0$  should be translation invariant in the  $x$  and  $y$  direction. The black brane is also assumed static so  $A_0$  is only dependent on  $r$ . Plugging this information in the above equation gives the nonzero components of the energy-momentum tensor:

$$T_{00} = \frac{1}{2}A(r)F_{01}^2, \quad T_{11} = -\frac{1}{2A(r)}F_{01}^2, \quad T_{22} = T_{33} = \frac{r^2}{2}F_{01}^2.$$

The Einstein-Hilbert action now includes the electric field:

$$S = \int dx^4 \sqrt{-g} \left[ -\frac{1}{4}F^2 + (R - \Lambda) \right]. \quad (2.5.10)$$

The Einstein equations then give the following differential equations:

$$R_{00} - \frac{1}{2}g_{00}R + \frac{1}{2}g_{00}\Lambda = -A \left( \frac{\dot{A}}{r} + \frac{A}{r^2} + \frac{\Lambda}{2} \right) = \frac{1}{2}A(r)F_{01}^2, \quad (2.5.11)$$

$$R_{11} - \frac{1}{2}g_{11}R + \frac{1}{2}g_{11}\Lambda = \frac{1}{A} \left( \frac{\ddot{A}}{r} + \frac{\dot{A}}{r^2} + \frac{\Lambda}{2} \right) = -\frac{1}{2A(r)}F_{01}^2, \quad (2.5.12)$$

$$R_{22} - \frac{1}{2}g_{22}R + \frac{1}{2}g_{22}\Lambda = r^2 \left( \frac{\ddot{A}}{2} + \frac{\dot{A}}{r} + \frac{\Lambda}{2} \right) = \frac{r^2}{2}F_{01}^2. \quad (2.5.13)$$

Subtracting equation (2.5.11) from equation (2.5.13) gives

$$\frac{\ddot{A}}{2} + \frac{2\dot{A}}{r} + \frac{A}{r^2} + \Lambda = 0 . \quad (2.5.14)$$

Putting in the ansatz

$$\frac{a}{r^2} + \frac{b}{r} + c + dr + er^2 ,$$

we find the conditions

$$c = 0, \quad d = 0, \quad e = -\frac{\Lambda}{6} ,$$

and the solution reads

$$A(r) = \frac{a}{r^2} + \frac{b}{r} - \frac{\Lambda r^2}{6} . \quad (2.5.15)$$

It is readily checked that the Maxwell equations are also satisfied. In analogy with the conventional Reissner-Nordström black hole we relate  $b$  to the mass by  $b = -2M$  and  $a$  to the charge by  $a = Q^2$ . The metric then reads

$$ds^2 = - \left( \frac{-2M}{r} + \frac{Q^2}{r^2} - \frac{\Lambda r^2}{6} \right) dt^2 + \frac{1}{\frac{-2M}{r} + \frac{Q^2}{r^2} - \frac{\Lambda r^2}{6}} dr^2 + r^2 (dx^2 + dy^2) . \quad (2.5.16)$$

This metric has a physical singularity at  $r = 0$  and a horizon at

$$\frac{\Lambda}{6Q^2} r^4 + \frac{2M}{Q^2} r - 1 = 0 . \quad (2.5.17)$$

Because  $\Lambda < 0$  and  $M > 0$  we see that there is exactly one solution if the derivative of the above equation is zero:

$$\frac{4\Lambda}{6Q^2} r^3 + \frac{2M}{Q^2} = 0 . \quad (2.5.18)$$

This case is called an extremal black hole. Plugging this solution into equation (2.5.17) gives the following relation between  $\frac{\Lambda}{Q^2}$  and  $\frac{M}{Q^2}$ :

$$\frac{2M}{Q^2} = 4 \left[ \left( \frac{-\Lambda}{6Q^2} \right)^{1/3} + 4 \left( \frac{6Q^2}{-\Lambda} \right)^{1/3} \right]^{-3/4} .$$

We then obtain the following result for the horizons of the Reissner-Nordström black brane:

$\frac{2M}{Q^2} < 4 \left[ \left( \frac{-\Lambda}{6Q^2} \right)^{1/3} + 4 \left( \frac{6Q^2}{-\Lambda} \right)^{1/3} \right]^{-3/4}$	no horizon
$\frac{2M}{Q^2} = 4 \left[ \left( \frac{-\Lambda}{6Q^2} \right)^{1/3} + 4 \left( \frac{6Q^2}{-\Lambda} \right)^{1/3} \right]^{-3/4}$	one horizon at $r_h = \left( -\frac{3M}{\Lambda} \right)^{1/3}$
$\frac{2M}{Q^2} > 4 \left[ \left( \frac{-\Lambda}{6Q^2} \right)^{1/3} + 4 \left( \frac{6Q^2}{-\Lambda} \right)^{1/3} \right]^{-3/4}$	two horizons at both sides of $r_h$

Under suitable conditions (if the charge is not too big) there can exist two horizons just like in the conventional Reissner-Nordström black hole, but now the horizons are planar instead of spherical.

### 2.5.4 Hyperbolic Black Holes in AdS

Apart from spherical symmetry (black hole) and planar symmetry (black brane) there can be hyperbolic symmetry. As opposed to Minkowski space it is possible to construct a so called hyperbolic black hole in AdS [18]. We will show that it is related to Rindler space. The following metric is a solution to Einstein's equations

$$ds^2 = - \left( -1 - \frac{2M}{r} - \frac{\Lambda r^2}{6} \right) dt^2 + \frac{dr^2}{-1 - \frac{2M}{r} - \frac{\Lambda r^2}{6}} + r^2 dH_2^2 , \quad (2.5.19)$$

where  $dH_2^2 = \frac{dx^2 + dy^2}{y^2}$  is the unit metric on the 2-dimensional hyperbolic space. We now show that for  $M = 0$  this metric is isometric to  $AdS_4$  but does not cover the whole manifold. This can already be seen from the above equation; for  $M = 0$  there is a horizon at  $r = \sqrt{\frac{6}{-\Lambda}}$  analogous to the Rindler horizon in equation (2.4.14). Therefore the coordinate patch is only valid for  $r \geq \sqrt{\frac{6}{-\Lambda}}$ .

Starting from

$$ds^2 = \frac{1}{r^2} (-dt^2 + dr^2 + dx^2 + dy^2) ,$$

and making the transformation  $r \rightarrow 1/r$  while extracting a factor  $-\Lambda/6$  we get AdS in Poincaré coordinates:

$$ds^2 = -\frac{\Lambda r^2}{6} (-dt^2 + dx^2 + dy^2) - \frac{6}{\Lambda r^2} dr^2 .$$

In light-cone coordinates  $u = t - y$ ,  $v = t + y$  this looks like

$$ds^2 = -\frac{\Lambda r^2}{6} (-dudv + dx^2) - \frac{6}{\Lambda r^2} dr^2 .$$

Now make the changes

$$r = \sqrt{-6/\Lambda} \tilde{r}/y , \quad u = -y \sqrt{1 + \frac{6}{\Lambda \tilde{r}^2}} e^{-t\sqrt{-\Lambda/6}} , \quad v = y \sqrt{1 + \frac{6}{\Lambda \tilde{r}^2}} e^{t\sqrt{-\Lambda/6}} ,$$

with  $\tilde{r} \geq \sqrt{\frac{6}{-\Lambda}}$ . The metric reads

$$ds^2 = - \left( -1 - \frac{\Lambda \tilde{r}^2}{6} \right) dt^2 + \frac{d\tilde{r}^2}{-1 - \frac{\Lambda \tilde{r}^2}{6}} + \tilde{r}^2 \frac{dy^2 + dx^2}{y^2} ,$$

which is the same as equation (2.5.19) with  $M = 0$ . In AdS/CFT one is always interested in what happens on the boundary of some spacetime. In this case the boundary is at  $r, \tilde{r} \rightarrow \infty$ . The metric (2.5.19) becomes asymptotically AdS when approaching the boundary and the transformation between Poincaré coordinates and hyperbolic coordinates becomes

$$r = \sqrt{-6/\Lambda} \tilde{r}/y , \quad u = -ye^{-t\sqrt{-\Lambda/6}} , \quad v = ye^{t\sqrt{-\Lambda/6}} .$$

The induced metric on the boundary then transforms as

$$\begin{aligned} ds_{ind}^2 &= \frac{-\Lambda r^2}{6}(-dudv + dx^2) \rightarrow \frac{-\Lambda \tilde{r}^2}{6} \left( -dt^2 - \frac{\Lambda}{6} \frac{dy^2 + dx^2}{y^2} \right) \\ &= \frac{\Lambda r^2}{6} \left( -y^2 \frac{-\Lambda}{6} dt^2 + dy^2 + dx^2 \right) = \frac{-\Lambda r^2}{6} ds_R^2 , \end{aligned}$$

where  $ds_R^2$  is the Rindler metric. From this we see that the boundary of a hyperbolic black hole in AdS is related to Rindler space by a conformal factor equal to  $r^2/\tilde{r}^2 = \frac{-6}{\Lambda y^2}$ .

# Chapter 3

## Black hole formation

In the previous chapter we investigated the remarkable black hole solutions that apparently can exist according to the general theory of relativity. Before we put too much effort into finding and understanding all the new physics these black hole solutions might exhibit, we would like to know how likely, if possible at all, the existence of black holes in nature really is. Therefore in this chapter we will study the various aspects of black hole formation.

In the first chapter we will show that a relatively big class of solutions (i.e. all spherically symmetric vacuum solutions) to Einstein's equations is inevitably the Schwarzschild solution. Next, we will discuss the likeliness of some spherical distribution of matter (like a star) being unable to withstand its own gravitational pull. If this happens, the star will collapse and create a black hole, which means that it will form a singularity and a horizon as a consequence of its own gravitational field. Finally, we will more abstractly investigate the sort of spacetimes that contain singularities and horizons. In particular, we will discuss the relationship between the two. All of this is done to argue on theoretical grounds that black hole solutions like the ones we studied in the previous chapter (and will study much further in chapters to come) might indeed occur in nature.

### 3.1 Birkhoff's Theorem

In this section we will consider the statement that the Schwarzschild metric is the *unique* vacuum solution for a spherical symmetric manifold. This statement is called: *Birkhoff's theorem*, and the proof was published by Birkhoff in 1923. To rigorously prove this theorem we would need to show that a spherically symmetric spacetime can be foliated by two-

spheres – in other words, that (almost) every point lies on a unique sphere that is left invariant by the generators of spherical symmetry. This will be beyond the scope of our book and instead we will just give a short description of what we mean by *spherically symmetric*. Furthermore, we would have to show that the metric on such a spacetime can always, locally, be put in the form

$$ds^2 = A(a, b)da^2 + 2B(a, b)dadb + C(a, b)db^2 + r(a, b)^2d\Omega^2, \quad (3.1.1)$$

where  $(a, b)$  are coordinates transverse to the 2-spheres used for the foliation, and  $r$  is a function of these coordinates. We will just assume that we can use this general metric. Places where these points are explicitly treated are Carroll [1], and more rigorously, Hawking and Ellis [4]. After deriving – or in our case assuming – (3.1.1), we have to plug this metric into Einstein’s equation in vacuum. This we will do in detail. First we do this for cosmological constant  $\Lambda = 0$ , from which we obtain the Schwarzschild metric as the unique and static solution. After this we will generalise to  $\Lambda > 0$  and  $\Lambda < 0$ , and we obtain respectively Schwarzschild-de Sitter and Schwarzschild-Anti-de Sitter metrics. It will turn out that for de Sitter there will be no Birkhoff’s theorem and for Anti-de Sitter there is.

We begin with describing what we mean by spherical symmetry. Suppose we have a four-dimensional spherically symmetric manifold  $M$ . Spherically symmetric means having the same symmetries as a two-sphere,  $S^2$ . These symmetries are the same as the rotations in three-dimensional Euclidean space, the special orthogonal group  $SO(3)$ . If we have a metric which is defined on the manifold, then symmetries are characterised by the existence of Killing vectors. The three Killing vectors of  $S^2$  in  $(\theta, \phi)$  coordinates are

$$\begin{aligned} R &= \partial_\phi, \\ S &= \cos\phi\partial_\theta - \cot\theta\sin\phi\partial_\phi, \\ T &= -\sin\phi\partial_\theta - \cot\theta\cos\phi\partial_\phi. \end{aligned} \quad (3.1.2)$$

How these Killing vectors can be found is for example shown by [1]. The main point now is that a manifold can be described as spherically symmetric manifold if it has the same three Killing vector fields as those on  $S^2$ . The challenge is to know when a set of Killing vectors on one manifold is the same as that on some other manifold in a coordinate-independent way. For this we can use commutation relations, because the structure of a set of symmetry transformations is given by the commutation relations of the transformations. The commutation relations give the difference in performing two infinitesimal transformations if their order is reversed. The commutation relations are expressed by the Lie algebra of the symmetry generators, while in differential geometry they are expressed by the commutators of the Killing vector fields. It can be shown that the commutators or the rotational

Killing vectors  $(R, S, T)$  satisfy

$$\begin{aligned} [R, S] &= T, \\ [S, T] &= R, \\ [T, R] &= S. \end{aligned} \tag{3.1.3}$$

This algebra of Killing vectors fully characterizes the kind of symmetry we have. Before, we said that a manifold is spherically symmetric if it has the same symmetries as  $S^2$ . Now, we can be a little more precise: A manifold is spherical symmetric if and only if its metric has three Killing fields satisfying the above algebra.

The next step would be to show that the metric on a spherically symmetric manifold is of the form

$$ds^2 = A(a, b)da^2 + 2B(a, b)dadb + C(a, b)db^2 + r(a, b)^2d\Omega^2. \tag{3.1.4}$$

Here  $2dadb = dadb + dbda$  and  $r(a, b)$  is some arbitrary function which has not yet been interpreted and to which is merely given a suggestive label. By looking at this general metric we can already see that the coefficients should not depend on the coordinates  $(\theta, \phi)$ , since otherwise the spherical symmetry would not exist. Again a more rigorous treatment can be found in [1, 4].

Now, starting from metric (3.1.4), we can just change coordinates from  $(a, b)$  to  $(a, r)$  by inverting  $r(a, b)$ . The metric then becomes

$$ds^2 = A(a, r)da^2 + 2B(a, r)dadr + C(a, b)dr^2 + r^2d\Omega^2. \tag{3.1.5}$$

We would like to try to get rid of the remaining cross terms  $2dadr$  in the metric. Our next step is thus to find a function  $t(a, r)$  such that in the  $(t, r)$  coordinate system there are no cross terms anymore. If  $t = t(a, r)$  then

$$dt = \frac{\partial t}{\partial a}da + \frac{\partial t}{\partial r}dr,$$

and

$$dt^2 = \left(\frac{\partial t}{\partial a}\right)^2 da^2 + 2\left(\frac{\partial t}{\partial a}\right)\left(\frac{\partial t}{\partial r}\right)dadr + \left(\frac{\partial t}{\partial r}\right)^2 dr^2.$$

In terms of this general function  $t(a, r)$  the metric looks like

$$(ds')^2 = A'(t, r)dt^2 + 2B'(t, r)^2dtdr + C'(t, r)dr^2 + r^2d\Omega^2. \tag{3.1.6}$$

Because the line element is invariant under coordinate transformations, we know that  $ds^2 = (ds')^2$ . Using this and plugging in the expressions for  $ds^2$  and  $(ds')^2$ , we can now

write (3.1.6) in the old coordinates:

$$\begin{aligned} (\mathrm{d}s')^2 = \mathrm{d}s^2 &= A'(t, r) \left( \frac{\partial t}{\partial a} \right)^2 \mathrm{d}a^2 + 2 \left[ A'(t, r) \left( \frac{\partial t}{\partial a} \right) \left( \frac{\partial t}{\partial r} \right) + B'(t, r) \left( \frac{\partial t}{\partial a} \right) \right] \mathrm{d}a \mathrm{d}r \\ &\quad + \left[ A'(t, r) \left( \frac{\partial t}{\partial r} \right)^2 + 2B' \left( \frac{\partial t}{\partial r} \right) + C'(t, r) \right] \mathrm{d}r^2. \end{aligned} \quad (3.1.7)$$

If we now compare with metric (3.1.5), we see that:

$$\begin{aligned} A &= A' \left( \frac{\partial t}{\partial a} \right)^2, \\ B &= A' \left( \frac{\partial t}{\partial a} \right) \left( \frac{\partial t}{\partial r} \right) + B' \left( \frac{\partial t}{\partial a} \right), \\ C &= A' \left( \frac{\partial t}{\partial r} \right)^2 + 2B' \left( \frac{\partial t}{\partial r} \right) + C'. \end{aligned} \quad (3.1.8)$$

where the first coefficients are functions of  $(a, r)$  and the primed coefficients are functions of  $(t, r)$ . The reason we introduced the new coordinate  $t(a, r)$  was to get rid of the cross terms  $\mathrm{d}a \mathrm{d}r$ . By looking at (3.1.6) we see that this corresponds to putting  $B'(t, r) = 0$ . Our general conditions for the coordinate transformation now become

$$\begin{aligned} A &= A' \left( \frac{\partial t}{\partial a} \right)^2, \\ B &= A' \left( \frac{\partial t}{\partial a} \right) \left( \frac{\partial t}{\partial r} \right), \\ C &= A' \left( \frac{\partial t}{\partial r} \right)^2 + C'. \end{aligned} \quad (3.1.9)$$

With this choice we are now able to put metric (3.1.6) in the form

$$(\mathrm{d}s')^2 = A'(t, r) \mathrm{d}t^2 + C'(t, r) \mathrm{d}r^2 + r^2 \mathrm{d}\Omega^2. \quad (3.1.10)$$

Important to note is that the two coordinates  $t$  and  $r$  are still undetermined. The only difference is that  $r$  is the function that is in front of the angular part in the metric. The reason for doing this was that the metric for flat Minkowski space in spherical coordinates can be written as  $\mathrm{d}s^2 = -\mathrm{d}t^2 + \mathrm{d}r^2 + r^2 \mathrm{d}\Omega^2$ , and because Minkowski space is itself spherically symmetric, it will therefore be described by (3.1.10). Another point we would like to mention is that the spacetime under consideration is Lorentzian, so either  $A'$  or  $C'$  will have to be negative. Again motivated by the form of Minkowski space in spherical coordinates, let us choose the coefficient  $A'$  in front of  $\mathrm{d}t^2$  to be negative. This choice is not completely

trivial, but we will assume it for now. For more on this see [4]. With this choice we can write  $A'$  and  $C'$  as exponentials of some new functions  $\alpha$  and  $\beta$ , so that the spherical symmetric metric becomes

$$ds^2 = -e^{2\alpha(t,r)}dt^2 + e^{2\beta(t,r)}dr^2 + r^2d\Omega^2. \quad (3.1.11)$$

We can not go further using only geometry and transformations. The functions  $\alpha(t, r)$  and  $\beta(t, r)$  can not be further specified by using spherical symmetry. To give a more specific form, we have to actually solve Einstein's equation in vacuum, so this will be our next step.

In solving the Einstein's equation we follow the usual scheme. We compute the nonvanishing Christoffel symbols and from them the nonvanishing components of the Riemann tensor. Then we calculate the components of the Ricci tensor and ultimately the Ricci scalar. I will just state the resulting non-zero components of the Ricci tensor, which can then be used to specify the form of the functions  $\alpha$  and  $\beta$ .

$$\begin{aligned} R_{tt} &= (\partial_t^2\beta + (\partial_t\beta)^2 - \partial_t\alpha\partial_t\beta) + e^{2(\beta-\alpha)} \left( \partial_r^2\alpha + (\partial_r\alpha)^2 - \partial_r\alpha\partial_r\beta + \frac{2}{r}\partial_r\alpha \right), \\ R_{rr} &= - \left( \partial_r^2\alpha + (\partial_r\alpha)^2 - \partial_r\alpha\partial_r\beta - \frac{2}{r}\partial_r\beta \right) + e^{2(\beta-\alpha)} (\partial_t^2\beta + (\partial_t\beta)^2 - \partial_t\alpha\partial_t\beta), \\ R_{tr} &= \frac{2}{r}\partial_t\beta, \\ R_{\theta\theta} &= e^{-2\beta}[r(\partial_r\beta - \partial_r\alpha) - 1] + 1, \\ R_{\phi\phi} &= R_{\theta\theta}\sin^2\theta. \end{aligned} \quad (3.1.12)$$

Then, we have to solve Einstein's equation in vacuum,  $R_{\mu\nu} = 0$ . From  $R_{tr} = 0$  we get

$$\partial_t\beta = 0. \quad (3.1.13)$$

Now, if we take the time derivative of  $R_{\theta\theta}$  and use  $\partial_t\beta = 0$ , we find

$$\partial_t\partial_r\alpha = 0. \quad (3.1.14)$$

We can therefore write

$$\begin{aligned} \beta &= \beta(r), \\ \alpha &= f(r) + g(t). \end{aligned} \quad (3.1.15)$$

The first term in the metric (3.1.11) is thus  $-e^{2f(r)}e^{2g(t)}dt^2$ . But we can always redefine our time coordinate such that  $dt \rightarrow e^{-g(t)}dt$ . This means that we can always choose  $t$  in such a manner that  $g(t) = 0$ , whence  $\alpha(t, r) = f(r)$ . So, we obtain

$$ds^2 = -e^{2\alpha(r)}dt^2 + e^{2\beta(r)}dr^2 + r^2d\Omega^2. \quad (3.1.16)$$

We see now that all of the metric coefficients are independent of  $t$ . This is very important, since we have shown now that any spherically symmetric metric in vacuum possesses a timelike Killing vector. A metric that has a Killing vector that is timelike near infinity is called *stationary*. A metric that is *also* invariant under  $t \rightarrow -t$  is called *static*. You could think of stationary as ‘doing exactly the same thing at every time’, while static means ‘not doing anything at all’. For example, the static spherically symmetric (3.1.16) will describe non-rotating stars or black holes, while rotating systems that keep rotating in the same way at all times will be described by metrics that are stationary but not static.”

By looking at the components of the Ricci tensor again, we see that since  $R_{tt} = R_{rr} = 0$  and because  $\partial_t\alpha = \partial_t\beta = 0$ , we have

$$0 = e^{2(\beta-\alpha)}R_{tt} + R_{rr} = \frac{2}{r}(\partial_r\alpha + \partial_r\beta). \quad (3.1.17)$$

We already know that  $\alpha = \alpha(r)$  and  $\beta = \beta(r)$ . Combining this with (3.1.17) we can now conclude that  $\alpha = -\beta + c$ , with some constant  $c$ . Like before, when we rescaled the  $g(t)$  away, we can similarly rescale the time coordinate  $t \rightarrow e^{-c}t$ , so that we effectively put  $c$  to zero. So, now we have

$$\alpha = -\beta. \quad (3.1.18)$$

If we now put this in  $R_{\theta\theta} = 0$ , we get

$$e^{2\alpha}(2r\partial_r\alpha + 1) = 1, \quad (3.1.19)$$

which is the same as

$$\partial_r(re^{2\alpha}) = 1. \quad (3.1.20)$$

Integrating both sides with respect to  $r$ , then relabeling the integration constant  $c = -R$  and dividing both sides by  $r$  gives us:

$$e^{2\alpha(r)} = 1 - \frac{R}{r}. \quad (3.1.21)$$

Plugging this result and  $\alpha = -\beta$  into equation (3.1.16) gives us

$$ds^2 = -\left(1 - \frac{R}{r}\right)dt^2 + \left(1 - \frac{R}{r}\right)^{-1}dr^2 + r^2d\Omega^2. \quad (3.1.22)$$

We now have no freedom left except for the constant  $R$ . We interpret this  $R$  as the Schwarzschild radius and we would like to express it in terms of some physical parameter. Our metric should reduce to the situation with a weak field when  $r \gg 2GM$ . From [1] can be found that in such a weak field limit we have

$$g_{tt} = -\left(1 - \frac{2GM}{r}\right), \quad (3.1.23)$$

where  $G$  is Newton's constant and  $M$  is a parameter, which we will interpret as the mass of the object. Because the coefficients should be the same in the weak field limit, we can now identify  $R = 2GM$ . Remember that in the last chapter we put  $G = 1$ , so we get  $R = 2M$ . Plugging  $R = 2M$  into equation (3.1.22), gives us finally the Schwarzschild metric:

$$ds^2 = - \left(1 - \frac{2M}{r}\right) dt^2 + \left(1 - \frac{2M}{r}\right)^{-1} dr^2 + r^2 d\Omega^2. \quad (3.1.24)$$

Before we form a conclusion, we might check whether the answer (3.1.21) makes sense. We can do this by putting (3.1.21) in  $R_{tt}$  or  $R_{rr}$ , because we used the linear combination (3.1.17) (and all other components) and so we have one component left over from the linear combination. Let's choose  $R_{rr}$ , which then has to be equal to 0 if we plug in (3.1.21). We first put  $\partial_t \beta$  and  $\alpha = -\beta$  already in  $R_{rr}$  and obtain

$$R_{rr} = - \left[ \partial_r^2 \alpha + 2(\partial_r \alpha)^2 + \frac{2}{r} \partial_r \alpha \right]. \quad (3.1.25)$$

From (3.1.21) we can then calculate

$$\partial_r^2 \alpha = \frac{1}{2} \left( \frac{1}{r^2} - \frac{1}{(r - R_S)^2} \right). \quad (3.1.26)$$

So that we then indeed obtain that  $R_{rr} = 0$ .

From (3.1.24) we can now form a conclusion. We found the unique, static, spherically symmetric vacuum solution to Einstein's equation. At this moment, you might wonder why the solution we found should be unique. We will give a physical argument for this. We arrived at (3.1.16) by only using spherical symmetry and some coordinate transformations. Because of general covariance, these different possible coordinates in which we can write down the solution, do not make physical difference. After this, we just plugged in (3.1.16) in the Einstein equations and we arrived at the solution (3.1.22) in which we only had the freedom to choose a constant. So, we derived the unique solution up to a constant. To make sure we arrived at the right result in the weak field limit, we had to fix the constant to  $R = 2GM$ . So, this is physically why we can consider the Schwarzschild metric as the *unique* solution. Important to say is that we derived this result only from the condition that the gravitational source exists in a spherically symmetric vacuum. In particular the solution of the spherically symmetric gravitational source is static, but the source itself doesn't have to be static at all. An important example for us is the case of a collapsing star; its exterior will still be described by the Schwarzschild metric! We will talk about gravitational collapse in more detail in section 3.3. Note that in the Schwarzschild metric, the parameter  $M$  can be interpreted as the Newtonian mass. However, it will not just be the sum of the different components that are curving spacetime, because the

gravitational binding energy also contributes to this curvature. Only in the weak field limit the quantities  $M_{Newton}$  and  $M_{GR}$  will be the same. Note also that, if we take  $M \rightarrow 0$ , we recover Minkowski space. And furthermore, if we take  $r \rightarrow \infty$ , the metric becomes more and more like Minkowski, this last property is known as ‘asymptotic flatness’.

We found the unique solution for a spherically symmetric manifold in *vacuum*. We will now attempt to generalize Birkhoff’s theorem to (Anti-)de Sitter spacetime by introducing a non-zero cosmological constant. If we look back we see that until (3.1.11) our derivation was very general and the metric (3.1.11) still holds in the case of adding a cosmological constant. What changes are Einstein’s equations in vacuum, which as we already saw – instead of  $R_{\mu\nu} = 0$  – now become

$$R_{\mu\nu} - \frac{1}{2}Rg_{\mu\nu} + \frac{1}{2}\Lambda g_{\mu\nu} = 0. \quad (3.1.27)$$

Contracting this equation with the metric, we obtain

$$R = 2\Lambda. \quad (3.1.28)$$

Substituting this result into (3.1.27) we get

$$R_{\mu\nu} = \Lambda \frac{1}{2}g_{\mu\nu}. \quad (3.1.29)$$

This is the generalized condition for the Ricci tensor for arbitrary values of  $\Lambda$ . Let’s start now again from  $R_{tr}$ :

$$R_{tr} = \frac{2}{r}\partial_t\beta = \frac{1}{2}\Lambda g_{tr} = 0. \quad (3.1.30)$$

Thus, we have  $\beta = \beta(r)$ , independent of the value of  $\Lambda$ . For  $R_{\theta\theta}$  we now have

$$R_{\theta\theta} = e^{-2\beta}[r(\partial_r\beta - \partial_r\alpha) - 1] + 1. \quad (3.1.31)$$

Taking the time-derivative of both sides, since  $\partial_t g_{\theta\theta} = 0$ , we get

$$e^{-2\beta}r\partial_t\partial_r\alpha = 0. \quad (3.1.32)$$

from which we get that

$$\alpha = f(r) + g(t). \quad (3.1.33)$$

And we can transform the  $g(t)$  away, by taking the transformation  $dt \rightarrow e^{-g(t)}dt$ . And thus, we obtain that  $\alpha = \alpha(r)$ . We have now (3.1.16), which we proved to be the same for  $\Lambda = 0$  and  $\Lambda \neq 0$ . Let’s look at the other components of the Ricci tensor. From the condition  $R_{\mu\nu} = \frac{1}{2}\Lambda g_{\mu\nu}$  we make a combination which vanishes once:

$$e^{-2\alpha}R_{tt} + e^{-2\beta}R_{rr} = \frac{1}{2}\Lambda(e^{-2\alpha}g_{tt} + e^{-2\beta}g_{rr}) = 0. \quad (3.1.34)$$

Equating this with the expressions for the Ricci tensor (3.1.12) and using  $\partial_t\alpha = \partial_t\beta = 0$ , we get:

$$0 = \frac{2}{r}(\partial_r\alpha + \partial_r\beta). \quad (3.1.35)$$

We already know that  $\alpha = \alpha(r)$  and  $\beta = \beta(r)$ . Combining this with (3.1.35) we can conclude that  $\alpha = -\beta + c$ , with some constant  $c$ . Now, we can transform the constant away by making the transformation  $dt \rightarrow e^{-c}dt$ , so that we once again have that

$$\alpha = -\beta, \quad (3.1.36)$$

independent of the value of  $\Lambda$ ! Incorporating this in  $R_{\theta\theta} = \Lambda g_{\theta\theta} = \Lambda r^2$ , we now obtain

$$\partial_r(re^{2\alpha}) = 1 - \Lambda r^2. \quad (3.1.37)$$

Integrating both sides with respect to  $r$ , naming the integration constant  $c = -R$  and dividing both sides by  $r$  we obtain:

$$e^{2\alpha} = 1 - \frac{R}{r} - \frac{\Lambda}{3}r^2. \quad (3.1.38)$$

Plugging this result and  $\alpha = -\beta$  into equation (3.1.16) and interpreting  $R = 2M$ , gives us

$$ds^2 = -\left(1 - \frac{2M}{r} - \frac{\Lambda}{3}r^2\right)dt^2 + \left(1 - \frac{2M}{r} - \frac{\Lambda}{3}r^2\right)^{-1}dr^2 + r^2d\Omega^2. \quad (3.1.39)$$

This is the Schwarzschild-de Sitter (Anti-de Sitter) solution if we introduce a  $\Lambda > 0$  ( $\Lambda < 0$ ).

To obtain Birkhoff's theorem we would have to find not only a unique solution, but also a *static*, unique solution. Let's see whether (3.1.39) gives us a static solution for both cases  $\Lambda > 0$  and  $\Lambda < 0$ . For a metric to be static, it has to have a timelike Killing vector. For such a Killing vector to exist, we first have to define what *time* is. The suggestion we will follow here is that time is the part of the metric for which there is an additional total minus sign. So, in (3.1.39) our time-coordinate would be  $t$  (as usual). We will see however, that something peculiar happens if  $\Lambda > 0$ . We can best see this if we let  $M \rightarrow 0$ , after which we obtain just the (Anti-)de Sitter metric:

$$ds^2 = -\left(1 - \frac{\Lambda}{3}r^2\right)dt^2 + \left(1 - \frac{\Lambda}{3}r^2\right)^{-1}dr^2 + r^2d\Omega^2. \quad (3.1.40)$$

For  $\Lambda > 0$  we see now that we have a cosmological horizon if  $r^2 = \frac{3}{\Lambda}$ . Important to see is that this horizon only exists for  $\Lambda > 0$  and thus not for  $\Lambda < 0$ . What does such a cosmological horizon mean? For  $r^2 > \frac{3}{\Lambda}$  in (3.1.40), we see that  $-g_{tt} \rightarrow g_{tt}$  and  $g_{rr} \rightarrow -g_{rr}$ . So, now we would define  $r$  to be our time-coordinate and not  $t$  anymore. This cosmological

horizon is not a real, intrinsic singularity, so it means that in order to cross the point  $r^2 = \frac{3}{\Lambda}$ , we would have to use a coordinate transformation. But that also means that in (3.1.40) no *global* time can be defined. And without a global time coordinate it is hard to see what a timelike Killing vector would mean. Thus, we can not find a static metric-solution to a spherically symmetric manifold with a cosmological constant  $\Lambda > 0$ , but we can find a static solution if the cosmological constant  $\Lambda < 0$ ! At this moment you might wonder that in the Schwarzschild metric there also appears to be a coordinate singularity at  $R = 2M$ , and thus in this case also no global time-coordinate can be defined. However, the Birkhoff's theorem only is about the exterior of the gravitational source, the massive object (star/black hole, etc). It does not say anything about the interior of that source, so the static solution is about the exterior. But in the case of the cosmological horizon of  $\Lambda > 0$ , there is a part in the exterior ( $r^2 > \frac{3}{\Lambda}$ ) in which the time-coordinate changes from  $t$  to  $r$ . In this case there's no global time defined, no time Killing vector, no static solution and thus no Birkhoff's theorem for the spherical symmetric stationary manifold with a cosmological constant  $\Lambda > 0$ . We can conclude now that from starting with a spherical manifold in vacuum we can find a unique and static metric for  $\Lambda = 0$  and  $\Lambda < 0$ , but we can not find a static solution for  $\Lambda > 0$  and thus in the latter case will be no Birkhoff's theorem. We only talked about the metric exterior of the gravitational source in this section; Birkhoff's theorem was valid independent of the dynamics of the gravitational source. In the next two sections we will talk about what happens in the interior of the gravitational source. In the next section we will talk about the conditions for a star to be in equilibrium or not. And in the section after that we will talk about gravitational collapse.

## 3.2 The Tolman-Oppenheimer-Volkoff Equation

The Tolman-Oppenheimer-Volkoff equation (TOV equation), named after the authors of the famous papers [19, 20, 21], governs the hydrostatic equilibrium of a perfect fluid in general relativity. Therefore it can be applied to stellar objects that are static and henceforth can predict certain limits on star mass and size.

For most of its lifetime, a star is in a static situation where protons in the core are fused to a bound state. The bound state has a lower energy than the two separated particles, so highly energetic photons are emitted. It is important to note that these photons generate an outward pressure: the radiation pressure. This outward pressure plays a large role in counteracting the inward gravitational force. That is why active stars have essentially no upper limit for the mass.

From astronomical observations it appears that there are several possibilities for the ‘end’ of the star. This is when the efficient fusion processes can no longer be maintained. We use the name ‘progenitor star’ for the original star, i.e. the star in its normal phase. What follows is a simplified categorization of stellar remnants. More info on stellar evolution can be found in e.g. [22].

- If the progenitor star is lighter than roughly 8 solar masses  $M_{\odot}$ , the star will collapse to a white dwarf: The star does not produce energy anymore and cools down slowly. The electron degeneracy at the core counteracts the gravitational force by means of the Pauli exclusion principle.
- If the white dwarf grows heavier than  $1.44 M_{\odot}$  (if the progenitor mass is larger than  $8 M_{\odot}$ , or if a white dwarf gathers mass from a neighbouring star), the inward gravitational force is larger than the force outwards resulting from the electron degeneracy. This means the static situation can no longer be maintained and as a consequence the electrons in the core fuse with the protons and become neutrons. This releases a catastrophic amount of gravitational potential energy so generally a large part of the star’s outer layers are blown away and a static neutron star is born. This explosion is called a supernova.

The mass limit of a white dwarf ( $1.44 M_{\odot}$ ) is called the Chandrasekhar limit, named after the physicist who derived it quantitatively[23].

- If the progenitor star was heavier than 15 to  $20 M_{\odot}$ , there is no stable solution for a neutron star since even the neutron degeneracy and strong nuclear interactions cannot cope with the gravitational force. No force in Nature can withstand the inward force so the neutron star collapses as well and a black hole is born. This can also happen if a neutron star gathers mass from a neighbouring star.

This limit corresponds to a mass of  $1.5 - 3.0 M_{\odot}$  for the neutron star and is called the TOV limit[21].

The Chandrasekhar and TOV limit can be calculated by using the TOV equation, which we derive in the next section.

### 3.2.1 Derivation of the Tolman-Oppenheimer-Volkoff Equation

Let us take a metric of the following form:

$$ds^2 = -e^{2\Phi} dt^2 + e^{2\lambda} dr^2 + r^2 d\Omega^2, \quad (3.2.1)$$

$$d\Omega^2 = d\theta^2 + \sin^2 \theta d\phi^2, \quad (3.2.2)$$

where  $\Phi$  and  $\lambda$  are functions of  $r$  only since we try to describe a static, spherically symmetric case. Additionally, we have left out any  $drdt$  product since that can be removed by a coordinate transformation, as shown in the previous section.

With this metric, we will use Einstein's equations to determine the equations for the structure of the star, so we can calculate the limits on the size and mass of the star. First we need some parameters to describe the star itself. We will use a perfect fluid to model the star's distribution of matter, since shear stresses, viscosity, or heat conduction are negligible on a hydrodynamic time scale because all fermion states are already occupied (full electron or neutron degeneracy). Therefore the star can be described in its rest frame by just two parameters: the mass density  $\rho(r)$  and isotropic pressure  $p(r)$ .

We define

$$u^\mu(r) = \frac{dx^\mu}{d\tau} \quad \text{The 4-velocity of the fluid,} \quad (3.2.3)$$

$$T^{\mu\nu}(r) = (\rho + p)u^\mu u^\nu + pg^{\mu\nu} \quad \text{The energy-momentum tensor.} \quad (3.2.4)$$

Because the star is static, the only nonzero component of  $u$  is  $u^t$ , whose value is determined by the fact that it is time-like:

$$-1 = g_{\mu\nu}u^\mu u^\nu = -e^{2\Phi}u^t u^t, \quad (3.2.5)$$

$$u^t = e^{-\Phi}. \quad (3.2.6)$$

This makes the energy momentum tensor (3.2.4) very simple:

$$T^t_t = -\rho, \quad (3.2.7)$$

$$T^r_r = T^\theta_\theta = T^\phi_\phi = p, \quad (3.2.8)$$

$$T^\mu_\nu = 0 \quad \text{otherwise.} \quad (3.2.9)$$

Now we can use Einstein's equation,  $R_{\mu\nu} - \frac{1}{2}Rg_{\mu\nu} + \frac{1}{2}\Lambda g_{\mu\nu} = 8\pi T_{\mu\nu}$ , to solve for the pressure and density function (please note that we deviate here from the definition of Einstein's equation used earlier by including the factor  $8\pi$ , since in this way the physical quantities will appear in a more natural way). We will ignore the cosmological constant  $\Lambda$  in this case because in our universe the presumed small and positive value of  $\Lambda$  will not have a notable influence on the hydrostatic equilibrium. However, as an academic exercise or as a useful result for AdS/CFT, solutions have been calculated for the TOV equation with nonzero cosmological constant[24].

Einstein's equations without cosmological constant give (prime denotes derivative with respect to  $r$ ):

$$-8\pi\rho = -e^{-2\lambda} \frac{-1 + e^{2\lambda} + 2r\lambda'}{r^2}, \quad (3.2.10)$$

$$8\pi p = \frac{-1 + e^{-2\lambda} (1 + 2r\Phi')}{r^2}, \quad (3.2.11)$$

$$8\pi p = e^{-2\lambda} \frac{-(\lambda' - \Phi') (1 + r\Phi') + r\Phi''}{r}. \quad (3.2.12)$$

Rewriting the  $(t, t)$  component of Einstein's field equations yields

$$G^t_t = r^{-2} \frac{d}{dr} (r(1 - e^{-2\lambda})) = 8\pi\rho. \quad (3.2.13)$$

This suggests that the quantity inside the brackets looks somewhat like an enclosed mass. Defining  $2m(r) \equiv r(1 - e^{-2\lambda})$ , this is confirmed for Newtonian physics:

$$m(r) = \int_0^r 4\pi r'^2 \rho(r') dr'. \quad (3.2.14)$$

However, we cannot use Newtonian physics if we are describing the inside of the star since we need to take the metric into account. It would be naive to just assume that  $m(r)$  is the enclosed mass, but we will try to provide some evidence that it really is the case. Only then we can relate this quantity to astronomical observations of stellar objects, and use its boundary conditions. To prove this, we first notice that the total energy of a star consists of the rest mass, the internal energy and the potential energy. We split up the energy density  $\rho$ ,

$$\rho = \mu_0 n + (\rho - \mu_0 n), \quad (3.2.15)$$

in which the first term is the total rest mass of  $n$  particles per unit volume with mass  $\mu_0$ , and the second term consists of the internal energy density. We will investigate what this means for the potential energy.

In general relativity, the proper volume of a spherical shell of thickness  $dr$  is

$$dV = 4\pi r^2 \sqrt{|g_{rr}|} dr = 4\pi r^2 (1 - 2m/r)^{-1/2} dr. \quad (3.2.16)$$

The total rest mass and the internal energy inside a sphere of radius  $r$  are then

$$m_0 = \int_0^r \mu_0 n dV = \int_0^r \mu_0 n 4\pi r'^2 (1 - 2m/r')^{-1/2} dr', \quad (3.2.17)$$

$$U = \int_0^r (\rho - \mu_0 n) dV = \int_0^r (\rho - \mu_0 n) 4\pi r'^2 (1 - 2m/r')^{-1/2} dr. \quad (3.2.18)$$

That means that if we subtract the two quantities from  $m$ , we should end up with the potential energy.

$$\begin{aligned} m(r) - (\text{energy calculated from GR}) \\ = \int_0^r 4\pi r^2 \rho (1 - (1 - 2m/r)^{-1/2}) dr \end{aligned} \quad (3.2.19)$$

$$\approx \int_0^r 4\pi r^2 (\rho m/r) dr. \quad (3.2.20)$$

The latter approximation is the Newtonian limit. It appears to be equal to the gravitational potential energy. This hints that we can take  $m(r)$  for the value of the total enclosed mass-energy in a sphere of radius  $r$ . We will use this interpretation in the next section, where we build a model of a star and derive some conclusions on limits on the star's mass and size.

We continue the derivation of the TOV equation by looking at the  $(r, r)$  component of the field equations:

$$G_r^r = r^{-2}(-1 + e^{-2\lambda} + 2re^{-2\lambda}\Phi') = 8\pi p. \quad (3.2.21)$$

This yields the equation for the gradient of  $\Phi$ , after using the freshly defined enclosed mass:

$$\frac{d\Phi}{dr} = \frac{m(r) + 4\pi r^3 p(r)}{r(r - 2m(r))}. \quad (3.2.22)$$

In the Newtonian limit,  $m/r = 1 - e^{-2\lambda} \ll 1$ , and ignoring the pressure contribution, this reduces to  $d\Phi/dr = m/r^2$  which is the classical gravitational force.

After combining the equation for  $p$ , the conservation of the energy-momentum tensor  $\nabla_\mu T^{\mu\nu} = 0$  (because of the Bianchi identity for the Einstein tensor) gives<sup>1</sup>:

$$-\frac{dp}{dr} = (\rho + p) \frac{d\Phi}{dr} \quad (3.2.23)$$

We can substitute the equation for  $\Phi$  into (3.2.23), yielding the famous TOV equation:

$$\frac{dp}{dr} = -\frac{(\rho + p)(m + 4\pi r^3 p)}{r(r - 2m)} \quad (3.2.24)$$

Let us cast this in a more suggestive form using  $dm(r) = 4\pi r^2 \rho(r) dr$ , to be able to read what this equation really tells.

$$\underbrace{4\pi r^2 dp(r)}_{\text{Force acting on the shell}} = -\underbrace{\frac{m(r)dm(r)}{r^2}}_{\text{Newtonian}} \left(1 + \frac{p(r)}{\rho(r)}\right) \left(1 + \frac{4\pi r^3 p(r)}{m(r)}\right) \left(1 - \frac{2m(r)}{r}\right)^{-1}. \quad (3.2.25)$$

---

<sup>1</sup>For a rigorous derivation, see for example [25].

The left hand side tells us what force is exerted by the pressure on a specific radius inside the star. If the star is in equilibrium, this outward pressure is counteracted with the gravitational force. This is the right hand side of the equation. We recognize the Newtonian gravitational attraction in the first term, and three correction terms due to relativistic effects. From the first and second correction terms it appears that not only mass but also pressure causes gravitational attraction.

The TOV equation has a larger numerator and a smaller denominator than the Newtonian equation so we expect higher pressure inside the star. Additionally the rise of the pressure is accelerated because of the pressure correction term in the numerator. This will ultimately imply that there are fundamental limits on masses for strongly gravitating objects. This is most easily seen from the fact that the star cannot be in equilibrium if  $2m(r) \geq r$  since the pressure gradient would blow up.

### 3.2.2 Physical Solutions of the Tolman-Oppenheimer-Volkoff Equation

Let us construct a stellar model with radius  $R$  and constant density  $\rho_0$ . This is not very realistic because it is known that stars do not have a constant density (see Section 3.2.3 for work on a more realistic approach). For now, the constant density will help us to keep the equation clean and focus on the physics.

A constant density means the following holds for the enclosed stellar mass:

$$m(r) = \begin{cases} 4/3\pi\rho_0r^3 & r < R \\ 4/3\pi\rho_0R^3 \equiv M & r > R \end{cases} \quad (3.2.26)$$

The line element, using the definition of  $m(r)$  in terms of  $\lambda$ , then takes the following form,

$$ds^2 = -e^{2\Phi}dt^2 + \frac{dr^2}{1 - 2m(r)/r} + r^2d\Omega^2. \quad (3.2.27)$$

We will use the equations derived in the previous section to learn about the metric and hydrostatic properties of the star. These equations are the mass equation (3.2.14), with boundary condition  $m(0) = 0$ , The TOV equation (3.2.24), with boundary condition  $p(R) = 0$  (no pressure at the boundary of the star), and the source equation for  $\Phi$  (3.2.22), with boundary condition  $\Phi(\infty) = 0$  (flat spacetime at infinity)

**Outside the star** The boundary of the star is defined as the point where  $p$  becomes zero (and stays zero due to the TOV equation because at the boundary also  $\rho$  is zero). Outside the star there is only vacuum, so only  $\Phi$  and  $\lambda$  are of relevance in this case. Integrating the equation for  $\Phi$  (3.2.22), we see:

$$\Phi(r) = \frac{1}{2} \log(1 - 2M/r) \quad (3.2.28)$$

Using this, the geometry reduces to the Schwarzschild metric in accordance with Birkhoff's theorem:

$$ds^2 = - \left(1 - \frac{2M}{r}\right) dt^2 + \left(1 - \frac{2M}{r}\right)^{-1} dr^2 + r^2 d\Omega^2 \quad (3.2.29)$$

**Inside the star** We can solve the TOV equation after plugging in the equation for  $m(r)$  (using e.g. Mathematica):

$$p(r) = \rho_0 \left\{ \frac{(1 - 2Mr^2/R^3)^{1/2} - (1 - 2M/R)^{1/2}}{3(1 - 2M/R)^{1/2} - (1 - 2Mr^2/R^3)^{1/2}} \right\} \quad (3.2.30)$$

This is an important result, because now the physical bounds on the star mass and size arise explicitly. Let us focus at first on the pressure at the core of the star:

$$p_c = p(0) = \rho_0 \left\{ \frac{1 - (1 - 2M/R)^{1/2}}{3(1 - 2M/R)^{1/2} - 1} \right\} \quad (3.2.31)$$

This reaches infinity for a limiting value of  $M/R = 4/9$  (this is an additional requirement for the star, alongside  $m(r)/2 > r$ ). This means the star can no longer be in equilibrium and thus something must happen. This will be the collapse of the stellar object. In Figure 3.1 this can be seen explicitly. The pressure inside a star is plotted for various mass/radius ratios. For  $M/R < 4/9$  the pressure at the core stays finite, and for  $M/R = 4/9$  the pressure scales like  $1/r^2$ , yielding an unphysical situation at the core.

In Figure 3.2 one can see how the central pressure develops as a function of the mass/radius ratio. The critical value,  $M/R = 4/9$ , is clearly visible. Interesting to see is how steep the central pressure increases near this threshold value. This is due to the occurrence of  $p(r)$  at the right hand side of the TOV equation. If  $p(r)$  is already large, it will increase even faster because its gradient (the left hand side) will also be large.

The precise meaning of the fundamental limit on the star's mass takes some effort to analyze, because one needs an equation of state, relating the pressure and density inside the star. Additionally, a star will of course collapse long before the pressure has reached infinity, because the fermion repulsion force is finite. The calculation of the TOV limit is

Figure 3.1: The pressure  $p$  exerted at a shell at radial position  $r$  inside the star for various ratios  $M/R$ . The green line corresponds to  $M/R = 4/9 \approx 0.44$  (this value causes the pressure to become infinite), yellow  $M/R = 0.42$ , red  $M/R = 0.4$ , blue  $M/R = 0.3$ .

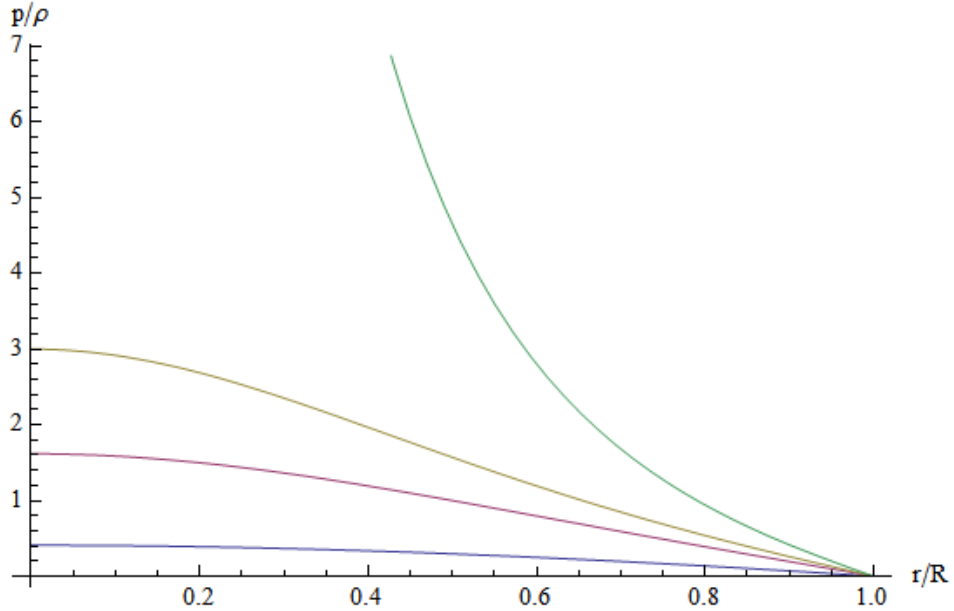
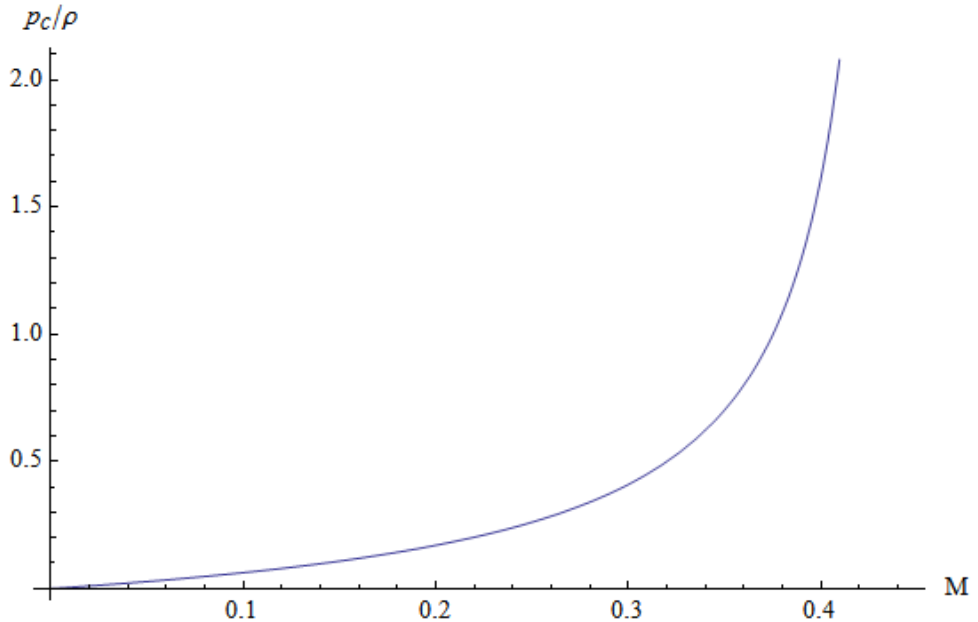


Figure 3.2: The pressure at the core of the star plotted against the mass/radius ratio  $M/R$ . The fundamental limit of this ratio is  $M/R = 4/9$ .



done in detail in [21] for neutron stars. The final result is that the mass of a neutron star cannot exceed 0.7 solar masses. Later this has been corrected to 1.5–3.0 due to increased

knowledge on the neutron star formation[26]. This uncertainty is largely due to the fact that we do not really know the structure of the neutron star. There might be a quark-gluon plasma inside, surrounded by a fermi liquid. For white dwarfs this limit is 1.44 solar masses. This outcome has been calculated by Chandrasekhar by other means before the TOV equation was discovered.

In Section 3.3 we will use a simplified model of a collapsing neutron star to check if a collapse into a black hole is a physically acceptable solution to Einstein's equations.

### 3.2.3 Realistic Stellar Models

So far we have treated a highly simplified model of a star. To achieve more realistic results, one needs to take extra factors into account. First of all, the density inside a star will not be constant (there is no such thing as an incompressible fluid). Secondly, a model of a stellar object that is rotating is of relevance because most neutrons stars are known to rotate very fast. Finally, also a charged star can be considered. However, charged stellar objects are not common because they neutralize by attracting oppositely charged particles.

Extension of the TOV equation for the charged case is done in *e.g.* [27]. By taking the Reissner-Nordström metric outside the star and assuming that the relation  $g_{00}g_{ii} = -1$  also holds for the interior solution for the metric, the equation of structure gets the following correction:

$$\frac{dp}{dr} = -\frac{(\rho + p)(m + 4\pi r^3 p)}{r(r - 2m)} + \frac{1}{8\pi r^4} \frac{d}{dr} q^2(r), \quad (3.2.32)$$

with  $q(r)$  the enclosed charge. This equation can be solved for a given charge distribution  $\sigma(r)$ , but then it appears that the total gravitational mass of the stellar object scales with this parameter. For  $\sigma = 0$ , also  $m(r) = 0$ . This means the gravitational mass is of purely electromagnetic origin, which is not the case for white dwarfs and neutron stars (made of hadrons). Unfortunately, this is the only case where one can solve the TOV equation explicitly for a charged stellar object.

Numerical analysis on normal (massive) charged stars has been performed [28]. It appears that a charge of  $10^{20}$ C is needed to have any noticeable effect on the star's structure. If these highly charged compact stars exist, they need to be isolated systems since outside the star, the Coulomb force would overwhelm the gravitational force. Any oppositely charged particle in the stellar atmosphere will be attracted and similarly charged particles will be repulsed by the charged star.

Rigidly rotating stars are treated in [29], but one has to resort to numerical methods to find solutions of the structure equation. It appears that in the rotating case, the mass can be about 20% larger than in the nonrotating case. However, the analysis of rigid rotation is limited by the spin rate at which the fluid at the equator moves on a geodesic, and any further speedup would lead to mass shedding of the stellar object. Therefore, so called ‘differentially rotating stars’ must be considered, further complicating the problem. This is treated in *e.g.* [30].

### 3.3 Gravitational Collapse

In the previous two sections, we have basically treated two prerequisites for the possibility of actually forming black holes in nature: first we have seen that under certain (physical) circumstances a star’s pressure is not big enough to keep it in equilibrium, and second we have seen that once a spherical distribution of matter is contained within its Schwarzschild radius, we can only find the Schwarzschild metric outside with its familiar “black hole” horizon. The part that is still lacking in order to argue that black holes might actually form in nature is the part in between: can we show the transition from a star that cannot withstand its gravitational pull, to a situation where all matter is within the Schwarzschild radius and the metric outside is Schwarzschild, is indeed a physical process?

Before we look at the particular example of a gravitationally collapsing spherical shell of dust that leaves behind the Schwarzschild metric, let’s quickly discuss the Newtonian analogue in order to appreciate the differences from a general relativistic treatment. To the reader it might seem obvious that in Newtonian theory a spherically symmetric body of dust ( $p = 0$ ), will collapse to some sort of singularity at  $r = 0$  (the gravitational force will blow up). However, we expect from Kepler’s laws of orbital motion, that as soon as we depart from perfect spherical symmetry, the dust particles will not fall all the way to  $r = 0$ , but will rather loop around it in some way (of course exact solutions in a non spherical case are hard to find). Also notice that the Newtonian solution to this problem is already less trivial than simply investigating the motion of a particle in some background gravitational field, because the background field is itself changing as a consequence of the motion of the dust particles. Like usually is the case, a full general relativistic treatment of this dynamic solution will result in a more complicated spacetime curvature and will require us to carefully define and treat the coordinates we use. Moreover, there are some fundamental physical differences too. First of all, we know that the Schwarzschild radius has some interesting physical implications and we want to make sure that we can properly

describe collapse through this radius, for which the horizon properties appear. Second, the sensitivity to a departure from spherical symmetry is much less. A first hint that this is the case can of course be found from the study of an infalling test particle in a background Schwarzschild metric: if the energy is large enough compared to the angular momentum, the particle will always fall into the singularity. Also, we have seen that once any matter passes the Schwarzschild radius, there is no returning: another aspect that clearly indicates the different nature of gravitational collapse in general relativity. A comprehensive figure that illustrates most features of gravitational collapse is included at the end of this section.

Having argued why we are interested in studying examples of gravitational collapse, we will next treat a first example of a solution to Einstein's equation that describes gravitational collapse. Later on we will briefly discuss what happens when we depart from this idealized situation, by considering different non spherical setups. A technical treatment of these, however, is outside the scope of this book and so we will stick to a qualitative discussion.

### 3.3.1 Infalling Spherical Shell of Dust

In general relativity language, the task of showing the reality of gravitational collapse, comes down to finding a metric that:

1. allows for a horizon in terms of the selected coordinates;
2. yields an energy momentum tensor, by means of the Einstein equation, that describes the motion of collapsing matter through a horizon.

This metric is actually relatively easily found in the case of a spherically symmetric, infinitely thin dust shell, radially falling in at the speed of light. The reason for this is that we can exploit the power of Birkhoff's theorem. Namely, in looking for a solution to the infalling spherical shell of dust, we already know that if we are going to find a solution, the interior as well as the exterior solution has to be Schwarzschild. In what follows, we shall start with the exterior Schwarzschild coordinates, transform them to new coordinates that describe the entire spacetime, and assume that the form of the metric in the interior region is very similar to the transformed Schwarzschild metric outside. Below we will display what exactly we mean by this statement and show that this way we indeed find a metric that describes gravitational collapse of dust infalling at almost the speed of light.

Let us first discuss the properties we want to find for the shell of dust. By definition, the energy momentum tensor of dust is

$$T_{\text{dust}}^{\mu\nu} = -\rho(x)u^\mu u^\nu \quad ; \quad u^\mu = \frac{dx^\mu}{d\tau}. \quad (3.3.1)$$

Note that dust is defined as a pressureless gas of non interacting massive particles, which means that formally it cannot move at the speed of light. What we will do is to consider dust that approaches the speed of light. This means that in terms of the exterior Schwarzschild coordinates  $u^r = -\Lambda$  goes to infinity. In order to be able to take a proper limit, i.e. without blowing up the energy momentum tensor, we will simultaneously be treating an ever less dense collection of particles: if the original rest mass was  $M$ , we will consider the speeded up dust to have rest mass  $M/\Lambda^2$ . Then, using  $u^\mu u_\mu = -1$  and solving for  $u^t$ , the four velocity in terms of the Schwarzschild coordinates becomes

$$u^\mu = \left( \sqrt{\frac{\Lambda^2}{(1-R_s/r)^2} + \frac{1}{1-R_s/r}}, -\Lambda, 0, 0 \right),$$

which in the limit  $\Lambda \rightarrow \infty$  becomes

$$u^\mu = \Lambda \left( \frac{1}{1-R_s/r}, -1, 0, 0 \right).$$

The initial condition of a shell of dust infalling at (almost) the speed of light from  $r = \infty$  at  $t = -\infty$  can be translated into the statement that at  $t \rightarrow -\infty$ , the energy momentum tensor looks like:

$$T_t^t = \frac{M}{4\pi r^2 \Lambda^2} \delta(r+t), \quad (3.3.2)$$

where the  $1/4\pi r^2$  term was inserted so that at infinity, where spacetime is just Minkowski spacetime (for which we have a good understanding of what energy conservation means), we have

$$E = \int_0^\infty dr 4\pi r^2 T_t^t(r, t) = M, \quad (3.3.3)$$

where we use that at  $t \rightarrow -\infty$ ,  $\rho(x) = \delta(r+t)M/(4\pi r^2 \Lambda^2)$ .

Now that we know what the energy momentum tensor in this setup looks like, our task is to find a metric that yields this energy momentum tensor in Schwarzschild coordinates. As we mentioned above, we are particularly interested in understanding gravitational collapse through the Schwarzschild radius. We have seen in the previous chapter that Schwarzschild coordinates are not the desired coordinates if we want to calculate the Einstein tensor in the entire spacetime. Therefore we change the exterior Schwarzschild coordinates to ingoing Eddington-Finkelstein coordinates, introduced in chapter 2, which are very convenient for infalling null geodesics. Then, because we know that the interior solution has to be

Schwarzschild too, we expect it to be a good choice to extend these coordinates to the entire spacetime, and assume that the only thing that will change from one region to the other is the mass parameter in the metric. We recall that these coordinates are defined by replacing the exterior Schwarzschild  $t$  with

$$v = t + r + R_s \log(r - R_s). \quad (3.3.4)$$

Note that  $v$  has the nice property that on null rays

$$\frac{dv}{dr} = \frac{1}{1 - R_s/r} + \frac{dt}{dr} = 0, \quad (3.3.5)$$

which means that the dust shell will approximately move on paths defined by  $v(s) = \text{constant}$ . This property becomes manifest by choosing the following metric in terms of the new coordinates:

$$ds_{\text{in}}^2 = -(1 - \frac{R_{s,\text{in}}}{r})dv^2 + 2dvdr + r^2d\Omega^2 \quad (3.3.6a)$$

$$ds_{\text{out}}^2 = -(1 - \frac{R_{s,\text{out}}}{r})dv^2 + 2dvdr + r^2d\Omega^2, \quad (3.3.6b)$$

for which the radial lightcone,  $ds^2 = 0$  has the two legs:

$$\frac{dv}{dr} = 0 \quad ; \quad \frac{dv}{dr} = \frac{2}{1 - R_s/r}. \quad (3.3.7)$$

Then our dust shell moves on the path  $v = 0$  (and possible subsequent shells will all move on paths given by  $v = \text{constant}$ ). This means that the parameter  $R_s$  should be a function of  $v$  only:

$$ds^2 = -\left(1 - \frac{R_s(v)}{r}\right)dv^2 + 2dvdr + r^2d\Omega^2. \quad (3.3.8)$$

In the slightly more general case of several dust shells radially infalling at the speed of light, we have

$$R_s(v) = \theta(v - v_i)2M_{out} + \theta(-v + v_i)2M_{in} \quad , \quad (3.3.9)$$

where  $M_{out} - M_{in} = M_i$ , the mass of the  $i$ -th shell, and  $\Theta$  is the step function. Relating the Schwarzschild radius, which is formally just a parameter in Birkhoff's theorem, to the mass in this way is suggested by considering the asymptotic regime, where the  $r$ -component of some shell becomes very large and the weak field approximations are valid. The metric components in these coordinates are thus:

$$\begin{aligned} g_{00} &= -1 + R_s/r & g_{01} = g_{10} = 1 & g_{11} = 0 & g_{22} = r^2 & g_{33} = r^2 \sin^2(\theta) \\ g^{11} &= 1 - R_s/r & g^{01} = g^{10} = 1 & g^{00} = 0 & g^{22} = \frac{1}{r^2} & g^{33} = \frac{1}{r^2 \sin^2(\theta)}. \end{aligned} \quad (3.3.10)$$

Now it is just a matter of calculating the Einstein tensor. Denoting  $\dot{R}_s = dR_s/dv$ , we find the nonzero Christoffel symbols:

$$\begin{aligned}\Gamma^0_{00} &= \frac{R_s}{2r^2} & \Gamma^1_{01} = \Gamma^1_{10} &= -\frac{R_s}{2r^2} & \Gamma^1_{00} &= \frac{\dot{R}_s}{2r} + \frac{R_s}{2r^2} - \frac{R_s^2}{2r^3} \\ \Gamma^0_{22} &= -r & \Gamma^0_{33} &= -r \sin^2(\theta) & \Gamma^1_{22} &= R_s - r \\ \Gamma^1_{33} &= (R_s - r) \sin^2(\theta) & \Gamma^2_{12} = \Gamma^2_{21} &= \frac{1}{r} & \Gamma^3_{13} = \Gamma^3_{31} &= \frac{1}{r} \\ \Gamma^2_{33} &= -\cos(\theta) \sin(\theta) & \Gamma^3_{23} = \Gamma^3_{32} &= \cot(\theta).\end{aligned}\quad (3.3.11)$$

To shorten the calculation, we note that

$$\partial_\rho (\log \sqrt{-g}) = \frac{1}{2} g^{\mu\nu} \partial_\rho g_{\mu\nu} = \Gamma_{\alpha\rho}^\alpha \quad , \quad (3.3.12)$$

so that we can write the Ricci tensor as

$$R_{\mu\nu} = -(\log \sqrt{-g})_{,\mu,\nu} + \Gamma_{\mu\nu,\alpha}^\alpha - \Gamma_{\alpha\mu}^\beta \Gamma_{\beta\nu}^\alpha + \Gamma_{\mu\nu}^\alpha (\log \sqrt{-g})_{,\alpha} \quad , \quad (3.3.13)$$

where  $\log \sqrt{-g} = 2 \log r + \log(\sin \theta)$ . Using this, we find that the only nonzero component of the Ricci tensor is

$$R_{00} = \frac{\dot{R}_s}{r^2}. \quad (3.3.14)$$

Hence the Ricci scalar is zero and upon inserting the factors of  $8\pi$  and using (3.3.9), the nontrivial part of the Einstein equation becomes:

$$8\pi G T_{00} = -\frac{\dot{R}_s}{r^2} = \frac{-2M_i \delta(v_i)}{r^2}. \quad (3.3.15)$$

This we compare to the energy momentum tensor of the dust shell. Note that our new coordinates are chosen such that the four momentum of the shell becomes  $u^\mu = (0, -\Lambda, 0, 0)$  and thus  $u_\mu = (-\Lambda, 0, 0, 0)$ . Substituting this into the Einstein equation yields

$$8\pi G \rho(x) \Lambda^2 = \frac{2M_i \delta(v_i)}{r^2}, \quad (3.3.16)$$

i.e.

$$\rho(x) = \frac{M_i \delta(v_i)}{4\pi r^2 \Lambda^2}. \quad (3.3.17)$$

In particular, for  $t \rightarrow -\infty$ ,  $\delta(v_i)$  can be replaced by  $\delta(r + t)$  in terms of the exterior Schwarzschild coordinates, which shows that the geometry is due to dust of mass  $M_i/\Lambda^2$  that was initially falling in at the speed of light and subsequently moves along a geodesic (constant  $v_i$ ) of this geometry. In other words, the shell of dust falls in as a consequence of its own gravitational field. Also, paths of constant  $v$  clearly cross the Schwarzschild radius. Figure 3.3 schematically shows what happens to the metric, in particular the horizon, when several spherical shells of mass fall in on paths of constant  $v$ .

Thus, we see that at least this idealized version of gravitational collapse through the Schwarzschild horizon is a viable solution to the Einstein field equation. The original example, that of a uniform-density ball of dust actually moving along non-null geodesics, can be found in the classic paper by Oppenheimer and Snyder [31].

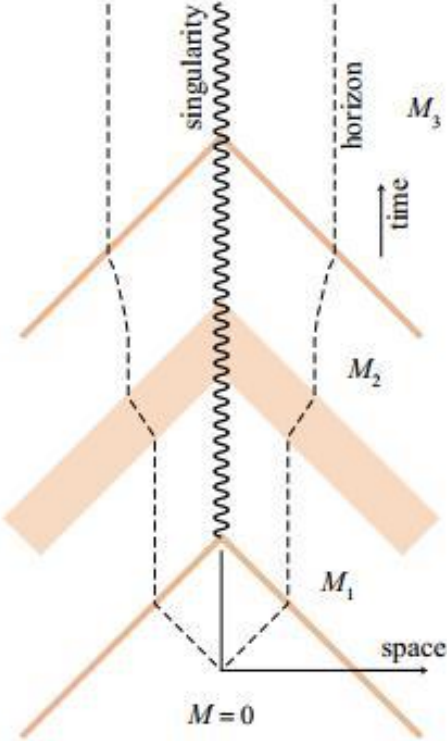


Figure 3.3: Schematic gravitational collapse of several shells of dust along null geodesics ( $v = \text{constant}$ ).

### 3.3.2 Realistic Gravitational Collapse

Like we mentioned before, one of the important differences between relativistic and Newtonian collapse lies in the ‘‘robustness’’ of the solutions with respect to non spherical perturbations. Generically, it is rather hard to solve Einstein’s equations in the presence of non spherical perturbations. This was the reason for a period of doubt in the 1960’s as to what the effects of such a perturbation would be. One viewpoint was that initially small perturbations would grow without bound, stopping the collapse or destroying the event horizon. Note that this means that the existence of black holes in nature was still highly doubted at that time. The opposite viewpoint was that collapse in case of non spherical perturbations behaves qualitatively the same as spherical collapse (below we will comment briefly on what the qualitative features of spherical collapse are). The most conclusive work that largely settled the issue seems to be [32]. In it he shows first and foremost that the perturbations neither disappear nor halt the collapse through the gravitational radius. Secondly, he shows that to an observer outside of the Schwarzschild radius, the metric approaches the spherical Schwarzschild solution as time goes to infinity, where we have to

keep in mind that to an outside observer it will take infinite time for matter to reach the Schwarzschild radius. Moreover, in later papers [33, 34] he shows that if we consider the small perturbations to be due to a spin-s field (spin-1 for electromagnetism and spin-2 for gravitational perturbations), the final field outside the horizon can only have contributions from multipoles with  $l < s$ . In other words, all multipole contributions to the outside field with  $l \geq s$  get radiated away to infinity or back to the black hole, as the nearly spherical mass collapses to a black hole. The latter goes under the name of Price's Theorem. Note that this is directly related to the “No Hair Theorems” discussed in the next chapter, stating that the only nonvanishing contribution to the electromagnetic field is the monopole Coulomb field and the only nonvanishing contributions to the gravitational field are the monopole field determined by the mass parameter and the dipole field determined by the angular momentum parameter. This is in accordance with the general solutions we found in the previous chapters and it shows that physical collapsing bodies will indeed leave behind those solutions as they cross the horizon. For a lengthier qualitative discussion of non spherical collapse we refer the reader to [25].

### 3.3.3 Consequences

The main differences between the Newtonian and relativistic treatments are the existence of a horizon and the nature of the singularity. The issue of singularities and their relation to the existence of a horizon will be investigated more generically in the next sections. Here we will just briefly comment on the physical implications of the horizon in gravitational collapse. First of all, as we have seen in the previous chapter, but as can also be seen from the “outgoing” leg in (3.3.7), the Schwarzschild radius really is a point of no return for the collapsing matter: as soon as it passes it, the only way is inward. Second, an outside observer sees the matter slow down and approach the horizon infinitely close, as can be inferred from the outgoing null geodesics of light sent from the matter. A question we therefore have to ask is in what sense a black hole actually can be called a black hole, if an outside observer will always see light coming from the object (see §33.1 in [25]). The argument here is that the signals coming from the surface of a collapsing star are strongly redshifted and hence the total observed luminosity of the star will decay rapidly: it goes dark. The original work on this is also the 1939 Oppenheimer and Snyder paper. A nice comprehensive image of what happens during gravitational collapse can be obtained from figure 3.4.

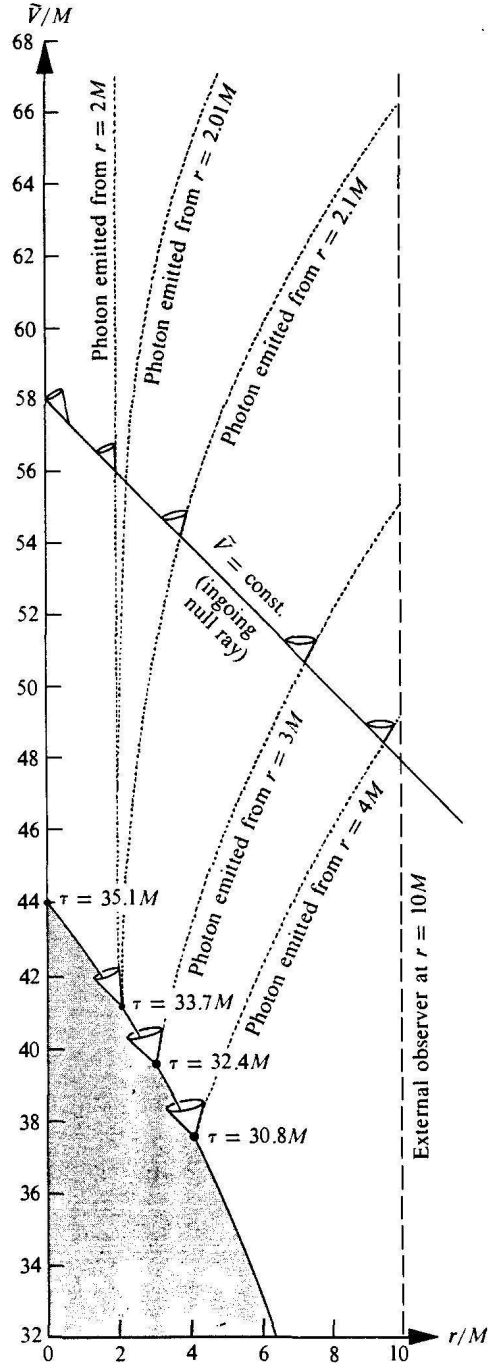


Figure 3.4: Gravitational collapse in ingoing Eddington-Finkelstein coordinates.

### 3.4 Singularity Theorems

After some exact solutions of the Einstein's equations were found, a fundamental question arose: are singularities in General Relativity characteristics of highly symmetric solutions

only, or are they actually present in the real world? Can it be, like in Newtonian mechanics, that as soon as perturbations are introduced, the singularities disappear from the theory? The singularities theorems by R. Penrose and S. Hawking answer these questions, by showing that, under certain conditions, singularities always arise, regardless of the details of their formation.

### 3.4.1 Conjugate Points and Definition of Singularity

To develop the framework in which such theorems can be proven the first step is to give a suitable definition of what a singularity actually is: naively one would claim that singularities are the points where the metric fails to be continuous (or differentiable). However the problem with this definition is that, in order to build a mathematical structure for the space-time, we have to assume it is everywhere  $C^2$ , and thus every allowed space-time has no singularities by the above definition. To have a precise definition of singularity one should think that it is a point *outside* the theory, which means that the future (or the past) of that point cannot be predicted with the means of the theory. We can make the intuition precise by requiring that any geodesic, the trajectory of a free falling body, must be extendable to arbitrary values of its affine parameter, then we say that space-time is *g-complete*. If the condition is not met, the space-time is *g-incomplete* and we shall say that our space contains a singularity. As an example one could consider the Schwarzschild black hole, where the origin of the coordinates is a singularity: an infalling body or photon will reach the singularity after finite value of the affine parameter and thus its geodesic will be inextensible after that point.

The second concept we are interested in is the notion of *conjugate points*: points  $p$  and  $q$  along a geodesic  $\gamma(s)$  are said to be conjugate iff nearby geodesics at  $p$  eventually collide at  $q$ . Since gravity is an attractive force, it focuses geodesics, and if the generated curvature is strong enough, conjugate points always develop, provided we can extend the geodesics arbitrarily far in the past and in the future.

To prove the above claim, we are going to look at a family of curves,  $\lambda(t)$  with tangent vector  $Z^\alpha$ . We will then define a vector field  $V^\alpha$  whose integral curves are geodesics, either time-like or light-like, and parallel transport  $\lambda(t)$  along  $V^\alpha$ . This construction generates a family of curves,  $\lambda(t, s)$ , where “ $s$ ” is the coordinate along which we parallel transport, called a *congruence* of geodesics. We want to look at the separation of nearby curves and for the conditions in which *conjugate points* arise if we assume extensibility. We have [4]

$$D_s Z^\alpha = Z^\beta \nabla_\beta V^\alpha, \quad (3.4.1)$$

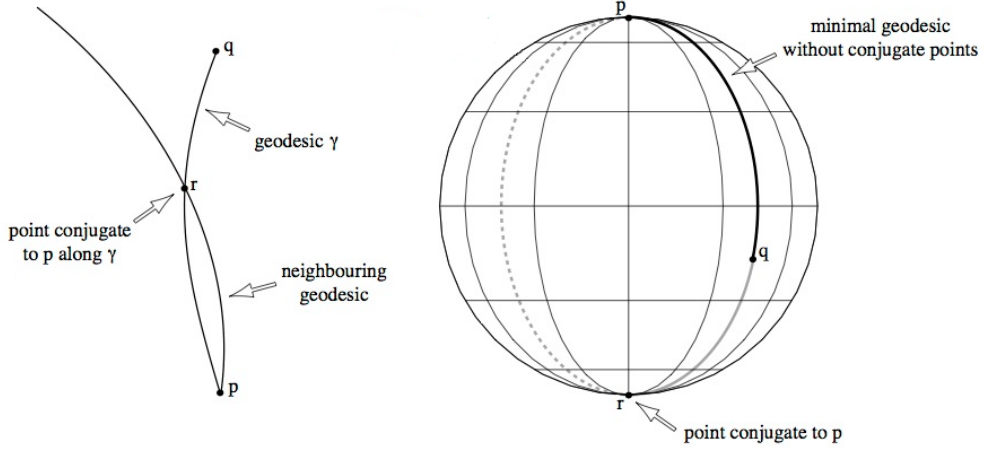


Figure 3.5: Schematic idea of conjugate points: on the left, nearby geodesics leaving  $p$  eventually meet at  $r$ ; on the right the example of a sphere, whose north and south poles are an example of conjugate points (but on a non lorentzian manifold).

where  $D_s$  means the covariant derivative of  $Z^\alpha$  along the coordinate  $s$ . We are interested in the separation between neighboring geodesics, not between points on the same geodesic, which means projecting the above equation on the subspace orthogonal to  $V^\alpha$ :

$$Z_\perp^\alpha = (\delta_\beta^\alpha + V^\alpha V_\beta) Z^\beta \equiv h_\beta^\alpha Z^\beta. \quad (3.4.2)$$

As it can be easily checked, the tensor  $h_\beta^\alpha$  projects any vector onto the subspace orthogonal to  $V^\alpha$ , if  $V^\alpha$  is time-like. The situation is slightly different if the geodesics are null, and it will be analyzed separately. The perpendicular part of  $Z^\alpha$  satisfies (3.4.1):

$$D_s Z_\perp^\alpha = Z_\perp^\beta \nabla_\beta V^\alpha. \quad (3.4.3)$$

If we project this onto the subspace perpendicular to  $V^\alpha$  and then take the covariant derivative, and project once more we get:

$$h_\beta^\alpha D_s (h_\gamma^\beta (D_s Z_\perp^\gamma)) = -R_{\beta\gamma\delta}^\alpha V^\beta V^\delta Z_\perp^\gamma, \quad (3.4.4)$$

where we used that, for a geodesic's tangent vector,  $V^\beta \nabla_\beta V^\alpha = 0$ . We now redefine our coordinate basis as  $\{e_\alpha\}_{\alpha=0,1,2,3}$ , where the basis elements are orthogonal. If we parallel transport this basis along the vector field  $V^\alpha$ , it will stay orthogonal because  $\lambda(t_0, s)$  is a geodesic. The definition of this new basis is given by  $V^\alpha e_\alpha = V^0 e_0$ . We have that  $Z_\perp = Z^\alpha e_\alpha$ , where  $\alpha = 1, 2, 3$  and<sup>2</sup>  $D_s = \frac{d}{ds}$ . The above equations simplify into:

$$\frac{dZ^\alpha}{ds} = \nabla_\beta V^\alpha Z^\beta, \quad (3.4.5)$$

---

<sup>2</sup>For a more detailed analysis of this claim see [4].

$$\frac{d^2 Z^\alpha}{ds^2} = -R_{0\delta 0}^\alpha Z^\delta = -R_{\beta\gamma\delta}^\alpha V^\beta V^\delta Z^\gamma. \quad (3.4.6)$$

Note that here, the sum with  $Z^\alpha$  runs for  $\alpha = 1, 2, 3$ , and we used the fact that  $R_{0\delta 0}^\alpha = R_{\beta\gamma\delta}^\alpha V^\beta V^\delta$ . The covariant derivative of  $V^\alpha$  has components for  $\alpha, \beta = 1, 2, 3$  in the equation. We shall then rewrite:

$$\nabla_\alpha V_\beta = S_{\alpha\beta} + A_{\alpha\beta} + \frac{1}{3}\theta h_{\alpha\beta}. \quad (3.4.7)$$

As a representation of a tensor into its symmetric traceless, antisymmetric and trace parts. Here  $\nabla_\beta V_\alpha$  is a  $3 \times 3$  matrix. To understand the physical meaning of this decomposition we make an analogy with fluid dynamics, and attribute to the vector field  $V^\alpha$  the meaning of flow lines, along which the curve  $\lambda(t)$  is flowing:

- $A_{\alpha\beta}$ , represents the vorticity of the lines and it is zero along geodesics, as they are “straight lines” in a geometrical sense [35].
- $S_{\alpha\beta}$  represents the shear, the change in shape of a small neighborhood of curves. However since it is traceless it does not contain information about the actual change of the volume.
- $\theta$  represents the divergence of nearby geodesics, and thus the change in volume of a small neighborhood of curves. It is the quantity we are interested in.

Plugging (3.4.5) into (3.4.6) and substituting the above decomposition we then get:

$$\frac{d\theta}{ds} = -S_{\alpha\beta}S^{\alpha\beta} - R_{\alpha\beta}V^\alpha V^\beta - \frac{\theta^2}{3}. \quad (3.4.8)$$

Typically known as the Raychaudhuri equation or *focusing theorem*.

For light-like geodesics the situation is slightly different, as the vector field along which we are transporting the curves,  $K^\alpha$ , satisfy  $K^\alpha K_\alpha = 0$ . Thus the subspace orthogonal to  $K^\alpha$  actually includes  $K^\alpha$ . However we can do the same analysis as before, but now we are interested in the projection of  $Z^\alpha$  onto the subspace orthogonal to  $K^\alpha$  not including  $K^\alpha$ . The basis  $e_\alpha$  has again  $e_0$  parallel to  $K^\alpha$ , but  $Z_\perp = Z^\alpha e_\alpha$ , where  $\alpha = 1, 2$ . This also implies that the decomposition (3.4.7) is done using  $2 \times 2$  matrices. (3.4.8) will then be:

$$\frac{d\theta}{ds} = -S_{\alpha\beta}S^{\alpha\beta} - R_{\alpha\beta}K^\alpha K^\beta - \frac{\theta^2}{2}. \quad (3.4.9)$$

Since  $\theta$  represents the divergence of nearby geodesics, when it becomes  $-\infty$ , all the neighboring curves will converge, meaning that conjugate points will form. From equation (3.4.8-3.4.9) we can see that, when  $R_{\alpha\beta}V^\alpha V^\beta \geq 0$  the divergence of neighboring geodesics always

decreases. In particular, if for some  $s_1$  the density  $\theta_1 < 0$ , then  $\theta \rightarrow -\infty$  for  $s \in [s_1, s_1 - \frac{n}{\theta_1}]$ <sup>3</sup> if we can extend the curve that far: this can be proven from the Raychaudhuri equation, by considering only the term  $\frac{\theta^2}{n}$  and integrating both sides<sup>4</sup>. It can be also shown that when  $R_{\alpha\beta}V^\alpha V^\beta \geq 0$  holds at point  $r$ , then there exists a conjugate point in the past of  $r$  and one in its future [4].

However, if we do not assume *g-completeness*, we may not be able to extend all geodesics until finding the conjugate point, given that the above conditions are respected. In other words, the existence of conjugate points along all geodesics requires  $R_{\alpha\beta}V^\alpha V^\beta \geq 0$  and that space-time is *g-complete*.

### 3.4.2 Energy Conditions

Let us give a closer look at the condition on the Riemann tensor for which conjugate points form. From Einstein's equations we can express the condition on the curvature in terms of the energy momentum tensor, to get:

$$R_{\alpha\beta} = T_{\alpha\beta} - \frac{T}{2}g_{\alpha\beta} + \frac{\Lambda}{2}g_{\alpha\beta},$$

where  $T$  is the trace of the energy momentum tensor.

- if the geodesic is null we have  $T_{\alpha\beta}K^\alpha K^\beta \geq 0$ . We shall call this the *weak energy condition*. It can also be expressed by saying that the energy density is positive in any reference frame. This is physically very reasonable and holds for most known matter scalar fields, electro-magnetic radiation and fluids with reasonable equation of state [36].
- if the geodesic is time-like we find  $T_{\alpha\beta}V^\alpha V^\beta \geq V^\alpha V_\alpha (\frac{T}{2} - \frac{\Lambda}{2})$ , which is stronger, but still met in most realistic physical systems. We shall call this the *strong energy condition*. This is less likely to hold than the weak energy condition, but it is still met, in an average sense, by most known space-times [36]. Note that the strong energy condition implies the weak for  $\Lambda \leq 0$ , but not otherwise.

Note that a pair of conjugate points can exist on null geodesics, but not on time-like geodesics, if the weak energy condition holds, but not the strong one. This means that a

<sup>3</sup> $n = 2$  for null geodesics,  $n = 3$  for time-like geodesics.

<sup>4</sup>We will then get  $\theta \leq \frac{n}{s - (s_1 - \frac{n}{\theta_1})}$ , which implies the above claim.

space-time can be null geodesically incomplete, but time-like geodesically complete, and the other way around.

### 3.4.3 The Schwarzschild Example

In this section, we illustrate the concepts developed in the previous one, by considering the geodesics of the Schwarzschild space-time, and show that they will converge at the singularity. In this case, the existence of conjugate points is implied by the Raychaudhuri equation, but the geodesics cannot be extended to find the conjugate point because of the singularity. For simplicity, we restrict ourselves to radial motion only. We also note that, in the Schwarzschild space-time, the energy conditions both hold with the equality sign.

Consider at first a massive particle falling from infinity towards the singularity. It will follow the geodesic equations

$$\frac{du^t}{d\tau} = -\frac{2M}{r^2(1-\frac{2M}{r})} u^t u^r, \quad (3.4.10)$$

$$\frac{du^r}{d\tau} = -\left(1-\frac{2M}{r}\right) \frac{M}{r^2} (u^r)^2 + \frac{M}{r^2(1-\frac{2M}{r})} (u^t)^2. \quad (3.4.11)$$

Where  $u^\alpha$  is the 4-velocity, and therefore the vector field generating the congruence of geodesics. Furthermore, we have the condition that the geodesic is time-like,  $u_\alpha u^\alpha = -1$ , which means

$$-1 = -\left(1-\frac{2M}{r}\right) (u^t)^2 + \left(1-\frac{2M}{r}\right)^{-1} (u^r)^2. \quad (3.4.12)$$

From (3.4.10) we get, integrating in  $u^t$

$$u^t = \left(1-\frac{2M}{r}\right)^{-1} C_1. \quad (3.4.13)$$

We find, by imposing that the particle has no radial motion at spatial infinity, that  $C_1 = 1$ . This condition can be derived from:  $-1 = u_t u^t$ , evaluated at radial infinity.

From (3.4.12) we can derive the expression for  $u^r$ , which turns out to be

$$u^r = \pm \sqrt{\frac{2M}{r}}. \quad (3.4.14)$$

As we want to analyze particles falling into the singularity, we pick the solution with the minus sign. We now have all the ingredients to calculate the divergence<sup>5</sup>

$$\tilde{\theta} = \Gamma_{tr}^t u^r + \partial_r u^r + \Gamma_{rr}^r u^r + \Gamma_{\theta r}^\theta u^r + \Gamma_{\phi r}^\phi u^r = -\frac{3}{2} \sqrt{\frac{2M}{r^3}}. \quad (3.4.15)$$

---

<sup>5</sup>The tilde sign on the divergence is only introduced to distinguish it from the coordinate  $\theta$ .

As expected,  $\tilde{\theta} \rightarrow -\infty$ , as  $r \rightarrow 0$ . This implies that nearby geodesics at infinity converge at  $r = 0$ , however, since the point  $r = 0$  is a singularity, the geodesic is not extendable that far. In principle, one could also check that the Raychaudhuri equation holds, using the non zero components of the shear

$$\begin{aligned} S_{tt} &= \sqrt{\frac{2M}{r}} \frac{2M}{r^2}, \\ S_{rr} &= \sqrt{\frac{2M}{r^3}} \frac{1}{\left(1 - \frac{2M}{r}\right)^2}, \\ S_{tr} &= \frac{2M}{r^2 \left(1 - \frac{2M}{r}\right)}, \\ S_{\theta\theta} &= \frac{1}{\sin^2(\theta)} S_{\phi\phi} = -\sqrt{\frac{Mr}{2}}, \end{aligned} \tag{3.4.16}$$

obtained with the formula

$$S_{\alpha\beta} = \frac{1}{2} (\nabla_\alpha u_\beta + \nabla_\beta u_\alpha) - \frac{\tilde{\theta}}{3} h_{\alpha\beta}.$$

Note that  $S_{\alpha\beta}$  is not a  $3 \times 3$  matrix, because we are expressing it in the usual coordinates  $\{t, r, \theta, \phi\}$  and not in the basis transported along the geodesics.

We now analyze the case of light-like geodesics: the above derivation holds for  $u^t$ , which will be then given by (3.4.13), but now equation (3.4.12) becomes

$$0 = - \left(1 - \frac{2M}{r}\right) (u^t)^2 + \left(1 - \frac{2M}{r}\right)^{-1} (u^r)^2, \tag{3.4.17}$$

which implies

$$u^r = \pm |C_1|. \tag{3.4.18}$$

Again we pick the solution with the minus sign and find the divergence

$$\tilde{\theta} = -\frac{2|C_1|}{r}. \tag{3.4.19}$$

Which proves that also light-like geodesics converge at  $r = 0$ , but cannot be extended that far. For completeness we give the non zero components of the shear, which will be:

$$\begin{aligned} S_{tt} &= \frac{MC_1}{r^2}, \\ S_{rr} &= \frac{MC_1}{r^2 \left(1 - \frac{2M}{r}\right)^2}, \\ S_{tr} &= \frac{MC_1}{r^2 \left(1 - \frac{2M}{r}\right)}. \end{aligned} \tag{3.4.20}$$

### 3.4.4 Trapped Surfaces

The last ingredient for the singularity theorem is the existence of trapped surfaces, which marks the presence of horizons. One should think that what is hidden behind an horizon can never go out, at least in a classical theory, in other words there exists some regions that are indeed trapped, because not even light can escape from them. To illustrate this, let us consider a closed, convex space-like surface  $S$  and a congruence of geodesics, orthogonal to  $S$ , leaving it at  $t = 0$ . At time  $t = \epsilon$  there will be three regions that can be distinguished:

- the causal future of  $S$ , namely the set that can be reached by time-like or null geodesics leaving  $S$  and traveling for  $\epsilon$  proper time, which we shall call  $V_3$ ;
- the region inside  $S$ , which we shall call  $V_2$ ;
- the region outside  $S$  whose points are not contained in the closure of  $V_3$ , which we call  $V_1$  (see fig. 3.6).

At any point  $q$  of  $S$ , we can introduce the basis formed by two space-like vectors tangent to  $S$ ,  $T_{1,\alpha}$  and  $T_{2,\alpha}$ , and two null vectors orthogonal to  $S$ ,  $N_{1,\alpha}$  and  $N_{2,\alpha}$ , which define two congruences of null geodesics normal to  $S$ .<sup>6</sup> We shall introduce two tensors on the surface  $S$ :

$$h_{\alpha\beta} = T_{1,\alpha}T_{1,\beta} + T_{2,\alpha}T_{2,\beta}, \quad (3.4.21)$$

$$\chi_{n,\alpha\beta} = -(\nabla_\delta N_{n,\gamma}) h_\alpha^\gamma h_\beta^\delta. \quad (3.4.22)$$

Which are called the *induced metric*, used to calculate the area of the surface and to project vectors onto the surface, and the *second fundamental form*, which represents the change of the area as it is moved on the null geodesics. There are two second fundamental forms, as there are two families of null geodesics leaving orthogonal to  $S$ , from now on labelled as 1,2. We will then define  $\theta_{1,2} = \chi_{1,2,\alpha\beta} g^{\alpha\beta}$ , representing the divergence of the surface area as we start moving it along the geodesics. We say that  $S$  is a *trapped surface* if  $\theta_{1,2} \leq 0$ . We say it is *marginally trapped* if the equality holds.<sup>7</sup>

This means that all of the causal future of  $S$  is shrinking and going back to  $S$  itself. For trapped surfaces we can prove the following theorem:

<sup>6</sup>The light-cones from  $S$  will have these 2 congruences as border.

<sup>7</sup>We also have that the largest trapped surface, which will be also the border of the trapped region, must be *marginally trapped*.

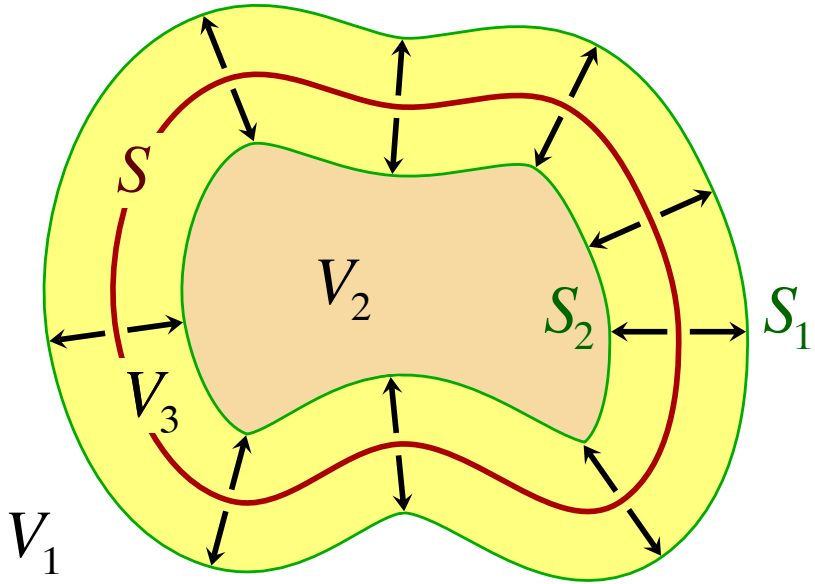


Figure 3.6: Representation of the idea behind a trapped surface: the region  $V_3$  represents the part of space-time that can be influenced by what happens at  $S$  at time  $t = 0$ . If the boundary of  $V_3$  is to shrink back to  $S$ , then  $S$  is a trapped surface.

*Theorem 3.4.1:* If everywhere in the closure of the trapped region the energy density  $T_{\alpha\beta}K^\alpha K^\beta \geq 0$ , then the trapped region remains trapped forever and the area of the largest trapped surface must stay constant or increase.

To illustrate this theorem we will apply the Raychaudhuri equation to a trapped surface. (3.4.5) and (3.4.6) hold for  $T_{1,2,\alpha}$  and as a consequence we can analyze the problem as before, only now with the congruence of geodesics the ones leaving orthogonal to  $S$  and the curve  $\lambda(t)$  lying on the surface. Thus we have that  $\theta_{1,2}$  is non increasing if  $T_{\alpha\beta}N_{1,2}^\alpha N_{1,2}^\beta \geq 0$ , as implied by the Raychaudhuri equation. This means that it cannot become positive if it was negative and the surface will stay trapped forever. If the surface is marginally trapped ( $\theta_{1,2} = 0$ ) then (3.4.9) implies that  $\theta_{1,2}$  either stays constant, in which case the largest trapped surface stays constant, or decrease, in which case the trapped region becomes larger.

As a consequence of this we see that, as long as matter respecting the weak energy condition is thrown into a black hole, the value of  $T_{\alpha\beta}K^\alpha K^\beta$  will be bigger or equal, so the largest trapped surface can either stay constant or start increasing, in which case the black hole has become larger. However, this result is a consequence of general relativity only and

does not take into account quantum effects, as the Hawking radiation, that actually allows a black hole to evaporate.

### 3.4.5 The Theorem

This concludes the necessary remarks, and we can state the singularity theorem in its most general form: *Theorem 3.4.2, Hawking-Penrose(1970)*: Space-time cannot satisfy all the following at the same time:

- i) There are no closed time-like curves.
- ii) Any geodesic contains a pair of conjugate points.
- iii) There exists a trapped surface.

The first condition is a general requirement on the causal structure of the universe and it should be true in all causal space-times, since the interpretative difficulties that arises in space-times containing closed time-like curves already characterize those space-times as singular. The second, as we saw before, is a consequence of the energy conditions and geodesic completeness, while the third describes the existence of an horizon.

There are several remarks that should be made. Firstly, one would hope that a space is *g-complete* for time-like geodesics, if and only if it is also *g-complete* for null geodesics. Unfortunately, this is not always the case. As we already pointed out an exception is when the weak energy condition is respected, but not the strong one. Furthermore, in deSitter space-time, we could have that the strong energy condition holds, but not the weak one. This suggests that time-like and light-like singularities are distinct concepts and are to be treated separately. Secondly, the theorem states that, in the presence of a trapped surface and when the energy conditions are met, the space-time is geodesically incomplete. It doesn't say anything about the character of the singularities themselves, nor if they are in the past or in the future. Thirdly, if there are no trapped surfaces there could still be a singularity according to the theorem, in which case we would say it is a *naked singularity*. In the next chapter we shall see how the naked singularities problem can be approached.

### 3.5 Cosmic Censorship

The Schwarzschild metric initially caused some concern among physicists. Though it was an exact solution to Einstein's equations, the infinite curvature at the singularity made it seem unphysical. Later on it was realised that such singularities were a generic feature of general relativity. Because there is an event horizon that 'shields' the singularity, the physics in the origin may get unpredictable, but it does not lead to any unpredictable situations outside the horizon.

Solutions to the Einstein equations which possess not-shielded, or naked, singularities are not difficult to find. Take for example the Reissner-Nordström solution of a charged spherically symmetric black hole with the radius of the event horizon given by equation (2.2.10),  $r_H = M + \sqrt{M^2 - Q^2}$ . We see that if  $Q$  is larger than  $M$ , the event horizon disappears, though the singularity at the origin remains and the metric is still a solution of the Einstein equations. If such a naked singularity existed, information from near the origin, where the physics gets unpredictable, could reach distant observers and it would spoil our view of general relativity as a deterministic theory. In 1969, Roger Penrose therefore came up with the hypothesis that naked singularities do not occur in Nature. This is what we now call the *weak cosmic censorship conjecture*. More precisely it states that singularities formed after physical gravitational collapse will not be visible to distant observers and thus realistic space-time is predictable and asymptotically flat. 'Physical' in this context means that we should impose an energy condition and that the initial data satisfies some appropriate boundary conditions.

If there is a weak, there is of course also a *strong cosmic censorship conjecture*. This would mean no singularities are visible for observers at future infinity, so even an observer falling past the horizon of a black hole will never see the singularity. More technically it means that all physically reasonable space-times are globally hyperbolic. This may sound stronger, because it applies to all observers, not only the distant ones. However, if the strong condition is met, this does not mean weak censorship is automatically satisfied. Imagine for example a singularity is formed which propagates to infinity. This destroys asymptotic flatness, but preserves global hyperbolicity.

### 3.5.1 Arguments for the Validity of the Weak Cosmic Censorship Conjecture

Though almost all physicists believe naked singularities can not exist in nature, cosmic censorship is still conjectural. It can be very hard to decide whether a solution to the Einstein equations is physical or not, thus it is not surprising that no one so far has managed to prove that any physical realizable solution can not contain naked singularities, or to put it differently, that any solution to Einstein's equations which contains naked singularities is unphysical.

The arguments for cosmic censorship are mostly philosophical. We want general relativity to be a deterministic theory, so any unpredictable situations should be hidden from any distant observers. Also, the theory of black holes is so beautiful, it would be a shame if it is not physically relevant. We also have some circumstantial proof for the hypothesis. We can try to make naked singularities starting from physical initial conditions and see if we succeed. All the attempts to find counterexamples to cosmic censorship in the past failed, as if there is some kind of conspiracy of Nature. As we look for example at a slightly perturbed Schwarzschild metric, we see that perturbations do not grow in time, but in fact disappear. Therefore it is a stable solution and the event horizon will not disappear when the black hole is slightly spherically asymmetric. Two other examples which we work out below are the attempts to overspin or overcharge a black hole.

Some other efforts trying to find counterexamples were more successful. For example the collapse of an inhomogeneous spherical dust cloud. This problem can be solved in an exact manner and then certainly leads to a naked singularity. At first sight this is a physical solution, but if we look closer we find out that the assumption of dust, pressureless matter, might not be an appropriate approximation for collapsing matter as the density blows up.

This is the way how research on the cosmic censorship conjecture is proceeding: trying to find another counterexample and thereafter, proof or argue it is not physically realizable after all. Every time another possible counterexample is found and disproved, this strengthens our belief in cosmic censorship, but it cannot be called a proof.

### 3.5.2 Overspinning a Kerr Black Hole

We saw in Section 2.3 that the solution to the Einstein equations for a rotating black hole is the Kerr metric, equation (2.3.4). It has an event horizon at  $r_H = M + \sqrt{M^2 - (J/M)^2}$ ,

if and only if  $a := J/M \leq M$ . However, for  $a > M$  it still satisfies the Einstein equations.

We start with an extremal black hole, i.e.  $a = M$ . One would think that if something is dropped in with enough angular momentum compared to its mass, the angular momentum of the new state becomes larger, such that  $a > M$ . If this could be done, we would end with a naked singularity, a violation of cosmic censorship.

We look at an object in the equatorial plane ( $\theta = \pi/2$ ) of the Kerr black hole, where the metric reduces to,

$$g_{\mu\nu} = \begin{pmatrix} -\left(1 - \frac{2M}{r}\right) & 0 & 0 & -\frac{2Ma}{r^2} \\ 0 & \frac{r^2}{\Delta} & 0 & 0 \\ 0 & 0 & r^2 & 0 \\ -\frac{2Ma}{r^2} & 0 & 0 & r^2 + a^2 + \frac{2Ma^2}{r} \end{pmatrix}, \quad (3.5.1)$$

where  $\Delta := r^2 - 2Mr + a^2$ .

The metric is independent of  $t$  and  $\phi$ , therefore we have two conserved quantities along a geodesic:

$$e := -\frac{1}{m} \frac{\partial \mathcal{L}}{\partial u^t} = -g_{t\mu} u^\mu = -g_{tt} u^t - g_{t\phi} u^\phi, \quad (3.5.2)$$

$$\ell := \frac{1}{m} \frac{\partial \mathcal{L}}{\partial u^\phi} = g_{\phi\mu} u^\mu = g_{\phi\phi} u^\phi + g_{\phi t} u^t, \quad (3.5.3)$$

with  $u^\mu := \frac{dx^\mu}{d\tau}$  the four-velocity. Because we can normalize the four-velocity we have, for timelike trajectories  $u \cdot u = -1$ ,

$$-1 = u \cdot u = g_{\mu\nu} u^\mu u^\nu = g_{tt}(u^t)^2 + 2g_{t\phi} u^\phi u^t + g_{\phi\phi}(u^\phi)^2. \quad (3.5.4)$$

Combining this with equations (3.5.2) and (3.5.3) and plugging in the metric (3.5.1), we find eventually

$$\frac{e^2 - 1}{2} = \frac{1}{2} \left( \frac{dr}{d\tau} \right)^2 + V_{\text{eff}}(r, e, \ell), \quad (3.5.5)$$

where the effective potential is

$$V_{\text{eff}}(r, e, \ell) = -\frac{M}{r} + \frac{\ell^2 - a^2(e^2 - 1)}{2r^2} - \frac{M(\ell - ae)^2}{r^3}. \quad (3.5.6)$$

If you threw a particle with rest mass  $m$  in, the mass of the black hole would increase by  $\delta M = me$ , the angular momentum would increase by  $\delta J = m\ell$ . The difference in  $a$  is then

$$\delta a = \frac{J + \delta J}{M + \delta M} - a = (J + \delta J) \frac{1}{M} \left( 1 - \frac{\delta M}{M} + O(\delta M^2) \right) - a$$

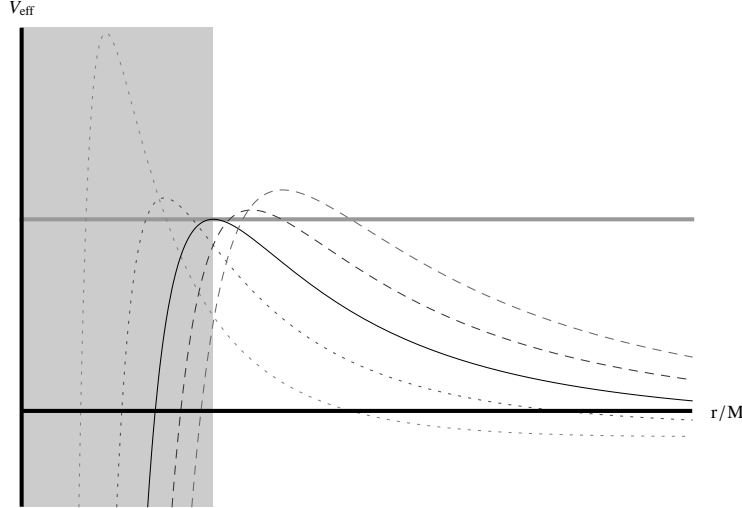


Figure 3.7: The effective potential (3.5.6) of an extremal Kerr Black hole for different values of  $\ell$ . We can see that for a particle with angular momentum  $\ell < 2Me$  (dotted lines) the effective potential is smaller than  $(e^2 - 1)/2$  (the solid gray line) everywhere outside the black hole (the gray region). For  $\ell > 2Me$  (dashed lines) there is a barrier which is too high to overcome outside the black hole, such that the particle will scatter. In the case of  $\ell = 2Me$  the potential at the horizon is just high enough to restrain the particle from falling in.

$$= \frac{1}{M}(\delta J - \delta Ma) = \frac{m}{M}(\ell - ae),$$

which is at the extremal case ( $a = M$ ) greater than  $\delta M$  if and only if  $\ell > 2Me$ . So we want to throw in a particle with rest mass  $m$  and angular momentum greater than  $2Me$  to blow off the horizon, but then the effective potential (3.5.6) has a maximum outside the horizon above  $(e^2 - 1)/2$  such that the particle will scatter off the black hole (figure 3.5.2).

### 3.5.3 Supercharging a Reissner-Nordström Black Hole

In a very similar way we attempt to drop a charged particle in a charged black hole, such that the horizon disappears. We saw in Section 2.2 that a charged black hole has metric (2.2.9) with an event horizon at  $r_H = M + \sqrt{M^2 - Q^2}$ , so we take the extremal case where  $Q = M$  as a starting point. We will look at a particle again in the equatorial plane and now infalling radially. With the Lagrangian of the particle of mass  $m$  and charge  $q$ ,

$$\mathcal{L} = \frac{1}{2}mg_{\mu\nu}u^\mu u^\nu + qA_\mu u^\mu,$$

with the field strength  $A_\mu = (Q/r, 0, 0, 0)$ . Because this metric is also time-independent, we can define the conserved quantity again,

$$e = -\frac{1}{m} \frac{\partial \mathcal{L}}{\partial u^t} = -g_{t\mu} u^\mu + \frac{q}{m} A_t = -g_{tt} u^t + g_{tt} \frac{qQ}{mr},$$

and use  $u \cdot u = -1$

$$-1 = u \cdot u = g_{\mu\nu} u^\mu u^\nu = g_{tt}(u^t)^2 + g_{rr}(u^r)^2,$$

from which we find

$$\frac{e^2 - 1}{2} = \frac{1}{2} \left( \frac{dr}{d\tau} \right)^2 + V_{\text{eff}},$$

with the effective potential

$$V_{\text{eff}}(r, q/m, e) = -\frac{M - Qeq/m}{r} + \frac{Q^2(1 - q^2/m^2)}{2r^2},$$

which in the extremal case, *i.e.*  $Q = M$  is

$$V_{\text{eff,extr}}(r, q/m, e) = -\frac{M}{r} \left( 1 - \frac{qe}{m} \right) + \frac{M^2}{2r^2} \left( 1 - \frac{q^2}{m^2} \right),$$

which has a maximum

$$V_{\text{eff,extr,max}}(q/m, e) = -\frac{1}{2} \frac{(1 - eq/m)^2}{1 - q^2/m^2}.$$

If we want to overcharge our extremal black hole, we should add a particle such that  $\delta Q > \delta M$ ,  $q > me$ , but for these values of  $q$ ,  $V_{\text{eff,extr,max}}(q/m, e) > \frac{e^2 - 1}{2}$ . Hence, a particle that is sufficiently charged to let the event horizon disappear will not fall into the black hole, because the repulsive electric force is larger than the attractive gravitational force. If you try to push harder, *e.g.* by attaching rockets to the particle, the energy and thus the mass will become higher, so this will not resolve your inability to overcharge an extremal charged black hole.

### 3.5.4 Censorship Violation in the Non-Homogeneous Dust Cloud

A famous example of a violation of cosmic censorship is found in the collapse of a spherical symmetric non-homogeneous dust cloud. For some density functions a light ray emanated

from the singular point at the origin of the collapsing dust cloud can escape to a distant observer.

We will use co-moving coordinates to describe this situation.  $R$  labels the infalling spherical dust shells and  $\tau$  is the proper time along the world lines of such shells. We choose the labels  $R$  such that at  $\tau = 0$ ,  $R$  equals the radius  $r(\tau, R)$  which is given by the parametric equation

$$r = \frac{R}{2}(1 + \cos \eta), \quad \tau = \sqrt{\frac{3}{32\pi a}}(\eta + \sin \eta),$$

with  $0 \leq \eta < \pi$  and

$$m(R) = 4\pi \int_0^R dS \rho(S) S^2, \quad a(R) = \frac{3m(R)}{4\pi R^3},$$

the initial mass distribution and mean density, respectively. For  $\eta = 0$  we are at the initial surface  $r = R$  and  $\tau = 0$ . The value  $\eta = \pi$  corresponds to the final singular surface, where  $r = 0$ , which is an essential singularity with

$$\tau_s(R) = \sqrt{\frac{3\pi}{32a(R)}}. \quad (3.5.7)$$

The metric of our space-time is

$$ds^2 = -d\tau^2 + \frac{r'^2}{1 - 2m/R} dR^2 + r^2 d\Omega^2,$$

and therefore an outgoing light ray satisfies

$$\frac{dR}{d\tau} = \frac{1}{r'} \sqrt{1 - \frac{2m}{R}}, \text{ and thus } \frac{dr}{d\tau} = \dot{r} + r' \frac{dR}{d\tau} = -\sqrt{\frac{2m}{r}} - \frac{2m}{R} + \sqrt{1 - \frac{2m}{R}}.$$

From this equation we see that for  $r$  greater (smaller) than  $2m$ , the light rays diverge (converge). Hence,  $r(\tau, R) = 2m(R)$  defines the turning points of the light rays, *i.e.* the apparent horizon

$$\tau_a(R) = \sqrt{\frac{3}{32\pi a(R)}} \left[ \arccos \left( \frac{4m(R)}{R} - 1 \right) + \sqrt{1 - \left( \frac{4m(R)}{R} - 1 \right)^2} \right].$$

This apparent horizon lies to the past of the singular surface of (3.5.7) for every  $R > 0$ , but for  $R = 0$  they are equal.

For weak cosmic censorship to be violated, a light ray should propagate from the singular surface to infinity. Therefore it should be earlier than the apparent horizon at the surface

of the cloud,  $R = R_0$ . Then it should be also earlier than the apparent horizon at all other  $0 < R < R_0$ . The only point on the singular surface where this light ray could have been emanated from is then the central point  $R = 0$ , where the singular surface and the apparent horizon coincide.

In the simplest case of a spherically symmetric homogeneous dust cloud no null geodesic emanated from the centre reaches spatial infinity. If we impose some conditions on the initial density however, such escaping light rays do exist. This was shown analytically by Christodoulou in 1984 [37] for an open set of spherically symmetric density functions  $\rho(R)$ . The few conditions he used all look physically very reasonable:

- If extended to the negative  $R$ -axis as an even function, the initial density distribution should be analytic everywhere;
- The density distribution must have compact support (there must be an  $R_0$  such that  $\rho(R) = 0$  for every  $R > R_0$ );
- In the initial dust cloud there is no horizon ( $2m(R) < R$  for all  $R$ );
- The density is ever decreasing ( $\rho'(R) < 0$  for all  $R > 0$ );
- The second derivative of the density at the centre is negative ( $\rho''(0) < 0$ ).

This might seem to indicate that the cosmic censorship conjecture is violated in Nature, but we have to take a closer look at the first assumption we made in the description of our model: it is made of dust, pressureless matter. Though this might be a good enough approximation in the initial matter cloud, when it is collapsing and the density is blowing up, the pressure is most likely not negligible any more. If we change dust for a perfect fluid,  $P = w\rho$ , Ori and Piran [38] showed that the existence of naked singularities depends on the value of  $w$ : if  $w > 0.011$  the naked singularities disappear. At this time we do not know whether we should rule out  $w < 0.011$  as being unphysical, because we do not know the equation of state of collapsing matter just before the formation of a singularity.

# Chapter 4

## No-hair Theorems

We have discussed the gravitational collapse that led us into black hole formation. In the following chapter we concern ourselves with the properties of a fully formed black hole and how we can describe such structures. For all purposes we must discuss the conjecture proposed by Wheeler in 1971 stating that quantum numbers such as baryon number or strangeness can have no place in the external description of a black hole [39]. This is now known as the statement that “black holes have no hair”. Originally inspired by Israel’s uniqueness theorems for Schwarzschild and Reissner-Nordström black holes [40] as well as the Kerr black hole uniqueness theorem by Carter and Wald [41], Wheeler figured that gravitational collapse would lead to a black hole described by its mass, charge and angular momentum and no other free parameters. The conjecture has long been regarded as a theorem by most, although no formal proof exists.

These unique parameters are all conserved quantities subject to a Gauss law which allows us to measure them from afar. One must also include the magnetic charge as a fourth parameter, but it is generally left out of discussion. We can obviously also make measurements of the position and momentum of the black hole, but these can be set to zero by choosing an appropriate reference frame and therefore they are not considered.

From here the need to probe for the existence or non-existence of “hair” arises. We define hair as any field not of gravitational or electromagnetic nature which is associated with the black hole. One may also define it as a set of free parameters which are not subject to a Gauss law. Finding the existence of solutions that allow the existence of hair would be interesting not just to disprove the conjecture, but also due to the fact that one cannot infer to the matter content of the black hole just by using the three parameters mentioned

by Wheeler.

In this chapter we will explore some examples for the non existence of hair in a variety of models, which are in agreement with the conjecture. The discussion of possible exceptions will also be done, however we shall see that these solutions are mostly unstable and do not qualify as sufficient to disprove the theorem. Finally we will discuss the probing of hair on a black hole with a cosmological background.

## 4.1 Bekenstein's Method

Many of the no-hair proofs for classical field theories utilize an elegant and powerful method first developed by Jacob Bekenstein [42]. We proceed to describe the formalism he used as well as his arguments so that we can apply it to some well known examples. In essence, it allows us to probe the behaviour of fields outside the event horizon.

We start by considering the exterior of a stationary black hole to be asymptotically flat, devoid of matter and any other fields that are not intrinsically associated to the black hole. These are standard assumptions since we will be dealing with Reissner-Nordström types.

Our asymptotically flat geometry is described by a coordinate system  $x^\mu$  spanning the black hole exterior and a metric tensor  $g_{\mu\nu}$  which is time independent. This metric reduces to flat space-time at infinity. The horizon is described by the equation  $F(x^i) = 0$ , where  $F$  is some function. Its normal  $n_\mu$ , given by  $n_\mu = \partial_\mu F$ , as well as its surface element  $dS_\mu$  have vanishing time components.

Now consider the action for a set of arbitrary local fields  $\Phi_k$  which are associated with the black hole exterior in a gravitational background:

$$S = \int d^4x \hat{\mathcal{L}} = \int d^4x \sqrt{-g} \mathcal{L}. \quad (4.1.1)$$

The variational principle  $\delta \int d^4x \sqrt{-g} \mathcal{L} = 0$  yields the familiar Euler-Lagrange equations. We then multiply them by  $d^4x \Phi_k$  and integrate by parts to get:

$$\sum_k \int_{\Omega} d^4x \partial_\mu \left[ \Phi_k \frac{\partial \mathcal{L}}{\partial(\partial_\mu \Phi_k)} \right] = \sum_k \int_{\Omega} d^4x \left[ \partial_\mu \Phi_k \frac{\partial \mathcal{L}}{\partial(\partial_\mu \Phi_k)} + \Phi_k \frac{\partial \mathcal{L}}{\partial \Phi_k} \right]. \quad (4.1.2)$$

The left side of this equation can be expressed as a surface integral  $\int_{\partial\Omega} dS_\mu b^\mu$ , where  $dS_\mu$  is the boundary element of the volume  $\Omega$  over which we integrate, and

$$b^\mu \equiv \sum_k \Phi_k \frac{\partial \mathcal{L}}{\partial(\partial_\mu \Phi_k)}. \quad (4.1.3)$$

Since we want to consider the admission of black hole solutions for our system and choose the four-volume where we integrate to be the black hole exterior, then  $\partial\Omega$  consists of the event horizon, spatial infinity as well as future and past timelike infinities. It is then important to infer on the behaviour of  $b^\mu$ . For all physically relevant fields it is easy to verify what happens through the use of the field equations and the asymptotic form of the metric. For massless fields,  $b^\mu$  vanishes asymptotically as  $1/r^3$  and for massive fields it vanishes exponentially<sup>1</sup>. Thus there are no contributions at spatial infinity to the left side of (4.1.2). Since  $dS_\mu$  is proportional to the hypersurface normal  $n_\mu$ , which we chose to satisfy  $n_i = 0$  as  $t \rightarrow \infty^2$ ,  $dS_\mu b^\mu$  will also vanish at timelike infinity when  $b^0 = 0$ . This condition for  $b^0$  is satisfied by static fields, therefore we have no non-horizon contributions to the surface integral in equation (4.1.2). From the fact that the horizon is a null hypersurface (satisfying the relation  $g_{ij}dS^i dS^j = 0$ ) and that  $g_{ij}$  is positive semi-definite on the horizon<sup>3</sup>, it can be shown that  $dS_\mu b^\mu$  vanishes on the boundary when  $b_\mu b^\mu$  is bounded there. Thus, for static fields with finite  $b_\mu b^\mu$  on the event horizon, equation (4.1.2) reduces to the following form:

$$\sum_k \int_{\Omega} d^4x \left[ \partial_\mu \Phi_k \frac{\partial \mathcal{L}}{\partial(\partial_\mu \Phi_k)} + \Phi_k \frac{\partial \mathcal{L}}{\partial \Phi_k} \right] = 0. \quad (4.1.4)$$

Having completed the formalism it is now clear how to probe for the non-existence of “hair”: if one can demonstrate that the integrand in (4.1.4) is negative or positive definite, then the only finite energy solutions satisfying the equation are those for which the integrand simply vanishes. For most physical Lagrangians, this implies that the fields must take on constant values over the black hole exterior, and so there is no hair.

We shall now use this method on some rather simple examples that establish the non existence of black hole hair, as shown by Bekenstein.

### 4.1.1 Scalar Fields

As a simple example, consider a massive, neutral and real valued scalar field  $\phi$ . The Lagrangian density used to describe this system is of the form

$$\mathcal{L} = -\frac{1}{2}(\partial_\mu \phi \partial^\mu \phi + m^2 \phi^2). \quad (4.1.5)$$

With the use of equation (4.1.2) we get the equation of motion

$$D_\mu D^\mu \phi - m^2 \phi = 0, \quad (4.1.6)$$

---

<sup>1</sup>This must be specifically seen according to the case that is being considered, although the procedure still involves simply plugging in the asymptotically flat form of the metric in the field equations.

<sup>2</sup>This is chosen so it is in agreement with staticity.

<sup>3</sup>See the Appendix.

which is simply the Klein-Gordon equation.

We find that the energy-momentum tensor is given by

$$T_{\mu\nu} = \partial_\mu \phi \partial_\nu \phi - \frac{1}{2} g_{\mu\nu} (\partial_\alpha \phi \partial^\alpha \phi + m^2 \phi^2). \quad (4.1.7)$$

Since we shall be dealing with the static case,  $\partial_0 \phi = 0$ , and  $T_{\mu\nu}$  is static. The expression (4.1.7) allows us to obtain the relations

$$\partial_\mu \phi \partial^\mu \phi = \sqrt{\frac{4}{3} (T_{\mu\nu} T^{\mu\nu}) - \frac{1}{3} T^2}, \quad (4.1.8)$$

and

$$m^2 \phi^2 = -\frac{1}{2} \sqrt{\frac{4}{3} (T_{\mu\nu} T^{\mu\nu}) - \frac{1}{3} T^2} - \frac{1}{2} T, \quad (4.1.9)$$

where  $T = g^{\mu\nu} T_{\mu\nu}$ .

We now point out that  $b^\mu = -\phi \partial_\mu \phi$  and therefore  $b^0 = 0$ . Relations (4.1.8) and (4.1.9) are used to verify our argument that  $b_\mu b^\mu = \phi^2 \partial_\mu \phi \partial^\mu \phi$  is bounded at the horizon<sup>4</sup>.

We then meet the criteria to vanish the right hand side of equation (4.1.2):

$$\int d^4x \sqrt{-g} (g_{ij} \partial^i \phi \partial^j \phi + m^2 \phi^2) = 0. \quad (4.1.10)$$

The spatial metric  $g_{ij}$  is positive definite in the black hole exterior at all times<sup>5</sup>. Therefore the above integral can only vanish if  $\phi$  goes to zero as well in the black hole exterior. This essentially means that the field  $\phi$  is in its ground state outside of the black hole and cannot be considered as a measurable quantity that characterizes the black hole, that is, it does not qualify as “hair”.

A treatment for the massless case is of increased subtlety. We take exactly the same equations computed above for the massive case but now set  $m = 0$ . Equation (4.1.9) will no longer insure that the quantity  $\phi^2$  is bounded at the event horizon. Also, equation (4.1.6) no longer has a mass term and determines  $\phi$  up to an additive constant. We impose the boundary condition ourselves:  $\phi$  should vanish at infinity and we interpret  $\phi^2$  as the invariant probability density for scalar mesons<sup>6</sup>.

<sup>4</sup>It is relevant to point out that physical scalars in general, and  $T$  and also  $T_{\mu\nu} T^{\mu\nu}$  in particular, are bounded on a non-singular horizon. An extensive discussion of this is made by Bekenstein in his original article: see reference [42].

<sup>5</sup>For now convince yourself of this statement; an extensive proof is present in the Appendix.

<sup>6</sup>The full argument for this interpretation is present in section VI of [42].

In this way, we can use exactly the same procedure as before and get that the field  $\phi$  must vanish outside the black hole in the same way as the massive scalar field. The additive constant mentioned above does not necessarily need to vanish, but it makes no appearance in any physical quantity, being unobservable. Since the massless field  $\phi$  is at its ground state outside the black hole, just like before, we establish the non-existence of hair for both classical massive and massless scalar fields. This result is in agreement with Wheeler's statement of the Israel-Carter conjecture.

### 4.1.2 Massive Vector Fields

The method that has been set out in the previous section will also be the guideline for the treatment of no-hair vector fields, following D. Bekenstein in his article *Nonexistence of Baryon Number for Static Black Holes* ([42]). The various assumptions made are still active and thus form the framework of our conclusion. We will first discuss a massive, neutral, real vector field  $B_\mu$ , followed by a massless vector field  $A_\mu$ . The latter will obviously correspond to the appearance of an electromagnetic field. Without jumping to conclusions it is clear that the Reissner-Nordström solution of Einsteins field equations represents a static, spherically symmetric black hole with an exterior electromagnetic field. Therefore we expect the treatment of the massless case to break down. In the final three sections we will consider a different Lagrangian, with general scalar couplings.

## Massive Vector Field

First we start by considering the Proca Lagrangian density

$$\mathcal{L} = F_{\mu\nu}F^{\mu\nu} - m^2B_\mu B^\mu,$$

where we take  $F_{\mu\nu} = \partial_\mu B_\nu - \partial_\nu B_\mu$ .

Just as in the scalar case we proceed by varying  $\mathcal{L}$  (Euler-Lagrange equations) and obtaining the Proca field equations

$$\partial_\nu F^{\mu\nu} + m^2 B^\mu = 0.$$

Since  $B_\mu$  is not subject to any gauge transformation, unlike  $A_\mu$  which we will encounter later on,  $B_\mu$  is a physical field.

In the scalar case we found the following equation

$$-\oint b^\mu dS_\mu + \sum_k \int (\partial_\mu \phi_k \frac{\partial \mathcal{L}}{\partial (\partial_\mu \phi_k)} + \phi_k \frac{\partial \mathcal{L}}{\partial \phi_k}) d^4x = 0.$$

where  $b^\mu = \sum_k \phi_k \frac{\partial \mathcal{L}}{\partial (\partial_\mu \phi_k)}$

Analogous to this scalar case we multiply the Proca field equations with  $B_\nu d^4x$ , integrate over the black-hole exterior, convert one term to a surface integral and use partial integration, to find:

$$-\oint b^\mu dS_\mu + \int (\partial_\mu B_\alpha \frac{\partial \mathcal{L}}{\partial (\partial_\mu B_\alpha)} + B_\alpha \frac{\partial \mathcal{L}}{\partial B_\alpha}) d^4x = 0,$$

which will take the following form:

$$-\oint b^\mu dS_\mu + \int (\partial_\mu B_\alpha) F^{\alpha\mu} d^4x - \int m^2 B_\alpha B^\alpha d^4x = 0, \quad (4.1.11)$$

where  $b^\mu = B_\alpha \frac{\partial \mathcal{L}}{\partial (\partial_\mu B_\alpha)} = B_\alpha F^{\mu\alpha}$ .

We want to apply the same reasoning as we did in the scalar case where we concluded that the boundary term is zero if  $b^\mu b_\mu$  is a physical scalar and if  $b^0 = 0$ . One way to see the boundary term vanish on the horizon is to assume regularity of  $B_\alpha F^{\mu\alpha}$  at the horizon. This means that the vector field and its derivative cannot be infinite at the horizon. The explicit way to see this is by trying to construct physical scalars from the energy-momentum tensor, e.g.  $T_{\mu\nu} T^{\mu\nu}$  and  $T_\mu^\mu$ . The energy-momentum tensor can be found using:

$$T_{\mu\nu} = \frac{-2}{\sqrt{-g}} \frac{\partial S}{\partial g^{\mu\nu}}.$$

In our case the energy-momentum tensor is given as follows:

$$T_{\mu\nu} = g_{\mu\nu} F_{\alpha\beta} F^{\alpha\beta} - 4F_\mu^\sigma F_{\sigma\nu} - m^2 g_{\mu\nu} B_\alpha B^\alpha + 2m^2 B_\mu B_\nu.$$

And we can construct a physical scalar from the energy-momentum tensor, for example:

$$T_\mu^\mu = g^{\mu\nu} T_{\mu\nu} = -2m^2 B_\alpha B^\alpha.$$

Now, using these equations, we can express  $B_\alpha F^{\mu\alpha}$  in physical scalars, which is left as an exercise for the reader. Thus,  $b^\mu b_\mu$  is a physical scalar and is bounded on the horizon. In the static case we have at hand here,  $b^0 = 0$ . Also assuming that  $b^\mu$  falls off as  $\frac{1}{r^3}$ , and following the same reasoning that is applied in the scalar case, the boundary term will then give a zero contribution at infinity. The conditions are met to conclude that the boundary term

is zero. A more mathematical explanation is given in the article by Eloy Ayo'n Beato ([43]).

The Proca Lagrangian has a few symmetries, one of which is time reversal, meaning it is invariant under:  $t \rightarrow -t$ . We assume this same time reversal symmetry in the metric and require it in the Proca field equations. In the metric this looks as follows:

$$dx^i dx^j \rightarrow dx^i dx^j, dt dt \rightarrow dt dt, dx^i dt \rightarrow -dx^i dt$$

Now writing the field equations explicitly we find:

$$-m^2 B^0 = \partial_0(\partial^0 B^0 - \partial^0 B^0) + \partial_i(\partial^0 B^i - \partial^i B^0),$$

and

$$-m^2 B^j = \partial_i(\partial^j B^i - \partial^i B^j).$$

These equations remain unchanged if  $B^i \rightarrow -B^i$  and if  $B^0 \rightarrow B^0$ . What follows is that  $F^{\mu\nu}$  will be invariant if (there are two ways to do this, we choose one)<sup>7</sup>  $F^{0i} \rightarrow F^{0i}$  and  $F^{ij} \rightarrow -F^{ij}$ . Since in this static situation it is required that no physical quantities should change, we can conclude that  $F^{ij} = 0$  and  $B^i = 0$ .

Let us now return to equation (4.1.11); the boundary term vanishes, the third term remains the same, but the second term we will rewrite.

$$(\partial_\mu B_\alpha) F^{\alpha\mu} = \partial_\mu B_\alpha \partial^\alpha B^\mu - \partial_\mu B_\alpha \partial^\mu B^\alpha = -\frac{1}{2}(\partial_\mu B_\alpha - \partial_\alpha B_\mu)(\partial^\mu B^\alpha - \partial^\alpha B^\mu) = -\frac{1}{2}F_{\mu\alpha}F^{\mu\alpha}.$$

Using this we can write (4.1.11) as follows:

$$\int \left( \frac{1}{2}F_{\mu\alpha}F^{\mu\alpha} + m^2 B_\alpha B^\alpha \right) d^4x = 0.$$

Since we concluded that  $F^{ij} = 0$  and  $B^i = 0$ , we can write:

$$\begin{aligned} \int \left( \frac{1}{2}F_{0i}F^{0i} + m^2 B_0 B^0 \right) d^4x &= 0, \\ \int g_{00} \left( \frac{1}{2}g_{ij}F^{0j}F^{0i} + m^2(B^0)^2 \right) d^4x &= 0. \end{aligned}$$

---

<sup>7</sup>The condition of time reversal invariance for Proca equations demands that the components  $B^0$  and  $F^{0i}$  remain unchanged while  $B^i$  and  $F^{ij}$  change sign, or the opposite scheme, i.e.,  $B^0$  and  $F^{0i}$  change sign as long as  $B^i$  and  $F^{ij}$  remain unchanged under time reversal. Therefore, for a time reversal invariant Proca field the components  $B^i$  and  $F^{ij}$  must vanish in the first case mentioned above, and the components  $B^0$  and  $F^{0i}$  vanish in the second one. Hence, time reversal invariance implies the existence of two separated cases: a purely electric case and a purely magnetic case.

In the second equation we introduced the metric. Since  $g_{ij} \geq 0$  and  $g_{00} < 0$  the integral will only vanish if  $F^{0i} = 0$  and if  $B^0 = 0$ . Because all the other components of these terms were already zero, we conclude that  $B^\mu$  is zero in the black-hole exterior.

## Massless Vector Field

Let's see what happens if we consider the massless case. Again we start from the Proca action leading to the Proca field equations:

$$\partial_\nu F^{\mu\nu} + m^2 B^\mu = 0.$$

Our field  $B_\mu$  is subject to a transformation:  $B_\mu \rightarrow B_\mu + \partial_\mu \phi$ . Here,  $\phi$  is a scalar function. Subsequently we see that the field  $F^{\mu\nu}$  is gauge invariant and the Proca field equations become:

$$\partial_\nu F^{\mu\nu} = -m^2(B^\mu + \partial^\mu \phi).$$

We can see that the transformation changes our field equations. When we then consider a massless vector field,  $m = 0$ , the right hand side will be zero, and the action and field equations will be unchanged by our gauge transformation. This results in making  $B^\mu$  an unphysical field. Yet, we know that the photon is the force carrier of the electromagnetic field and the Reissner-Nordström metric is a solution for the Einstein equations having exactly this massless field incorporated. This massless field makes the no hair theorem break down. The only known massless, neutral (abelian)<sup>8</sup> vector field is the electromagnetic field.

### 4.1.3 A Complex Scalar Field Minimally Coupled with Electromagnetism

Consider now the case of a charged (complex) scalar field  $\psi$  which is minimally coupled to an electromagnetic field described by a vector potential  $A_\mu$  and an associated electromagnetic tensor  $F_{\mu\nu}$ . Its Lagrangian density is of the form

$$\mathcal{L} = -(D^\alpha \psi D_\alpha \psi^* + m^2 \psi \psi^*) - \frac{F^{\mu\nu} F_{\mu\nu}}{16\pi}, \quad (4.1.12)$$

where  $D_\alpha \psi = \partial_\alpha \psi - ieA_\alpha \psi$  and  $e$  is simply the elementary charge. The energy-momentum tensor associated with  $\psi$  is then given by

$$T_{\mu\nu} = D_\mu \psi D_\nu \psi^* + D_\mu \psi^* D_\nu \psi - g_{\mu\nu} (D^\alpha \psi D_\alpha \psi^* + m^2 \psi \psi^*). \quad (4.1.13)$$

---

<sup>8</sup>Non-abelian gluon fields are also massless and have spin 1.

This theory is invariant under the gauge transformation

$$\psi \rightarrow \psi \exp(ie\Lambda), \quad A_\mu \rightarrow A_\mu + \partial_\mu \Lambda, \quad (4.1.14)$$

where  $\Lambda$  is an arbitrary real scalar function. This gauge invariance gives rise to a conserved electric current

$$j_\mu = ie(\psi D_\mu \psi^* - \psi^* D_\mu \psi). \quad (4.1.15)$$

Once again we consider the static case giving that  $\partial_0 A_0 = 0$ , and we can take the gauge choice  $A_i = 0$ . Staticity will also lead to  $j^i = 0$  and  $\partial_0 j^0 = 0$ . It then follows from equation (4.1.15) that  $\psi\psi^*$  must be time independent and the phase of  $\psi$  must be of the form  $\omega x^0 + \varphi$ , where  $\omega$  and  $\varphi$  are real constants. We can now make a second gauge transformation with  $\Lambda = -(\omega x^0 + \varphi)/e$  that makes  $\psi$  real and time-independent without making any change on our conditions for  $A_\mu$ <sup>9</sup>. We can then calculate  $b^\mu$  by doing the explicit sum in (4.1.3) over  $\psi$  and  $\psi^*$ , which gives  $b_\mu = -(\psi D_\mu \psi^* + \psi^* D_\mu \psi)$ . It is quite easy to see that  $b^0 = 0$  and  $b^i$  is real.

To show that  $b^\mu b_\mu$  is bounded to our horizon we once again go to the energy-momentum tensor (4.1.13) to obtain the following relations

$$T = -2D^\mu \psi D_\mu \psi^* - 4m^2 \psi \psi^* \quad (4.1.16)$$

and

$$T_{\mu\nu} T^{\mu\nu} = 2|D^\mu \psi D_\mu \psi|^2 + \frac{3}{4} T D^\mu \psi D_\mu \psi^* + \frac{1}{16} T^2 + \frac{1}{2} (D^\mu \psi D_\mu \psi^*)^2. \quad (4.1.17)$$

Since both  $T$  and  $T_{\mu\nu} T^{\mu\nu}$  are physical scalars they are bounded on the horizon by assumption. To make the statement that  $b^\mu b_\mu$  is indeed bounded on the horizon totally clear we proceed with a more thorough explanation: we see that both of the terms in equation (4.1.17) which are explicitly fourth order in  $D_\mu \psi$  are positive. It is therefore necessary that both  $D_\mu \psi D^\mu \psi$  and  $D^\mu \psi D_\mu \psi^*$  be bounded on the horizon since if either one of them or both became unbounded, the same would happen to  $T_{\mu\nu} T^{\mu\nu}$ . It then follows from equation (4.1.16) that  $\psi\psi^*$  is also bounded on the horizon. Recall that in our gauge  $\psi$  is real so that  $b^\mu b_\mu = \psi\psi^*(D^\mu \psi D_\mu \psi + D^\mu \psi^* D_\mu \psi^* + 2D^\mu \psi D_\mu \psi^*)$ .

Since all the necessary requirements are now met to apply our method, we can now write equation (4.1.4) in the form

$$\int d^4x \sqrt{-g} \left\{ g_{ij} \partial^i \psi \partial^j \psi + [m^2 + g_{00}(eA^0)^2] |\psi^2| \right\} = 0. \quad (4.1.18)$$

---

<sup>9</sup>Specifically,  $A_0$  gets shifted by a factor  $\omega$ .

The metric components satisfy  $g_{00} \leq 0$  and  $g_{ij}$  is positive definite in the black hole exterior. The integrand of equation (4.1.18) is not positive definite if  $A^0 \neq 0$ , however  $A^0$  must vanish in our gauge if the scalar field is present. This can be proven as follows: in our gauge we obtain from equation (4.1.15) that  $j^0 = -2e^2 A^0 |\psi^2|$ .  $|\psi^2|$  is interpreted as the invariant probability density for charged scalar mesons. Since  $\sqrt{-j^\mu j_\mu}$  is the invariant charge density we can see that the specific charge per meson of the field, given by  $\sqrt{-j^\mu j_\mu}/|\psi^2|$ , is also a physical scalar and must be bounded on the horizon. Since  $j^i = 0$ , the quantity  $g_{00}(A^0)^2$  is also bounded. The quantity  $F_{\mu\nu}F^{\mu\nu}$  is itself a physical scalar, and therefore for the static case,  $g_{00}g_{ij}F^{0i}F^{0j}$  will also be bounded.

Now we compute the sum (4.1.3) for the electromagnetic field over  $A_\mu$ , giving us  $b^\mu = -F^{\mu\nu}A_\nu/4\pi$  so that in our gauge  $b^0 = 0$ . From all these results it follows immediately that  $b^\mu b_\mu$  is bounded on the horizon. This allows us to use the formalism of (4.1.4) for the electromagnetic field;

$$\int d^4x \sqrt{-g} g_{00} (g_{ij} F^{0i} F^{0j} / 4\pi + 2(eA^0)^2 |\psi^2|) = 0. \quad (4.1.19)$$

From the properties of the metric it follows that the above integrand is negative definite in the black hole exterior, so the only way for it to vanish is for  $A^0$  to vanish throughout the exterior. Returning now to equation (4.1.18) we can see that its integrand is positive definite, so  $\psi$  must vanish identically over the entire black hole exterior. It follows from (4.1.14) that this is true up to a gauge choice, which is not obviously observable.

It is also possible to treat the case of an electrically neutral but complex scalar field in the way shown above by coupling  $\psi$  minimally to a fictitious  $A_\mu$  which is itself a gradient. This ghost field makes no contribution to any physical quantity by virtue of gauge invariance, but does allow us to take over our results for the charged scalar field.

We therefore conclude by stating that a static, bare black hole has no exterior scalar field of any type.

#### 4.1.4 Different Couplings to Scalar Field Functions

Consider the following Lagrangian:

$$\mathcal{L} = f(\phi) F_{\mu\nu} F^{\mu\nu} + g(\phi) \partial_\mu \phi \partial^\mu \phi - V(\phi).$$

In this section we will work out Bekenstein's theorem for the more general Lagrangian,

setting first  $f(\phi) = 0$ , then  $g(\phi) = 0$ , subsequently  $f(\phi) \neq 0$ ,  $g(\phi) \neq 0$ . Here  $f(\phi)$ ,  $g(\phi)$  and  $V(\phi)$  are functions of multiple scalar fields, not constant. We will try to find if hair is possible in each configuration, and whether there are any restrictions on the result.

### The case where $f(\phi) = 0$

In this configuration the Lagrangian has the following basic form:

$$\mathcal{L} = g(\phi)\partial_\mu\phi\partial^\mu\phi - V(\phi).$$

The equations of motion resulting from this Lagrangian are:

$$2\partial_\alpha(g(\phi)\partial^\alpha\phi) - \frac{\partial g(\phi)}{\partial\phi}\partial_\mu\phi\partial^\mu\phi + \frac{\partial V(\phi)}{\partial\phi} = 0.$$

We apply the same method as before: assuming only dependence on the radial component  $r$  of the scalar field, we multiply the equation by  $\phi$ , then we integrate from the boundary of the horizon,  $r_h$ , to infinity, and apply partial integration. From this we find the following equation:

$$-[\phi g(\phi)\partial^\alpha\phi]_{r_h}^\infty + \int_{r_h}^\infty d\rho \left( 2\partial_\mu\phi g(\phi)\partial^\alpha\phi - \phi \frac{\partial g(\phi)}{\partial\phi}\partial_\mu\phi\partial^\mu\phi + \phi \frac{\partial V(\phi)}{\partial\phi} \right) = 0.$$

When looking solely at the boundary term we note that since the scalar field only depends on  $\rho$  we can rewrite it as:

$$-[\phi g(\phi)\partial^\alpha\phi]_{r_h}^\infty = -[\phi g(\phi)g^{\rho\rho}\partial_\rho\phi]_{r_h}^\infty.$$

Then we can reason as before. Since we have by definition that  $g^{\rho\rho}$  at the boundary,  $r_h$ , is zero, the term is zero on the boundary. Also, if we look at this term at infinity, it is again zero. See the section on scalar fields for a full explanation.

We are left with the following equation:

$$\int_{r_h}^\infty d\rho \left( 2\partial_\mu\phi g(\phi)\partial^\alpha\phi - \phi \frac{\partial g(\phi)}{\partial\phi}\partial_\mu\phi\partial^\mu\phi + \phi \frac{\partial V(\phi)}{\partial\phi} \right) = 0.$$

Before, we tried to reason that the only way for this integral to be zero is for  $\phi$  to be zero. However, this reasoning breaks down in this case. Note that we now have an extra term

in the integral in comparison with the scalar case treated in a previous section. Of course, one way for the integral to vanish everywhere is when  $\phi = 0$ , and  $V(\phi)$  is of the form  $V(\phi^2)$  and obtains its extremum  $\frac{\partial V(\phi^2)}{\partial \phi^2} = 0$ , at  $\phi = 0$ . There are other ways. The second term in the integral can cancel the other two terms in the integral for some  $\phi(\rho)$ . Therefore we can not conclude that in the exterior of the black hole the scalar field takes some trivial form, constant or zero. This last result is obtained by considering a potential of any form. Also, the functions  $f(\phi) = 0$  and  $g(\phi)$  have no restrictions on them. From this result we can deduce that the possibility of finding scalar hair is present. This result, in any case, needs further research.

### The case where $g(\phi) = 0$

From this condition the Lagrangian takes the form:

$$\mathcal{L} = f(\phi)F_{\mu\nu}F^{\mu\nu} - V(\phi).$$

Again, we write the equations of motion. However, we now have equations of motion with respect to the scalar field  $\phi$  and with respect to the vector field  $A_\mu$ . Hence for the scalar field:

$$-\frac{\partial f(\phi)}{\partial \phi}F_{\mu\nu}F^{\mu\nu} + \frac{\partial V(\phi)}{\partial \phi} = 0,$$

and for the vector field:

$$\partial_\mu(F^{\mu\nu}f(\phi)) = 0.$$

We multiply the equation by  $\phi$  or  $A_\mu$  respectively, then we integrate from the boundary of the horizon,  $r_h$ , to infinity, and apply partial integration. From this we find the following two equations. For the scalar case, the Bekenstein procedure gives the following:

$$\int_{r_h}^{\infty} d\rho [\phi \frac{\partial f(\phi)}{\partial \phi} F_{\mu\nu}F^{\mu\nu} - \phi \frac{\partial V(\phi)}{\partial \phi}] = 0.$$

And in the case of  $A_\mu$  we find:

$$-[A_\mu F^{\mu\nu}f(\phi)]_{r_h}^{\infty} + \int_{r_h}^{\infty} d\rho \partial_\alpha A_\mu F^{\alpha\mu}f(\phi) = 0.$$

By reasoning the same way as in the complex scalar case discussed before, we can set the boundary term to zero in this last expression, leaving us with:

$$\int_{r_h}^{\infty} d\rho \partial_\alpha A_\mu F^{\alpha\mu}f(\phi) = 0.$$

Then by rewriting  $\partial_\alpha A_\mu F^{\alpha\mu}$  as  $-\frac{1}{2}F_{\alpha\mu}F^{\alpha\mu}$ , the equation looks like:  $\int_{r_h}^\infty d\rho -\frac{1}{2}F_{\alpha\mu}F^{\alpha\mu}f(\phi) = 0$ , from which we can conclude that  $F_{\mu\nu}$  has to be zero (we do not want to consider  $f(\phi) = 0$  here). Using this condition on the scalar equation (4.1.4), we end up with:

$$-\int_{r_h}^\infty d\rho \phi \frac{\partial V(\phi)}{\partial \phi} = 0.$$

So, the only way for the integral to be zero, is for  $\phi = 0$ . This implies no scalar hair in this case, if we have the condition that our potential  $V(\phi)$  is not constant. However, we only have a restriction on  $F_{\alpha\mu}$  and not on  $A_\mu$ , so we can not exclude in this case the possibility of finding hairy solutions for  $A_\mu \neq 0$ .

## The More General Lagrangian

In this section we combine our previously found results and try to see if it is possible to find hair using the more general Lagrangian:

$$\mathcal{L} = f(\phi)F_{\mu\nu}F^{\mu\nu} + g(\phi)\partial_\mu\phi\partial^\mu\phi - V(\phi).$$

Again we have two sets of equations of motion, one for the scalar field  $\phi$  and one for the vector field  $A_\mu$ . First consider the equations of motion for the scalar field for this Lagrangian:

$$\partial_\alpha(g(\phi)\partial^\alpha\phi) - \left( \frac{\partial f(\phi)}{\partial\phi}F_{\mu\nu}F^{\mu\nu} + \frac{\partial g(\phi)}{\partial\phi}\partial_\mu\phi\partial^\mu\phi - \frac{\partial V(\phi)}{\partial\phi} \right) = 0.$$

As we have seen multiple times by now, we apply Bekenstein's procedure and find the following equation for the scalar field in the exterior of the black hole:

$$-[\phi g(\phi)\partial^\alpha\phi]_{r_h}^\infty + \int_{r_h}^\infty d\rho \left( 2\partial_\alpha\phi g(\phi)\partial^\alpha\phi + \phi\left(\frac{\partial f(\phi)}{\partial\phi}F_{\mu\nu}F^{\mu\nu} + \frac{\partial g(\phi)}{\partial\phi}\partial_\mu\phi\partial^\mu\phi - \frac{\partial V(\phi)}{\partial\phi}\right) \right) = 0.$$

As we showed before, we can rewrite the boundary term in such a way that it includes a  $g^{\rho\rho}$ , which by definition is zero at the boundary. And since the fields fall off as  $\frac{1}{r}$  they vanish at infinity, such that our boundary term drops. This leaves:

$$\int_{r_h}^\infty d\rho \left( 2\partial_\alpha\phi g(\phi)\partial^\alpha\phi + \phi\left(\frac{\partial f(\phi)}{\partial\phi}F_{\mu\nu}F^{\mu\nu} + \frac{\partial g(\phi)}{\partial\phi}\partial_\mu\phi\partial^\mu\phi - \frac{\partial V(\phi)}{\partial\phi}\right) \right) = 0.$$

Lets now try to do the same for the vector field, starting with the equations of motion with respect to  $A_\mu$ , we immediately write the corresponding integral over the exterior and the boundary term:

$$-[A_\mu F^{\mu\nu} f(\phi)]_{r_h}^\infty + \int_{r_h}^\infty d\rho (\partial_\mu A_\alpha F^{\alpha\mu} f(\phi)) = 0.$$

For the same reasons as in the previous section, the boundary term drops. Then rewriting  $(\partial_\mu A_\alpha F^{\alpha\mu}) = -\frac{1}{2}F_{\alpha\mu}F^{\alpha\mu}$ , we can conclude that the only way this integral vanishes, is for  $F_{\alpha\mu} = 0$ . This however does not imply that  $A_\mu = 0$ . Now going back to our scalar equation, setting  $F_{\mu\nu} = 0$ , we find:

$$\int_{r_h}^\infty d\rho \left( 2\partial_\alpha \phi g(\phi) \partial^\alpha \phi + \phi \frac{\partial g(\phi)}{\partial \phi} \partial_\mu \phi \partial^\mu \phi - \phi \frac{\partial V(\phi)}{\partial \phi} \right) = 0.$$

This is exactly the same equation we found earlier. There we concluded that there are non-trivial forms of  $\phi$ , not constant nor zero, that could make this integral vanish. Thus it leaves the option to find scalar hair for this Lagrangian open. Additionally, since we cannot conclude that  $A_\mu$  is zero, there is a possibility to find vector hair.

## 4.2 No-hair theorem for Spinor Fields

In this section we will follow a very different but rather physical way of investigating the problem of black hole hair. It is based on the idea that the observable properties characterizing a black hole should normally be possible to be measured with an experiment, let it be the trajectory of a charged particle or the scattering off a black hole for instance.

As shown in the previous sections, massive vector fields induce a short-range Yukawa potential  $V_{Yukawa} \sim \frac{e^{-\mu r}}{r}$  and yield no-hair on the black hole. On the other hand, masslessness favors infinite range interactions. That's the case for the photon field which also charges the Kerr-Newman black hole. The rest of the quantum interactions of the Standard Model are significantly weak in magnitude and range. However, Wheeler's conjecture that a black hole carries no information about the fermionic identity of the imploded star is extremely hard to chew. A star consisting of an enormous number of leptons and baryons cannot just “delete” all of them to form a black hole. Could there be a way to check that? As proved by Feinberg and Sucher, there is a classical component of the weak interaction, mediated by the exchange of a virtual neutrino-antineutrino pair, that survives and propagates in large distances as they were considered massless in the 70's. More specifically, it is shown<sup>10</sup> that

---

<sup>10</sup>A complete treatment of this long range interaction can be found in [44].

the weak potential mediated between two static lumps of matter with leptonic numbers  $L_1$  and  $L_2$  is  $V(r) = \frac{G_W^2}{4\pi^3} \frac{L_1 L_2}{r^5}$ . However small the interaction, it could be used to deduce the lepton content of a star collapsing to a black hole. This renders checking if this flat space interaction survives in the background of a black hole quite interesting.

The physical question our model will try to answer is if matter decouples from interaction as it approaches the event horizon. To simplify things, matter's backreaction will be neglected so in practice we will have field perturbations in a standard Schwarzschild geometry<sup>11</sup>. In addition, while the force field will be quantized, the source will be treated classically, thus neglecting processes as pair production or annihilation. Calculations get also easier if the source will not be geodesically falling but quasistatically falling, thus reducing the full problem to a sequence of static identical problems.

On general grounds, the quantum field can always be written as

$$\psi(x) = \psi_{free}(x) + \tilde{\psi}(x)$$

where  $\psi_{free}(x)$  is the field propagating in curved background without any other external coupling while  $\tilde{\psi}(x)$  captures this external interaction. Namely,

$$\tilde{\psi}(x) = \int d^4x' \sqrt{-g(x')} S_R(x; x') J(x') \quad (4.2.1)$$

where  $J(x')$  is the classical source while  $S_R(x; x')$  is the retarded propagator in curved background.

The question of decoupling now is translated as the study of the limit of the above integral as the source is on the horizon, that is  $r' \rightarrow 2M$ . The conversation gets more specific in our case of right-handed neutrinos interacting with classical leptons. A covariant effective action<sup>12</sup> is

$$S = \int d^4x \sqrt{-g} [\bar{\psi} \gamma^\mu D_\mu \psi + i \frac{G_W}{\sqrt{2}} N_\mu(x) \bar{\psi} \gamma^\mu (1 + \gamma^5) \psi]$$

where  $\psi$  is a Dirac spinor and the vector potential  $N_\mu(x)$  describes the lepton current.

The equation of motion for  $\bar{\psi}$  reads

$$[\gamma^\mu(x) D_\mu + i \frac{G_W}{\sqrt{2}} \gamma^\mu(x) N_\mu(x) (1 + \gamma^5)] \psi = 0.$$

Equation (4.2.1) now is

$$\tilde{\psi}(x) = -i \frac{G_W}{\sqrt{2}} \int d^4x' \sqrt{-g(x')} S_R(x; x') \gamma^\mu(x') N_\mu(x') (1 + \gamma^5) \psi(x'),$$

---

<sup>11</sup>The Kerr-Newman case will be calculation-wise more involved but follows the same lines.

<sup>12</sup>To see how spinor fields couple covariantly to gravity you are referred to the Appendix A3.

which can be solved with a perturbative expansion. We will restrict to first order, namely we will calculate

$$\tilde{\psi}_1(x) = -i \frac{G_W}{\sqrt{2}} \int d^4x' \sqrt{-g(x')} S_R(x; x') \gamma^\mu(x') N_\mu(x') (1 + \gamma^5) \psi_{free}(x'), \quad (4.2.2)$$

with  $S_R(x; x')$  the retarded propagator satisfying the normal equation

$$\gamma^\mu(x) D_\mu S_R(x; x') = \delta^{(4)}(x - x') \mathbf{I}_{4 \times 4}, \quad (4.2.3)$$

with the boundary conditions discussed soon. For  $L$  leptons at rest on a spherical shell of radius  $R$  we have  $N_\mu(x) = L \delta_\mu^t \frac{\delta(r-R)}{r^2 \sin \theta}$ . Plugging this into (4.2.2)

$$\tilde{\psi}_1(x) = -iL \frac{G_W}{\sqrt{2}} \int d\theta' d\phi' \sqrt{^{(3)}g(R, \Omega')} S_R(x; R, \Omega', t') \gamma^t(R, \Omega') (1 + \gamma^5) \psi_{free}(R, \Omega', t') \quad (4.2.4)$$

where  $^{(3)}g_{\mu\nu}$  is the induced metric on the  $r = R$  hypersurface.

Suppressing the angular integration for notational convenience and exploiting the staticity of the set-up to Fourier transform time as

$$\begin{aligned} S_R(x; x') &= \int_{-\infty}^{+\infty} \frac{d\omega}{\sqrt{2\pi}} S_R(\vec{x}; \vec{x}'; \omega) e^{-i\omega(t-t')}, \\ \psi(x') &= \int_{-\infty}^{+\infty} \frac{d\omega}{\sqrt{2\pi}} \psi(\vec{x}'; \omega) e^{-i\omega t'}, \end{aligned}$$

the previous equation reads

$$\tilde{\psi}_1(x) = -iL \frac{G_W}{\sqrt{2}} \int_{-\infty}^{+\infty} d\omega e^{-i\omega t} \sqrt{^{(3)}g(R')} S_R(\vec{x}; R; \omega) \gamma^t(R) (1 + \gamma^5) \psi_{free}(R; \omega). \quad (4.2.5)$$

Formulation of the boundary conditions on the retarded propagator in a general spherical symmetric black hole metric such as

$$ds^2 = -f(r) dt^2 + \frac{1}{f(r)} dr^2 + r^2 d\Omega_2^2$$

is facilitated by using the ‘‘tortoise coordinate’’  $r^* = \int \frac{dr}{f(r)} \Big|_{f(r)=1-2M/r} = r + 2M \ln(\frac{r}{2M} - 1)$ , which extends the problem to the entire  $r^*$  real line.

The desired behavior of the retarded Green’s function of a massless field at the space boundaries is

$$S_R(\vec{x}, \vec{x}'; \omega) \underset{r^* \rightarrow \pm\infty}{\overset{\omega \geq 0}{\sim}} \begin{cases} \exp[i(\omega^2)^{1/2}|r^*|], & \omega^2 > 0 \\ \exp[-(-\omega^2)^{1/2}|r^*|], & \omega^2 < 0 \end{cases}$$

The exponential damping for superluminal propagation is a general property required for physical Green's functions. The wave-like propagation for  $\omega^2 > 0$  corresponds to the specific retarded Green's function.

Since we seek expressions for  $S_R$  and  $\psi_{free}$  we need to solve their differential equations. To begin with, the source-free ( $N_\mu = 0$ ) and massless Dirac equation in curved spacetime is

$$\gamma^\mu(x)D_\mu\psi(x) = 0 \rightarrow \gamma^\mu(x)[\partial_\mu + \Gamma_\mu(x)]\psi(x) = 0. \quad (4.2.6)$$

where the connection is  $\Gamma_\mu = \frac{1}{8}[\gamma^a, \gamma^b]e_a^\nu[\partial_\mu e_{b\nu} - \Gamma_{\mu\nu}^\sigma e_{b\sigma}]$ . One can easily derive the frame fields

$$e_a^\mu = \text{diag}\left[\frac{1}{\sqrt{f(r)}}, \sqrt{f(r)}, \frac{1}{r}, \frac{1}{r \sin \theta}\right].$$

The general coordinate gamma matrices are

$$\gamma^t = \frac{1}{\sqrt{f(r)}}\gamma^0, \gamma^r = \sqrt{f(r)}\gamma^1, \gamma^\theta = \frac{1}{r}\gamma^2, \gamma^\phi = \frac{1}{r \sin \theta}\gamma^3.$$

We choose the following representation of the Clifford Algebra

$$\gamma^0 = \begin{pmatrix} -i & 0 \\ 0 & i \end{pmatrix}, \gamma^i = \begin{pmatrix} 0 & -i\sigma^i \\ i\sigma^i & 0 \end{pmatrix}, \gamma^5 = i\gamma^0\gamma^1\gamma^2\gamma^3 = \begin{pmatrix} 0 & 1 \\ 1 & 0 \end{pmatrix}.$$

Consequently, the connection coefficients are

$$\Gamma_t = \frac{1}{4}f'(r)\gamma_0\gamma_1, \Gamma_r = 0, \Gamma_\theta = \frac{1}{2}\sqrt{f(r)}\gamma_1\gamma_2, \Gamma_\phi = \frac{1}{2}[\sin\theta\sqrt{f(r)}\gamma_1 + \cos\theta\gamma_2]\gamma_3.$$

Substituting this in (4.2.6)

$$\left[ -\frac{\gamma_0}{\sqrt{f}}\partial_t + \sqrt{f}\gamma_1\left(\partial_r + \frac{1}{r} + \frac{f'}{4f}\right) + \frac{\gamma_2}{r}\left(\partial_\theta + \frac{\cot\theta}{2}\right) + \frac{\gamma_3}{r \sin\theta}\partial_\phi \right]\psi = 0,$$

making the transformation  $\psi(x) = \frac{f^{-\frac{1}{4}}(r)}{r}\Phi(x)$ , and using the tortoise coordinate  $r^*$  we get

$$\left[ -\frac{\gamma_0}{\sqrt{f}}\partial_t + \frac{\gamma_1}{\sqrt{f}}\partial_{r^*} + \frac{\gamma_2}{r}\left(\partial_\theta + \frac{\cot\theta}{2}\right) + \frac{\gamma_3}{r \sin\theta}\partial_\phi \right]\Phi = 0.$$

Looking for positive energy solutions and definite  $(k, m)$  states<sup>13</sup>

$$\Phi(x) = e^{-i\omega t} \begin{pmatrix} F_k(r)\chi_k^m(\theta, \phi) \\ G_k(r)\chi_{-k}^m(\theta, \phi) \end{pmatrix}.$$

---

<sup>13</sup>To be more specific,

$$\chi_k^m(\theta, \phi) = \begin{pmatrix} \sqrt{\frac{j+m}{2j}}Y_l^{m-\frac{1}{2}}(\theta, \phi) \\ \sqrt{\frac{j-m}{2j}}Y_l^{m+\frac{1}{2}}(\theta, \phi) \end{pmatrix} \text{ for } j = l + \frac{1}{2}, k = j + \frac{1}{2}$$

The reason for using the new integer quantum number<sup>14</sup>  $k$  is for practical convenience as it summarizes the total angular momentum  $j$  and the parity  $(-1)^l$  into

$$j = |k| - \frac{1}{2}, \text{ parity} = (-1)^{j+\frac{\text{sgn}(k)}{2}}.$$

More specifically, while  $\mathbf{s}^2$ ,  $\mathbf{j}^2$ ,  $j_z$  and not  $\mathbf{l}^2$  commute with the Dirac Hamiltonian, the operator  $k = \gamma^0(\mathbf{l}\cdot\mathbf{s} + 1)$  commutes with  $\vec{j}$  and relates with parity in the manner above. Parity in the presence of the weak interaction is not a good quantum number but chirality is. For practical simplicity we will turn to the chirality basis only in the end of the whole calculation.

The resulting equations are

$$\begin{aligned}\frac{dF}{dr^*} &= -\frac{k}{r}\sqrt{f(r)}F + \omega G, \\ \frac{dG}{dr^*} &= \frac{k}{r}\sqrt{f(r)}G - \omega F.\end{aligned}$$

Differentiating once more we decouple the two variables

$$\frac{d^2F}{dr^{*2}} + [\omega^2 - V_k(r^*)]F = 0, \quad (4.2.7)$$

$$\frac{d^2G}{dr^{*2}} + [\omega^2 - V_{-k}(r^*)]G = 0, \quad (4.2.8)$$

without ever forgetting that  $G = \frac{1}{\omega} \left[ \frac{dF}{dr^*} + \frac{k}{r}\sqrt{f}F \right]$ .

Now we have a scattering problem (4.2.7) in the real line  $-\infty < r^* < +\infty$  with effective potential

$$V_k(r^*) = \left(1 - \frac{2M}{r}\right)^{\frac{1}{2}} \left[ \frac{k^2}{r^2} \left(1 - \frac{2M}{r}\right)^{\frac{1}{2}} + \frac{k}{r^2} \left(1 - \frac{2M}{r}\right) + \frac{M}{r^3} \right]$$

where we explicitly used the Schwarzschild metric  $f(r) = 1 - \frac{2M}{r}$ .

and

$$\chi_{-k}^m(\theta, \phi) = \begin{pmatrix} \sqrt{\frac{j+1-m}{2j+2}} Y_l^{m-\frac{1}{2}}(\theta, \phi) \\ -\sqrt{\frac{j+1+m}{2j+2}} Y_l^{m+\frac{1}{2}}(\theta, \phi) \end{pmatrix} \text{ for } j = l - \frac{1}{2}, k = -j - \frac{1}{2}$$

define the spinor harmonics

$$\mathcal{Y}_{k,m}(\theta, \phi) = \begin{pmatrix} \chi_k^m(\theta, \phi) \\ \chi_{-k}^m(\theta, \phi) \end{pmatrix}$$

which satisfy the eigenvalue equation

$$\left[ \gamma_2 \left( \partial_\theta + \frac{\cot\theta}{2} \right) + \frac{\gamma_3}{\sin\theta} \partial_\phi \right] \mathcal{Y}_{k,m}(\theta, \phi) = ik \mathcal{Y}_{k,m}(\theta, \phi).$$

<sup>14</sup>Details to be found in [45].

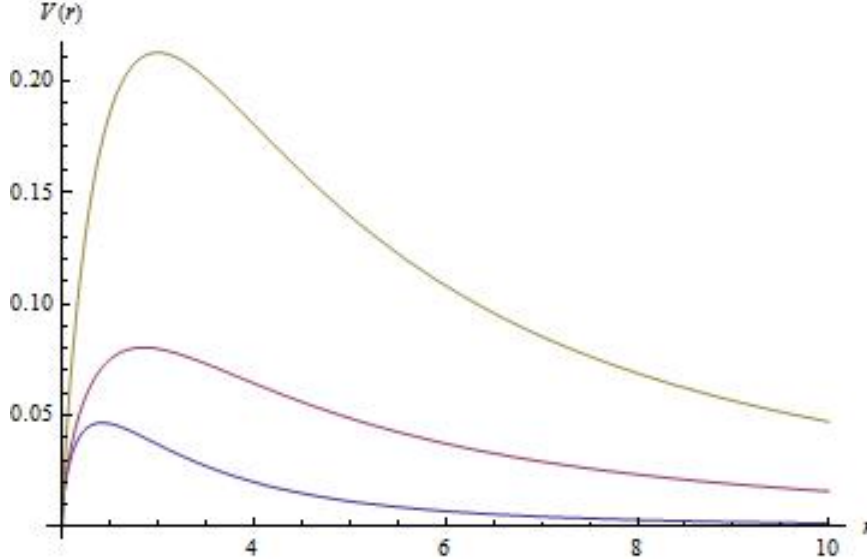


Figure 4.1: Plot of  $V_k(r)$  for  $M = 1$  and  $k = 2, 1$  and  $-1$  in order of decreasing  $V$ .

Equation (4.2.7) has two linearly independent solutions and the vanishing of  $V_k$  at the asymptotic regions enables us to formulate them as two different scattering scenarios and assign two quantum numbers<sup>15</sup>  $\alpha = \pm$ : at the first a neutrino wave is coming from the horizon ( $\alpha = +$ ) which reflects back to  $r^* \rightarrow -\infty$  and transmits partially to infinity:

$$F_{k\omega}^{(+)} = \begin{cases} e^{i\omega r^*} + R_k^{(+)}(\omega) e^{-i\omega r^*}, & r^* \rightarrow -\infty \\ T_k^{(+)}(\omega) e^{i\omega r^*}, & r^* \rightarrow +\infty \end{cases}$$

At the second case we have a neutrino incoming from spatial infinity ( $\alpha = -$ ):

$$F_{k\omega}^{(-)} = \begin{cases} T_k^{(-)}(\omega) e^{-i\omega r^*}, & r^* \rightarrow -\infty \\ e^{-i\omega r^*} + R_k^{(-)}(\omega) e^{i\omega r^*}, & r^* \rightarrow +\infty \end{cases}$$

Through the relation between  $F$  and  $G$  one easily shows that  $iG_{k\omega}^{(\alpha)} = -\alpha F_{-k\omega}^{(\alpha)}$  and consequently  $T_k^{(+)} = T_k^{(-)} = T_{-k}^{(\pm)} \equiv T_k$  and  $R_k^{(\alpha)} = -R_{-k}^{(\alpha)}$ .

Finally, we obtain the full set of solutions of the Dirac equation with energy  $\omega$

$$\psi_{km\omega}^{(\alpha)}(\vec{x}) = \left(1 - \frac{2M}{r}\right)^{-\frac{1}{4}} \frac{1}{r} \begin{pmatrix} F_{k\omega}^{(\alpha)} \chi_k^m \\ -\alpha F_{-k\omega}^{(\alpha)} \chi_{-k}^m \end{pmatrix}.$$

Now the neutrino field has an eigenmodes expansion in creation and annihilation operators

$$\psi_{free}(x) = (8\pi)^{-1} \sum_{km\alpha} \int_0^{+\infty} d\omega [e^{-i\omega t} \psi_{km\omega}^{(\alpha)}(\vec{x}) b_{km\omega}^{(\alpha)} + e^{i\omega t} \psi_{km,-\omega}^{(\alpha)}(\vec{x}) d_{km\omega}^{(\alpha)\dagger}]. \quad (4.2.9)$$

<sup>15</sup>This quantum number exists in contrast with flat space where regularity of the solutions is required at the origin.

The field is quantized with anticommutation relations on an equal-time spacelike hypersurface

$$\{\psi_a(\vec{x}, t), \psi_b^\dagger(\vec{x}', t)\} = \delta_{ab}\delta(\vec{x} - \vec{x}')^{(3)}g^{-\frac{1}{2}}$$

yielding the fermionic creation-annihilation algebra on the operators

$$\{b_{km\omega}^{(\alpha)}, b_{k'm'\omega'}^{(\alpha')\dagger}\} = \{d_{km\omega}^{(\alpha)}, d_{k'm'\omega'}^{(\alpha')\dagger}\} = \delta_{\alpha\alpha'}\delta_{kk'}\delta_{mm'}\delta(\omega - \omega')$$

with all the rest vanishing, therefore  $b$  annihilates a neutrino and  $d^\dagger$  creates an antineutrino.

Besides the expansion for  $\psi_{free}$ , we need an expansion for  $S_R$  in terms of the free solutions above. From (4.2.3) it is clear that  $S_R$  will be discontinuous at the singularity at  $x'$ . The solutions to this equation which satisfies the boundary conditions have branches

$$S_R(\vec{x}; \vec{x}'; \omega) = \sum_{k,m} \begin{cases} \psi_{km\omega}^{(+)}(\vec{x})\phi_{km\omega}^{(-)\dagger}(\vec{x}'), & r^* > r^{*\prime} \\ \psi_{km\omega}^{(-)}(\vec{x})\phi_{km\omega}^{(+)\dagger}(\vec{x}'), & r^* < r^{*\prime} \end{cases} \quad (4.2.10)$$

with the spinor  $\phi$  defined as

$$\phi_{km\omega}^{(\alpha)} = \left(1 - \frac{2M}{r}\right)^{-\frac{1}{4}} \frac{1}{r} [2iT_k^*(\omega)]^{-1} \begin{pmatrix} F_{k\omega}^{(\alpha)*} \chi_k^m \\ -\alpha F_{-k\omega}^{(\alpha)*} \chi_{-k}^m \end{pmatrix}.$$

We are ready to calculate the first order correction  $\tilde{\psi}_1$  to the neutrino field by plugging (4.2.9),(4.2.10) into (4.2.5), restore the angular integration and use the orthonormality relation  $\int d\Omega \chi_k^{m\dagger} \chi_{k'}^{m'} = \delta_{kk'} \delta_{mm'}$ . The result is cutely neat

$$\begin{aligned} \tilde{\psi}_1(x) = & -iL \frac{G_W}{\sqrt{2}} (16\pi R^2)^{-1} \int_0^{+\infty} d\omega \sum_{km\alpha} [T_k(\omega)]^{-1} [F_{k\omega}^{(-)}(R)F_{k\omega}^{(\alpha)}(R) + \alpha F_{-k\omega}^{(-)}(R)F_{k\omega}^{(\alpha)}(R)] \times \\ & \times \{e^{-i\omega t} [\psi_{km\omega}^{(\alpha)}(\vec{x}) - \psi_{-km\omega}^{(\alpha)}(\vec{x})] b_{km\omega}^{(\alpha)} + e^{i\omega t} [\psi_{km-\omega}^{(\alpha)}(\vec{x}) - \psi_{-k,m,-\omega}^{(\alpha)}(\vec{x})] d_{km\omega}^{(\alpha)\dagger}\}. \end{aligned} \quad (4.2.11)$$

We will be interested to what happens when the lepton source sits near the horizon, that is  $R \rightarrow 2M$  or  $r^{*\prime} \rightarrow -\infty$ . Hartle [46] has shown that  $F_{k\omega}^{(-)}(R) \xrightarrow{R \rightarrow 2M} T_k(\omega)e^{-i\omega R}[1 + \mathcal{O}(\sqrt{1 - \frac{2M}{R}})]$ . It follows that the  $\alpha = -$  term in (4.2.11) will die as  $\sqrt{1 - \frac{2M}{R}}$ . On the other hand, the  $\alpha = +$  term gives a finite contribution and in total we have a residual value for  $\tilde{\psi}_1$

$$\begin{aligned} \lim_{R \rightarrow 2M} \tilde{\psi}_1(x) = & -iL \frac{G_W}{\sqrt{2}} (8\pi M^2)^{-1} \sum_{km} \int_0^{+\infty} d\omega [e^{-i\omega t} (\psi_{km\omega}^{(+)}(\vec{x}) - \psi_{-km\omega}^{(+)}(\vec{x})) b_{km\omega}^{(+)} \\ & + e^{i\omega t} (\psi_{km-\omega}^{(+)}(\vec{x}) - \psi_{-km-\omega}^{(+)}(\vec{x})) d_{km\omega}^{(+)\dagger}]. \end{aligned}$$

Finally, we switch to chirality states  $\lambda = \pm 1$  by defining the normalized states  $\psi_{jm\lambda\omega}^{(+)} = \frac{\psi_{km\omega}^{(+)} - \psi_{-km\omega}^{(+)}}{\sqrt{2}}$  and normalized annihilation operators  $b_{jm\lambda\omega}^{(+)} = \frac{b_{km\omega}^{(+)} - b_{-km\omega}^{(+)}}{\sqrt{2}}$  and  $d_{jm\lambda\omega}^{(+)} = \frac{d_{km\omega}^{(+)} - d_{-km\omega}^{(+)}}{\sqrt{2}}$ .

Ultimately, only positive chirality states survive

$$\lim_{R \rightarrow 2M} \tilde{\psi}_1(x) = -iL \frac{G_W}{\sqrt{2}} (4\pi M^2)^{-1} \sum_{\substack{jm \\ \lambda=+1}} \int_0^{+\infty} d\omega [e^{-i\omega t} \psi_{jm\lambda\omega}^{(+)} b_{jm\lambda\omega}^{(+)} + e^{i\omega t} \psi_{jm\lambda-\omega}^{(+)} d_{jm\lambda\omega}^{(+)\dagger}]. \quad (4.2.12)$$

So for a spherical source situated at the event horizon, only the positive chirality part of the incoming from the horizon neutrino field gets modified. More specifically, by contrasting the zeroth order to the weak coupling field

$$\psi_{free}(x) = (4\pi)^{-1} \sum_{jm\lambda\alpha} \int_0^{+\infty} d\omega [e^{-i\omega t} \psi_{jm\lambda\omega}^{(\alpha)}(\vec{x}) b_{jm\lambda\omega}^{(\alpha)} + e^{i\omega t} \psi_{jm\lambda,-\omega}^{(\alpha)}(\vec{x}) d_{jm\lambda\omega}^{(\alpha)\dagger}]$$

with (4.2.12) it follows that the  $\alpha = +, \lambda = +1$  states get just augmented by a factor of  $-iL \frac{G_W}{\sqrt{2}M^2}$ . Iterating this first order perturbative correction we conclude that this part of the neutrino field is multiplied by a constant phase factor  $\text{Exp}[-i \frac{G_W}{\sqrt{2}M^2}]$ .

Even though the neutrino field does not decouple from the source, this field phase shift is not observable because in any general coordinate bilinear quantity of physical relevance, such as the potential  $\langle 0 | \bar{\psi}(x) \gamma^\mu(x) (1 + \gamma^5) \psi(x) | 0 \rangle$ , will yield identity. Thus, the residual field cannot be detected in the vacuum. Thereafter the lepton properties, if any, of a Schwarzschild black hole are not measurable. On the contrary, they should be “hidden” and not counted as the hair we already know. The result is also not significantly altered when taking into account higher-order corrections because they only give non-trivial contributions such as frequency-dependent phase factor, which would cause a time delay in neutrino scattering.

To conclude, the same method based on the concept of near-horizon decoupling has been applied to other kind of fields, proving that scalars and massive vector fields do decouple from sources on the horizon as  $\sqrt{1 - \frac{2M}{R}}$  and  $(1 - \frac{2M}{R})$  respectively. On the other hand, a massless vector field does not decouple thanks to gauge invariance and the Gauss Law. Those results support our treatment as being complementary to the one used in the previous section.

### 4.3 Hairy Black Hole Solutions

This section is devoted to the analysis and explanation of counter-examples on the original no-hair conjecture. Ever since the 70's when the conjecture was formed, people have contemplated on proofs. Some special cases have been explicitly shown above, but even the most general of proofs make certain assumptions, usually about the form of the action. This intrigued people to try and find counter-examples of the no hair theorem, i.e. hairy solutions (or just hair) as we shall call them hence forth. Not much had been done, until suddenly in the early 90's a plethora of hairy solutions was discovered. Since then more than 20 years have passed and it has been shown that hairy solutions are present with any kind of fields (scalars, vectors, fermions etc.).

In order to make sense out of this abundance of literature, we will attempt a kind of categorization and further discuss specific educative examples. We will be restricted to models with scalar fields and/or vector fields. First, we want to group together all gauge fields, Abelian like electromagnetism or non-Abelian like the Yang Mills fields, which were the main block of the hairy solutions discovered during the early 90s [47, 48, 49, 50, 51, 52]. From these 90s references, reference [53] with Skyrme hair is of particular importance, since it is a hairy example that you can find and is not an unstable solution [53] hence it is a true counter example (another nice example of stable hair, although not asymptotically flat, is that of global monopole [54]). We will not treat those examples because of their complexity.

A general remark is in order before we go into details in some educative examples. The no hair conjecture is conceptually connected to black hole thermodynamics, since if we would have a small finite amount of parameters that characterized our black hole, we could associate an entropy to it. That is why we are looking for static and stable solutions, since they would be the equivalent of equilibrium states of thermodynamics. Because unstable solutions will decay into stable ones, they cannot correspond to equilibrium thermodynamic states, as a result they do not really limit the conjecture. Also, we want to mention that in the literature there are some solutions with non-zero fields outside the event horizon, but measuring them does not give any information about the black hole. So the fields do not characterize the black hole, but rather the space time outside the black hole. This categorizes them as “dressing”, or secondary hair when the value of the field is dependent only on  $Q$  and  $M$ , which is not true hair. True hair or “primary hair”, as they are often called in literature, are hairy solutions which add at least one more independent parameter in our black hole solution. The distinction is made because if you do not get any extra

information from the fields about the structure of the black hole, the “entropy” remains unchanged.

### 4.3.1 BBM(B) Model

A really pedagogical hairy solution is that of the BBM(B) model, named after Bocharova, Bronnikov and Melnikov, who first discovered it [55]. The paper was in Russian and unknown to the west, so some time after them Bekenstein rediscovered the solution (hence the B in parenthesis). What characterizes this kind of solution is that the field is singular at the horizon. The generic action for an Abelian scalar field theory is

$$S = S_{EHM} - \frac{1}{2} \int d^4x \sqrt{-g} [(D_\alpha \psi)(D^\alpha \psi)^* + \xi R \psi^* \psi + V(\psi^* \psi)] . \quad (4.3.1)$$

Where  $S_{EHM}$  is the standard Einstein-Hilbert-Maxwell action used previously (2.2.1). Now this action, for the specific value of the conformal coupling  $\xi = 1/6$  has the following solution

$$ds^2 = -(1 - M/r)^2 dt^2 + (1 - M/r)^{-2} dr^2 + r^2 d\Omega^2, \quad (4.3.2)$$

$$F_{\mu\nu} = Qr^{-2}(\delta_\mu^r \delta_\nu^t - \delta_\mu^t \delta_\nu^r) \text{ for } Q < M, \quad (4.3.3)$$

$$\psi = \pm(3/4\pi)(M^2 - Q^2)^{1/2}(r - M)^{-1}. \quad (4.3.4)$$

Remember that since we are looking for counter examples it is just enough to make an *ansatz* and then check that it satisfies the equations of motion. One can easily verify that in our case. A useful remark here is that the metric form (4.3.2) is very similar to that of the ordinary Schwarzschild solution, apart for the square in the first two terms and the fact that the horizon is at  $r = M$  and not at  $r = 2M$ .

When looking at this solution, two comments are in order. First, one might wonder why this solution qualifies as a counter example, since its only parameters are the  $M$  and  $Q$ , which is in compliance with the no-hair conjecture. On a closer inspection though one notices the  $\pm$  in front of the scalar field which is a dichotomic parameter but still represents some freedom in our solution even if it is discontinuous and discrete. Second, when inspecting the form of the scalar field, one observes that it is divergent at the horizon  $r = M$ , after which we are tempted to say, that, by virtue of the divergence, our solution is non-physical. It turns out that this is wrong; in order to conclude that a solution is non-physical we have to actually think of a physical observable that would be divergent or a thought-experiment that will give physically unacceptable results. It turns out that for our solution every experiment we expected to go wrong does not and we mention three

illustrative examples, the first two of which we work out. Trajectories of (charged or not) particles do not terminate abruptly; in finite proper time, particles coupled to the scalar field do not encounter an infinite potential barrier and finally, it can also be proven that tidal forces between pairs of nearby trajectories do not diverge. We look for all that on the horizon, since that is where the field diverges; hence where one would expect non-physical results. Also, using the obvious similarity of our solution to a Reissner-Nordstrom black hole. we only need to check what happens for particles with scalar charge. We will now proceed proving some of the statements.

We start by specifying the action for the test particle coupled to the scalar field

$$S = - \int d\lambda (\mu + f\psi) \left( -g_{\alpha\beta} \frac{dx^\alpha}{d\lambda} \frac{dx^\beta}{d\lambda} \right)^{1/2}, \quad (4.3.5)$$

so  $\mu$  is the rest mass of the particle and  $f$  is the coupling to the scalar field  $\psi(x)$  (scalar charge of the particle). This action is the most natural one (it is like the minimal coupling of electromagnetism). It is the simplest coupling that is invariant under the same symmetries as the free field action [56]. Varying the action with respect to  $x$  gives

$$(\mu + f\psi) \frac{D^2x^\nu}{d\lambda^2} = \left[ \frac{1}{2} (\mu + f\psi) \frac{d}{d\lambda} \ln A - f \partial_\alpha \psi \frac{dx^\alpha}{d\lambda} \right] \frac{dx^\nu}{d\lambda} - f A \partial^\nu \psi, \quad (4.3.6)$$

$$\text{where } A = -g_{\alpha\beta} \frac{dx^\alpha}{d\lambda} \frac{dx^\beta}{d\lambda}. \quad (4.3.7)$$

Now we have the freedom to choose  $\lambda$  so for  $\lambda = \tau$  (proper time) we get  $A = 1$  and (4.3.6) becomes

$$(\mu + f\psi) \frac{D^2x^\nu}{d\tau^2} = -f \left( \psi^\nu + \psi_{,\alpha} \frac{dx^\alpha}{d\tau} \frac{dx^\nu}{d\tau} \right). \quad (4.3.8)$$

This is the most common choice, used in text books. We will be using a different  $\lambda$ , we can set what multiplies  $dx^\nu/d\lambda$  in (4.3.6) equal to zero then  $A = \mu^{-2}(\mu + f\psi)^2$  so the equations of motion give

$$\frac{D^2x^\nu}{d\lambda^2} = -\mu^{-2} f(\mu + f\psi) \psi^{\nu}, \quad (4.3.9)$$

$$-g_{\alpha\beta} \frac{dx^\alpha}{d\lambda} \frac{dx^\beta}{d\lambda} = \left( \frac{d\tau}{d\lambda} \right)^2 = \mu^{-2}(\mu + f\psi)^2. \quad (4.3.10)$$

For our solution we can find that we have a constant of motion  $E$

$$E = (1 - M/r)^2 (dt/d\lambda). \quad (4.3.11)$$

The easiest way to see that is by using a timelike killing vector. If for simplicity we restrict our motion to be radial (and define  $q = (3/4\pi)(M^2 - Q^2)^{1/2}$ ) we have that (4.3.10) gives

$$\frac{dr}{d\lambda} = \pm \left[ E^2 - (1 - M/r)^2 \left( 1 + \frac{fq}{\mu} \frac{1}{r - M} \right)^2 \right]^{1/2}. \quad (4.3.12)$$

So we see that for sufficiently small  $f$  (or  $|fq/(\mu M)|$ ), then  $dr/d\lambda$  never becomes zero (for  $r \geq M$ ) so from this its clear that we do not get an infinite potential barrier. Since for small scalar charge of the particle ( $f$ ) the particle speed never becomes zero (for  $r \geq M$ ), the particle does not encounter a potential wall to bounce back.

Now, to check what happens with the particle trajectories in finite proper time we start from (4.3.10), which in our problem can now be recast as

$$\frac{d\tau}{d\lambda} = \pm \left( 1 + \frac{fq}{\mu} \frac{1}{r - M} \right) \quad (4.3.13)$$

and

$$E = \left( 1 + \frac{fq}{\mu} \frac{1}{r - M} \right) (1 - M/r)^2 \frac{dt}{d\tau}, \quad (4.3.14)$$

solving using (4.3.12), near  $r = M$  we have

$$\frac{dr}{d\tau} = \pm \left[ \left( \frac{E\mu}{fq} \right)^2 - 1 \right]^{1/2} M^{-1}(r - M). \quad (4.3.15)$$

Which shows that the particle approaches the horizon only asymptotically at infinite proper time, so the trajectory never terminates. Thus this solution cannot be dimmed non-physical yet, but it is proven to be linearly unstable [57] so it not important for our purposes, since as we discussed earlier we can not assign to an unstable solution the “role” of an equilibrium thermodynamic state.

### 4.3.2 Nielsen-Olesen Vortex

The other hairy example we want to mention here is that of a black hole threaded or pierced by a string-like object for example a cosmic string or a Nielsen Olesen vortex. This hairy solution has the privilege of resembling actual hair (since it is a line (hair) that is connected to a spherical black hole (head)). The existence of the Nielsen-Olesen vortex married to a Schwarzschild black hole has been proven numerically [58], so we will not go into more detail apart mentioning that it is proven to be linearly unstable [59]. We will however attempt to explain a little what a Nielsen-Olesen vortex is, so that the interested reader can follow the discussion on the papers, and also because it is useful to know not only in black hole physics but in various other examples as well. For that reason we consider an Abelian Higgs model (in flat space at the moment)

$$\mathcal{L} = -\frac{1}{4}F_{\mu\nu}F^{\mu\nu} + (D_\mu\phi)^*(D^\mu\phi) - V(\phi). \quad (4.3.16)$$

With a Mexican hat potential

$$V(\phi) = \frac{1}{4}\lambda(|\phi|^2 - a^2)^2, \quad (4.3.17)$$

where as always

$$D_\mu = \partial_\mu + ieA_\mu, \quad (4.3.18)$$

$$F_{\mu\nu} = \partial_\mu A_\nu - \partial_\nu A_\mu. \quad (4.3.19)$$

In canonical form we recast the Hamiltonian density as

$$\mathcal{H} = \frac{1}{2}(\mathbf{E}^2 + \mathbf{B}^2) + \pi^*\pi + (\mathbf{D}\phi)^*(\mathbf{D}\phi) + V(\phi); \quad H = \int d^3x \mathcal{H}(\vec{x}). \quad (4.3.20)$$

It is standard procedure to re-parametrize our scalar field as follows

$$\phi(\vec{x}) = \rho(\vec{x})e^{i\theta(\vec{x})}. \quad (4.3.21)$$

Looking at (4.3.20) in order to have finite energy we need our fields to satisfy asymptotically as  $|x| \rightarrow \infty$

$$\begin{aligned} \mathbf{B}(\vec{x}) &\rightarrow 0, \\ \mathbf{D}\phi(\vec{x}) &= (\nabla - ie\mathbf{A}(\vec{x}))\phi(\vec{x}) \rightarrow 0, \\ \phi(\vec{x}) &\rightarrow ae^{i\theta(\vec{x})}. \end{aligned}$$

Where first line comes from first term in (4.3.20), the next comes from the third and the last line comes from the potential term (thus  $a$  is the same  $a$  of the potential). Since each term in (4.3.20) is positive it means that each term separately must vanish. So from the above we get the asymptotic behaviour for the gauge field

$$\mathbf{A}(\vec{x}) = \frac{1}{ie}\nabla \ln \phi(\vec{x}) = \frac{1}{e}\nabla\theta(\vec{x}). \quad (4.3.22)$$

We go to cylindrical coordinates and check boundary conditions

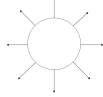
$$\phi(\vec{x}) = \phi(r, \varphi) \xrightarrow{r \rightarrow \infty} ae^{i\theta(\varphi)}, \quad e^{i\theta(\varphi+2\pi)} = e^{i\theta(\varphi)}, \quad (4.3.23)$$

$$\theta : S^1 \rightarrow S^1, \quad \theta(\varphi + 2\pi) = \theta(\varphi) + 2n\pi. \quad (4.3.24)$$

Trying to compute the magnetic flux and taking the surface bounded by an asymptotic curve  $C$  gives

$$\Phi_B^n = \int_{\Sigma} d^2x B = \oint_C ds \mathbf{A} = \frac{1}{e} \oint_C ds \nabla\theta(x) = n \frac{2\pi}{e}. \quad (4.3.25)$$

Which for the trivial case  $n = 0$ , flux is zero, but when we have non-zero  $n$ , we have flux for example for  $n = 1$  we get



In general it will also look like a vortex; hence the name Nielsen-Olesen vortex. This  $n$  is kind of a winding number (for the string enthusiasts out there).

Having explained the name we will now attempt to show why it looks like a string. In order to see that the scalar fields have cylindrical symmetry (this will be useful also later in order to explore their coupling to gravity, if the interested reader decides to explore it) we will redefine

$$\Phi(x^\alpha) = aX(x^\alpha)e^{i\chi(x^\alpha)}, \quad (4.3.26)$$

$$A_\mu(x^\alpha) = \frac{1}{e} \left[ P_\mu(x^\alpha) - \nabla_\mu \chi(x^\alpha) \right]. \quad (4.3.27)$$

When we write our equations of motion with those fields and choose  $n = 1$  and our gauge such that

$$\Phi = aX_0(R)e^{i\phi}; P_\mu = P_0(R)\nabla_\mu\phi. \quad (4.3.28)$$

For  $R = \sqrt{\lambda}ar$  the equations of motion take the form

$$-X_0'' = \frac{X_0'}{R} + \frac{P_0^2 X_0}{R^2} + \frac{1}{2}X_0(X_0^2 - 1) = 0, \quad (4.3.29)$$

$$-P_0'' + \frac{P_0'}{R} + \beta^{-1}X_0^2 P_0 = 0. \quad (4.3.30)$$

Where we see that the Nielsen-Olesen vortex solution represents an infinite straight static solution with cylindrical symmetry. What people did [58] in order to marry it with a black hole and get hair, is put it on a Schwarzschild background metric and numerically study back reaction. They get some nice numerical results, however this solution is also proven to be linearly unstable. One important aspect of this solution, is that it is also not asymptotically flat, even if we start with Schwarzschild metric. The solution asymptotically has an angle deficit, a trade that is also shared by the global monopole hair. A space with deficit solid angle has the following metric :

$$ds^2 = -dt^2 + dr^2 + (1 - 8\pi G\eta^2)r^2 d\Omega^2. \quad (4.3.31)$$

One can see this metric as a metric that is asymptotically de-Sitter so it is equivalent to having a non-zero cosmological constant  $\Lambda$ . This is a very interesting aspect of those solutions, since you couple the vortex, string or monopole with an asymptotically flat Schwarzschild metric but you end up with a metric that is asymptotically de-Sitter. The de-Sitter and anti-de-Sitter cases reserve a complete treatment, since measurements put us

in a universe with non-zero cosmological constant. So our next section is devoted on those cases.

### 4.3.3 Final remarks

To conclude this section we would like to stress what is worth taking home. First that there exist stable solutions which are hairy and have yet to show any pathologies. Second that you can not say if your solution is non-physical just by having a divergent field like we discussed on the BBM(B) model. Last but not least the value of the no hair conjecture increases if we have a thermodynamic point of view. Since it makes the analogy between stable black hole solutions and equilibrium states in thermodynamics natural. As we will see further on black hole thermodynamics is one of the most important parts of black hole physics.

## 4.4 No-hair theorems and Hairy Black Holes for $\Lambda \neq 0$

As we have already mentioned, the no hair theorem states that we need, at most, three different variables to describe a black hole. These variables are the mass, the angular momentum and the electric charge of the black hole. All the examples we have seen until now, are based on the assumption that the space-time is asymptotically flat. But what if the Universe has a non zero cosmological constant and so the space-time is either asymptotically de-Sitter ( $\Lambda > 0$ ) or Anti-de Sitter ( $\Lambda < 0$ )? In this section we consider a scalar field in a convex potential ( $\frac{d^2V}{d\phi^2} > 0$ ) coupled to gravity and give a more general proof to the no-hair theorem that extends both to de Sitter and anti-de Sitter space-times.

### 4.4.1 A Black Hole with a Scalar Field in both the dS and AdS Case

We consider the action of a scalar field coupled to gravity with non zero cosmological constant

$$S = \int d^4x \sqrt{-g} \left[ \frac{1}{16\pi G} (R - \Lambda) - \frac{1}{2} (\nabla\phi)^2 - V(\phi) \right] , \quad (4.4.1)$$

and because we want spherical symmetry we assume a form similar to the Schwarzschild metric as done by Takashi, Kengo and Makoto [60]:

$$ds^2 = -fe^{-2\delta}dt^2 + f^{-1}dr^2 + r^2d\Omega^2 , \quad (4.4.2)$$

with  $f = 1 - \frac{2Gm(r,t)}{r} - \frac{\Lambda}{6}r^2$ . Moreover,  $\delta = \delta(r, t)$  and  $m = m(r, t)$  are just functions of distance and time. From now on we are going to use the dimensionless variables in order to simplify our work, given by

$$\sqrt{|\Lambda|}t \rightarrow t, \quad \sqrt{|\Lambda|}r \rightarrow r, \quad \sqrt{G}\phi \rightarrow \phi \quad \text{and} \quad \frac{G}{|\Lambda|}V \rightarrow V ,$$

such that  $f = 1 - \frac{2m}{r} + \frac{r^2}{6}$ . By varying (4.4.1) with respect to the metric we can find the stress energy-tensor

$$T^{\mu\nu} = -\frac{2}{\sqrt{-g}}\frac{\delta S}{\delta g_{\mu\nu}}.$$

It's then possible, with the help of Einstein's equations, to find the metric which correspond to the above action. By comparing this metric with our assumption (4.4.2), we get the following field equations

$$m' = 4\pi r^2\left(\frac{1}{2}f^{-1}e^{2\delta}\dot{\phi}^2 + \frac{1}{2}f\phi'^2 + V(\phi)\right) , \quad (4.4.3)$$

$$\delta' = -4\pi r(f^{-2}e^{2\delta}\dot{\phi}^2 + \phi'^2) , \quad (4.4.4)$$

$$\dot{m} = 4\pi r^2f\dot{\phi}\phi' , \quad (4.4.5)$$

$$-\frac{d}{dt}(e^\delta f^{-1}\dot{\phi}) + \frac{1}{r^2}\frac{d}{dr}(r^2e^{-\delta}f\phi') = e^{-\delta}\frac{dV(\phi)}{d\phi} , \quad (4.4.6)$$

where we use the dot and the prime to show derivatives of dimensionless variables  $t$  and  $r$  respectively.

#### 4.4.2 Boundary Conditions

Since we are studying a black hole we expect a regular black hole event horizon at  $r = r_b$ , we also demand regularity for  $r > r_b$ . Furthermore when we consider the AdS case we don't expect a cosmic event horizon while in dS case we do. We find  $r_b$  by taking  $f = 0$  and so we get:

$$2m(r_b) = r_b - \frac{r_b^3}{6} . \quad (4.4.7)$$

In the dS case there will also be a Cosmic event horizon at  $r = r_c$ . The condition  $f = 0$  also holds in this case, and so we get:

$$2m(r_c) = r_c - \frac{r_c^3}{6} . \quad (4.4.8)$$

In the AdS case, there is no other horizon apart from the Black hole event horizon and so the regularity condition reads  $f(r) > 0$  for  $r > r_b$ , hence:

$$2m(r) < r - \frac{r^3}{6}. \quad (4.4.9)$$

In addition, we impose smoothness of  $\phi$  everywhere, apart from the singularity ( $r = 0$ ). We define the effective cosmological constant to be

$$\lambda_{eff} = 8\pi V(\phi_\infty) - 1, \quad (\text{where } V(\phi_\infty) = \lim_{\phi \rightarrow \infty} V(\phi)). \quad (4.4.10)$$

We end up having 3 different possibilities for the asymptotic behaviour of our system, depending on the value of  $\lambda_{eff}$ :

- $\lambda_{eff} < 0 \rightarrow$  AdS case ,
- $\lambda_{eff} > 0 \rightarrow$  dS case ,
- $\lambda_{eff} = 0 \rightarrow$  asymptotically flat case .

Let's start by considering static solutions within an AdS asymptotic structure. For our metric functions it is reasonable to define, for spatial infinity ( $\lim_{r \rightarrow \infty}$ ):

- (a)  $f \sim Ar^2 \Rightarrow 1 - \frac{2m}{r} - \frac{r^2}{6} \sim Ar^2 \Rightarrow m \lesssim$  (lower or the same order of)  $Br^3$ , where A is a positive constant and  $B < \frac{1}{12}$  in the case that  $m \sim r^3$  or simply a constant otherwise;
- (b)  $\delta \rightarrow \delta_\infty$  where  $\delta_\infty$  is just a constant.

For more details about the asymptotic behavior of the metric return to the second chapter at formulas 2.1.19-2.1.20. To continue we integrate the equation (4.4.3) which gives us:

$$m = 4\pi \int_{r_b}^r dr \left( \frac{1}{2} f \phi'^2 + V(\phi) \right) \sim 4\pi \int_{r_b}^r dr \left( \frac{1}{2} Ar^4 \phi'^2 + V(\phi)r^2 \right). \quad (4.4.11)$$

However, as we have already mentioned,  $m \lesssim Br^3 \Rightarrow \phi' \lesssim O(r^{-1})$  otherwise  $m$  would be of higher order than  $r^3$ . We also have that

$$\delta = -4\pi \int_{r_b}^r dr (r \phi'^2) + \delta_B, \quad (4.4.12)$$

and because of the boundary condition (b) we get that  $\phi' < O(r^{-1})$ . If  $\phi'$  was of the same or higher order than  $O(r^{-1})$  then  $\delta$  would diverge at infinity, but as we said before  $\delta$  approaches

a constant value at infinity. Therefore, when  $V(\phi_\infty) > 0$ , the gradient contribution to  $m$  becomes asymptotically sub-dominant implying that  $\lim_{r \rightarrow \infty} (m(r)) \sim 4\pi \int_{r_b}^r dr V(\phi) r^2$ . To proceed further we impose staticity on equation (4.4.6) giving us

$$Ar^2\phi'' + 4Ar\phi' - \frac{dV}{d\phi} = 0 \Rightarrow Ar^4\phi'' + 4Ar^3\phi' = r^2 \frac{dV}{d\phi} ,$$

and by integrating both parts we get:

$$Ar^4\phi' = \int dr \left( r^2 \frac{dV}{d\phi} \right) . \quad (4.4.13)$$

We have already found that  $\phi' < O(r^{-1}) \Rightarrow r^4\phi' < O(r^3)$  and so  $\int dr \left( r^2 \frac{dV}{d\phi} \right) < O(r^3) \Rightarrow \frac{dV}{d\phi} \lesssim O(r^{-\epsilon})$  (where  $>$ ,  $<$  and  $\sim$  refer to higher, lower or same order, respectively), therefore:

$$\frac{dV}{d\phi} \rightarrow 0 \text{ as } r \rightarrow \infty \Rightarrow \lim_{\phi \rightarrow \infty} V(\phi) , \quad (4.4.14)$$

is an extremum. Due to equation (4.4.10),  $V(\phi_\infty) < \frac{1}{8\pi}$ , otherwise  $\lambda_{eff}$  ceases being negative and the space-time approaches dS or another exotic one. By using this asymptotic behaviour, we can prove the non existence of hair for a convex potential ( $\frac{d^2V}{d\phi^2} > 0$ ) in both de Sitter and anti-de Sitter cases. No-hair theorems hold if there are not any non-trivial solutions for the field equations<sup>16</sup> The existence of trivial solutions ( $\phi$  constant everywhere) does not violate the no-hair theorem because it does not give an additional parameter for the description of the black hole. There are two types of convex potentials: one with a minimum somewhere and one which approaches its minimum asymptotically i.e.  $V(\phi) = e^{-\phi}$ . We are going to study them separately.

#### 4.4.3 Potential with Minimum at Finite $\phi$

For simplicity we set the minimum at  $\phi = 0$  and we also consider  $\phi(r_b) \neq 0$  to avoid trivial solutions. Without loss of generality we take  $\phi(r_b) > 0$ . Then we consider equation (4.4.6) and impose staticity to get:

$$\frac{1}{r^2} \frac{d}{dr} (r^2 \phi' f) = \frac{dV(\phi)}{d\phi} , \quad (4.4.15)$$

and for the case of  $r = r_b \Rightarrow f = 0$  we end up with:

$$f'\phi' = \frac{dV}{d\phi} . \quad (4.4.16)$$

---

<sup>16</sup>If there were non-trivial solutions, an additional parameter  $\phi = \phi(r)$  would be necessary for the description of the black hole, and the no-hair theorem would not hold.

The quantity  $f'$  turns out to be always positive. Moreover, we have taken  $\phi(r_b) > 0$ , since the minimum of the potential is at  $\phi = 0$  and the potential is convex. For positive  $\phi$  we have that  $\frac{dV}{d\phi} > 0$ , but then both  $f'$  and  $\frac{dV}{d\phi}$  are positive and so  $\phi'$  should also be positive, hence  $\phi$  increases at the horizon, while by considering equation (4.4.15) at  $\phi' = 0$  we take

$$f\phi'' = \frac{dV}{d\phi}. \quad (4.4.17)$$

As long as we have no cosmic event horizon,  $f > 0$  everywhere outside the black hole event horizon. Furthermore  $\frac{dV}{d\phi}$  is positive for  $\phi > 0$  making  $\phi''$  also positive. The above analysis shows that  $\phi$  is a monotonically increasing function. Since  $\phi$  does not diverge, we can have three cases for the asymptotic behaviour of the scalar field:

1.  $\phi_\infty > \phi_0$  (where  $V(\phi_0) = \frac{1}{8\pi}$ ) ,
2.  $\phi_\infty < \phi_0$  (where  $\phi_\infty$  is the asymptotic value of the scalar field) ,
3.  $\phi_\infty = \phi_0$  .

We are going to look at these three cases separately.

### Case 1

In this case  $V(\phi)$  becomes larger than  $V(\phi_0)$  at some finite  $r$ . As a result, the effective cosmological constant ( $\lambda_{eff} = 8\pi V(\phi_\infty) - 1$ ) becomes positive, hence the cosmic event horizon appears at finite  $r$ . Equation (4.4.16) holds on the cosmic event horizon ( $f = 0$ ), nevertheless we have that  $f' < 0$  while  $\frac{dV}{d\phi}$  is still positive, meaning that we should also have  $\phi' < 0$  which ends up contradicting our previous analysis.

### Case 2

For this case,  $V(\phi)$  never becomes higher than  $V(\phi_0)$  and so  $\lambda_{eff}$  is always negative. We can use the AdS asymptotic behaviour here:  $f \sim Ar^2$  (with  $A > 0$ ) and  $\delta = \text{finite}$  and, because of equation (4.4.12),  $\phi'$  is of lower order than  $O(r^{-1})$  (otherwise  $\delta$  would diverge). This implies that  $r^2\phi'e^{-\delta}f = Ar^4\phi'e^{-\delta}$  is of lower order than  $O(r^3)$  and so  $\frac{d}{dr}(Ar^4\phi'e^{-\delta})$  is of lower order than  $O(r^{-2})$ . As a result  $\lim_{r \rightarrow \infty} \frac{1}{r^2} \frac{d}{dr}(Ar^4\phi'e^{-\delta}) \rightarrow 0$ . The left hand side of equation (4.4.15) goes to zero as  $r \rightarrow \infty$  while the right hand side remains positive and so we reach again a contradiction<sup>17</sup>.

---

<sup>17</sup>When we say  $\phi'$  is of lower order than  $O(r^{-1})$  it is enough for  $\phi'$  to be proportional to  $r^{-1-\epsilon}$  where  $\epsilon$  is an infinitesimal constant.

**Case 3**

Here the space-time becomes asymptotically flat, since  $\lambda_{eff} = 0$  at  $r \rightarrow \infty$  and also  $f = 1 - \frac{2m}{r}$  is of the same order as  $O(r^0)$  at infinity. The quantity  $\delta$  is finite and due to equation (4.4.12)  $\phi'$  should be of lower order than  $O(r^{-1})$ . This means that the left hand side of equation (4.4.15) is again equal to 0 at infinity while the right hand side is positive. Thus, again we reach a contradiction.

So by supposing that there exists non-trivial solutions for the field equations we have reached a contradiction in all three cases. Hence there are no non-trivial solutions for the case of convex potential with a minimum at finite  $r$ . Now we will show that the same holds for the case where we have a convex potential with a minimum at infinity i.e  $V(\phi) = e^{-\phi}$

#### 4.4.4 Scalar field in a Convex Potential which Approaches its Minimum at $\phi \rightarrow \infty$

We treat a potential which approaches its extremum at infinity, meaning that  $\frac{dV}{d\phi} \rightarrow 0$  at infinity, but  $\frac{dV}{d\phi}$  is a monotonically increasing function because  $\frac{d^2V}{d\phi^2} > 0$ . Hence  $\frac{dV}{d\phi}$  should start by a negative value. Furthermore, equation (4.4.16) should hold again at the horizon. Since now  $f' > 0$  while  $\frac{dV}{d\phi} < 0$ , we get that  $\phi' < 0$  at the horizon. On top of that (4.4.17) still holds at the extremum of the scalar field. Nevertheless, we find that  $\phi'' < 0$ . Therefore, we have shown that in this case the scalar field is a monotonically decreasing function. We can also notice that the potential is a monotonically decreasing function of  $\phi$  because  $\frac{dV}{d\phi}$  is always negative. Again we have three different possibilities, depending on the value of  $\lambda_{eff}$ . In the first case we have  $V(\phi_\infty) > V(\phi_0)$  and so  $\lambda_{eff} > 0$  which makes the cosmic event horizon appear. Equation (4.4.16) should also hold in this case. However,  $f'$  becomes negative on the horizon and  $\frac{dV}{d\phi}$  is also negative, hence  $\phi'$  should be positive (increasing  $\phi$ ), but we have already shown that  $\phi$  is a monotonically decreasing function for this kind of potential, so again we reach a contradiction. We can also treat the other two cases in the same way as before which leads us to contradictions. Finally we have shown that there are no non-trivial solutions for the case of static black hole with a scalar field in a convex potential which implies that the no-hair theorem holds.

#### 4.4.5 Example of a Hairy black hole Coupled to a Scalar Field in AdS

We will consider a neutral scalar field minimally coupled to gravity in a self-interacting potential  $V(\phi)$  as done in [61]. We will also take the cosmological constant to be  $\Lambda = -\frac{6l^{-2}}{k}$ , where  $l$  is the length of the AdS space and  $\kappa = 8\pi G_N$  the Newton Constant. We will incorporate the cosmological constant in the potential as  $\Lambda = V(0)$ . The action then is:

$$S = \int d^4x \sqrt{-g} \left( \frac{1}{2\kappa} R - \frac{1}{2} g^{\mu\nu} \nabla_\mu \phi \nabla_{\nu} \phi - V(\phi) \right), \quad (4.4.18)$$

and the energy momentum tensor:

$$T_{\mu\nu}^{(\phi)} = \nabla_\mu \phi \nabla_\nu \phi - g_{\mu\nu} \left[ \frac{1}{2} g^{\rho\sigma} \nabla_\rho \phi \nabla_\sigma \phi + V(\phi) \right], \quad (4.4.19)$$

and by substituting (4.4.18) and (4.4.19) to Einstein's equations we get:

$$R_{\mu\nu} - \kappa (\partial_\mu \phi \partial_\nu \phi + g_{\mu\nu} V(\phi)) = 0, \quad (4.4.20)$$

We will consider the metric ansatz:

$$ds^2 = -f(r)dt^2 + f^{-1}(r)dr^2 + \alpha^2(r)d\Omega^2 \quad (4.4.21)$$

By using the ansatz to (4.4.20) we get the following differential equations:

$$f''(r) + 2\frac{\alpha'(r)}{\alpha(r)}f'(r) + 2V(\phi) = 0 \quad (4.4.22)$$

$$\frac{\alpha'(r)}{\alpha(r)}f'(r) + \left( \frac{(\alpha'(r))^2}{\alpha^2(r)} + \frac{\alpha''(r)}{\alpha(r)} \right) f(r) - \frac{k}{\alpha^2(r)} + V(\phi) = 0 \quad (4.4.23)$$

$$f''(r) + 2\frac{\alpha'(r)}{\alpha(r)}f'(r) + \left( 4\frac{\alpha''(r)}{\alpha(r)} + 2(\phi'(r))^2 \right) f(r) + 2V(\phi) = 0 \quad (4.4.24)$$

where  $k$  denotes the curvature of the spatial 2-section. We eliminate the potential to the above equations and we obtain:

$$\alpha''(r) = \frac{1}{2}(\phi'(r))^2 \alpha(r) = 0 \quad (4.4.25)$$

$$f''(r) - 2 \left( \frac{(\alpha'(r))^2}{\alpha^2(r)} + \frac{\alpha''(r)}{\alpha(r)} \right) f(r) + \frac{2k}{\alpha^2(r)} = 0 \quad (4.4.26)$$

To find exact hairy black hole solutions the differential equations (4.4.22)-(4.4.24) have to

be supplemented with the Klein Gordon equation of the scalar field which in general reads as:

$$\square\phi = \frac{dV}{d\phi} \quad (4.4.27)$$

There is a well known solution of the above differential equations [62] with:

$$\alpha^2(r) = \frac{r(r + 2G_N\mu)}{(r + 2G_N\mu)^2} r^2 \quad , \quad (4.4.28)$$

$$f(r) = \frac{r(r + 2G_N\mu)}{(r + 2G_N\mu)^2} F(r) \quad , \quad (4.4.29)$$

with  $F(r) = \frac{r^2}{l^2} - \left(1 + \frac{G_N\mu}{2}\right)^2$ . The scalar field is given by:

$$\phi = \sqrt{\frac{3}{4\pi G_N}} \operatorname{Arctanh} \frac{G_N\mu}{r + G_N\mu} \quad , \quad (4.4.30)$$

where the potential is found to be:

$$V(\phi) = \Lambda \sinh^2 \sqrt{\frac{4\pi G_N}{3}} \phi \quad . \quad (4.4.31)$$

This is the simplest known hairy black hole solution of a scalar field coupled conformally to gravity. Now if we want to abandon the conformal gravity with a curvature one we can still find the solutions of the differential equations (4.4.22)-(4.4.26). They have the form:

$$\alpha^2(r) = r^2, \quad (4.4.32)$$

$$f(r) = \frac{r(r + 2r_0)}{(r + r_0)^2} F(r) \quad (4.4.33)$$

with

$$F(r) = \frac{r^2}{l^2} - g \frac{r_0}{l^2} r - 1 + g \frac{r_0}{l^2} - \left(1 - 2g \frac{r_0^2}{l^2}\right) \frac{r_0}{r} \left(2 + \frac{r_0}{r}\right) + g \frac{r^2}{sl^2} \ln \left(1 + 2 \frac{2r_0}{r}\right) .$$

The potential is:

$$\begin{aligned} V(\phi) &= \frac{\Lambda}{4\pi G_N} \sinh^2 \sqrt{\frac{4\pi G_N}{3}} \phi + \frac{g\Lambda}{6\pi G_N} \\ &\times [2\sqrt{3\pi G_N} \cosh \left( \sqrt{\frac{16\pi G_N}{3}} \phi \right) \\ &- \frac{9}{8} \sinh \left( \sqrt{\frac{16\pi G_N}{3}} \phi \right) \\ &- \frac{1}{8} \sinh(4\sqrt{3\pi G_N} \phi)]. \end{aligned}$$

#### 4.4.6 Final Remarks

We have studied the case of a scalar field in a convex potential which couples to gravity in a more general way. We found out that for this case the no-hair theorem holds for both dS and AdS space-times as well as the asymptotically flat space-time. It essentially generalizes Bekenstein's procedure for the scalar field presented at the beginning of this chapter, which is also taken for convex potentials. We have shown this more general proof by supposing that the field equations have non-trivial solutions and contradicting our starting assumptions. It should be mentioned that the whole analysis holds only if we have a scalar field in a convex potential. In the case of a non-convex potential, or another kind of fields, it is possible to find hairy solutions. An example of this is when we couple a Higgs field to gravity [63]. However such solution is regarded unstable and therefore not a threat to the Israel-Carter conjecture.

# Chapter 5

## The Laws of Black Hole Mechanics

In this chapter we will discuss one of the most intricate equivalences in theoretical physics, namely the idea that black holes can be considered as thermodynamic systems. This field of study has appropriately been named “black hole thermodynamics”, as for every law of thermodynamics there is a law of black hole mechanics. In this chapter we consider the laws of black hole mechanics in a purely classical sense. This means that the equivalence between black hole and thermodynamics is only an analogy. This comes from the fact that classical black holes cannot radiate and thus do not have a temperature. The quantum mechanical treatment is postponed until Chapter 7. The first four paragraphs will introduce the four laws of black hole mechanics. Subsequently, paragraph five will present the analogy between black holes and thermodynamics, focussing on the first and second laws of thermodynamics. The final paragraph will do the same for the zeroth and third law.

### 5.1 Zeroth Law: Surface Gravity

In this section we will introduce the concept of surface gravity, an important idea in the study of black hole thermodynamics which, as we will see later, is associated with the temperature of a black hole. Before introducing this concept it is necessary to introduce the definition of Null-hypersurface and Killing horizon. After doing this we will explain the relation between event horizons and Killing horizons. Then we proceed stating and giving a brief account of the proof of the zeroth law of black mechanics, which states that the surface gravity is constant along the event horizon. Finally, we will show how to calculate the surface gravity for the case of the Schwarzschild solution.

In this section we will make an effort not to be too technical in the mathematical intricacies. For readers interested in these details we will refer you to references where these topics are studied in more detail.

### 5.1.1 Null-Hypersurfaces and Killing Horizons

A *hypersurface* in the 4-dimensional space-time of general relativity is basically a 3-dimensional sub-manifold. Families of hypersurfaces can be defined by imposing a condition of the form:

$$S(x) = \text{Const},$$

where  $S(x)$  is a smooth function depending on the coordinates  $x^\mu$ .

A hypersurface that is part of such a family has a normal vector which can be written as

$$l = N(x)\partial^\mu S \partial_\mu = N(x)g^{\mu\nu}\partial_\nu S\partial_\mu, \quad (5.1.1)$$

$$l^\mu = N(x)\partial^\mu S = N(x)g^{\mu\nu}\partial_\nu S, \quad (5.1.2)$$

where  $N(x)$  is an arbitrary function that sets the normalization of  $l$ , while  $\partial_\mu$  is a basis vector for the vector space of directional derivatives (recall [1]). Here we also used the fact that  $\partial_\mu S$  is normal to the hypersurface.

A *null-hypersurface*  $\Sigma$  is defined as a hypersurface  $\Sigma$  for which its normal vector  $l$  satisfies the following condition

$$l^2|_\Sigma = l^\mu l_\mu|_\Sigma = 0. \quad (5.1.3)$$

This equation implies that  $l$  is orthogonal to itself and therefore  $l$  is also a tangent vector to the hypersurface.

A *Killing horizon* is a null-hypersurface  $\Sigma$ , for which there exists a Killing vector  $\xi$  that is normal to  $\Sigma$ . Since  $\xi$  is normal to  $\Sigma$ , at the Killing horizon it is clear that the Killing vector and normal vector satisfy

$$\xi = fl \text{ at } \Sigma, \quad (5.1.4)$$

for some function  $f$ . From this we see that

$$\xi^2|_\Sigma = f^2 l^2|_\Sigma = 0. \quad (5.1.5)$$

We will now use a result often derived in the literature (see [64, 65]), which is the fact that we have the freedom to choose  $N(x)$  in equation (5.1.2) such that

$$l^\sigma \nabla_\sigma l^\mu|_\Sigma = 0,$$

for a null-hypersurface  $\Sigma$ .

From this expression and equation (5.1.4) it is easy to verify that

$$\xi^\sigma \nabla_\sigma \xi^\mu|_\Sigma = \kappa \xi^\mu , \quad (5.1.6)$$

where  $\kappa$  is known as the *surface gravity* and it is given by

$$\kappa = \xi^\sigma \partial_\sigma \ln f .$$

For the case of a static asymptotically flat space-time,  $\kappa$  will correspond to the acceleration of a static observer near the horizon, as it is seen by a static observer at infinity (for more details see [1]). In Section 5.6 we will see that this quantity is associated with the temperature of a black hole, consequently it will play a very important role in black hole thermodynamics.

We will now proceed to rewrite equation (5.1.6). For this we use Frobenius' theorem, which states that a sufficient and necessary condition in order for a vector field  $A$  to be orthogonal to a surface, is that

$$A_{[\alpha} \nabla_\beta A_{\gamma]}|_\Sigma = 0.$$

Using this property for the Killing vector  $\xi$  and the Killing equation, it is possible (after some lengthy algebra) to rewrite equation (5.1.6) in the following way

$$\kappa^2 = -\frac{1}{2} (\nabla^\alpha \xi^\beta) (\nabla_\alpha \xi_\beta)|_\Sigma . \quad (5.1.7)$$

From this equation it is clear that for a given Killing horizon the value of  $\kappa^2$  will depend on the normalization of  $\xi$ . In order to avoid this ambiguity, and thus guarantee the uniqueness of  $\kappa$  for a given Killing horizon, we will choose a specific normalization for  $\xi$ . The normalization that we will use corresponds to fixing  $\xi$  such that

$$\lim_{r \rightarrow \infty} \xi^2 = -1 .$$

This particular choice of normalization is motivated by the fact that we are interested in spacetimes that are asymptotically flat, thus we want the normalization of  $\xi$  for large values of  $r$  to correspond to the one used for  $\partial_t$  in Minkowski space.

### 5.1.2 Killing Horizons and Event Horizons

As we saw in the previous section, the concept of a Killing horizon is in itself a mathematical construct independent of our definition of event horizon. However, these different concepts are very related in the case of space-times with time translational symmetry.

The connection between these two topics has been achieved by means of the “rigidity theorems”, the first of which was proven by Carter [66]. He showed using only geometrical concepts that: For a static black hole  $\xi = \partial_t$  is normal to the event horizon, while for an axisymmetric stationary black hole the linear combination

$$\xi = \partial_t + \Omega_H \partial_\phi , \quad (5.1.8)$$

with  $\Omega_H$  some constant related to the angular velocity of the black hole, is normal to the event horizon [67]. Therefore, for any black hole having one of these symmetries, the event horizon would be a Killing horizon, provided it is a null-surface.

For this the following simple argument holds: Choose coordinates such that the event horizons are surfaces of constant  $r$ , therefore the vector  $\partial_r$  will be normal to them. For the event horizon to be a null-hypersurface it is then needed that

$$0 = \partial_\mu r \partial_\nu r \ g^{\mu\nu}|_{\text{Horizon}} = g^{rr}|_{\text{Horizon}} ,$$

but this is always true since this is basically the recipe for finding the horizon once a specific metric is given (recall [1]). As a final comment it is important to point out that this theorem proves that for stationary axisymmetric and static black holes, the event horizons are Killing horizons, but the converse is not true.

### 5.1.3 Zeroth Law

The zeroth law of black hole mechanics states that the surface gravity  $\kappa$  is constant along the event horizon. A rigorous proof of this statement is beyond the scope of this text, however, we will try to give a sketch of the proof (for more details see [64, 65, 68]).

From the field equations of Einstein we have that

$$R_{\mu\nu} - \frac{1}{2}g_{\mu\nu}R = T_{\mu\nu} .$$

We now introduce the Killing vector  $\xi$  normal to the horizon. Multiplying by  $\xi^\mu \xi^\nu$  on both sides this becomes

$$\xi^\mu \xi^\nu R_{\mu\nu} - \xi^2 R = T_{\mu\nu} \xi^\mu \xi^\nu . \quad (5.1.9)$$

We now evaluate this expression at the horizon  $\Sigma$ . From equation (5.1.5) we have that  $\xi^2|_\Sigma = 0$ . On the other hand, Raychaudhuri’s identity (recall Section 3.4.1) at the horizon states that:

$$R_{\mu\nu} \xi^\mu \xi^\nu|_\Sigma = 0 .$$

Thus the left hand side of (5.1.9) vanishes, leaving us with

$$T_{\mu\nu}\xi^\mu\xi^\nu|_\Sigma = 0 . \quad (5.1.10)$$

Since the Killing vector is normal to the horizon, the equation above implies that  $\xi^\nu T_{\mu\nu}$  is a vector tangent to the Killing horizon.

Recall that the Killing horizon is a 3-dimensional null-hypersurface made of vectors orthogonal to the normal vector  $l$ : Because we are in a null-hypersurface,  $l$  will be among these vectors. By choosing 2 other vectors  $\varsigma^{(1)}$  and  $\varsigma^{(2)}$  that are orthogonal to  $l$ , we can create a basis in which we can decompose any vector orthogonal to  $l$ . Doing this for  $\xi^\nu T_{\mu\nu}$  we get:

$$\xi^\nu T_{\mu\nu} = a\xi_\mu + b\varsigma_\mu^{(1)} + c\varsigma_\mu^{(2)} ,$$

where  $a, b, c$  are coefficients and we used the fact that at the horizon  $\xi$  and  $l$  are parallel (recall equation (5.1.4)).

For null-hypersurfaces it turns out that the tangent space at any point is made of space-like vectors except in one direction (in this case  $l$ ) [69]. This implies that  $\varsigma^{(1)}$  and  $\varsigma^{(2)}$  are space-like vectors. This, combined with equation (5.1.5) implies that  $\xi^\nu T_{\mu\nu}$  is either a space-like or a null vector (the latter only if  $b = c = 0$ ).

If we assume the dominant energy condition we have that  $\xi^\nu T_{\mu\nu}$  must be a time-like or null vector. Therefore, for this two conditions to be compatible it is needed that  $b = c = 0$ . Consequently we have that  $\xi^\nu T_{\mu\nu} \propto \xi^\mu$ . This implies that these 2 vectors are proportional to each other and therefore commute

$$\xi_{[\rho} T_{\sigma]}^\lambda \xi_\lambda|_\Sigma = 0 .$$

Using Einstein's field equation and equation (5.1.5), this becomes

$$\xi_{[\rho} R_{\sigma]}^\lambda \xi_\lambda|_\Sigma = 0 .$$

After using several identities for Killing vectors and some lengthy algebra (see [64]) it is possible to write this in the following way:

$$\xi_{[\sigma} R_{\rho]}^\lambda \xi_\lambda|_\Sigma = \xi_{[\rho} \partial_{\sigma]} \kappa|_\Sigma = 0 .$$

This expression implies that  $\xi$  and  $\partial\kappa$  commute and therefore  $\xi \propto \partial\kappa$ . Since  $\xi$  is normal to the horizon this means that the change in  $\kappa$  ( $\partial\kappa$ ) is normal to the horizon, therefore for any vector  $t$  tangent to the horizon it holds that:

$$t_\alpha \partial^\alpha \kappa = 0 .$$

Since this holds for all  $t$  tangent to the horizon,  $\kappa$  is therefore constant along the horizon.

### 5.1.4 Surface Gravity of the Schwarzschild Solution

Let us now give an example on how to calculate the surface gravity for the simplest case, the Schwarzschild solution. Instead of using coordinates  $(r, t, \theta, \phi)$  for the calculation, we will use incoming Eddington-Finkelstein coordinates:

$$v = t + r_*, \quad \text{with} \quad r_* = r + 2M \ln \left( \frac{r - 2M}{2M} \right) .$$

In this coordinates the line element looks like:

$$ds^2 = - \left( 1 - \frac{2M}{r} \right) dv^2 + 2dvdr + r^2 d\Omega^2 ,$$

and the inverse metric is given by:

$$g^{\mu\nu} = \begin{bmatrix} 0 & 1 & 0 & 0 \\ 1 & 1 - \frac{2M}{r} & 0 & 0 \\ 0 & 0 & \frac{1}{r^2} & 0 \\ 0 & 0 & 0 & \frac{1}{r^2 \sin^2 \theta} \end{bmatrix} .$$

We will be interested in hypersurfaces of the form  $S(x) = r = \text{const}$ , since this family of hypersurfaces has the same structure as the event horizon  $r = 2M$ . From equation (5.1.2) we have that:

$$l = N(x)g^{\mu r}\partial_\mu = N(x)[g^{vr}\partial_v + g^{rr}\partial_r] = N(x)\left[\partial_v + \left(1 - \frac{2M}{r}\right)\partial_r\right] . \quad (5.1.11)$$

We will now check under which conditions  $S(x) = r$  defines a null-surfaces:

$$\begin{aligned} l^2 &= l^\mu l^\nu g_{\mu\nu} = N^2(x)g^{\mu\sigma}\partial_\sigma S(x)g^{\nu\rho}\partial_\rho S(x)g_{\mu\nu} \\ &= N^2(x)g^{\mu r}g^{\nu r}g_{\mu\nu} = N^2(x)g^{rr} = N^2(x)\left(1 - \frac{2M}{r}\right) . \end{aligned}$$

Therefore, the event horizon  $r = 2M$  will correspond to a null-hypersurface, which we will denote by  $\Sigma$ .

Since the metric is time independent we have that  $\xi = \partial_t$  is a Killing vector. In incoming Eddington-Finkelstein coordinates it becomes

$$\xi = \partial_t = \frac{dv}{dt} \frac{\partial}{\partial v} = \partial_v .$$

From this result and the result for  $l$  we see that indeed  $\xi \propto l$  at the Killing horizon ( $r = 2M$ ), just as in equation (5.1.4).

Taking this into account we now proceed to calculate the surface gravity by using equation (5.1.6):

$$\begin{aligned}\xi^\alpha \nabla_\alpha \xi^v|_\Sigma &= \xi^\alpha \Gamma_{\alpha\rho}^v \xi^\rho|_\Sigma = \Gamma_{vv}^v|_\Sigma = \frac{1}{2} g^{v\sigma} (\partial_v g_{v\sigma} + \partial_v g_{\sigma v} - \partial_\sigma g_{vv})|_\Sigma \\ &= \frac{1}{2} (2\partial_v g_{vr} - \partial_r g_{vv})|_\Sigma = \frac{M}{4M^2} = \frac{1}{4M} = \frac{1}{4M} \xi^v.\end{aligned}$$

Comparing with equation (5.1.6), we conclude that the surface gravity is

$$\kappa = \frac{1}{4M}. \quad (5.1.12)$$

Using a similar procedure one can calculate the surface gravity for the Reissner-Nordström (already introduced in equation (2.3.12)) and Kerr solutions, which are presented in the Appendix A.4.

## 5.2 First Law of Black Hole Mechanics

The first law of black hole mechanics is based on the following question: what is the mass difference between two solutions of the Einstein equation, when these solutions have a infinitesimally different area, charge and angular momentum? A more physical way of stating this question is: how does the mass/area of a black hole change if we throw in a particle with a certain mass, charge and angular momentum?

To answer the question we will first need to define mass in general relativity, because we need a rigorous definition of the mass of a black hole in order to answer the above question. For this we will introduce the Komar mass [70], which is a geometric expression for the mass contained inside a closed surface. Analogous to this we will introduce how to define the angular momentum of a black hole. With this new definition of mass we are in a position to calculate the mass of a black hole. Then we can see what happens to the mass if we vary the parameters in the expression by an infinitesimal amount. This is a very general derivation of the first law, which holds for every axisymmetric stationary asymptotically flat solution to the Einstein equation. The first law will take the following form:

$$dM = \frac{\kappa(M, J, Q)}{8\pi} dA + \Omega(M, J, Q) dJ + \Phi(M, J, Q) dQ. \quad (5.2.1)$$

However, by now the physical interpretation of the parameters present in this equation is not yet clear, they are just some functions that appear in front of  $dA$ ,  $dJ$  and  $dQ$ . To give the functions a physical interpretation we use a simpler way to derive the first law for a more specific example, namely by calculating  $dM$  of a Kerr-Newman black hole. Then we

have the opportunity to give a physical interpretation to the quantities  $\kappa$ ,  $\Omega$  and  $\Phi$  is. Our starting point for this is a Kerr-Newman black hole with mass  $M$ , charge  $Q$  and angular momentum  $J$ . With the relatively simple derivation for the first law of a Kerr-Newman black hole, we will determine that  $\kappa$  is the surface gravity of the previous section,  $\Omega$  the angular velocity of the black hole and  $\Phi$  the electrostatic potential difference between the horizon and infinity.

### 5.2.1 Mass in GR

When we try to define the mass of a black hole, we run into several problems (for a nice discussion, see [70]). Usually we try to define the mass using the energy-momentum tensor  $T_{\mu\nu}$ . However, for a black hole all matter is inside the event horizon, an inaccessible region. Therefore we can not really define a  $T_{\mu\nu}$  for a black hole. Our only option then is to define the mass (energy) of the black hole as energy contained in the gravitational field. This is where we run into difficulties, because there is (yet) no way to get a well defined energy-momentum tensor of the gravitational field itself. This is mainly because the gravitational field itself is determined by the energy-momentum tensor via Einstein's equation. With the energy-momentum eliminated as a way to define the mass of a black hole, we try to use the Ricci tensor  $R_{\mu\nu}$ . We make this choice because we know that the information about the gravitational field is contained in this tensor, and that it is related to the energy-momentum tensor via the field equations.

In this section we will define the mass of a black hole via the quantity known as the Komar quantity. There are other ways to define the mass of a black hole, but we will not go into details for this section (some of the different definitions even turn out to be equal [70]).

Let us first define the notations.  $S$  is a space-like hypersurface, which is obtained after taking a time-slice of our 3+1 spacetime ( $S$  is then just the 3d space at a certain time) with a time-like unit normal vector  $a_\mu$ . The metric of our 3+1 space-time is  $g_{\mu\nu}$ . Define the induced metric on the hypersurface  $S$  as  $\gamma_{\mu\nu}$ . We then define  $\partial S$  as a closed 2-surface embedded in  $S$  with a space-like unit normal vector  $b_\mu$ . We can choose  $a_\mu$  and  $b_\mu$  to be orthogonal ( $a_\mu b^\mu = 0$ ). We define the induced metric on  $S$  as  $\gamma_{\mu\nu}$  and on  $\partial S$  as  $q_{\mu\nu}$  given by the following formulae:

- $\gamma_{\mu\nu} = g_{\mu\nu} + a_\mu a_\nu$ ,
- $q_{\mu\nu} = \gamma_{\mu\nu} - b_\mu b_\nu$ .

When integrating tensors over  $\partial S$  or  $S$  it is useful to define the surface or volume elements as tensors. We can do this in the following way:

- $dS_{\mu\nu} = (b_\mu a_\nu - b_\nu a_\mu) \sqrt{q} d^2x,$
- $dS_\mu = a_\mu \sqrt{\gamma} d^3x.$

Here  $dS_{\mu\nu}$  is a surface element of  $\partial S$ ,  $dS_\mu$  is a volume element of  $S$  and  $q$  and  $\gamma$  are the determinants of  $g_{\mu\nu}$  and  $\gamma_{\mu\nu}$  respectively.

With this notation we can define the Komar quantity in the following way

$$Q_K \equiv -\frac{1}{4\pi} \int_{\partial S} dS_{\mu\nu} \nabla^\mu \xi^\nu, \quad (5.2.2)$$

where  $\xi^\mu$  is a Killing vector of the 3+1 space-time and the factor  $-\frac{1}{4\pi}$  is a normalization factor, determined in such a way that we get the right physical quantities from this mathematical expression. We can rewrite this quantity by using Gauss' law in GR,

$$\int_S dS_\mu \nabla_\nu A^{\mu\nu} = \int_{\partial S} dS_{\mu\nu} A^{\mu\nu}, \quad (5.2.3)$$

and the useful identity for Killing vectors,

$$\nabla_\nu \nabla^\mu \xi^\nu = R_\nu^\mu \xi^\nu, \quad (5.2.4)$$

to write the Komar quantity as

$$Q_K = -\frac{1}{4\pi} \int_S dS_\mu \nabla_\nu \nabla^\mu \xi^\nu = -\frac{1}{4\pi} \int_S dS_\mu R_\nu^\mu \xi^\nu, \quad (5.2.5)$$

One can derive that  $R_\nu^\mu \xi^\nu$  is a conserved quantity

$$\begin{aligned} \nabla_\mu (R_\nu^\mu \xi^\nu) &= \nabla_\mu \nabla_\nu \nabla^\mu \xi^\nu, \\ &= \nabla_\nu \nabla_\mu \nabla^\mu \xi^\nu + R_{\alpha\mu\nu}^\mu \nabla^\alpha \xi^\nu + R_{\alpha\mu\nu}^\nu \nabla^\mu \xi^\alpha, \\ &= \nabla_\nu \nabla_\mu \nabla^\mu \xi^\nu = 0. \end{aligned} \quad (5.2.6)$$

In the second line we have used the commutator of covariant derivatives when working on a 2-tensor. The last two terms in the second line vanish because the Riemann tensors reduce to a Ricci tensor. The Ricci tensor is symmetric but from the Killing equation we know that  $\nabla^\mu \xi^\nu$  is anti-symmetric, thus these terms vanish. From the above equation we see that this expression is symmetric in switching the first 2 covariant derivatives, but we

know that  $\nabla^\mu \xi^\nu$  is anti-symmetric. Therefore we can conclude that  $\nabla_\mu \nabla_\nu \nabla^\mu \xi^\nu$  must equal 0, verifying that  $R_\nu^\mu \xi^\nu$  is a conserved quantity.

This tells us that we can relate a conserved quantity to a Killing vector via the Ricci-tensor. An important property of this conserved quantity is that we can write it as a surface integral. The advantage is that we then do not have to worry about what happens inside the surface. The Komar quantity is a perfect candidate to define the mass of a black hole. Note also that the conserved quantity contains the Ricci-tensor, which is what we were looking for when we wanted to define mass/energy.

Since the metric of a static and axisymmetric black hole is independent on  $t$  and  $\phi$ , we know that it has the following two Killing vectors:  $\xi = \partial_t$ , and  $\xi = \partial_\phi$ . Now it is very straightforward to define the mass as the (conserved) Komar quantity associated with the time-like Killing vector. We choose the time like Killing vector because of the fact that energy density is the  $T_0^0$  component of the energy-momentum tensor and that energy conservation is associated with time-translation symmetry. The definition of the Komar mass is then

$$M_K \equiv -\frac{1}{4\pi} \int_{\partial S} dS_{\mu\nu} \nabla^\mu k^\nu, \quad (5.2.7)$$

where we have defined  $k^\mu$  as the Killing vector associated to  $\partial_t$ . In the same way we can define the angular momentum as the Komar quantity associated with the rotational killing vector, since conservation of angular momentum is associated with symmetry under  $\phi$  translations. the definitions of the Komar angular momentum is then

$$J_K \equiv -\frac{1}{8\pi} \int_{\partial S} dS_{\mu\nu} \nabla^\mu \tilde{k}^\nu, \quad (5.2.8)$$

where we have defined  $\tilde{k}^\mu$  as the Killing vector associated to  $\partial_\phi$ . The definition of the angular momentum has a extra factor of  $\frac{1}{2}$  which is another normalization factor.

It is important to realize that, since  $R_{\mu\nu}$  is 0 in vacuum, we have a freedom in choosing our surface. We can alter  $\partial S$  as we like without changing the value of the integral, as long as we do not include new matter inside the new surface  $\partial S$ . In other words: if we want to change the surface we only have to be careful that there is no non-zero  $R_{\mu\nu}$  (so no non-zero  $T_{\mu\nu}$ ) inside the new surface, because that will alter the outcome of the integral.

Lastly let us note two important points. First, this definition of mass and angular momentum is purely geometric in the sense that it is coordinate independent. Second, this definition does not refer to the particular embedding in  $S$ , it only depends on the closed 2-surface that is chosen.

### 5.2.2 Mass of an Axisymmetric Black Hole

With this definition of the mass of a black hole we are ready to calculate it. In this section we will confine ourselves to a stationary axisymmetric asymptotically flat space. We know that in such a space we have two Killing vectors, a time-translational and a rotational Killing vector associated with  $\partial_t$  and  $\partial_\phi$  respectively. Remember that in the previous section we defined  $k^\mu$  as the Killing vector associated to  $\partial_t$  and  $\tilde{k}^\mu$  as the Killing vector associated to  $\partial_\phi$ . We will start by taking the identity (5.2.4) for  $k^\mu$  and integrate both sides over hypersurface  $S$ . We can then use Gauss law (5.2.3) to write it as follows

$$-\int_S dS_\mu R_\nu^\mu k^\nu = \int_{\partial S} dS_{\mu\nu} \nabla^\mu k^\nu. \quad (5.2.9)$$

We will choose  $S$  to contain the whole 3 dimensional space except for the interior of the black hole. The surface of  $S$  then consists of a surface at infinity and a surface where  $S$  crosses the horizon of the black hole,  $\partial B$ . We have excluded the interior of the black hole since it is inaccessible. According to the newly given definition of mass (5.2.7), the right hand side integrated over the surface at infinity will be equal to the total mass inside  $S$ ,  $M$ , times  $-4\pi$  and the integral over  $\partial B$  equals the mass of the black hole

$$M = \frac{1}{4\pi} \int_S dS_\mu R_\nu^\mu k^\nu + \frac{1}{4\pi} \int_{\partial B} dS_{\mu\nu} \nabla^\mu k^\nu. \quad (5.2.10)$$

If we now substitute  $k^\mu = \xi^\mu - \Omega \tilde{k}^\mu$  (remember  $\xi = \partial_t + \Omega \partial_\phi$ ) in the expression for the black hole mass, this term then splits in two. The term involving  $\tilde{k}^\mu$  is twice the Komar angular momentum according to the definition 5.2.8, making this term equal to  $2\Omega J_{BH}$ . If we then use Einstein's equation to rewrite the Ricci tensor we get

$$M = \int_S (2T_\nu^\mu - T\delta_\nu^\mu) k^\mu dS_\nu + 2\Omega J_{BH} + \frac{1}{4\pi} \int_{\partial B} \nabla^\mu \xi^\nu dS_{\mu\nu}. \quad (5.2.11)$$

Now let us look at the last term. We know that  $dS_{\mu\nu}$  can be expressed using the normal vectors to the surface. We have already seen that  $\xi^\mu$  is orthogonal to the event horizon. Let us call the other null-vector orthogonal to  $\partial B$   $n^\mu$ , which we can choose such that  $\xi^\mu n_\mu = -1$ . We can now use the two normal vectors  $\xi^\mu$  and  $n^\mu$  in our expression for  $dS_{\mu\nu}$ . We can also rewrite the equation for  $\kappa$  (5.1.7) by multiplying it with  $n_\mu$  and get:

$$\kappa = -n_\mu \xi^\nu \nabla^\mu \xi^\nu. \quad (5.2.12)$$

Now we see that, since  $\nabla^\mu \xi^\nu$  is anti-symmetric, the last term in (5.2.11) is simply the surface gravity integrated over the area. This term is equal to the surface gravity  $\kappa$ , which

is constant over the area according to the zeroth law. This term then equals  $\kappa$  times the area and we get for the total mass  $M$  inside  $S$ :

$$M = \int_S (2T_\nu^\mu - T\delta_\nu^\mu) k^\mu dS_\nu + 2\Omega J_{BH} + \frac{\kappa}{4\pi} A. \quad (5.2.13)$$

Here the first term is the contribution from the mass outside the black hole and the last two terms form the mass of the black hole itself.

### 5.2.3 The First Law

Now we can calculate what happens to this expression if take a small variation of the parameters. The full calculation is done in [68], which is long and cumbersome, so here we will only give a rough outline and the results. By varying the mass formula we actually compare two slightly different stationary axisymmetric black holes. Therefore we have a freedom in choosing which points will correspond. A convenient choice is letting the surfaces  $S$  and  $\partial B$  of the two different solutions coincide, as well as the Killing vectors  $k^\mu$  and  $\tilde{k}^\mu$ . This gives us the following equations:

$$\begin{aligned} \delta k^\mu &= \delta \tilde{k}^\mu = 0, & \delta k_\mu &= \delta g_{\mu\nu} k^\nu, & \delta \tilde{k}_\mu &= \delta g_{\mu\nu} \tilde{k}^\nu, \\ \delta \xi^\mu &= \delta \Omega \tilde{k}^\mu, & \delta \xi_\mu &= h_{\mu\nu} \xi^\nu + \delta \Omega \tilde{k}_\mu. \end{aligned} \quad (5.2.14)$$

If we rewrite  $T = -\frac{1}{8\pi}R$  and use the variation of the Ricci scalar, it can be shown that the variation of the term involving  $T$  in (5.2.13) can be converted in a surface integral. The integral over infinity gives  $-\delta M$  and the integral over  $\partial B$  gives  $-\frac{\delta\kappa}{4\pi} - 2\delta\Omega J_{BH}$ , which will obviously cancel with two other terms when taking the variation of (5.2.13). The variation of the term involving  $T_\nu^\mu$  will give contributions from the matter surrounding the black hole (which is assumed not to fall into the black hole). We will take this to be zero in our discussion (the interested reader can see [68] for a discussion when this term is not taken to be zero). Putting all of this together in one equation we get

$$\delta M = -\delta M - \frac{\delta\kappa}{4\pi} - 2\delta\Omega J_{BH} + 2\delta(\Omega J_{BH}) + \delta\left(\frac{\kappa A}{4\pi}\right), \quad (5.2.15)$$

$$\delta M = \Omega\delta J_{BH} + \frac{\kappa}{8\pi}\delta A. \quad (5.2.16)$$

This equation is the first law of black hole mechanics.

### 5.2.4 The First law for the Kerr-Newman Black Hole

In the previous section we have done a formal derivation of the first law, where we only assumed an axisymmetric stationary asymptotically flat black hole. However, charge was

not yet included and the physical interpretation of  $\Omega$  is yet unclear. In this section we will derive the first law assuming that we have the Kerr-Newman solution. We will start by calculating the area of the event horizon of a Kerr-Newman black hole. This is the area of the 2-surface created by fixing  $t = t_0$  and  $r = r_+ = M + \sqrt{M^2 - Q^2 - J^2/M^2}$ , both  $t_0$  and  $r_+$  are a constant, in the metric of a Kerr-Newman black hole. The induced metric  $h_{\mu\nu}$  on this 2-surface is then as follows

$$h_{\mu\nu} = \begin{pmatrix} g_{\theta\theta} & 0 \\ 0 & g_{\phi\phi} \end{pmatrix}, \quad (5.2.17)$$

where  $g_{\theta\theta}$  and  $g_{\phi\phi}$  are components of the Kerr-Newman metric. The area is then given by

$$A = \int \sqrt{\det(h_{\mu\nu})} d\theta d\phi. \quad (5.2.18)$$

Using the expressions for  $g_{\theta\theta}$  and  $g_{\phi\phi}$ , (2.3.2), and evaluating them at the horizon  $r = r_+$ , we get  $\det(h_{\mu\nu}) = (r_+^2 + a^2)^2 \sin^2(\theta)$ , where  $a = \frac{J}{M}$ . Now we can calculate the area

$$A = \int_0^\pi d\theta \int_0^{2\pi} d\phi (r_+^2 + a^2) \sin(\theta) = 4\pi(r_+^2 + a^2), \quad (5.2.19)$$

that can be expressed in terms of  $M$ ,  $J$  and  $Q$ :

$$A = 4\pi \left( 2M^2 - Q^2 + 2M\sqrt{M^2 - Q^2 - a^2} \right). \quad (5.2.20)$$

Now we can set up  $dA = \frac{\partial A}{\partial M} dM + \frac{\partial A}{\partial Q} dQ + \frac{\partial A}{\partial J} dJ$  by simply determining the derivatives:

$$\begin{aligned} \frac{\partial A}{\partial M} &= 4\pi \left( 4M + \frac{4M^3 - 2Q^2M}{\sqrt{M^4 - Q^2M^2 - J^2}} \right), \\ \frac{\partial A}{\partial Q} &= 4\pi \left( -2Q + \frac{-2QM^2}{\sqrt{M^4 - Q^2M^2 - J^2}} \right), \\ \frac{\partial A}{\partial J} &= \frac{-8\pi J}{\sqrt{M^4 - Q^2M^2 - J^2}}. \end{aligned}$$

Then rewrite the differential for  $dA$ , using some simple algebra, as a differential for  $dM$

$$dM = \frac{1}{16\pi} \frac{r_+ - r_-}{r_+^2 + a^2} dA + \frac{a}{r_+^2 + a^2} dJ + \frac{Qr_+}{r_+^2 + a^2} dQ. \quad (5.2.21)$$

## 5.2.5 Physical Interpretations

We can see by comparing equations (5.2.1) and (5.2.21) that  $\kappa = \frac{r_+ - r_-}{2(r_+^2 + a^2)}$ . In the appendix the surface gravity of the Kerr-Newmann black hole is calculated, in A.4.2. Comparing our

expression with the result we see that our  $\kappa$  equals  $\kappa_+$  of equation (A.4.2). The physical interpretation of this term is then the surface gravity of the black hole.

The coefficient in front of  $dJ$ ,  $\frac{a}{r_+^2 + a^2} = \Omega$ , may also be familiar. In the appendix (A.4.2) it has been calculated that this is the coefficient that makes the Killing vector  $\xi$  a null factor on the horizon, by solving  $\xi^2 = 0$ . However, we can also give a nice physical interpretation to this coefficient: the angular velocity of the black hole. At first it might seem strange to even give an angular velocity to a black hole, but we can define the angular velocity of the black hole using the frame dragging effect of the Kerr solution. In section 2.3 we saw that if you throw in a particle at rest with 0 angular momentum, it will gain an angular velocity with respect to infinity. A definition we can then give to the angular velocity of a black hole is the angular velocity that a particle has once it reaches the horizon, if it started from rest with zero angular momentum at infinity. Let us calculate this quantity. Since the Kerr-Newman metric does not depend on  $t$  and  $\phi$ , there are two conserved quantities related to this:

$$E = 2g_{tt}\dot{t} + 2g_{t\phi}\dot{\phi}, \quad L = 2g_{t\phi}\dot{t} + 2g_{\phi\phi}\dot{\phi}. \quad (5.2.22)$$

Here the dot denotes differentiation with respect to the proper time. These expressions can be solved for  $\dot{t}$  and  $\dot{\phi}$ . Dividing these two quantities then gives us  $\frac{d\phi}{dt}$ , the angular velocity of the particle with respect to an observer stationary with respect to the black hole. If we then set  $L = 0$  (initially the particle goes straight towards the black hole) we see that the particle still gets an angular velocity due to the  $g_{t\phi}$  term, equal to:

$$\frac{d\phi}{dt} = \frac{g_{t\phi}}{g_{\phi\phi}} = \frac{a(r^2 + a^2 - \Delta)}{(r^2 + a^2)^2 - \Delta a \sin^2(\theta)}, \quad (5.2.23)$$

where  $\Delta = (r - r_+)(r - r_-)$ . The phenomenon for which the particle starts to rotate along with the black hole even though it had no angular momentum is called the frame dragging effect, which can be seen as that the black hole 'drags' the space-time along with it.

According to an observer at infinity the particle will never cross the horizon, but we can take the limit  $r \rightarrow r_+$ ,  $\Delta \rightarrow 0$ , and get the following result:

$$\Omega = \frac{d\phi}{dt} = \frac{a}{r_+^2 + a^2}. \quad (5.2.24)$$

From this we immediately recognize the term in front of  $dJ$  in (5.2.21). Note that this is a quantity constant over the horizon (independent of  $\theta$ ). Therefore we can say this is a property of the black hole, confirming the name 'angular momentum of the black hole'.

Lastly we want to know what  $\Phi$  is. As we will see this quantity is the electrostatic potential of the black hole (with respect to infinity). This is a very logical way of interpreting this

quantity since taking a charge from infinity to the event horizon will give it an extra energy equal to the potential difference. However, we can make this more concrete. In electrodynamics the electrostatic potential is the  $t$ -component of the electromagnetic 4-vector  $A_\mu$ . We can write it more formally as  $k^\mu A_\mu$ , where  $k^\mu$  is the time-like Killing vector. As argued before, this Killing vector is related to the energy. But there is a problem if we want to define the electrostatic potential on the event horizon. We know that an observer can not follow a path along the time translational Killing vector inside the ergosphere. However, we have seen that for a rotating black hole frame dragging occurs where the space-time is dragged along with the black hole. This changes our Killing vector and therefore the definition of the electrostatic potential:

$$\xi^\mu A_\mu, \quad \xi^\mu = t^\mu + \Omega\phi^\mu, \quad (5.2.25)$$

with  $t^\mu$  and  $\phi^\mu$  the unit vectors in the  $t$  and  $\phi$  directions respectively. Now we can define the electrostatic potential of the black hole as the difference in  $\xi^\mu A_\mu$  between infinity and the horizon. We know the electromagnetic potential of a Kerr-Newman black hole from a previous chapter, equation (2.3.16), which has the property that it is 0 at infinity. Putting this all together gives us the following expression for the potential difference:

$$\Phi = (A_t + \Omega A_\phi)|_{r=r_+} = \frac{Qr_+}{r_+^2 + a^2 \cos^2(\theta)} - \frac{a^2}{r_+^2 + a^2} \frac{Qar_+ \sin^2(\theta)}{r_+^2 + a^2 \cos^2(\theta)} = \frac{Qr_+}{r_+^2 + a^2} \quad (5.2.26)$$

This is the same as the term in front of  $dQ$ , verifying that this is the electrostatic potential of the black hole. Note that this too is constant over the event horizon.

### 5.3 The Second Law: the Area Theorem

After seeing the first law of black hole mechanics written in full generality in equation (5.2.1), one could wonder whether there are any restrictions on the possible changes in the mass, area, charge or angular momentum of a black hole. From a given set of initial values, can these quantities be tuned to become any value?

It turns out that the answer is no: not all of these quantities can be tuned at will. There is at least one restriction: the area  $A$  of the event horizon of a black hole cannot decrease in time, thus  $\frac{dA}{dt} \geq 0$ , under a couple of fairly general conditions. This result was obtained by Stephen Hawking and goes by the name of (Hawking's) Area Theorem [4]. It is a very general result and holds in any asymptotically flat spacetime containing a black hole, if the cosmic censorship conjecture is true and the weak energy condition is obeyed. It is, however, a classical result and does not account for quantum effects. We will see in Chapter

7 that the area of the event horizon can shrink due to Hawking radiation. In order to go in depth into the proof, we do need some concepts, which we will introduce in the next two sections. After that, we can see the validity of a very interesting theorem by Penrose, which we can then use to prove the Area Theorem. Lastly, we revisit the Penrose process, to see whether it violates the Area Theorem.

### 5.3.1 Causality

In Section 3.4.1, we already started thinking about congruences of geodesics in a spacetime and the causal future and past of subsets of spacetime. These concepts will be very useful to formalize, because we will use them often in the remainder of the section and can also be found in [65].

By a *causal curve* we mean a curve in a spacetime  $M$  that is nowhere space-like. If two points  $p$  and  $q$  in spacetime are connected by a causal curve from  $p$  to  $q$ , we say that  $p$  lies in the *causal past* of  $q$  and write  $p \prec q$ . Similarly, if this curve goes from  $q$  to  $p$  we say that  $p$  lies in the *causal future* of  $q$  and write  $q \prec p$ . Using these definitions we can also define the causal past and future of a subset  $S$ :

$$\begin{aligned} \text{causal past of } S : J^-(S) &= \{x \in M | \exists s \in S \text{ such that } s \in S \text{ s.t. } x \prec s\} \\ \text{causal future of } S : J^+(S) &= \{x \in M | \exists s \in S \text{ such that } s \in S \text{ s.t. } s \prec x\}. \end{aligned} \quad (5.3.1)$$

Similarly, we can define a *chronological curve* as a curve that is time-like everywhere and use this to define the *chronological future* and *chronological past* of a given subset  $S$  in complete analogy with the causal case treated above: we write  $p \ll q$  when there exists a chronological curve from  $p$  to  $q$ . Now we can define also the following sets:

$$\begin{aligned} \text{chronological past of } S : I^-(S) &= \{x \in M | \exists s \in S \text{ such that } s \in S \text{ such that } x \ll s\} \\ \text{chronological future of } S : I^+(S) &= \{x \in M | \exists s \in S \text{ such that } s \ll x\}. \end{aligned} \quad (5.3.2)$$

It follows straight from the definitions that  $I^\pm \subset J^\pm$ , since every time-like curve is also nowhere space-like. From this observation, we can define the *boundary of the causal past* of a set as the set  $\partial J^-(S) = J^-(S) \setminus I^-(S)$ . This set contains points which can only be connected to  $S$  by a null geodesic; we say that  $\partial J^-(S)$  is generated by a set of null geodesics, *the null geodesic generators* of  $\partial J^-(S)$ . Also, we can observe the following facts about relations between points in spacetime:

1. If  $p \ll q$  and  $q \ll r$ , then also  $p \ll r$ .

2. If  $p \prec q$  and  $q \prec r$ , then also  $p \prec r$ .
3. If  $p \ll q$  and  $q \prec r$ , then also  $p \ll r$ .

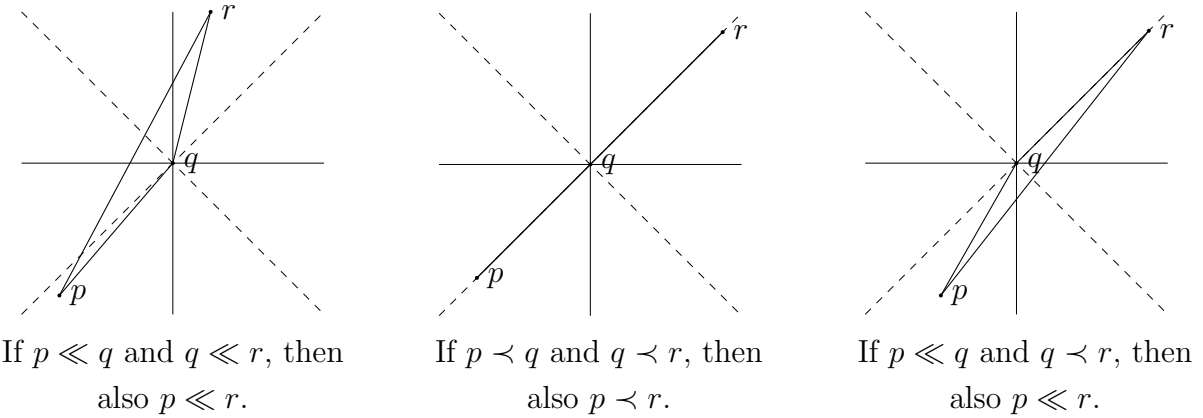


Figure 5.1: Spacetime diagrams to give some intuition to the abstract relations between different points in spacetime given above. The dashed lines indicate the lightcone, the solid lines indicate paths between points.

Using these definitions, we can already prove an important result, first proven by Roger Penrose in 1967 [71]:

**Lemma 5.3.1** *for any subset  $S \subset M$ , a null geodesic generator of  $\partial J^-(S)$  cannot have a future endpoint on  $\partial J^-(S)$ .*

This means that null geodesic generators may indeed enter  $\partial J^-(S)$ , but cannot leave  $\partial J^-(S)$ . The proof of this claim formally requires some mathematical theorems, but nothing we cannot tackle using physical intuition. In addition, the breakthroughs in this field were all accomplished by arguments such as the ones in the proof of Penrose and it would be a shame not to let the reader taste these arguments.

**Proof .** Suppose that  $\gamma$  is a null geodesic generator of  $\partial J^-(S)$  and suppose that  $p \in \partial J^-(S)$  is a future endpoint of  $\gamma$ . We can find a patch  $V$  around  $p$  with Riemann normal coordinates, such that the causal relations in  $V$  are those of Minkowski space. This  $V$  is usually small, but we can always make it such that it has compact boundary<sup>1</sup>. We can then find a sequence of points  $p_i \in V \cap I^-(S)$  such that they converge to  $p$  as  $i \rightarrow \infty$ . For these  $p_i$ , there exist time-like geodesics  $\mu_i$  connecting the  $p_i$  to  $S$ . These geodesics  $\mu_i$

<sup>1</sup>Formally, we can do this because every manifold is locally compact.

leave the region  $V$  at points which we call  $q_i$ . Because we had ensured that the boundary of  $V$  is compact, the sequence of points  $q_i$  has a convergent subsequence which converges to a point  $q$ . Also the curves  $\mu_i$  belonging to this subsequence converge to a curve  $\mu$ . We cannot be sure that this curve is still time-like, but continuity ensures that it is at least not space-like anywhere: the limit of all these curves must lie in the closure of  $I^-(S)$ . The curve  $\mu$  shows that  $p \prec q$ . Also, we assumed that  $p$  is an endpoint of a null geodesic, thus  $q \notin \partial J^-(S)$ . Since the  $q_i$  were elements of  $I^-(S)$ , it follows that also  $q \in I^-(S)$ . This implies that  $q \ll S$ , which is shorthand for stating that there is a point  $s \in S$  for which  $q \ll s$ . By the relations given above, we find that  $p \ll S$ . However, this means that there exists a time-like curve from  $p$  to  $S$ , implying that  $p \notin J^-(S)$ . This is a contradiction, thus our assumption that  $p$  is an endpoint of  $\gamma$  must be false. We may conclude that  $\gamma$  has no future endpoint on  $J^-(S)$ .

### 5.3.2 Horizons

The Area Theorem is a statement about the area of the event horizon of a black hole. In Section 3.4, we have already seen that the area of the largest trapped surface cannot decrease, which seems to be a very similar statement. However, there is a distinction in the various definitions. A trapped surface was defined as a surface on which  $\theta_{1,2} \leq 0$ , i.e. all the null geodesics leaving such a surface converge. In general trapped surfaces are closed surfaces inside the event horizon. The largest trapped surface is called the *apparent horizon*<sup>2</sup> and one can wonder whether this is actually also the event horizon. Although this is the case in some simple examples, this is not true in general. The most important difference between these two types of horizons is that the apparent horizon is observer dependent, whereas the event horizon is not. Indeed, Robert Wald and Vivek Iyer [72] showed that in the case of the Schwarzschild black hole, the trapped surfaces (and thus also the apparent horizon) can be transformed away by a suitable transformation, whereas the true event horizon is a topological property of the spacetime. We will therefore not use trapped surfaces to define the event horizon.

We can define a black hole as the collection of points in spacetime from which light cannot escape, which we can write as  $M \setminus J^-(\mathcal{I}^+)$ , where we defined  $\mathcal{I}^+$  as future null infinity already in Chapter 2. The event horizon then lies at the edge of this set and is thus characterized by  $\partial J^-(\mathcal{I}^+)$ <sup>3</sup>. This definition is very useful in our context, since it allows us

<sup>2</sup>Or more precise: the boundary of the collection of all the trapped surfaces is called the apparent horizon.

<sup>3</sup>The event horizon characterized in this way does not overlap with  $J^-(\mathcal{I}^+)$ , because one can prove that

to talk about spacetimes with an arbitrary number of black holes in any possible configuration, as long as it is asymptotically flat. However, it is prudent to also indicate a few drawbacks: it is firstly highly unpractical to use in reality, since it is quite impossible to actually reconstruct all light-like geodesics ending up in  $\mathcal{I}^+$ . This means it is impossible using this definition to actually find the event horizon. Secondly, there is a somewhat philosophical issue: the event horizon given in this definition seems to respond in advance to future events. Finally, this definition is unlocal, which makes it very difficult to use it in local theories such as quantum gravity [4].

We have thus defined the event horizon as the causal past of a set and thus, by the Penrose theorem, we see that null geodesic generators of  $\partial J^-(\mathcal{I}^+)$  cannot leave  $\partial J^-(\mathcal{I}^+)$ .

### 5.3.3 Hawking's Area Theorem

Equipped with all the terminology and the theorems of the previous sections, we can now tackle *Hawking's Area Theorem*. The area of the event horizon is actually the area of the intersection of the event horizon  $\partial J^-(\mathcal{I}^+)$  with a space-like hypersurface, i.e. the spatial area of the event horizon at some point in time. From now on, this is what we mean by the area of the event horizon. For this area, the following is true, as has been proven by Hawking<sup>4</sup>:

**Theorem 5.3.2** *For an asymptotically flat black hole spacetime<sup>5</sup>, the area of the event horizon  $\partial J^-(\mathcal{I}^+)$  cannot decrease in time, if the weak energy condition holds and the cosmic censorship conjecture is true.*

Using the theorems we saw before and the machinery that was already set up in Chapter 3, it is not very difficult to prove this theorem:

**Proof .** The area of the even horizon is closely related to the divergence of the null geodesics on this surface, which we indicated by  $\theta$  (see Section 3.4). If  $\theta \geq 0$  everywhere on the event horizon, this means that the area is nowhere shrinking, thus the area cannot

this set is open.

<sup>4</sup>The original paper on the area theorem [73] proves the area theorem for the case of two colliding black holes. It can however be proven for a more general case, the proof of which can be found in [4]. The proof presented here can be found in [65].

<sup>5</sup>This ensures that the compactification of spacetime is such that every null geodesic has future endpoints on the boundary of the compactified spacetime.

decrease as a whole. Suppose on the contrary that there is a point  $p$  on the event horizon for which  $\theta < 0$ . If we assume the cosmic censorship conjecture holds, then the region in spacetime outside the black hole is geodesically complete. Also, the null geodesic generators of  $\partial J^-(\mathcal{I}^+)$  form a geodesic congruence (as defined in Chapter 3.4). Then, as was already stated in Section 3.4.1 (p.88), there is a finite parameter value for which  $\theta \rightarrow -\infty$ , if also the weak energy condition holds. This means that there is full convergence of all the null geodesics from a neighbourhood of  $p$  at a conjugate point  $q$  to  $p$ , which is connected to  $p$  by a null geodesic  $\gamma$ . It can be shown that not all the null geodesics converging at  $q$  can continue [71], thus there is at least one null geodesic that ends at  $q$ . Now, if  $q$  lies in  $\partial J^-(\mathcal{I}^+)$ , this immediately leads to a contradiction, since Penrose's theorem showed that null geodesic generators cannot have future endpoints on  $\partial J^-(\mathcal{I}^+)$ . However, if  $q \notin \partial J^-(\mathcal{I}^+)$ , this means that  $\gamma$  left the event horizon at some point  $q'$  earlier in time. This would then be an endpoint for the light-like geodesic  $\gamma$  and also run into contradiction using Penrose's theorem. Hence, it must be that  $\theta \geq 0$  everywhere on the event horizon and so the area of the event horizon cannot shrink.

This proves the Area Theorem, also known as the *second law of black hole mechanics*.

### 5.3.4 Penrose Process

After coming across the Area Theorem for the first time, it is natural to try to come up with physical processes in which the Area Theorem might be false after all. In Chapter 2, we came across a process which was intended to do just this for the statement that the energy of a black hole cannot decrease: the Penrose process. We showed there that using the Penrose process it is possible to extract rotational energy from a Kerr black hole. What happens to the area of the event horizon of the black hole in such a case?

Since the particle that travels away from the black hole takes with it some of the rotational energy, it must be that the particle falling into the black hole has angular momentum opposite to that of the black hole. To see whether the area of the event horizon can decrease, we must investigate the maximum efficiency of this process. Let the particle that falls into the black hole have four-momentum  $p^\mu = (E, 0, 0, L)^T$ , which must be a future-pointing time-like vector (or null if the particle has no mass). Here  $E$  is the energy and  $L$  is the angular momentum of the particle. We already found in Section 5.1 that the vector  $\xi = \partial_t + \Omega_H \partial_\phi$  is normal to the event horizon, a null hypersurface. This implies that  $\xi$ , which incidentally generates translations along the null geodesic generators of the event horizon, is also a null vector. As the particle crosses the horizon, its four-momentum

must still be future-pointing, thus it must be that  $p \cdot \xi \geq 0$ . This leads to the estimate  $E - \Omega_H L \geq 0$ , thus  $L \leq E/\Omega_H$ . In the previous section, we found that

$$\delta M = \frac{\kappa}{8\pi G} \delta A + \Omega_H \delta J, \quad (5.3.3)$$

which holds for the black hole. We can rearrange this to give

$$\frac{\kappa}{8\pi G} \delta A = \delta M - \Omega_H \delta J. \quad (5.3.4)$$

By identifying  $\delta M = E$  and  $\delta J = L$ , we see that the right-hand side cannot be smaller than zero, because we saw  $E - \Omega_H L \geq 0$ . Thus the area  $A$  cannot decrease during this process. This shows that the Penrose process does obey the Area Theorem [1, p. 214].

The fact that the area of the event horizon of a black hole cannot decrease in any classical process is already very interesting in itself. Its proof relies only on the truth of the weak energy condition and the Cosmic Censorship Conjecture and is true for any asymptotically flat black hole spacetime. We will see in Section 5.5, however, that the second law has a much deeper interpretation.

## 5.4 The Third Law of Black Hole Mechanics

Historically, the third law of black hole dynamics was first stated as the fact that [68]

*“It is impossible by any process, no matter how idealised, to reduce the surface gravity  $\kappa$  to zero in a finite sequence of operations.”*

Although this first formulation lacks the mathematical rigour ostentiated in the derivations of the other laws, it should be possible to arrive at a more precise restatement by considering the dynamical processes that could potentially lead to a vanishing surface gravity. In order to come to this conclusion we will take a graphical approach based on the Penrose diagrams of such situations and formalise the methods to extract the required information from them. Finally, we will also consider a process in which a charged black hole emits chargeless particles as Hawking radiation. We will show such a procedure cannot make  $\kappa$  vanish either, in spite of the fact that this is not a classical phenomenon.

### 5.4.1 Extremal Black Holes Cannot Be Formed Continuously

The surface gravity of, for example, the Reissner-Nordström solution is given by

$$\kappa_{RN\pm} = \pm \frac{\sqrt{M^2 - Q^2}}{(M \pm \sqrt{M^2 - Q^2})^2} = \pm \frac{r_+ - r_-}{2r_\pm^2}, \quad (5.4.1)$$

where  $r_\pm$  refers to the outer horizon and inner horizon respectively. It is obvious that the situation  $\kappa = 0$  corresponds to the description of an extremal black hole with  $|Q| = M$  and coinciding horizons,  $r_+ = r_-$ . Let us take a closer look at extremal black holes and how they may be formed by interaction with the environment. For simplicity, we take these black holes to be Reissner-Nordström, although the conclusions can be generalised and so applies to Kerr-Newmann black holes as well [68, 74]. First of all, a simple thought experiment shows that extremisation can be achieved in finite advanced time in some highly idealised, discrete processes that are not subjected to the third law. Consider a spherically symmetric, extremally charged ( $|Q| = M$ ) infinitesimally thin shell with a supercritical mass  $M$  larger than the commonly accepted Chandrasekhar limit for black hole formation. The black hole resulting from the gravitational collapse of such a shell will certainly be extremal. Furthermore, it will become clear that extremal black holes can be realised by the injection of neutral matter with a negative energy density into a subextremal black hole, so that it will shrink in size but maintain a constant charge. However, this process will give way to other mechanisms that can lead to the creation of naked singularities, so that it is also in contradiction with the widely-accepted cosmic censorship conjecture that was argued for in Section (3.5).

In more realistic scenarios, absorption of an (overcharged) thick spherical shell causes the charge/mass ratio of an ordinary charged black hole to increase gradually, but never quite reach unity. Two such processes are depicted in the Penrose diagrams of Figures 5.2-5.3. These diagrams that are essentially an adaptation of the canonical diagram for the Reissner-Nordström solution that reflects the fact that the black hole was formed by the collapse of the matter on the left-hand side. The diagram for a normal RN black hole is mirror symmetric in the vertical axis, which separates the non-black hole regions into a universe on the right hand side and a copy on the left. If we now stipulate that the black hole is formed through gravitational collapse of matter in the right universe, only the causal future of the matter will have interesting effects and so the left hand side of the diagram is duly neglected. Before the matter passes the (coordinate  $r_+$  of the) outer horizon, the coordinate  $r = 0$  is just the centre of the spherical shell. Afterwards, however, it will be the location of the singularity. Remember that the normal diagram has two lines

designating the singularity. In this adaptation, the left hand one of the two is still present, but obfuscated by the surrounding matter.

Now, the interaction of the black hole with the thick mass shell will cause the black hole to change in size by contracting or expanding its horizon. In order to create an extremal black hole then, we wish to add matter in such a way that the inner and outer apparent horizons move closer together, squeezing out the trapped surfaces in between. This situation is shown in Figure 5.2, where  $r_+$  and  $r_-$  have indeed approached each other (i.e. smaller distance  $\Delta u = r_-(u) - r_+(u)$ ) after the mass shell has passed through both the outer and inner outgoing horizon. However, this will have significant repercussions for the fate of a radially outgoing light ray, moving towards the upper right corner in the Penrose diagram, that crosses the inner apparent horizon in the transition region. Preceding the crossing of the matter shell over the inner horizon, such a light ray will certainly end up at the singularity to the right as depicted by the blue arrow in the figure. After the crossing, however, the light ray will no longer be doomed to converge to the singularity but instead is able to escape from the black hole and diverge to infinity like the red arrow. Therefore, we must conclude that the horizon displacement caused by the matter shell has a strongly diverging effect. By Raychaudhuri's equation (3.4.8) this implies that the energy density of the infalling matter is negative, at least locally when it passes the inner horizon. Therefore, any relevant crossing over the outgoing sheet of the inner horizon would violate the Weak Energy Condition (WEC) [74].

Notice from the equations

$$r_+ = M + \sqrt{M^2 - Q^2} \quad r_- = M - \sqrt{M^2 - Q^2} \quad (5.4.2)$$

that it is, in fact, possible to throw in a particle with a charge  $q$  that is larger than its (positive) mass  $m$  and reduce the distance  $\Delta r = r_+ - r_-$  between the inner and outer horizon. This situation clearly cannot correspond to Figure 5.2, since there the horizons will only approach each other if the energy density of the matter is negative. Therefore, consider the alternate scenario, in which the matter shell falls through the ingoing sheet of the inner horizon. If we demand the matter to respect the WEC at the moment of crossing, we obtain the situation of Figure 5.3. The positive energy density of the matter has a converging action, so that the inner horizon is deformed upwards in the diagram. Evidently,  $r_+$  is perpendicular to the ingoing sheet of  $r_-$ , so that the two will never coincide. The exception is future spacelike infinity  $i^+$ , where they meet. We must conclude that extremisation, which occurs only when the inner and outer horizons coalesce and all trapped surfaces are squeezed out, is deferred until an infinite amount of advanced time has passed [74]. This behaviour inspires the following informal reformulation of the third law [74]:

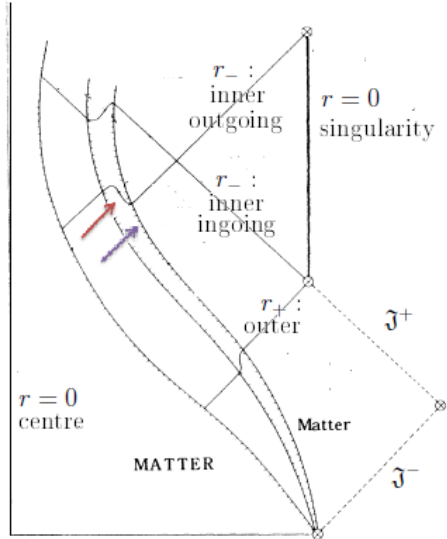


Figure 5.2: The crossing of matter through the outgoing sheet of the inner horizon has a diverging effect on outgoing light rays. By Raychaudhuri's equation, this implies that the absorbed matter must locally have a negative energy density when crossing the inner horizon, violating the WEC [74].

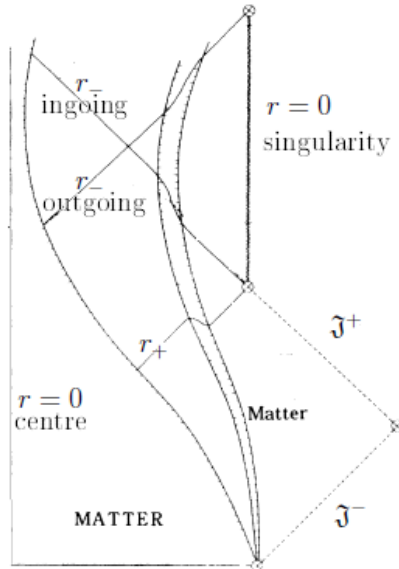


Figure 5.3: The crossing of matter with a positive energy density through the ingoing inner horizon has a converging action on ingoing light rays, so that the inner horizon is shifted upwards and extremisation will take an infinite amount of advanced time to attain [74].

*“A non-extremal black hole cannot become extremal (i.e. lose its trapped surfaces) at a finite advanced time in any continuous process in which the stress-energy tensor of accreted matter stays bounded and satisfies the Weak Energy Condition in a neighbourhood of the outer apparent horizon.”*

### 5.4.2 Formalisation of the Third Law

In what follows, we will develop the mathematical framework to formalise this statement of the third law. We will be required to introduce the notion of *strongly future asymptotic predictability* [74].

**Definition** We say a spacetime is *strongly future asymptotically predictable* if the domain of dependence  $D^+(\mathcal{S})$  of some partial Cauchy surface  $\mathcal{S}$  (i.e. the causal future of  $\mathcal{S}$ ) contains not only future timelike infinity  $\mathfrak{J}^+$  and a complete future segment of the event horizon as required for canonical asymptotic predictability, but also encompasses the outermost trapped surfaces closest to the outer horizon.

With this definition, it becomes possible to foliate this enhanced domain of dependence  $D^+(\mathcal{S})$  by a collection of partial Cauchy surfaces  $\mathcal{S}(\tau)$ . In other words,  $D^+(\mathcal{S})$  is divided into an infinite amount of spacelike hypersurfaces  $\mathcal{S}(\tau)$ , or slicings of the particular region of spacetime. These partial Cauchy surfaces intersect  $\mathfrak{J}^+$  in such a way that for each positive  $\tau$  after  $\mathcal{S}$  itself,  $\mathcal{S}(\tau)$  serves as a complete Cauchy surface for  $D^+(\mathcal{S}(\tau))$ , i.e. for the part of  $D^+(\mathcal{S})$  that lies to its future. As such, the parameter  $\tau$  can be interpreted as some (non)-unique time function that is globally defined over all of  $D^+(\mathcal{S})$ . All evolution between surfaces  $D^+(\mathcal{S}(\tau))$  is completely described by ordinary quantum field theory with  $\tau$  as guiding time coordinate. It is this parameter  $\tau$  that can be interpreted as the ‘advanced time’ a network of observers surrounding the black hole’s horizon at various distances will see tick away on their clocks. A more formal statement of the third law can then be given by [74]

*“In a strongly future asymptotically predictable black hole spacetime, let there be a continuous process in which  $\mathcal{S}(\tau)$  contains trapped surfaces for all  $\tau < \tau_{ext}$ , but none for  $\tau > \tau_{ext}$ . Then the Weak Energy Condition is necessarily violated in a neighbourhood of the apparent horizon on  $\mathcal{S}(\tau)$ . ”*

A simple way to see that this will indeed hold is to apply a lemma that is based strongly on Raychaudhuri’s equation of null congruences [74]:

**Lemma 5.4.1** *Let  $S_0$  be a trapped 2-surface. Consider then an extension of  $S_0$  to a 3-cylinder  $\Sigma$  composed of slicings formed by 2-sections  $S(\tau)$ , which has the three properties that (i) - the extension  $\Sigma$  is ‘semi-rigid’, i.e. the area of the 2-sections  $S(\tau)$  is locally preserved, and such that the ingoing light rays orthogonal to  $S(\tau)$  converge. (ii) -  $\Sigma$  is*

regular (iii) - the Weak Energy Condition holds on  $\Sigma$ . Such an extension  $\Sigma$  is everywhere spacelike, so that all subsequent 2-sections  $S(\tau)$  are trapped.

With this lemma, we can easily check if a certain process is eligible for the extremisation of a charged black hole. We first choose a trapped 2-surface  $S_0$ , from which we will try to draw spacelike extensions  $\Sigma$  that change their nature and become timelike upon crossing the inner horizon (where the signature of the spacetime itself will also flip!), like in Figure 5.4. The conclusion of the lemma may hereby be avoided and the process will have caused a dichotomy of the extension into a piece with and a piece without trapped surfaces, so that extremisation is achieved. However, this will not go by impunatively, since one of the premisses of the lemma will have to be violated in order for its conclusion to be rendered void. While ingoing light rays starting from  $\Sigma$  will surely converge and the extension is regular, we will indeed find the WEC is not satisfied on  $\Sigma$ . If, however, we try to construct a similar spacelike-becoming-timelike extension through the ingoing inner horizon as in Figure 5.5, the WEC will be satisfied but the ingoing convergence condition (i) will no longer hold. In that case, the spacetime is no longer strongly asymptotically predictable and the third law no longer applies. This enables the extremisation of the charged black hole, albeit only in infinite advanced time.

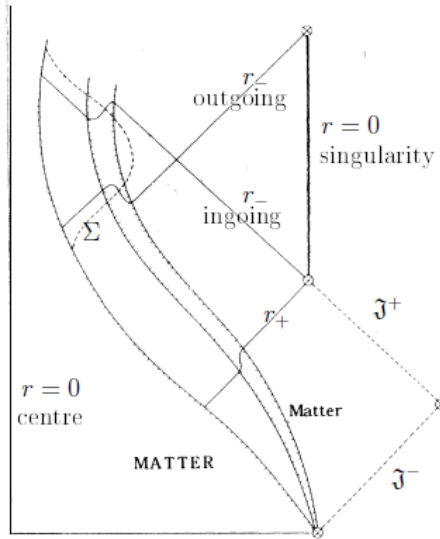


Figure 5.4: An extension  $\Sigma$  of a trapped surface  $S_0$  that starts out with spacelike nature, consisting of trapped surface  $S(\tau)$  for  $\tau$  before the crossing of the outgoing inner horizon, and continues as a timelike curve without trapped surfaces for  $\tau$  after the crossing, must violate one of the premises of lemma (5.4.1). Indeed, the WEC is not satisfied [74].

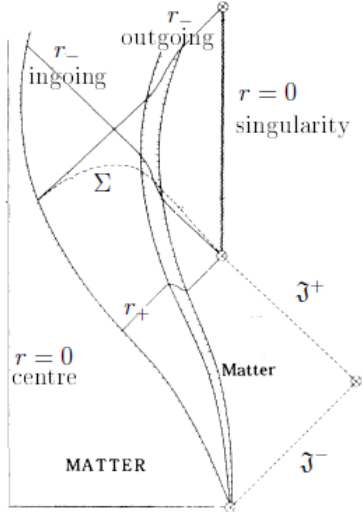


Figure 5.5: An extension  $\Sigma$  of a trapped surface  $S_0$  that starts with spacelike nature, consisting of trapped surface  $S(\tau)$  for  $\tau$  before the crossing of the outgoing inner horizon, and continues as a timelike curve without trapped surfaces for  $\tau$  after the crossing, must violate one of the premises of lemma (5.4.1). Indeed, the first prerequisite (i) is not satisfied [74].

### 5.4.3 Surface Gravity Cannot Become Zero by Hawking Radiation

Although hitherto we have kept to a classical treatment of black holes and have not yet arrived at the phenomenon of Hawking radiation, we here include a short paragraph on the validity of the third law when including such quantum effects. The full semi-classical derivation of Hawking radiation will be presented in Chapter 7. Only by sending out a particle with a lower charge/mass ratio will a RN black hole become more extremal. Consider therefore the situation in which the black hole sends out an uncharged but massive particle, so that its charge  $Q$  remains constant but its mass  $M$  decreases. It will turn out that the temperature at which a black hole emits its Hawking radiation is given by  $T = \kappa/2\pi = 1/8\pi M$ , so that by the Stefan-Boltzmann's law we obtain

$$\frac{dM}{dt} = -CAT^4 = -C \frac{(M^2 - Q^2)^2}{(M + \sqrt{M^2 - Q^2})^6}. \quad (5.4.3)$$

where  $C$  is some numerical constant. In this fashion, the evaporation time up to a certain point in the evolution of a black hole can be computed by the integral

$$t = \int dt = \int dM \left[ -\frac{1}{C} \frac{(M + \sqrt{M^2 - Q^2})^6}{(M^2 - Q^2)^2} \right]. \quad (5.4.4)$$

Now, we have that a similar integral over  $x$  yields

$$\begin{aligned} - \int dx \frac{(x + \sqrt{x^2 - 1})^6}{(x^2 - 1)^2} &= -16x - \frac{32x^3}{3} + \frac{x}{2(x^2 - 1)} - \sqrt{x^2 - 1} \left( \frac{64}{3} + \frac{32x^3}{3} - \frac{6}{\sqrt{x^2 - 1}} \right) \\ &\quad + \frac{35}{4} \ln \left( \frac{1+x}{1-x} \right), \end{aligned} \tag{5.4.5}$$

which will certainly diverge when  $x \rightarrow 1$ . Hence, putting  $x = |Q|/M$  shows conclusively that the time it takes for the black hole to radiate in such a way that it becomes extremal (when  $|Q|/M = 1$ ) is in fact infinite [75], and such a process is unattainable.

## 5.5 Black Holes and Entropy

In the previous four sections of this chapter, we have treated the four laws of black hole mechanics. In this section and the following section we will make plausible that the laws of black hole mechanics all have a corresponding law of thermodynamics. This is really just an analogy at the classical level, as we will argue that classical, non-radiating black holes have zero temperature. The analogy becomes much deeper when we consider a quantum mechanical treatment of black holes, which shall yield Hawking radiation and a non-zero black hole temperature. This treatment will be done in Chapter 7.

In this section we shall focus on the first and second law, in the following section on the zeroth and third law. The title of this section is not coincidentally the same as the article by Bekenstein from 1973 [76]. In this beautifully written article the correspondence between black hole mechanics and thermodynamics was laid out thoroughly for the first time. We shall follow the article closely here. In the following we use units in which  $c = G_N = k_B = 1$ , but  $\hbar \neq 1$ . This last choice will turn out to be crucial in the treatment, as we will be talking about fundamental units of information, which have a true quantum mechanical behaviour.

### 5.5.1 Relating Black Hole Physics to Thermodynamics

We have already seen several hints at the intricate relation between black holes and thermodynamics. A first hint is given by the no-hair theorems which we discussed in Chapter 4. Effectively the theorem states that a highly complicated object like a black hole can be characterized by just three parameters: its mass  $M$ , its electric charge  $Q$  and its angular momentum  $J$ . Putting aside the possible flaws of the no-hair theorem, we can compare

this to the situation in statistical mechanics. From statistical mechanics we know that we can describe a system of a gigantic amount of particles with just three macroscopic parameters, for instance  $\mu$ ,  $V$ ,  $T$  for the grand canonical ensemble. Noting that both the complicated black hole and the enormous number of particles can be described by just three macroscopic parameters is a first clue of the relation between black hole mechanics and thermodynamics.

Furthermore, we can compare the first law of thermodynamics in infinitesimal form:

$$dE = TdS - pdV, \quad (5.5.1)$$

where  $T$  is temperature,  $S$  entropy,  $p$  pressure and  $V$  volume, to the first law of black hole mechanics derived in the second paragraph of this chapter:

$$dM = \Theta d\alpha + \Omega dJ + \Phi dQ, \quad (5.5.2)$$

where  $\alpha := A/4\pi$  is the rationalized area and  $\Theta$ ,  $\Omega$  and  $\Phi$  are functions of the available parameters. Noting that  $E = m$  (remember  $c = 1$ ) we are tempted to identify the above equations with one another. We know from thermodynamics that  $-pdV$  represents the work done on the system. What should we identify as the work terms in the first law of black hole mechanics? This is a priori not clear, it could be any term from equation (5.5.2). Luckily, we have another piece of information. From Hawking's area theorem we know that  $dA \propto d\alpha \geq 0$ . Recalling that the second law of thermodynamics states that  $dS \geq 0$ , this gives us a reason to associate the area of a black hole to some kind of entropy. If we reason further like this, the terms  $\Omega dJ + \Phi dQ$  should represent the work done on the black hole, i.e.  $-pdV$ . As discussed before,  $\Omega$  plays the role of rotational angular frequency and  $\Phi$  the role of electric potential of the black hole.

As another source of inspiration, recall the Penrose process: the idea is that an object falls into a Kerr black hole and once it is in the ergosphere, it splits up. One part of the object moves against the rotation of the black hole and has negative energy, whereas the other part moves out of the ergosphere again, towards infinity, with a larger energy than the composite object had before it entered the black hole. The energy is extracted from the black hole by decreasing the angular momentum. In discussing the Penrose process, one can introduce the concept of irreducible mass:

$$M_{\text{irr}}^2 := \frac{A}{16\pi}. \quad (5.5.3)$$

It can be shown that  $\delta M_{\text{irr}} > 0$  for any process and we shall use this later. Note that we can interpret this irreducible mass as the analogue of energy which cannot be converted

into work in the case of thermodynamics! This is another hint at the relation between black holes and thermodynamics.

The following table summarizes the analogy between black hole mechanics and thermodynamics:<sup>6</sup>

Law	Thermodynamics	Black Holes
0th	A system in thermal equilibrium has a constant temperature $T$ everywhere.	A stationary black hole has a constant surface gravity $\kappa$ over its event horizon.
1st	$dE = TdS - pdV + \mu_i dN^i$	$dM = \Theta d\alpha + \Omega dL + \Phi dQ$
2nd	$dS \geq 0$	$d\alpha \geq 0$
3rd	$T$ cannot be brought to zero by a finite number of operations.	$\kappa$ cannot be brought to zero by a finite number of operations.

We shall elaborate more on the first and second law in this paragraph. The following paragraph will treat the zeroth and third law. Before we continue, it is important to note that the correspondence between classical black holes and thermodynamics is really an analogy. To illustrate this, consider a black hole which is in thermal equilibrium with an external 'normal' body. The normal body will emit radiation, of which a part is absorbed by the black hole. However, the black hole cannot emit radiation by its very definition, rendering the total system out of equilibrium. This is a contradiction, such that the temperature of the classical black hole must be zero. When one considers quantum effects, black holes can radiate and then the correspondence becomes formal. We shall see this in Chapter 7 explicitly.

Having made the relation between the laws of black holes and the laws of thermodynamics, we now turn to a formal discussion of information theory, enabling us to derive an explicit expression for the black hole entropy.

### 5.5.2 The Relation Between Entropy and Information

When the concept of entropy is introduced in a bachelor course on thermodynamics, the interpretation of order/disorder is often given: the entropy is high when the amount of disorder of the system is high. On the other hand, one might identify the amount of order of a system with the amount of information one has on the system. Consider a system

---

<sup>6</sup>Inspired by a similar table in Fay Dowker's lecture notes [65] on black holes.

which can be in  $N$  different states. In the thermodynamic limit we have of course  $N \rightarrow \infty$ . Suppose now that the probability  $p_n$  indicates that the system is in the  $n$ th state. We can then associate the *Von Neumann entropy* to the system given by:

$$S = - \sum_n p_n \ln(p_n) \quad p_n \in [0, 1] \quad \sum_n p_n = 1, \quad (5.5.4)$$

which is an analogue of the Gibbs entropy in statistical mechanics. Note that the formula above is completely generic: it does not depend on the system under consideration at all.

Suppose now that we obtain some new information  $\Delta I$  on the system. This means that we have some constraints on the  $p_n$ 's. Effectively, this will mean that some of the  $p_n$ 's are zero. The fact that you have more information on the system means that some states are not occupied any more, such that their probabilities are zero. As  $p_n \ln(p_n) < 0$  for  $p_n \in (0, 1)$ , all terms in the entropy are strictly larger than zero and thus we have a decrease in the entropy under the new constraints:  $\Delta I = -\Delta S$ . From this point of view entropy can be understood easily: when a non-equilibrium system evolves, its initial conditions get washed out, reducing the available information on the system ( $\Delta I < 0$ ), thus increasing the entropy of the system.

The smallest unit of information is called a *bit* and is the amount of information available when the answer to a yes-or-no question is known. Noting that the smallest amount of information corresponds to a maximum entropy, we can calculate the maximum of our freshly introduced entropy function. Firstly, we can write it in terms of  $p_{\text{yes}}$  only, using  $p_{\text{no}} + p_{\text{yes}} = 1$ :

$$S = -p_{\text{yes}} \ln(p_{\text{yes}}) - p_{\text{no}} \ln(p_{\text{no}}) = -p_{\text{yes}} \ln(p_{\text{yes}}) - (1 - p_{\text{yes}}) \ln(1 - p_{\text{yes}}).$$

Now we take the derivative and set it to zero:

$$\frac{\partial S}{\partial p_{\text{yes}}} = -\ln(p_{\text{yes}}) - 1 + \ln(1 - p_{\text{yes}}) + 1 = 0 \quad \Rightarrow \quad p_{\text{yes}} = p_{\text{no}} = 1/2.$$

Plugging this back into the entropy function, we find that one bit is equal to  $\ln(2)$  of information.

What does the concept of information have to do with black hole mechanics? Recall that a thermodynamic system in equilibrium can be described by a few macroscopic quantities, e.g. temperature and pressure. From the no-hair theorems we know that the same is the case for black holes: in most cases they are described by their mass  $M$ , charge  $Q$  and angular momentum  $J$ . Effectively we have already seen this in equation (5.5.2). However, exactly because we cannot cross the event horizon, obtain information, and return, black

holes with the same set  $(M_0, Q_0, J_0)$  may still have different internal configurations. Of course, we expect that the internal structure of a black hole formed by the collapse of a neutron star is different from the collapse of, say, our moon. The entropy we want to assign to the black hole is a measure of the inaccessibility of this information on the internal configuration. It is very important to understand that for a given set of equivalent black holes, all with the same set of parameters  $(M_0, Q_0, J_0)$ , we consider the entropy to distinguish between the different possible internal situations.

Inspired by Hawking's theorem of the non-decreasing area of a black hole, we conjecture that the entropy of a black hole must be a monotonically increasing function of the rationalized area  $\alpha$  of the black hole. Because  $d\alpha \geq 0$ , we know that  $d(\alpha)^n \geq 0$ , for some  $n \in \mathbb{Q}_{>0}$ . Of course, this also holds for  $n \in \mathbb{R}_{>0}$ , but let us apply Occam's razor for now. How do we know what  $n$  to choose? Bekenstein presents in his article only a counter argument for the choice  $n = 1/2$  and then simply continues with the choice  $n = 1$ , as it is “the next simplest choice”. Because of Hawking's later result, we know that the latter is the correct choice, but Bekenstein did not really give a solid argument. However, we can argue why  $n = 1/2$  is impossible. Suppose we have two black holes in a vacuum with mass  $M_1$  and  $M_2$ . After merging, we have  $S_1 + S_2 < S_{\text{merged}}$ . Because  $S \propto \sqrt{\alpha} \propto M_{\text{irr}}$ , we also have  $M_1 + M_2 < M_{\text{merged}}$ . But that is impossible, as we just merge two black holes in a vacuum: where should the additional mass come from? This contradiction does not hold in the  $n = 1$  case, because we then have  $S \propto \alpha \propto M_{\text{irr}}^2$ , yielding  $M_1^2 + M_2^2 < M_{\text{merged}}^2$ . As we always have  $(M_1 + M_2)^2 > M_1^2 + M_2^2$ , we have no contradiction. Let us thus continue with the choice of  $n = 1$ :

$$S_{BH} = \gamma \alpha, \quad (5.5.5)$$

where  $\gamma$  is a positive constant. We assume that we may introduce  $S_{BH}$  for an arbitrary black hole.

In our units the entropy is dimensionless ( $k_B = 1$ ), thus we must have  $[\gamma] = m^{-2}$ . The only constant with the correct units would be  $\hbar^{-1}$ .<sup>7</sup> So we have:

$$S_{BH} = \frac{\eta \alpha}{\hbar}, \quad (5.5.6)$$

where  $\eta$  is a dimensionless constant which we will estimate in the next section. Note that at this point, the occurrence of  $\hbar$  in the above equation is just based on dimensional arguments. Intuitively, we know that its occurrence makes sense: the entropy is a count of the states of the system and such states are always ‘quantum’. In the next section we shall use the expression for the Compton wavelength in a qualitative way. Again, this

---

<sup>7</sup>This is exactly the reason why we chose a unit system with  $\hbar \neq 1$ .

points us to the quantum mechanical nature of the problem at hand, but a full quantum mechanical treatment, in which we can associate the known value to  $\hbar$ , was given a year after Bekenstein by Hawking.

### 5.5.3 Estimating the Black Hole Entropy

As a thought experiment, consider an elementary particle which falls into the black hole. The minimum amount of information we have of the particle before it falls into the black hole is that it exists. Recall that we defined a bit as the answer to a yes or no question. In this case this question would be: “Does the particle exist?”. Before it has fallen into the black hole, the answer is yes. After it has fallen in, we do not know this any more. Having lost at least one bit of information, we expect the entropy to have increased.

We thus want to calculate the minimum possible increase in the area of the black hole, due to the absorption of one particle. Christodoulou<sup>8</sup> showed that if a point particle falls freely into a black hole, the area of the black hole is left unchanged. We shall therefore consider a spherical particle with a finite radius  $b > 0$  and mass  $\mu$ . Bekenstein derives in his article that

$$(\Delta\alpha)_{\min} = 2\mu b. \quad (5.5.7)$$

The derivation uses the Kerr metric and considers a point just outside of the horizon,  $r_0 = r_+ + \delta$ , such that it is located a proper distance  $b$  outside the horizon. Using the first integrals of the metric and some specific inequalities for the Kerr black hole (like  $a^2\Omega^2 \leq 1/4$ ), one can then show equation (5.5.7) to first order in  $b$ .

Having found the minimum possible increase in the black hole area, we must think about the values  $b$  can take on. Two length scales are important here: the Compton wavelength  $\lambda = \hbar/\mu$  and the Schwarzschild radius  $\tilde{\lambda} = 2\mu$  of the particle. Demanding that  $b > \tilde{\lambda}$  ensures that we are not dealing with a little black hole falling into a bigger black hole and demanding  $b > \lambda$  ensures that we can really consider our particle to be a particle instead of a wave. We have  $\lambda > \tilde{\lambda}$  for  $\mu < \sqrt{\hbar/2}$ , but  $\tilde{\lambda} > \lambda$  for  $\mu > \sqrt{\hbar/2}$ . In both cases, we obtain the smallest possible increase in the black hole area  $(\Delta\alpha)_{\min} = (2\mu b)_{\min} = 2\hbar$ , due to the loss of one bit of information.

We can now calculate the dimensionless constant  $\eta$  from equation (5.5.6). We just use the

---

<sup>8</sup>He did this in his PhD thesis, to which Bekenstein refers. Unfortunately, it cannot be found in your standard library or web shop.

fact that we found that one bit is equal to  $\ln(2)$  of information:

$$\ln(2) = (\Delta S_{BH})_{\min} = \frac{\eta}{\hbar}(\Delta\alpha)_{\min} = \eta\hbar^{-1} \cdot 2\hbar \quad \Rightarrow \quad \eta = \frac{1}{2}\ln(2). \quad (5.5.8)$$

We must note that the calculation for the value of  $\eta$  is crucially based on the assumption that the smallest possible radius of particle is exactly equal to its Compton wavelength. The actual radius is not so sharply defined. Doing a truly quantum mechanical calculation, one will find a different value, but it is close to  $S \approx 0.11A/(4\hbar)$ . Indeed, a year after Bekenstein's article, Hawking showed (by doing a full quantum mechanical treatment) that  $S = \alpha\pi/\hbar = A/(4\hbar)$ . We will do this calculation explicitly in Chapter 7.

We have thus found the entropy of a black hole. Upon reintroducing the elementary constants, we obtain:

$$S_{BH} = \frac{\ln(2)k_B c^3}{8\pi\hbar G} A. \quad (5.5.9)$$

To get a feeling for the numbers, let us consider the sun collapsing to form a Schwarzschild black hole. The area of the black hole is then given by  $A = 4\pi(r_+^2 + a^2)|_{a=0,Q=0} = 16\pi M^2 \equiv 16\pi M^2 G^2 c^{-4}$  and the entropy becomes:

$$\begin{aligned} S &= \frac{\ln(2)}{8\pi\hbar} k_B c^3 G \cdot 16\pi \frac{G^2 M^2}{c^4} \\ &= \frac{2\ln(2)GM^2 k_B}{\hbar c} \\ &\approx 10^{53} J/K, \end{aligned}$$

which is quite large.

### 5.5.4 The Generalized Second Law of Black Hole Thermodynamics

If one throws a box of entropy into a black hole, the total entropy of the universe minus the black hole has decreased, seemingly violating the second law of thermodynamics. We can easily solve this by requiring that "*The common entropy in the black-hole exterior plus the black-hole entropy never decreases*". We call this the generalized law of black hole thermodynamics. Note that a consequence of this statement is that we really consider the entropy of a black hole to be a genuine contribution to the entropy content of the universe. At this point, this formulation of the second law does not make so much sense yet, because we argued that classically the black hole temperature should be zero. After Hawking's treatment, this statement is formally true.

Let us write this generalized second law down mathematically. Consider an object with entropy  $S$ . If we add this body to the black hole, the information about the internal configuration of the body become inaccessible. We thus expect the black hole entropy to increase by at least  $S$ . Defining  $\Delta S_c \equiv -S$  the generalized second law becomes

$$\Delta S_{BH} + \Delta S_c > 0. \quad (5.5.10)$$

## 5.6 Temperature and Euclidean Gravity

In the first four sections of this chapter, the four laws of black hole mechanics were discussed. These laws appear to be very similar to the laws of thermodynamics. In Section 5.5 we started discussing this correspondence in greater detail. Here, we will continue this discussion. While the previous section mainly concentrated on defining the entropy of a black hole, in this section we will focus on the concept of black hole temperature.

The black hole temperature is related to the surface gravity of the black hole. We will start this section by arguing this. Subsequently, we will relate the zeroth and the third law of black hole mechanics to the ones of thermodynamics, thereby strengthening the relationship between temperature and surface gravity. After this, we will review the introduction of temperature in quantum field theories. Finally we will apply this to derive a relation between temperature and surface gravity by means of Euclidean gravity.

### 5.6.1 Surface Gravity as Black Hole Temperature

In the previous section, we argued that the area of a black hole plays the role of the black hole entropy. Similarly, we will argue here that the surface gravity is related to the black hole temperature. By viewing the entropy as a measure of the amount of inaccessible information, the relation to the black hole area became manifest. Unfortunately, the relation between surface gravity and black hole temperature is less intuitive.

One can name a few similarities, e.g. the surface gravity of a stationary black hole is positive, as is the temperature in thermodynamics (at least classically). Furthermore, we have seen that the surface gravity can be interpreted as the gravitational acceleration of an object near the event horizon as measured by an observer at infinity, but only for a stationary black hole. For a dynamical black hole, this interpretation does not hold, since the event horizon is no Killing horizon (see also Section 5.1). Similarly, it is harder to define

thermodynamic temperature for non-equilibrium systems. Recall that the thermodynamic temperature is defined in terms of the entropy  $S$  and the internal energy  $U$  of the system by

$$\frac{1}{T} = \left( \frac{\partial S}{\partial U} \right)_{N,V}, \quad (5.6.1)$$

for constant number of particles  $N$  and at a constant volume  $V$ .

The easiest way to see the relation between the surface gravity  $\kappa$  and the temperature  $T$  is by looking at the first law of black hole mechanics, given by equation (5.2.1). Ignoring the terms that represent the work done, we get

$$dM = \frac{\kappa}{8\pi} dA, \quad (5.6.2)$$

whilst the first law of thermodynamics is

$$dE = TdS. \quad (5.6.3)$$

As the area  $A$  is related to the entropy  $S$ , it follows that the surface gravity  $\kappa$  is the analogue of the temperature  $T$ , up to a constant.

The previous argument of relating the surface gravity to the temperature was proposed in a paper by Bardeen, Carter and Hawking a paper from 1973 [68]. However, they emphasize that this temperature must not be considered a thermodynamic temperature of the black hole. Their motivation is that a black hole can never be in equilibrium with a body at a finite temperature. Indeed, in this case black body radiation would be emitted into the black hole, while the black hole cannot emit any radiation itself. Thus, the classical black hole temperature must be zero. It was Hawking himself who two years later showed that black holes actually do radiate [77] (see also Chapter 7). Therefore they do have a finite temperature, which can be related to the surface gravity.

Black hole radiation is a quantum mechanical effect. Hence, we require a quantum mechanical treatment of black holes to obtain the exact relation between the temperature and the surface gravity. Such a treatment is done in Hawking's paper from 1975 [77] and his approach shall be treated in Chapter 7. Here, we will pursue the analogy between the laws of black hole mechanics and the laws of thermodynamics.

### 5.6.2 Black hole mechanics and Thermodynamics: Zeroth and Third Law

In Section 5.1, we showed that the surface gravity  $\kappa$  of a stationary black hole is constant along its event horizon. This is the zeroth law of black hole mechanics. The zeroth law of thermodynamics states that the temperature  $T$  is constant over a set of systems in thermal equilibrium. Again, one can clearly see that  $\kappa$  is the analogue of the temperature  $T$  here.

In Section 5.4, we covered the third law of black hole mechanics. As explained there, this law states that the surface gravity cannot be brought to zero by a finite number of operations. Similarly, a version of the third law of thermodynamics is that it is impossible to reach the absolute zero  $T = 0$  by a finite number of operations, making again clear the analogy between  $\kappa$  and  $T$ .

Classically, the correspondence between the laws of black hole mechanics and thermodynamics is nothing more than an analogy. Indeed, as stated above, a classical black hole has zero temperature. Also, if the no-hair theorem holds, then  $S = 0$ , since there is only one classical state of the black hole for a given mass, angular momentum and charge. Hence we cannot identify the temperature with the surface gravity, or the entropy with the area. Only if we incorporate quantum mechanics we will be able to make the exact identifications. In the next subsections, we will derive the temperature for the Schwarzschild and the Reissner-Nordström black holes, using the Euclidean gravity approach.

### 5.6.3 Introducing Temperature in Quantum Field Theory

Shortly after Hawking derived the exact relation between the black hole temperature and the surface gravity, the same result was derived again with a back-of-the-envelope calculation, e.g. in [78]. We will present this calculation in the next subsections for two specific cases. However, we first review how to introduce finite temperature in a quantum field theory.

We start with the path integral formulation of quantum mechanics. Consider a Hamiltonian operator

$$H(q, p) = \frac{p^2}{2m} + V(q) \quad (5.6.4)$$

and quantum states  $|q\rangle$  of a particle at position  $q$ . Then the amplitude for the particle to

go from position  $q_1$  to  $q_2$  in a time  $t_0$  is given in the path integral formulation by

$$\langle q_1 | e^{-iHt_0} | q_2 \rangle = \int \mathcal{D}q(t) e^{iS[q(t)]} \quad (5.6.5)$$

where the path integral is over all paths such that  $q(0) = q_1$  and  $q(t_0) = q_2$  and where  $S[q(t)]$  is the classical action (here  $\hbar = 1$ ). We now perform a Wick rotation by replacing the time  $t$  by the imaginary time  $\tau = it$ , such that we get

$$\langle q_1 | e^{-H\tilde{t}_0} | q_2 \rangle = \int \mathcal{D}q(\tau) e^{-S[q(\tau)]}. \quad (5.6.6)$$

where  $\tilde{t}_0 = it_0$ . The minus in the exponent is due to the definition of the action in imaginary time

$$S[q(\tau)] = \int_0^{\tilde{t}_0} \left( \frac{m}{2} \left( \frac{dq}{d\tau} \right)^2 + V(q(\tau)) \right) d\tau, \quad (5.6.7)$$

with  $p = m \frac{dq}{dt} = im \frac{dq}{d\tau}$ . To study the system at finite temperature, we must look at the partition function of the system. The partition function for a system in thermal equilibrium with a heat bath at temperature  $T$  is given by

$$Z = \text{Tr}[e^{-\beta H}] = \sum_n \langle n | e^{-\beta H} | n \rangle. \quad (5.6.8)$$

where  $\beta = T^{-1}$  ( $k_B = 1$ ). The sum is over a complete set of states  $\{|n\rangle\}$ . Evaluating this further by inserting (5.6.6) evaluated at imaginary time  $\tilde{t}_0 = \beta$  in (5.6.8) with  $|q_1\rangle = |q_2\rangle = |n\rangle$  yields

$$Z = \int \mathcal{D}q(\tau) e^{-S[q(\tau)]} \quad (5.6.9)$$

where because of the sum in (5.6.8), the path integral is now over all paths such that  $q(0) = q(\beta) \equiv q$ , where we integrate over all positions  $q$ . Note that we used here that the states  $|q\rangle$  form a complete set in the sense that  $\int dq |q\rangle \langle q| = 1$ . Thus, we have found a path integral representation of the partition function. The extension to a field theory happens in the same way as for the usual quantum mechanical path integral. It is easy to show that this yields

$$Z = \int \mathcal{D}\phi e^{-S[\phi(\tau)]}, \quad (5.6.10)$$

where the path integral is over all paths such that  $\phi(\mathbf{x}, 0) = \phi(\mathbf{x}, \beta)$ . Note that the action is now an integral of the Lagrangian density over space and over the imaginary-time interval  $[0, \beta] / \sim$ . Here the  $\sim$  is an equivalence relation which makes the two boundary points of the interval equivalent. This means we have compactified range of the imaginary time to the circle. We have now introduced the temperature in the quantum field theory, noticing that  $\beta$  is the inverse temperature.

To summarize, we can introduce a temperature in our theory by performing a Wick rotation and subsequently compactifying the imaginary time dimension to the circle, such that the inverse temperature is identified with the circumference  $\beta$  of this circle.

### 5.6.4 Euclidean Gravity: Schwarzschild Solution

We now present an extremely simple derivation of the black hole temperature. This approach is also found in [78], for example. As stated before, we require a quantum mechanical description for this. Let us ignore all details for the moment and just assume that we have quantized our theory. Then we can introduce a temperature in our theory by performing the steps above. Hence, we perform a Wick rotation and compactify the imaginary time coordinate  $\tau \in [0, \beta]/\sim$ . We then get a Euclidean metric (signature +++) where  $\beta = T^{-1}$  is the inverse temperature of a heat bath with which the black hole is in thermal equilibrium. Equation (2.1.1) then becomes

$$ds^2 = \left(1 - \frac{2M}{r}\right) d\tau^2 + \left(1 - \frac{2M}{r}\right)^{-1} dr^2 + r^2 d\Omega^2. \quad (5.6.11)$$

We are interested in the black hole temperature, so we determine the behaviour near the event horizon  $r = 2M$ . Define a new coordinate  $\xi = r - 2M$ , so that  $\xi \downarrow 0$  as we approach the event horizon from outside the black hole. Expanding the metric tensor components to lowest order in  $\xi$  then yields

$$\begin{aligned} ds^2 &= \frac{\xi}{r} d\tau^2 + \frac{r}{\xi} dr^2 + r^2 d\Omega^2 \\ &\approx \frac{\xi}{2M} d\tau^2 + \frac{2M}{\xi} d\xi^2 + (2M)^2 d\Omega^2. \end{aligned} \quad (5.6.12)$$

We now define a new coordinate  $\rho^2 = 8M\xi$ ,  $\rho \in \mathbb{R}_+$  such that we get

$$ds^2 = \frac{\rho^2}{16M^2} d\tau^2 + d\rho^2. \quad (5.6.13)$$

where we ignored the  $S^2$  part of the metric. We see that the result is just a conical metric  $ds^2 = r^2 d\phi^2 + dr^2$ , if we identify the angle  $\phi$  with  $\frac{\tau}{4M}$ . This means that we also have conical singularities<sup>9</sup> unless we require that  $\phi \in [0, 2\pi]/\sim$ , in which case our metric just describes flat space in polar coordinates. Comparing with (5.6.13), we then see that here we should

---

<sup>9</sup>To see this, suppose  $\phi \in [0, \alpha]/\sim$  and  $\alpha = \pi$ . The resulting spacetime then looks like a half-plane, say  $\{(x, y) \in \mathbb{R}^2 | y \geq 0\}$ , with the rays  $x > 0$  and  $x < 0$  glued together. Due to this gluing, the point  $(0, 0)$  will look like the apex of a cone. Such a singularity occurs for any  $\alpha \neq 2\pi$ . Manifolds with such conical singularities are sometimes called *conifolds*.

require that  $\tau \in [0, 8\pi M]/\sim$ . But we already compactified the imaginary time coordinate such that  $\tau \in [0, \beta]/\sim$ . Hence we find that

$$\beta = 8\pi M \quad (5.6.14)$$

or, using that the surface gravity for the Schwarzschild black hole is given by  $\kappa = \frac{1}{4M}$  (see equation (5.1.12)),

$$T = \frac{\kappa}{2\pi}. \quad (5.6.15)$$

This is exactly the result Hawking found by using much more difficult methods which will be explained in Chapter 7. Note that, consistent with our interpretation of the surface gravity, this is the temperature as measured by an observer at infinity. Like frequency (inverse real time), the temperature (inverse imaginary time) also experiences a redshift [78].

From this we can calculate that the entropy is given by

$$dS = \frac{dM}{T} = 8\pi M dM \Rightarrow S = 4\pi M^2 = \pi R^2 = \frac{A}{4}, \quad (5.6.16)$$

using that the radius of the black hole is  $R = 2M$ . This result corresponds to the entropy Hawking found, as stated in Section 5.5.

Restoring the physical constants, the temperature is given by

$$T = \frac{\hbar c^3}{8\pi GM k_B}. \quad (5.6.17)$$

According to this formula, the temperature of a black hole with the mass of the sun in thermal equilibrium would be approximately  $6 \cdot 10^{-8}$  K, which is negligible compared to the cosmic microwave background ( $\approx 2.7$  K). A black hole with a temperature which approximately corresponds to the cosmic microwave background would have a mass comparable to that of our Moon.

The above result yields evidence for the thermal nature of quantum field theory in a black hole background. Therefore, this result led to many physicists striving for an understanding of the statistical mechanics of black holes. One hopes that this will yield a deeper understanding of quantum gravity, in much the same way as understanding the statistical mechanics of black body radiation led to a greater understanding of quantum mechanics.

### 5.6.5 Euclidean Gravity: Reissner-Nordström Solution

Here, we will derive the black hole temperature once more, using the same Euclidean gravity approach, but this time for the Reissner-Nordström black hole. We consider the

case  $M^2 > Q^2$ , which is the physical solution, as explained in Section 2.2. First, we write the metric (2.2.9) in the form

$$ds^2 = -\frac{1}{r^2}(r - r_+)(r - r_-)dt^2 + \frac{r^2}{(r - r_+)(r - r_-)}dr^2, \quad (5.6.18)$$

where we ignored the  $S^2$  part of the metric and where  $r_+$  and  $r_-$  are defined by (2.2.10). Performing the Wick rotation and compactifying the imaginary time to  $\tau \in [0, \beta]/\sim$  yields

$$ds^2 = \frac{1}{r^2}(r - r_+)(r - r_-)d\tau^2 + \frac{r^2}{(r - r_+)(r - r_-)}dr^2. \quad (5.6.19)$$

We determine the behaviour near the outer event horizon  $r_+$ . Therefore we define a new coordinate  $\zeta = r - r_+$ , so that  $\zeta \downarrow 0$  as we approach the event horizon from outside the black hole. Using  $\delta \equiv r_+ - r_-$ , the metric now reads

$$ds^2 = \frac{\zeta(\zeta + \delta)}{(\zeta + r_+)^2}d\tau^2 + \frac{(\zeta + r_+)^2}{\zeta(\zeta + \delta)}d\zeta^2. \quad (5.6.20)$$

Expanding the metric tensor components to lowest order in  $\zeta$  then yields

$$ds^2 \approx \frac{\delta\zeta}{r_+^2}d\tau^2 + \frac{r_+^2}{\delta\zeta}d\zeta^2. \quad (5.6.21)$$

Now note that we can write this in terms of the surface gravity  $\kappa$  at the outer horizon, which is equal to  $\kappa = \frac{\delta}{2r_+^2}$  (see equation (A.4.1)), as follows:

$$ds^2 = 2\kappa\zeta d\tau^2 + \frac{1}{2\kappa\zeta}d\zeta^2. \quad (5.6.22)$$

But this is exactly the same as equation (5.6.12), since there  $\kappa = \frac{1}{4M}$ ! Therefore, following the exact same steps as in the previous subsection, the end result will also be the same:

$$T = \frac{\kappa}{2\pi}, \quad (5.6.23)$$

but the value of  $\kappa$  is different from the Schwarzschild case, of course.

Being able to derive these intricate results from such elementary computations seems almost too good to be true. As expected, there are a few subtleties we ignored. The most important of these subtleties concerns the Wick rotation. In quantum field theory in Minkowski spacetime, performing Wick rotation can be justified as follows. Propagators in quantum field theory are integrals over momentum space and have poles on the real  $p^0$  axis. The divergence of these integrals is resolved by adding an arbitrarily small but nonzero contribution  $\pm i\epsilon$  to the poles, with  $\epsilon > 0$ . After doing so, the integral over  $p^0$  can be treated as a contour integral in the complex plane. The Wick rotation is then just a

particular deformation of this contour. This deformation is allowed, if no poles are crossed when deforming the contour. This is true, provided the poles were shifted in the way which defines the Feynman propagator.

However, in quantum gravity, it is far less obvious whether performing a Wick rotation is allowed. One of the reasons is that in the path integral approach in curved spacetime we must also include a path integral over the metric tensor. In the approach followed above, all seems to work out well for the Schwarzschild metric, the charged Reissner-Nordström metric and as shown in appendix A.5, also for the Kerr metric. However, it is not a priori clear that a path integral over Euclidean spacetime should be equivalent to a path integral over Lorentzian spacetime. Therefore unsurprisingly, Euclidean quantum gravity is still a hot topic in physics.

# Chapter 6

## Perturbations of Black Hole Geometries

In this chapter we study the effect of perturbing the various spacetime geometries that were considered in the previous chapters. We have already seen that isolated black holes in equilibrium are intrinsically simple objects as they can be completely described by their mass, angular momentum and charge. A real black hole on the other hand, such as those at the centre of a galaxy, is always in a perturbed state. By analysing these perturbations one can investigate how a black hole will interact with its astrophysical environment and whether or not the system will in fact be stable. In particular one may study the oscillations of a newly formed black hole, which due to its compactness, can be strong enough to be detected by existing gravitational-wave observatories. Since our current understanding of the universe outside the Solar System comes almost exclusively from observations of electromagnetic radiation, neutrinos and cosmic rays, the advent of gravitational-wave physics would open up an entirely new window onto energetic phenomena in the distant universe. Furthermore on the theoretical side, the motivation has a more transcendent interest: it provides insight, in its simplest and purest context, into the deeper aspects of space and time as conceived by general relativity.

A black hole can be perturbed in a variety of ways, a few examples being by incident gravitational waves, in-falling objects or by the accretion of matter surrounding it. The question one would like to ask is then as follows: Do black holes possess a distinct set of 'pure tones' representing the time evolution of some initial displacement from their equilibrium state? Several numerical analyses have proven that indeed they do; during a certain time interval, the evolution of some initial perturbation is dominated by damped

single frequency oscillations, namely quasinormal modes. In contrast to a idealised closed system, perturbed black hole systems are intrinsically dissipative due to the presence of an event horizon. This precludes a normal-mode analysis because the system is time-asymmetric and therefore the associated boundary value problem is not Hermitian. In general, quasinormal modes will have complex characteristic frequencies, with the real part representing the frequency of the oscillation and the imaginary part representing the damping. Similar to the normal-mode analysis one finds that the frequencies and decay rates of the quasinormal modes are independent of the particular perturbation and depend only on the parameters of the black hole. At first sight the existence of these modes may seem bemusing, as a black hole does not posses any material which could sustain such oscillations. Furthermore the horizon, although often regarded as a kind of membrane, is also not the main carrier of these oscillations. The oscillations essentially involve the metric *outside* the horizon, illustrating the fact that in general relativity the spacetime is not merely a stage where physical processes occur, rather it is a dynamical entity itself.

In normal-mode analysis one usually has a system of ordinary differential equations, and imposes boundary conditions to the effect that the wave function must vanish outside a finite region of space. This system is described by a self-adjoint operator with a discrete spectrum and a complete set of normal modes. In the system under consideration the perturbation of the black hole will propagate throughout all space, we cannot therefore demand that they should be zero outside a finite region. Instead we must impose that no gravitational radiation unrelated to the initial perturbation disturbs the system at a later time. Specifically this means that nothing is supposed to come in from spatial infinity or to come out of the black hole's horizon. Consequently, the spectrum of the corresponding operator is continuous, this seems to contradict the existence of the single quasinormal frequencies. The issue pertains to the fact that the quasinormal modes will generally not form a complete set, meaning that we are unable to describe the time evolution of any initial perturbation as a superposition of such quasinormal modes that has existed forever and will continue to exist forever without changing. Instead one should regard the quasinormal modes as quasi-stationary states and hence consider them as a solution only at a particular instant in time.

## 6.1 Quasinormal Modes of a Schwarzschild Black Hole

### 6.1.1 Normal Modes and Quasinormal Modes

Because quasinormal modes have a couple of properties in common with normal modes, we begin with recalling what normal modes are.

Normal modes (also called harmonics) are periodic solutions of oscillating systems without dissipation (hence no energy loss), which can be fully specified by their frequency and amplitude. Normal modes can be expressed as

$$\psi_n(t, x) = e^{i\omega_n t} \psi_n(x), \quad (6.1.1)$$

where  $\psi_n(x)$  is some complex-valued field and  $\omega_n$  is real. The general solution to the system can be expressed by

$$\psi(t, x) = \sum_{n=1}^{\infty} a_n \psi_n(t, x). \quad (6.1.2)$$

A well-known example of a system, for which the solutions are normal modes, is a string which is fixed at its endpoints. The normal modes then describe how the string vibrates.

Now consider quasinormal modes. They differ from normal modes because they are not stationary but damped. Quasinormal modes depend on time as

$$\psi(t) \sim e^{-i\omega t}, \quad (6.1.3)$$

with  $\omega$  a complex number. The real part of  $\omega$  is responsible for the oscillating behavior of the quasinormal modes and the imaginary part of  $\omega$  causes the damping.

An example of quasinormal modes, which will be familiar to everyone, is the ringing of a glass after we have (gently) hit it with a knife or a spoon. We hear the modes of the glass, which almost sound like normal modes only that they do not live on forever but they damp.

### 6.1.2 Perturbing a Schwarzschild Black Hole

In this section we will show how we can describe the behavior of perturbations of a Schwarzschild black hole as a one-dimensional wave equation with a potential term.

We start out with the familiar Schwarzschild metric, see equation (2.1.1). We perturb this equilibrium state. We can do that in several different ways. We can perturb the metric, include a scalar field, include an electromagnetic field, etc. Here we will derive the earlier mentioned wave equation by considering a perturbation in the metric and then linearize the Einstein equations. If we would include a matter field, for example a scalar field, we would deduce the wave equation by solving the equations of motion. That is if we would assume that there is no back-reaction, thus the metric is not changed by adding the matter field and we do not have to solve the Einstein equations again.

Consider a small gravitational perturbation,  $h_{\mu\nu}$ , on the Schwarzschild metric background

$$\tilde{g}_{\mu\nu} = g_{\mu\nu} + h_{\mu\nu}. \quad (6.1.4)$$

Now we will calculate the Ricci tensor up to linear order in the perturbation. We already know that the background metric solves the Einstein equations. We also want the perturbed metric,  $\tilde{g}_{\mu\nu}$ , to be a solution to the Einstein equations (in vacuum), hence we get that

$$R_{\mu\nu} = 0, \quad (6.1.5)$$

$$\delta R_{\mu\nu} = 0. \quad (6.1.6)$$

We now want to write out an expansion for  $h_{\mu\nu}$  by using properties of the background metric. We can reduce the complexity of the deduced perturbation equations by using that our background metric, the Schwarzschild metric, is spherically symmetric. We expand  $h_{\mu\nu}$  in the following way

$$h_{\mu\nu} = \sum_{l=0}^{\infty} \sum_{m=-l}^l \sum_{i=1}^{10} C_{lm}^i(t, r) (Y_{lm}^i)_{\mu\nu}(\theta, \phi), \quad (6.1.7)$$

where  $(Y_{lm}^i)_{\mu\nu}(\theta, \phi)$  are tensor spherical harmonics and  $C_{lm}^i(t, r)$  are expansion coefficients. We have a summation from  $i = 1$  to  $i = 10$  because  $h_{\mu\nu}$  is symmetric, hence has ten independent components. This tensor function expansion is a generalization of the expansion for a scalar function in terms of spherical harmonics, which we know from for example the motion of an electron in an hydrogen atom. We have to use tensor spherical harmonics because  $h_{\mu\nu}$  should transform as a rank two tensor under rotations. More about this expansion for  $h_{\mu\nu}$  can be found in [79, 80].

We can simplify the problem by considering a gravitational perturbation with a specific  $l$ . We can do that because, due to spherical symmetry in the background metric, perturbations with different  $l$  will not mix in the perturbation equations. The same holds for  $m$ . Actually when we work out the perturbation equations (as is done in [79]) we find that the

equations for the time and radial component will not depend on  $m$ , hence we just leave  $m$  out. On top of that we can distinguish two types of perturbations by looking at how they transform under space inversion

$$(\theta, \phi) \rightarrow (\pi - \theta, \pi + \phi). \quad (6.1.8)$$

When a perturbation gets a factor  $(-1)^l$  under space inversion we call it a polar perturbation. When it gets a factor  $(-1)^{l+1}$  we call it an axial perturbation. Since our background metric is invariant under space inversions the perturbation equations do not mix polar and axial contributions, hence we can consider them separately.

After quite some calculational work, see Section 2 in [79], we get the time-dependent master wave equation. In this master wave equation our wavefunction is of the form

$$\psi(t, r) = \frac{1}{r} \left( 1 - \frac{2M}{r} \right) C(t, r). \quad (6.1.9)$$

Here  $C(t, r)$  is a specific expansion coefficient from the decomposition of  $h_{\mu\nu}$ . We get this, because during our derivation it turned out that the other expansion coefficients can be expressed in terms of  $C(t, r)$ , see Section 2 in [79]. Now we find the master wave equation itself

$$\left( \frac{\partial^2}{\partial t^2} - \frac{\partial^2}{\partial r^{*2}} + V(r^*) \right) \psi(t, r^*) = 0, \quad (6.1.10)$$

where  $r^*$  is the tortoise coordinate, which is given in equation (2.1.3). The tortoise coordinate maps the horizon,  $r = 2M$ , to  $-\infty$ , hence we only look at the spacetime outside the horizon. In the next section we give the explicit form of the potential  $V(r^*)$  for different types of perturbations.

### 6.1.3 Perturbations and Their Effective Potentials

In the foregoing section we saw the reduction of a complicated system involving a black hole in a perturbed state, to a relatively simple system analogous to a one-dimensional scattering problem of a particle in the presence of a potential. Moreover it is a remarkable fact that the same wave equation will describe the evolution of different perturbations with only the effective potential differing. For the axial and polar perturbations considered, we find the Regge-Wheeler and Zerilli potentials respectively [81, 80]

$$V_{RW}(r) = \left( 1 - \frac{2M}{r} \right) \left( \frac{l(l+1)}{r^2} - \frac{6M}{r^3} \right), \quad (6.1.11)$$

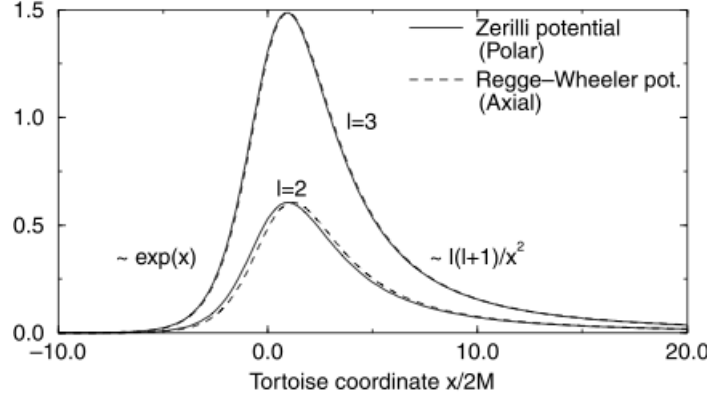


Figure 6.1: Regge-Wheeler and Zerilli potentials as a function of the normalized tortoise co-ordinate  $r^*/2M$  for  $l=2$  and  $3$ .

$$V_Z(r) = \left(1 - \frac{2M}{r}\right) \left\{ \frac{72M^3}{r^5\lambda^2} - \frac{12M}{r^3\lambda^2}(l-1)(l+2) \left(1 - \frac{3M}{r}\right) \right\} \\ \left\{ \frac{l(l-1)(l+1)(l+2)}{r^2\lambda} \right\}, \quad (6.1.12)$$

where  $\lambda = l(l+1) - 2 + 6M/r$ .

The Regge-Wheeler and Zerilli potentials (see figure 6.1) show that despite the functional form of the potentials being quite different, the shape of the curves are almost the same.

As an alternative to perturbing the black hole metric itself, one may introduce a matter field to the spacetime. That is we study the dynamics of the matter field on the fixed background metric, ignoring the influence that the corresponding energy-momentum tensor will have on the metric. As with the metric tensor we decompose the matter field into the appropriate spherical harmonic functions and again find that the expansion coefficients satisfy the same wave equation. Furthermore, if one considers a scalar or electromagnetic test field as the source of the perturbation, astonishingly we find that the potential is exactly of the Regge-Wheeler type

$$V(r) = \left(1 - \frac{2M}{r}\right) \left( \frac{l(l+1)}{r^2} + \frac{2M(1-s^2)}{r^3} \right), \quad (6.1.13)$$

where  $s \in \{0, 1, 2\}$  denotes the electromagnetic, scalar and axial gravitational perturbation respectively [82].

### 6.1.4 Quasinormal Modes as an Eigenvalue Problem

From the previous sections we have seen that in a spherically symmetric background, the study of black hole perturbations due to linearized fields of spin  $s$ , can be reduced to the study of a second order partial differential equation, namely the wave equation with a potential. The numerically observed single-frequency oscillation suggests that we could assume a harmonic time dependence for our perturbation and study the conditions which allow such a solution to exist. In other words, we will attempt to carry out a normal-mode analysis of black hole perturbations and will see why and how this approach fails. We will assume that the solution of the perturbation equation has the harmonic dependence  $\psi(t, r^*) = \exp(i\omega t)\phi(r^*)$ . Substituting this into the wave equation yields an ordinary differential equation in the radial co-ordinate (the time-independent wave equation),

$$\frac{\partial^2 \phi}{\partial r^{*2}} = (V(r^*) - \omega^2)\phi. \quad (6.1.14)$$

To determine the oscillation modes of a black hole, which correspond to the solutions of this ordinary differential equation, one must impose physically appropriate boundary conditions at the horizon ( $r^* \rightarrow -\infty$ ) and at spatial infinity ( $r^* \rightarrow \infty$ ). It is these boundary conditions and their consequences for the solutions of the time-independent wave equation that we turn to now.

### 6.1.5 Boundary Conditions

In a normal-mode analysis, a general perturbation can be represented as a continuous Fourier transform of solutions to the wave equation (6.1.14). For a Sturm-Liouville type problem, such as the finite string, one can reduce the continuous Fourier transform to a sum over individual frequencies, will this be possible for our system? From the considerations of the preceding chapters we suspect not, and this is indeed the case. The potentials under consideration are positive everywhere, vanishing towards the horizon and towards spatial infinity. Consequently they will not admit bound states and therefore we cannot impose that the solutions vanish at the boundary. This therefore precludes a normal-mode analysis, however let us press on with this procedure and see what problems will arise from it. As  $|r^*| \rightarrow \infty$  the asymptotic solutions to equation (6.1.14) will be a combination of in and out-going plane waves. Our boundary conditions come from the physical considerations that we do not want gravitational radiation to enter from spatial infinity or to appear from the black hole horizon. We must therefore impose that asymptotic solutions

should resemble purely out-going waves (where out-going means falling into the black hole thereby leaving the domain we are studying), i.e.  $\phi(r^*) \sim e^{\pm i\omega r^*}$  as  $r^* \rightarrow \pm\infty$  thus discarding unphysical waves entering from spatial infinity and non-classical waves emerging from the horizon. The solutions to equation (6.1.14) are precisely the quasinormal modes with discrete quasinormal frequencies  $\omega$ . Their normal-ness relates to the fact they are determined in a similar fashion to normal modes, whereas their quasi-ness expresses the fact that, unlike normal modes, they are not stationary solutions due to their strong damping.

### 6.1.6 The Mashhoon Method and Approximation With the Pöschl-Teller Potential

In this section we analytically compute the quasinormal modes by solving the wave equation with the so called Pöschl-Teller potential, which will serve as a prototype model to illustrate the physical essence of the problem. The original solution was found via the Mashhoon method, which is physically quite transparent [83]. The idea is as follows: Let  $R(\omega)$  and  $T(\omega)$  be the reflection and transmission amplitudes for the potential under consideration. The quasinormal frequencies correspond to those singular points of  $R(z)$ , the analytically continued  $R(\omega)$  to the complex plane, for which  $R(z) \neq 0$  and  $T(z)/R(z)$  is neither zero nor infinite. Heisenberg taught us that the singularities of the scattering amplitude are related to bound states. We can then extend this idea to barrier potentials by establishing a correspondence between the quasinormal modes and the bound states of the inverted potential. All we then have to do is to approximate this inverted potential by a potential for which we know there exists an analytic solution to the wave equation. One such example is the Pöschl-Teller potential,

$$V_{\text{PT}}(x) = \frac{V_0}{\cosh^2[\alpha(x - x')]} \tag{6.1.15}$$

where  $V_0 = V(x')$  is the maximum of the potential such that  $\partial V_{\text{PT}}(x')/\partial x = 0$  and  $-2V_0\alpha = \partial^2 V_{\text{PT}}(x')/\partial x^2$  is the curvature of the potential at its maximum. This potential therefore contains free parameters which can be adjusted to approximate the black hole effective potential near its maximum. The time independent wave equation becomes

$$\frac{\partial^2 \phi}{\partial r^{*2}} + \left( \omega^2 - \frac{V_0}{\cosh^2[\alpha(r^* - r^{*'})]} \right) \phi = 0. \tag{6.1.16}$$

The solutions of equation (6.1.16) are precisely the quasinormal modes, to find them we will take a more direct route. We start by defining a new independent variable  $\xi = (1 + e^{-2\alpha(r^* - r^{*'})})^{-1}$ , such that  $\xi \in (0, 1)$ . Substituting this into equation (6.1.16) we find

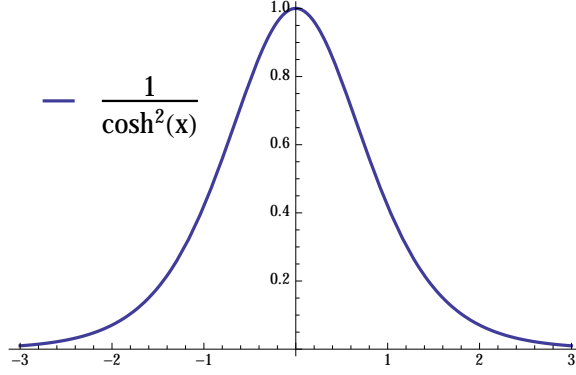


Figure 6.2: The Pöschl-Teller potential for  $V_0 = 1$ ,  $x' = 0$  and  $\alpha = 1$ .

$$\xi^2(1-\xi)^2 \frac{\partial^2 \phi}{\partial r^{*2}} - \xi(1-\xi)(2\xi-1) \frac{\partial \phi}{\partial \xi} + \left( \frac{\omega^2}{4\alpha^2} - \xi(1-\xi) \frac{V_0}{\alpha^2} \right) \phi = 0. \quad (6.1.17)$$

Our wave equation now looks unnecessarily complicated, however if we redefine our unknown function in terms of a new unknown function  $\phi = y(\xi(1-\xi))^{-i\omega/2\alpha}$ , and make the definitions  $a = (\alpha + \sqrt{\alpha^2 - 4V_0} - 2i\omega)/2\alpha$ ,  $b = (\alpha - \sqrt{\alpha^2 - 4V_0} - 2i\omega)/2\alpha$  and  $c = 1 - iw/\alpha$ , we find that our wave equation has an identical form to Euler's hypergeometric differential equation for a hypergeometric function  $y$ ,

$$\xi(1-\xi) \frac{\partial^2 y}{\partial \xi^2} + (c - (a+b+1)\xi) \frac{\partial y}{\partial \xi} - aby = 0. \quad (6.1.18)$$

Solutions to equation (6.1.18) are built out of the hypergeometric series

$${}_2F_1(a, b; c; \xi) = \sum_{n=0}^{\infty} \frac{(a)_n (b)_n}{(c)_n} \frac{\xi^n}{n!} \quad |\xi| < 1, \quad (6.1.19)$$

with

$$(q)_n = \begin{cases} 1 & n = 0 \\ q(q+1) \cdots (q+n-1) & n > 0. \end{cases}$$

If  $c$  is not a non-positive integer, the two independent solutions around the point  $\xi = 0$  (i.e. the horizon) are  ${}_2F_1(a, b; c; \xi)$  and  $\xi_2^{1-c} F_1(1+a-c, 1+b-c; 2-c; \xi)$ . The general solution can therefore be represented as the following linear combination

$$\begin{aligned} \phi = A \xi^{i\omega/2\alpha} (1-\xi)^{-i\omega/2\alpha} {}_2F_1(1+a-c, 1+b-c; 2-c; \xi) \\ + B (\xi(1-\xi))^{-i\omega/2\alpha} {}_2F_1(a, b; c; \xi), \end{aligned} \quad (6.1.20)$$

with  $A$  and  $B$  constant coefficients.

From equation (6.1.19) we find that  ${}_2F_1(a, b; c; 0) = 1$  and near the horizon  $\xi^{i\omega/2\alpha} \sim e^{i\omega r^*}$ , we notice therefore that the first term represents, according to our convention, a wave emerging from the horizon which is classically forbidden, as a consequence  $A = 0$ . The second term represents an out-going wave at the horizon, and therefore by our boundary conditions it should vanish at spatial infinity. Here one may use the transformation law  $\xi \rightarrow 1 - \xi$  for the hypergeometric function, which inverts the domain of  $\xi$  such that spatial infinity is now at  $\xi = 0$ .

$$\begin{aligned} {}_2F_1(a, b; c; \xi) &= (1 - \xi)^{c-a-b} \frac{\Gamma(c)\Gamma(a+b-c)}{\Gamma(a)\Gamma(b)} \\ &\quad {}_2F_1(c-a, c-b; c-a-b+1; 1-\xi) \\ &\quad + \frac{\Gamma(c)\Gamma(c-a-b)}{\Gamma(c-a)\Gamma(c-b)} {}_2F_1(a, b; 1+a+b-c; 1-\xi). \end{aligned} \quad (6.1.21)$$

The boundary condition at spatial infinity implies that either  $1/\Gamma(a) = 0$  or  $1/\Gamma(b) = 0$ , which are satisfied when the quasinormal frequencies are as follows,

$$\omega = \pm \sqrt{V_0 - \alpha^2/4} - i\alpha(2n+1)/2, \quad n = 0, 1, 2, \dots, \quad (6.1.22)$$

where  $n$  is the *overtone index*.

We have found that the out-going mode solutions to equation (6.1.16) oscillate at quasinormal frequencies given by (6.1.22), which are quantised in their *imaginary* part, but their *real* part is independent of  $n$ . The free parameters may now be used to approximate the black-hole potential near its maximum, resulting in a good approximation of the lowest frequencies, and in particular the fundamental frequency. However the highly damped modes remain elusive due to the fact that they are more sensitive to changes in the potential far from the maximum, and consequently are less well approximated.

It seems as though we have almost succeeded in analysing the perturbations of a Schwarzschild black hole in terms of their characteristic modes and frequencies. However there is a big caveat here, alluded to in the introduction to the chapter. The boundary conditions given in section 6.1.5 diverge exponentially near the horizon and at spatial infinity. The upshot of this is that the solutions satisfying these boundary conditions are not to be considered as solutions at any point in space, but rather as asymptotic solutions specifying the behaviour as we approach the boundaries. This then explains the incompleteness of the quasinormal modes mentioned in the introduction to this chapter. The incompleteness of the quasinormal modes can be seen in our approximation by the fact that their frequencies are limited in their real parts. It is therefore unlikely that an initial perturbation containing high-frequency components, will be completely represented as a sum over such a set of

incomplete quasinormal modes. It has been argued in [79] that any potential, falling off faster than exponentially towards infinity in the tortoise coordinate, will admit a complete set of quasinormal modes. Unfortunately both the Regge-Wheeler and Zerilli potentials decay with a power law dependence towards spatial infinity as shown by figure 6.1. As a result we must modify equation (6.1.2) as follows,

$$\psi(t, x) = \sum_{n=1}^{\infty} a_n \psi_n(t, x) + (\text{other contributions}). \quad (6.1.23)$$

The most important of the other contributions is the late time power-law tail. In the next section we will discuss this power-law tail and some other features that can be seen from the result of numerically integrating the time-dependent wave equation.

### 6.1.7 Numerical Results

In figure 6.3 an example of the waveform of a quasinormal mode is shown. In this example the observer is at  $r = 400 * 2M$ . This figure was obtained from numerical integration of the time-dependent wave equation for a Schwarzschild black hole with a gravitational perturbation, caused by a close limit approximation for a head-on black hole collision, [84]. We can clearly distinguish three different phases in the solution plotted on logarithmic scale. The first phase, which lasts until  $\frac{t}{2M} = 400$ , describes the propagation of the initial perturbation to the distant observer. The second phase, which starts around  $\frac{t}{2M} = 400$ , contains the quasinormal modes. The third phase, which starts around  $\frac{t}{2M} = 480$ , consists of a power law tail, which as previously mentioned, comes from other contributions in the solution of the wave equation, and dominates the behavior of the gravitational wave after a while. The power law tail is present throughout the whole signal but remained hidden until the quasinormal modes had decayed enough for it to take over.

In figure 6.4, quasinormal frequencies obtained from numerical calculations are depicted. We may notice that the frequencies are countably infinite and quantized in their imaginary part, in agreement with the analytical calculation presented in Section 6.1.6. Also mentioned in the previous section was that the frequencies are bounded in their real parts, which we can also clearly see from the numerical calculation. The fundamental ( $n = 0$ ) mode is the most interesting from an experimental point of view because it is the most likely mode to be detected from far away distances. This is due to it being the least damped mode because it has the smallest imaginary part. It will also oscillate the fastest because it has the largest real part. We can also see that both  $l = 2$  and  $l = 3$  have one special

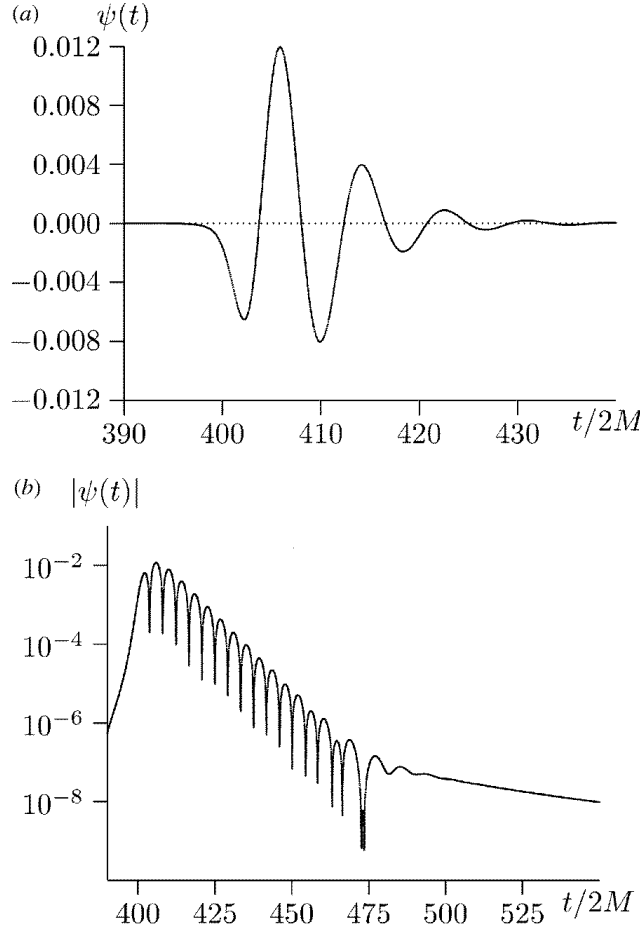


Figure 6.3: Taken from [79]. The typical form of a quasinormal mode, on a) linear scale and on b) in absolute value on a logarithmic scale, as seen by an observer at  $r = 400\frac{2}{M}$ . All values are in the geometric unit system.

mode which has zero real part, so meaning it actually does not oscillate. There is some discussion whether or not this solution should be seen as a quasinormal frequency. We see, clearly for  $l = 2$ , that for increasing modes the real part of the frequency remains constant while the imaginary part increases proportionally to the number of the mode. From this we see that the Pöschl-Teller potential is not a good approximation for lower modes, because it gives constant real part for all the modes. In this figure both the positive and negative solutions to the real part of the frequency are shown, this is only because they both are correct mathematical solutions but from the physics point of view only one of them already gives us all the information.

A very interesting numerical result, taken from [82], is

$$\omega M \approx 0.3737 - 0.0890i, \quad (6.1.24)$$

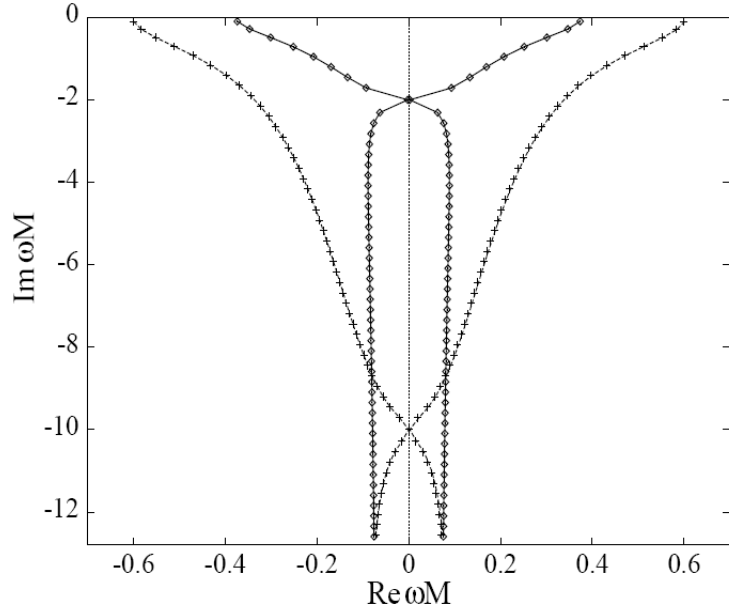


Figure 6.4: Taken from [85]. Numerical solutions of quasinormal frequencies for  $l = 2$  (diamonds) and  $l = 3$  (crosses) for the Schwarzschild black hole. On the horizontal axis is the real part of the frequency and on the vertical axis is the imaginary part of the frequency. The different points correspond to different modes. The frequencies are given in geometrical units and for conversion into kHz one should multiply by  $2\pi(5142\text{Hz}) * \frac{M_\odot}{M}$ .

with  $\omega$  the frequency of the quasinormal fundamental mode in geometrical units and  $M$  the mass of the Schwarzschild black hole in geometrical units. If we want to express the frequency in kHz (physical units) one should multiply by  $2\pi(5142\text{Hz}) * \frac{M_\odot}{M}$ , in agreement with figure 6.4. We get equation (6.1.24) from a WKB method like approximation for the frequency of the fundamental mode. Since equation (6.1.24) tells us that the frequency of the fundamental mode is inversely proportional to the mass of the Schwarzschild black hole we could derive the mass of the black hole if we could measure the frequency of the fundamental mode.

## 6.2 Quasinormal Modes in AdS

In this section we will look at quasinormal modes in asymptotically AdS. This turns out to be a very useful topic through the AdS/CFT correspondence. First, we will look at a massive scalar field perturbation to Schwarzschild AdS (SAdS) and how to derive the wave equation. Then we will examine the pure AdS case, which gives the exact result of

normal modes. Next, we will see another exact solution of the wave equation, namely the BTZ (2+1 dimensional) black hole. We will then give some analytical arguments about the quasinormal modes we find in SAdS. Finally, we will explain the interpretation of quasinormal modes in the AdS/CFT correspondence.

### 6.2.1 Scalar Field Perturbations in AdS

Following [86], we will now look at a scalar field perturbation in the AdS vacuum, that is  $\Phi = \Phi^{BG} + \phi$  with  $\Phi^{BG} = 0$ .

Our general metric for SAdS<sub>4</sub> is given by

$$ds^2 = -f dt^2 + f^{-1} dr^2 + r^2 d\Omega_2^2, \quad f(r) = 1 + r^2/L^2 + r_0/r, \quad (6.2.1)$$

where  $d\Omega_2^2$  is the metric of the 2-sphere. The AdS curvature radius  $L$  is related to the cosmological constant by  $L^2 = -3/\Lambda$  and  $r_0$  is related to the mass by  $M = r_0/2$ . This metric describes pure AdS<sub>4</sub> when  $r_0 = 0$ .

We assume that there is no “backreaction,” that is, we assume  $T_{\mu\nu} = 0$  in Einstein’s equations. The action for the scalar field is then given by

$$S_{\text{matter}} = \int d^4x \sqrt{-g} (\partial_\mu \Phi \partial^\mu \Phi - m^2 \Phi^2). \quad (6.2.2)$$

The equation of motion for the scalar field is the Klein-Gordon equation in its covariant form

$$(\nabla_\mu \nabla^\mu - m^2) \Phi = 0. \quad (6.2.3)$$

We can write this with explicit metric dependence in terms of the fluctuation  $\phi$  as

$$\frac{1}{\sqrt{-g}} \partial_\mu (\sqrt{-g} g^{\mu\nu} \partial_\nu \phi) - m^2 \phi = 0. \quad (6.2.4)$$

Since the metric is time independent and spherically symmetric we can decompose  $\phi$  as

$$\phi(t, r, \Omega_2) = \int d\omega \sum_{lm} r^{-3/2} \psi(r) Y_{lm}(\Omega_2) e^{-i\omega t}, \quad (6.2.5)$$

where  $Y_{lm}$  are the spherical harmonics on  $S^2$ , satisfying  $\Delta_{\Omega_2} Y_{lm} = -l(l+1) Y_{lm}$  with  $\Delta_{\Omega_2}$  the Laplace operator on the two angles,  $\Omega_2$ .

Now, plugging (6.2.5) into (6.2.4), we can write a wave equation for the radial function  $\psi(r)$

$$f^2 \psi'' + f f' \psi' + (\omega^2 - V) \psi = 0, \quad (6.2.6)$$

with the radial potential  $V$  given by

$$V(r) = f \left[ \frac{l(l+1)}{r^2} + \frac{f'}{r} + m^2 \right]. \quad (6.2.7)$$

It is convenient to use the “tortoise” coordinate  $r_*$ , which is defined by  $dr_*/dr = 1/f$ . Now we can rewrite the wave equation (6.2.6)

$$\frac{d^2\psi}{dr_*^2} + (\omega^2 - \tilde{V}(r_*)) \psi = 0, \quad (6.2.8)$$

with  $\tilde{V}$  denoting the potential in the new coordinate  $r_*$ . Since quasinormal modes describe the decay of the field, we must impose certain boundary conditions on this wave equation. We demand that the solution at the horizon is purely outgoing (into the black hole)  $e^{i\omega r_*}$  and at infinity it is purely outgoing  $e^{-i\omega r_*}$  (no incoming wave is allowed at infinity). For asymptotically AdS, the potential diverges near infinity, in contrast to the asymptotically flat case where the potential vanishes near infinity. Therefore we demand that  $\Phi$  vanishes at infinity.

### 6.2.2 Pure AdS

Pure AdS (equation (6.2.1) with  $r_0 = 0$ ) is interesting to study not only because it is one of the few exact solutions, but also because it is something quite different from what we find in flat space. First let us look at the “tortoise” coordinate in this space. We have

$$\frac{dr_*}{dr} = \frac{1}{1+r^2/L^2}, \quad (6.2.9)$$

which gives us

$$r_* = L \text{Arctan} \left( \frac{r}{L} \right). \quad (6.2.10)$$

Since  $r_*$  has a finite range, we may deduce from the wave equation (6.2.8) that our  $\omega$  will correspond to normal (real) modes.

These normal modes were originally calculated for a scalar field perturbation by Burgess and Lütken [87]. In  $d = 4$ , the scalar field modes satisfy

$$L\omega = 2n + l + 3, \quad n = 0, 1, 2, \dots \quad (6.2.11)$$

It is also interesting to note that the exact solutions for gravitational perturbations have a similar form [86]

$$L\omega = 2n + l + 3, \quad n = 0, 1, 2, \dots \quad \text{tensor-type} \quad (6.2.12)$$

$$L\omega = 2n + l + 2, \quad n = 0, 1, 2, \dots \quad \text{vector-type, scalar-type.} \quad (6.2.13)$$

### 6.2.3 BTZ Black Hole

We will now look at a second exact solution for quasinormal modes following [88]. This is for massless scalar perturbations in the BTZ (2+1 dimensional) black hole in asymptotically AdS. The analytic solution for scalar perturbations, as well as electromagnetic and Weyl, was first found by Cardoso and Lemos [88]. The metric is given by

$$ds^2 = -f dt^2 + f^{-1} dr^2 + r^2 d\theta^2, \quad f = -M + \frac{r^2}{L^2}, \quad (6.2.14)$$

where  $M$  is the black hole mass. The horizon radius is  $r_+ = M^{1/2}L$ . The equation of motion is given by (6.2.4) with  $m = 0$ . The ansatz we make for our scalar field is simpler since we only have one angular coordinate

$$\phi = \frac{1}{r^{1/2}} \psi(r) e^{-i\omega t} e^{il\theta}, \quad (6.2.15)$$

with  $l$  the angular number. We define the “tortoise” coordinate as before through the relation  $dr_*/dr = 1/f$ , which gives

$$r = -M^{1/2} \coth(M^{1/2} r_*). \quad (6.2.16)$$

Note that  $r_* \rightarrow -\infty$  corresponds to  $r = r_+$  and  $r_* = 0$  corresponds to  $r \rightarrow \infty$ .

The wave equation can be written in the same form as equation (6.2.8) with

$$V(r) = \frac{3r^2}{4L^2} - \frac{M}{2L^2} - \frac{M^2}{4r^2} + \frac{m^2}{L^2} - \frac{Mm^2}{r^2}. \quad (6.2.17)$$

By making a coordinate transformation followed by a transformation of the wavefunction  $\psi$ , we can put this wave equation in the form of a standard hypergeometric equation. Then, enforcing the boundary conditions as discussed in section 6.2.1, we find the relation for the quasinormal modes to be

$$L\omega = \pm l - 2iM^{1/2}(n+1), \quad n = 0, 1, 2, \dots \quad (6.2.18)$$

### 6.2.4 Schwarzschild AdS

Following [89], we will examine the quasinormal modes of SAdS<sub>4</sub> using the metric (6.2.1). We will now consider the scalar field perturbations to be massless and since the solutions can only be found numerically, we will restrict ourselves to a summary of some results. The

equation of motion of the scalar fluctuation is equation (6.2.3) with  $m = 0$ . The Hawking temperature is given by

$$T = \frac{f'(r_+)}{4\pi} = \frac{3r_+^2 + L^2}{4\pi r_+ L^2}. \quad (6.2.19)$$

The wave equation can be written in the standard form (6.2.8). The potential  $\tilde{V}$  is positive and vanishes exponentially at the horizon of the black hole which corresponds to  $r_* \rightarrow -\infty$  and diverges at  $r \rightarrow \infty$  which corresponds to a finite value of  $r_*$ . Since the potential vanishes at the horizon, there is no power law tail for the quasinormal modes in SAdS [89].

In SAdS there are two dimensionful parameters: the AdS radius  $L$  and the black hole radius  $r_+$ . Therefore we can examine large black holes ( $r_+ \gg L$ ), small black holes ( $r_+ \ll L$ ), and intermediate black holes ( $r_+ \sim L$ ). In [89] it is shown that for large black holes, the quasinormal modes only depend on temperature  $T \sim r_+/L^2$ . However, if you start decreasing  $r_+$  below  $L$ , though the temperature begins to increase, the imaginary part of the frequency continues to decrease approximately linearly with  $r_+$ . This is not how a black hole in asymptotically flat space behaves, since in that case the quasinormal modes must be multiples of the temperature, the only dimensionful parameter.

## AdS/CFT Interpretation

The famous AdS/CFT correspondence relates an operator  $\hat{\mathcal{O}}$  in a  $d$ -dimensional conformal field theory with a field  $\phi$  in  $\text{AdS}_{d+1}$ . The interpretation of quasinormal modes of an asymptotically  $\text{AdS}_{d+1}$  space is that they correspond to the poles of the retarded Green's functions of the dual  $d$ -dimensional field theory. Additionally, when the field theory has a finite temperature, the dual gravitational background must have a horizon and the Hawking temperature corresponds to the temperature of the field theory [82]. As first presented by Horowitz and Hubeny [89], the perturbation of a black hole corresponds to the perturbation of the thermal state of the field theory. The imaginary part of the quasinormal modes will give the thermalization time scale on the field theory side.

Unfortunately, this proposition for the interpretation of quasinormal modes in AdS/CFT is difficult to prove since the Green's functions on the field theory side are in general hard to calculate for four dimensions and higher. But there have been confirmations of this nevertheless. For instance, the results of Birmingham, Sachs, and Solodukhim [90] show that there is an exact agreement of the quasinormal modes for the BTZ black hole in equation (6.2.18) and the poles of the retarded Green's functions in the two dimensional CFT.

### 6.3 Breitenlohner Freedman Bound

In this section we are going to discuss the perturbative stable solutions for a massive scalar field in AdS space, from which we will see that a negative  $m^2$  does not necessarily lead to any instabilities, as long as it is not too negative. The negative lower bound for  $m^2$ , guaranteeing at least one stable solution, is called the Breitenlohner Freedman Bound. In  $AdS_4$  space the BF Bound reads:  $m^2 \geq -\frac{9}{4L^2}$ [91, 92], where  $L$  is the AdS length, which we will set to 1 in the rest of the section.

#### 6.3.1 Stability Bound in Minkowski Space

To get a clue for the perturbative stability problem in AdS space, we first consider that in a simpler Minkowski space. Here we consider a massive scalar field in 4-dimensional Minkowski spacetime. The simplest solutions for Klein-Gorden equation are plane waves

$$\begin{aligned}\phi &= \exp(-i\omega t + i\vec{k} \cdot \vec{x}); \\ m^2 &= \omega^2 - \vec{k}^2; \quad \omega := k_0.\end{aligned}\tag{6.3.1}$$

When  $m^2 < 0$ , in the range  $\vec{k}^2 \leq -m^2$ ,  $\omega$  is pure imaginary, hence the solution  $\phi$  grows exponentially in time. Thus we obtain a tachyonic unstable solution. By setting  $\vec{k} = 0$  we achieve the stability bound for massive scalar field in Minkowski space as  $m^2 \geq 0$ .

Equivalently, consider energy-momentum tensor

$$T_{\mu\nu} = \partial_\mu \phi \partial_\nu \phi - \frac{1}{2} g^{\mu\nu} [\partial\phi \cdot \partial\phi + m^2 \phi^2] + \chi [g_{\mu\nu} \square - \nabla_\mu \partial_\nu + R_{\mu\nu}],\tag{6.3.2}$$

where  $\chi$  originates from a conformal coupling of  $\phi$  to the scalar curvature  $R$  of background spacetime, and can be setted as any arbitrary value[91, 93]. In Minkowski space energy momentum tensor for the plane wave simplifies to

$$T_{\mu\nu} = 2k_\mu k_\nu\tag{6.3.3}$$

Energy density  $T_{00}$  is negative for  $m^2 + \vec{k}^2 < 0$ , suggesting the presence of instability. Therefore by analysing the energy momentum tensor we get the same stability bound as  $m^2 \geq 0$ .

### 6.3.2 Stability Bound in AdS Space

We can use the same idea as in last subsection to find the stability bound in AdS space. However the AdS case is much more complicated since we cannot find a solution as simple as (6.3.1). Using a proper coordinate system, Poincaré coordinates in this case, does simplify things a bit. First we introduce the metric for Poincaré coordinates in  $AdS_4$

$$ds^2 = \frac{dz^2 + \eta^{\mu\nu}dx_\mu dx_\nu}{z^2} \quad (6.3.4)$$

$z \in [0, \infty)$  is the radial  $AdS$  coordinate. Assuming a space time dependence  $\exp(-i\omega t + i\vec{k} \cdot \vec{x})$  of our solutions, the equation of motion simplifies to

$$\partial_z^2 \phi - \frac{2}{z} \partial_z \phi - \frac{m^2}{z^2} \phi = k^2 \phi. \quad (6.3.5)$$

A standard way to solve this differential equation is to write  $\phi(z) = A(z)\psi(z)$ , substitute it back into (6.3.5), and find a proper  $A(z)$  to let the first order derivative of  $\psi$  vanish, to arrive at a Schrödinger like quation. We can choose  $A(z) = z \times \text{Const}$ , and we set  $\vec{k} = 0$ . Then the equation of motion for  $\psi$  becomes

$$-\partial_z^2 \psi + \frac{m^2 + 2}{z^2} \psi = k^2 \phi. \quad (6.3.6)$$

This is a 1-dimensional Schrödinger equation with inverse square potential of strength  $\alpha = m^2 + 2$ , and with energy  $E = k^2 = \omega^2 - \vec{k}^2$  [94].

In analogy with Minkowski case, an imaginary  $\omega$  will cause instability, which in the quantum mechanical language corresponds to  $E = \omega^2 < 0$  (See [94] for more detailed discussion in how stability of solution for AdS wave equation is related to normalizability in quantum mechanical sense), and we can find the stability bound as  $\alpha \geq -\frac{1}{4}$ , i.e:

$$m^2 \geq -\frac{9}{4} \quad (6.3.7)$$

The above inequality is the celebrated Breitenlohner Freedman Bound. When this condition is satisfied, we have a repulsion (for  $\alpha > 0$ ) or weak attracting (for  $-\frac{1}{4} \leq \alpha < 0$ ), which gives stable modes.

Another way to arrive at Breitenlohner Freedman Bound is to check the solutions directly. Solutions to the Schrödinger equation of form (6.3.6) can be expressed in terms of Bessel

functions

$$\begin{aligned}\psi(z) &= \sqrt{z}[C_1 J_a(wz) + C_2 Y_a(wz)], \\ a_{\pm} &= \pm \frac{1}{2}\sqrt{9 + 4m^2},\end{aligned}\tag{6.3.8}$$

where  $C_1, C_2$  are constants,  $J_a, Y_a$  are order  $a$  Bessel functions of first and second kind respectively.

Extensive works on (6.3.6) [95, 96, 97] tells us that only real value of  $a$  gives us convergent  $\psi(z)$ , which is a stable solution. This is also a manifestation of the Breitenlohner Freedman Bound (6.3.7).

### 6.3.3 Another Derivation of the BF Bound

We have already found the solution (6.3.8) for Schrödinger like wave equation (6.3.6), from which we can see there exist two different modes for a massive scalar field in AdS space, namely  $\sqrt{z}J_a(wz)$  and  $\sqrt{z}Y_a(wz)$ . The Breitenlohner Freedman Bound guarantees that we have at least one mode that is stable. However, we have difficulties in analysing the Bessel functions for large  $z$  asymptotically, because of the zeros all the way out the infinity[98]. So here we are going back to the original work of Breitenlohner and Freedman[91, 92], and try to find out an explicit expression for the wave equation. There we introduce a new metric for  $AdS_4$

$$ds^2 = (\cos\rho)^{-2}[dt^2 - d\rho^2 - \sin^2\rho(d\theta^2 + \sin^2\theta d\phi^2)]\tag{6.3.9}$$

where  $0 \leq \theta < \pi$  and  $0 \leq \phi < 2\pi$  are angles,  $0 \leq \rho < \pi/2$ .  $r = 0$  maps to  $\rho = 0$ , while  $r = \infty$  maps to  $\rho = \pi/2$ .

Then if substitute the ansatz

$$\phi = e^{-iwt}Y_l^m(\theta, \phi)R_{wl}(\rho)\tag{6.3.10}$$

into the wave equation, we find an equation for radial function  $R_{wl}(\rho)$ , which can be written in terms of hypergeometric equation, and then gives an analytic solution as [91, 92, 99]

$$\begin{aligned}R_{wl}^{\pm}(\rho) &= (\sin\rho)^l(\cos\rho)^{\lambda_{\pm}} {}_2F_1(a, b, c, \sin^2\rho), \\ a &= \frac{1}{2}(l + \lambda - \omega), \\ b &= \frac{1}{2}(l + \lambda + \omega), \\ c &= l + \frac{3}{2},\end{aligned}\tag{6.3.11}$$

$$\lambda_{\pm} = \frac{3}{2} \pm \frac{1}{2}\sqrt{9 + 4m^2}, \quad (6.3.12)$$

where  ${}_2F_1$  is the hypergeometric function. The stability of above modes demands the conservation and positivity of the energy for scalar fluctuations. Global energy is actually conserved only if its flux at spatial infinity vanishes. The flux is given by

$$\int dS_i \sqrt{g} T_0^i = \int d\Omega [\rho^2 \sqrt{g} n_i T_0^i]_{\rho=\pi/2} \quad (6.3.13)$$

Substituting in the energy momentum tensor and analysing asymptotically for  ${}_2F_1(a, b, c, \sin^2(\rho))$  at  $\rho = \pi/2$ , we get the following two equations [99]

$$\omega = \lambda + l + 2n, \quad n, l = 0, 1, 2, \dots, \quad (6.3.14)$$

$$[(\cos\rho)^{2\lambda-1}]_{\rho=\pi/2} = 0. \quad (6.3.15)$$

We have already argued that complex frequency  $\omega$  leads to instabilities, thus from Eq.(6.3.14), we see that  $\lambda$  must be real. Using this condition for (6.3.12), we find again the Breitenloher Freedman Bound (6.3.7).

Now we see that actually the frequency is discrete, therefore we can express hypergeometric functions in terms of Jacobi polynomials

$$R_{wl}^{\pm}(\rho) = N(\sin\rho)^l (\cos\rho)^{\lambda_{\pm}} P_n^{[\pm\sqrt{9+4m^2}/2, l+\frac{1}{2}]}, \quad (6.3.16)$$

where  $N$  is a normalization factor.

Notice now we have two separate sets of modes, as for  $\lambda_{\pm}$ . The question is: do they all appear in (6.3.16)? To answer this question we have to go back to (6.3.15), where we see, as  $\rho \rightarrow \pi/2$ , i.e.  $\cos\rho \rightarrow 0$ , the equation only holds for  $2\lambda - 1 > 0$ . As from (6.3.12), for  $\lambda_+$  this inequality always holds; for  $\lambda_-$ , however, we need an extra condition

$$m^2 < -\frac{5}{4}. \quad (6.3.17)$$

The  $\lambda_+$  modes are sometimes called regular modes, and  $\lambda_-$  ones irregular modes[100]. For  $-\frac{9}{4} \leq m^2 < -\frac{5}{4}$  both regular and irregular modes exist for stable solutions; when  $m^2 \geq -\frac{5}{4}$ , the irregular modes are not stable, only regular modes exist.

## Connection with AdS/CFT Correspondence

Eq (6.3.12) may actually be familiar for people who know AdS/CFT. In fact, the equation for  $\lambda$  is

$$\lambda(\lambda - 3) = m^2, \quad (6.3.18)$$

which is the same as the famous equation for conformal dimension of  $CFT_3$  operators (here we still discuss  $AdS_4$ ). It was shown in [101] that if we have  $m^2 \leq -\frac{5}{4}$ , a single gravity theory in the bulk describes one conformal field theory  $CFT_+$ , the CFT operator  $O$  dual to the scalar field has scaling dimension  $\lambda_+$ . When  $-\frac{9}{4} \leq m^2 < -\frac{5}{4}$ , a single gravity theory in the bulk describes two different conformal field theories,  $CFT_+$  and  $CFT_-$ , which have  $\lambda_+$  and  $\lambda_-$  respectively as scaling dimensions.

## 6.4 Quasinormal Modes in Astrophysics

In this section we will discuss the applications of quasinormal modes (QNMs) to astrophysics. Today there is strong evidence of the astrophysical reality of black holes from electromagnetic observations [102]. Gravitational wave observation, will incontrovertibly show if these compact objects are indeed Kerr black holes as predicted by general relativity or some exotic alternative like a boson star [103]. Furthermore QNMs can be used to test the no-hair theorem [103]. The two detectors that are considered in this chapter are the (advanced) Laser Interferometer Gravitational-Wave Observatory (LIGO), with a frequency range between  $20 - 7000\text{Hz}$  [104] and the planned Laser Interferometer Space Antenna (LISA) with a frequency range of  $10^{-5} - 10^{-1}\text{Hz}$  [105].

### 6.4.1 Quasinormal Modes of Astrophysical Black Holes

The most general solution describing stationary axisymmetric black holes is the Kerr-Newman metric. However astrophysical black holes are not found in isolation and the astrophysical environment of a black hole e.g. a massive accretion disk is thought to short out the electric charge of a black hole. Thus the charge of a black hole is negligible in the astrophysical context, which leaves us with the Kerr metric. Therefore we can characterize any astrophysical black hole solely by its mass  $M$  and angular momentum parameter  $a$ . The complex frequency of a QNM yields two observables, the frequency  $f_{lmn} = \text{Re}(\omega_{lmn})/(2\pi)$  and the damping time  $\tau_{lmn} = |\text{Im}(\omega_{lmn})|$  of the oscillation. The QNM frequencies are

sorted by increasing imaginary part with index  $n$ , called overtones, where  $n = 0$  is the least damped mode. Furthermore the frequencies carry indices  $l$  and  $m$  from the spherical harmonics decomposition (6.1.7). For a thorough discussion of the theory behind these modes see Section 6.1. For each mode these two observables depend only on  $M$  and  $a$ . Thus if we can perform a measurement of the frequency and damping time of a QNM we can find the mass and angular momentum of a black hole with potentially high accuracy. There are three types of black holes considered in astrophysics:

- Stellar-mass black holes with  $M \sim 5 - 20M_{\odot}$ ,
- Intermediate-mass black holes with  $M \sim 10^2 - 10^5M_{\odot}$ ,
- Supermassive black holes with  $M \sim 10^6 - 10^{9.5}M_{\odot}$ .

There is strong and growing observational evidence for stellar mass and supermassive black holes. No such observational evidence exists for intermediate black holes. Stellar-mass black holes are usually found in X-ray binaries, whereas supermassive black holes are found in the center of galaxies in particular in Active Galactic Nuclei (AGN).

When black holes form or are excited they are expected to emit a characteristic radiation called ringdown waves. Since the various modes have complex frequencies we expect the QNM frequencies with small imaginary parts (low  $n$ -modes) to have the longest damping time. According to the literature [106]  $l = m = 2$  modes, corresponding to gravitational perturbations, have the longest damping time and thus should dominate the signal. Black holes can form or be excited in various ways:

- Excitation by accretion,
- Stellar collapse to a black hole,
- Mergers of compact objects.

It is important to stress that the QNMs do not depend on the initial physical process that caused the black hole to form or be excited. However the phase and amplitude do depend on the initial perturbation (see Section 6.4.2). Even though the QNMs may in principle fall inside the frequency range of our detectors the amplitude may be too small to detect the signal. As an example we consider a  $\sim 2.7 - 2.9M_{\odot}$  neutron star - neutron star (NS-NS) merger with subsequent collapse into a black hole. The frequency of the  $l = m = 2$  mode is  $\sim 6.5 - 7\text{kHz}$  with an amplitude of  $\sim 10^{-22}m$  at a distance of 50 Mpc [86]. While the

frequency lies within LIGO's range (barely) the amplitude of the signal is incredibly small. This makes it unlikely that we will be able to detect ringdown waves from NS-NS mergers with current and planned observatories. For the remainder of this chapter we will not consider the initial physical process and focus on the QNMs of astrophysical objects.

### 6.4.2 Important Quantities for Detection

Detecting ringdown waves from these black holes depends on the sensitivity of the detector and the extent to which QNMs are excited in an astrophysical setting. The frequency of the ringdown waves depend only on the mass and the angular momentum of the black hole and not on the source of the excitation. Gravitational wave detectors like LIGO and in the future LISA are located at very large distances from astrophysical black holes. Therefore a QNM measured by a detector is well approximated by its asymptotic behaviour at spacial infinity  $\psi(t, r) \sim e^{i\omega(t+r_*)}$ .

The waveform measured at the detector can be expressed as a linear superposition of the gauge-invariant polarization amplitudes  $h_+$  and  $h_\times$ . We have

$$h_+ = \frac{M}{r} \sum_{lmn} \text{Re} \left[ A_{lmn}^+ e^{i(\omega_{lmn} t + \phi_{lmn}^+)} e^{-t/\tau_{lmn}} S_{lmn}(\iota, \beta) \right], \quad (6.4.1)$$

$$h_\times = \frac{M}{r} \sum_{lmn} \text{Im} \left[ A_{lmn}^\times e^{i(\omega_{lmn} t + \phi_{lmn}^\times)} e^{-t/\tau_{lmn}} S_{lmn}(\iota, \beta) \right], \quad (6.4.2)$$

where  $A_{lmn}^{+,\times}$  and  $\phi_{lmn}^{+,\times}$  are the real amplitude and phase, which are determined by the specific process that formed the final black hole [103].  $S_{lmn}(\iota, \beta)$  are the spin-weighted spheroidal harmonics of spin-weight -2 [107]. The angles  $\iota$  and  $\beta$  are adapted to the source such that the  $z$ -axis is aligned with the spin of the black hole. Detectors are sensitive to the so called effective strain defined by

$$h = h_+ F_+ + h_\times F_\times, \quad (6.4.3)$$

where  $F_{+,\times}$  are the so called pattern function which depend on the orientation of the detector, the direction of the source and the polarization angle.

Another important quantity for gravitational wave detection is the signal-to-noise ratio (SNR) defined as

$$\rho = \left( 4 \int_0^\infty \frac{\tilde{h}^*(f) \tilde{h}(f)}{S_h(f)} df \right)^{1/2}, \quad (6.4.4)$$

where  $\tilde{h}(f)$  is the Fourier transform of the waveform and  $S_h(f)$  is the noise spectral density of the detector. Measurement errors scale inversely proportionally with the SNR making this a very important quantity.

The ringdown efficiency is defined as the fraction of the total mass-energy of the system radiated away in ringdown waves and is denoted  $\epsilon_{rd}$ , which is well approximated by

$$\epsilon_{rd} \approx \frac{Q_{lmn} M \omega_{lmn}}{32\pi} [(A_{lmn}^+)^2 + (A_{lmn}^\times)^2], \quad (6.4.5)$$

where  $Q_{lmn} = \text{Re}(\omega)/(2\text{Im}(\omega))$  is the quality factor. Note that for weakly damped modes the quality factor is large.

### 6.4.3 Detectability of Fundamental Modes

The ringdown efficiency together with the mass and angular momentum are the three main parameters that determine whether we can detect the ringdown waves. In most cases the frequency and damping time of the emitted radiation will be dominated by the fundamental mode. For a Schwarzschild black hole the frequency and damping time of the fundamental mode are given by [86, 103]

$$f_{200} = 1.207 \cdot 10^{-2} (10^6 M_\odot / M) \text{Hz}, \quad (6.4.6)$$

$$\tau_{200} = 55.37 (M / (10^6 M_\odot)) \text{s}. \quad (6.4.7)$$

Earth-based detectors are limited by a seismic cutoff frequency  $f_s$ . For advanced LIGO the seismic cutoff is estimated at  $f_s \sim 20 \text{Hz}$ . Solving (6.4.6) for  $M$  we find

$$M < 1.27 \cdot 10^4 (\text{Hz}/f_s) M_\odot \approx 0.63 \cdot 10^3 M_\odot. \quad (6.4.8)$$

Therefore in principle advanced LIGO should be able to detect non-rotating stellar-mass black holes and low mass intermediate-mass black holes. For a more realistic black hole we want to look at the frequencies of the fundamental mode of Kerr black holes. From Table 6.1 [108] we see that in principle LIGO will be able to detect astrophysical realistic stellar-mass black holes and lower intermediate-mass black holes. LISA will be able to detect ringdown waves from supermassive black holes. For example a supermassive black hole with  $a/M = 0.8$  and  $M \sim 4 \cdot 10^6 M_\odot$  that radiates 1% of its mass at a luminosity distance of 3 Gpc and redshift  $z = 0.54$  will be detected by LISA with  $\rho \sim 10^4$  [108]. Since the measurement error is inversely proportional to the SNR these measurements of the QNM frequencies should be very precise.

Table 6.1: Upper limit on detectable black hole mass for which the fundamental QNM  $l = m = 2$  would be detectable by LISA and LIGO for rotation parameter  $a$ .

With  $f_s \sim 20\text{Hz}$

	$a/M = 0$	$a/M = 0.6$	$a/M = 0.7$	$a/M = 0.98$
LIGO	$1200M_\odot(\frac{10\text{Hz}}{f_s})$	$1600M_\odot(\frac{10\text{Hz}}{f_s})$	$1720M_\odot(\frac{10\text{Hz}}{f_s})$	$2670M_\odot(\frac{10\text{Hz}}{f_s})$
LISA	$4 \cdot 10^8 M_\odot$	$5.3 \cdot 10^8 M_\odot$	$5.7 \cdot 10^8 M_\odot$	$8.9 \cdot 10^8 M_\odot$

#### 6.4.4 A Black hole Versus a Boson Star

By the no-hair theorem the Kerr spacetime is completely specified by the first two multipole moments, the mass and angular momentum. An alternative to a supermassive Kerr black hole, that is not ruled out by experiment and is compatible with general relativity, is a rotating boson star [103]. Boson stars are very compact objects (without an event horizon) and deviations in the properties of orbiting objects occur close to the Schwarzschild radius. This makes it very hard to distinguish between a boson star and a black hole by electromagnetic observations. Numerical calculations indicate that the spacetime of a rotating boson star is determined by three multipole moments. The maximum boson star mass, for a non-interacting scalar field, and the Chandrasekhar mass for regular fermion stars in terms of the Planck mass are given by

$$M_{max,boson} \sim 0.633m_p^2/m_b, \quad (6.4.9)$$

$$M_{Ch} \sim m_p^3/m_H^2, \quad (6.4.10)$$

where  $m_b$  and  $m_H$  are the boson particle mass and fermion (hydrogen) particle mass respectively. For a non-interacting scalar field the maximum boson star mass is much smaller than the Chandrasekhar mass. As a numerical example we find for a supermassive black hole with a mass  $\sim 10^6 M_\odot$ ,  $M_\odot \approx 1.12 \cdot 10^{57}\text{GeV}$  an ultralight boson mass  $m_b = 8.41 \cdot 10^{-26}(10^6 M_\odot / M_{max,boson})\text{GeV}$  [103]. Thus to have an astrophysical sized object we require ultralight bosons. To get around this requirement we can consider a self-interacting scalar field with a quartic interaction term  $\lambda\phi^4/4$  with a coupling constant  $\lambda \gg (m_b/m_p)^2$ . This gives [109]

$$M_{max,boson} \sim 0.062\lambda^{1/2}m_p^3/m_b^2. \quad (6.4.11)$$

Plugging in the same numbers as before we find that astrophysical supermassive objects can exist for  $m = 3.2 \cdot 10^{-4}\lambda^{1/4}(10^6 M_\odot / M_{max,boson})^{1/2}\text{GeV}$ . There are other self-interacting

potentials we can choose to obtain different boson masses  $m$ . As we can see from the two examples above the boson masses needed to support supermassive objects differ by many orders of magnitude.

To test a boson star against a suspected astrophysical (Kerr) black hole we must consider rotating boson stars. Stable rotating boson stars were obtained by Ryan [109] who showed that for a pure state for a scalar field of the form  $\phi = \Phi(r, \theta)e^{i(s\varphi - \Omega t)}$  the structure was completely determined by the three independent parameters  $\lambda^{1/2}/m^2$ ,  $\tilde{\Omega} = \Omega/m$  and  $\tilde{s} = s/(\lambda^{1/2}/m)^4$ . Ryan's numerical calculations showed that these three parameters correspond to the first three multipole moments of the star, the mass, spin and quadrupole moment. To test the boson star against a Kerr blackhole we require the QNM frequencies for rotating boson stars. Unfortunately these QNM frequencies have not yet been calculated to our knowledge so we take an alternative approach. We consider a non-rotating miniboson star, for which the QNM frequencies are known and compare it to (6.4.6) and (6.4.7). The dominant modes are given by  $\omega/m_b = 2.3 + 0.13i$  [103], which gives

$$f = 4.7 \cdot 10^{-2}(10^6 M_\odot / M_{max,boson}) \text{Hz}, \quad (6.4.12)$$

$$\tau = 60(M_{max,boson} / (10^6 M_\odot)) \text{s}. \quad (6.4.13)$$

Naively setting the boson mass equal to the mass of a typical supermassive black hole brings the QNM frequency in the range where LISA could detect it. Finding QNM frequencies consistent with a black hole would give us confirmation of general relativity in the strong-field regime. If instead they correspond to frequencies of a boson star measuring two QNMs would be enough to determine all three boson star parameters.

We have seen that with LIGO and LISA, once operational, we should be able to get very precise gravitational measurements of black hole masses and angular momenta. In combination with electromagnetic observations this will lead to a broader understanding of black hole physics.



# Chapter 7

## Hawking Radiation

In this section we will focus on the quantum field theory (QFT) in a Schwarzschild spacetime in order to understand the main ingredients of Hawking radiation. We start with a recap of the quantum theory of a free scalar field in flat spacetime. It might sound irrelevant to the scope of this book because applications of QFT in flat spacetime (like particle physics and condensed matter physics) focus on interaction between fields, while we are primarily interested in studying the effects of gravity on these fields. But by generalizing this theory to curved spacetime later in this chapter we can do exactly that and work towards a derivation of the famed Hawking radiation.

We do not (and cannot) generalize to a full theory of quantum gravity, but since we are working on sufficiently large scales we assume we can work instead with an effective semi-classical theory. This is accomplished by splitting the metric into a background spacetime and a perturbation which represents the gravitational wave. The perturbation field will be treated as part of the energy momentum tensor. Then the background spacetime is taken to be fixed but the matter fields propagate on the curved spacetime and are quantized.

Particle creation by gravity can be accomplished when the metric is time-dependent or for a spacetime in which a horizon is present. Particle creation due to the presence of a horizon is the one we will only consider in this chapter and arises in case of a Schwarzschild black hole<sup>1</sup>.

In this section we will focus on QFT in a Schwarzschild spacetime in order to understand

---

<sup>1</sup>For an example of particle creation completely due to the time-dependence of the metric one can think of an expanding universe as described by the Friedmann Robertson Walker metric.

the main ingredients of Hawking radiation<sup>2</sup>. We will see that the vacuum and particles are observer dependent objects whereas in QFT in flat spacetime they are unambiguously defined in the inertial frame. Also the importance of a horizon will be highlighted. An intuitive picture to keep in mind is that the vacuum constantly creates particles and anti-particles borrowing energy from the gravitational field. Due to the horizon one escapes to infinity and is detected by a far away observer while the other particle falls into the black hole. We start with recapping QFT in flat spacetime and focus on the vacuum and particle concepts. Finally we use a similar analysis in the Schwarzschild spacetime and see how the horizon obscures the notion of a vacuum and particles. This obscurity of the vacuum leads to the fact that different observers do not agree on the vacuum state and thus can detect particles in each others vacuum state.

To keep matters manageable we will restrict ourselves to the simplest case of dynamic spinless scalar fields propagating in a classical spacetime background. While these may not give the most realistic description, they allow us to illustrate the processes involved without obscuring the facts by dense calculations.

Readers interested in the reason for turning to the second quantization formalism can refer to Appendix A.6 for a broader context.

## 7.1 Recap: Quantization of a Scalar Field in Quantum Field Theory

In this subsection we briefly recap the quantum theory of a free scalar field in flat spacetime<sup>3</sup>. We will generalize the theory to curved spacetime in the next subsection and we are primarily interested in the effects of gravity on the fields and not in the interactions between the matter fields. We will see that in curved spacetime the notions of the vacuum and particles become ambiguous, therefore in this subsection we pay special attention to the vacuum and particle states in QFT in flat spacetime.

---

<sup>2</sup>For the interested reader: this theoretical framework is also used in the field of cosmology. The theory of inflation predicts that vacuum fluctuations of the quantum fields in the early universe are responsible for cosmological perturbations which are the seeds for the large scale structure in our universe. The cosmological perturbations have been mapped among other things by the detection of the cosmic microwave background radiation and galaxy distribution. Therefore in cosmology we might be able to probe effects of strong gravity.

<sup>3</sup>This section is based on [1, Sec. 9.1, 9.3, 9.4] [110, Ch. 4] and [111, Ch. 3.3].

We start with a classical theory of a free scalar field as described by the action

$$S[\phi] = -\frac{1}{2} \int d^4x [\eta^{\mu\nu} \partial_\mu \phi \partial_\nu \phi + m^2 \phi^2]. \quad (7.1.1)$$

Using inertial coordinates  $(t, \mathbf{x})$  the equations of motion become

$$\ddot{\phi} - \nabla^2 \phi + m^2 \phi = 0,$$

which can be rewritten as an infinite set of decoupled harmonic oscillators

$$\ddot{\phi}_{\mathbf{k}} + (k^2 + m^2) \phi_{\mathbf{k}} = 0, \quad (7.1.2)$$

by making a Fourier transformation of the field

$$\phi(t, \mathbf{x}) = \int \frac{d^3\mathbf{k}}{(2\pi)^{3/2}} e^{i\mathbf{k}\cdot\mathbf{x}} \phi_{\mathbf{k}}(t).$$

Next we canonically quantize the field by promoting the classical field and its conjugate momentum  $\pi(t, \mathbf{x}) = \partial_t \phi(t, \mathbf{x})$  to operators and impose the equal-time commutation relations

$$[\hat{\phi}(t, \mathbf{x}), \hat{\pi}(t, \mathbf{y})] = i\delta(\mathbf{x} - \mathbf{y}), \quad [\hat{\phi}(t, \mathbf{x}), \hat{\phi}(t, \mathbf{y})] = [\hat{\pi}(t, \mathbf{x}), \hat{\pi}(t, \mathbf{y})] = 0. \quad (7.1.3)$$

By using the Fourier transformation we can equivalently introduce the mode operators  $\hat{\phi}_{\mathbf{k}}$  and  $\hat{\pi}_{\mathbf{k}}$  and we reduce the problem to quantizing a simple harmonic oscillator for each  $\mathbf{k}$ . We know from quantum mechanics it is useful to introduce creation and annihilation operators which can be expressed in terms of  $\hat{\phi}_{\mathbf{k}}$  and  $\hat{\pi}_{\mathbf{k}}$ . Instead of going through all the algebra we proceed by making directly an ansatz for the expansion of the field operator in creation and annihilation operators

$$\hat{\phi}(t, \mathbf{x}) = \int \frac{d^3\mathbf{k}}{(2\pi)^{3/2}} [v_{\mathbf{k}}^*(t) e^{i\mathbf{k}\cdot\mathbf{x}} \hat{a}_{\mathbf{k}}^- + v_{\mathbf{k}}(t) e^{-i\mathbf{k}\cdot\mathbf{x}} \hat{a}_{\mathbf{k}}^+]. \quad (7.1.4)$$

where we impose the appropriate commutation relations

$$[\hat{a}_{\mathbf{k}}^-, \hat{a}_{\mathbf{p}}^+] = \delta(\mathbf{k} - \mathbf{p}), \quad [\hat{a}_{\mathbf{k}}^-, \hat{a}_{\mathbf{p}}^-] = [\hat{a}_{\mathbf{k}}^+, \hat{a}_{\mathbf{p}}^+] = 0. \quad (7.1.5)$$

In order to make them compatible with the commutation relations (7.1.3) the Wronskian of the mode functions  $v_{\mathbf{k}}$  and  $v_{\mathbf{k}}^*$  equals

$$\dot{v}_{\mathbf{k}}(t) v_{\mathbf{k}}^*(t) - \dot{v}_{\mathbf{k}}^*(t) v_{\mathbf{k}}(t) = 2i.$$

Furthermore the mode functions should satisfy the equations of motion (7.1.2) as well. Analogous to quantum mechanics we would like to assume there exists a vacuum state which is annihilated by each  $\hat{a}_{\mathbf{k}}$

$$\hat{a}_{\mathbf{k}}^- |0\rangle = 0, \quad \forall \mathbf{k}$$

and we can build the Fock basis which spans the entire Hilbert space by repeatedly acting with creation operators on the vacuum. But note that the mode functions are not completely defined by these constraints, which means that the operators  $\hat{a}_{\mathbf{k}}^-$  and  $\hat{a}_{\mathbf{k}}^+$  are ambiguous and hence the vacuum state  $|0\rangle$  is undefined. To solve the problem we assume in addition that the vacuum is the lowest energy eigenstate of the Hamiltonian, which corresponds to the intuitive picture of the vacuum. The Hamiltonian expressed in terms of the mode functions and creation and annihilation operators becomes

$$\hat{H}(t) = \frac{1}{2} \int d^3\mathbf{k} [(\dot{v}_{\mathbf{k}}^2 + \omega_k v_{\mathbf{k}}^2) \hat{a}_{\mathbf{k}}^+ \hat{a}_{-\mathbf{k}}^+ + h.c. + (|\dot{v}_{\mathbf{k}}|^2 + \omega_k |v_{\mathbf{k}}|^2) (2\hat{a}_{\mathbf{k}}^+ \hat{a}_{-\mathbf{k}}^- + \delta(\mathbf{0}))]$$

Computing the expectation value of the energy

$$\langle 0 | \hat{H} | 0 \rangle = \int d^3\mathbf{k} (|\dot{v}_{\mathbf{k}}|^2 + \omega_k |v_{\mathbf{k}}|^2) \delta(\mathbf{0}),$$

using the fact that  $\delta(\mathbf{0})$  represents the infinite total volume of space [110, p. 72], the energy density becomes

$$\epsilon = \int d^3\mathbf{k} (|\dot{v}_{\mathbf{k}}|^2 + \omega_k |v_{\mathbf{k}}|^2).$$

This yields the additional constraints on the mode functions

$$|\dot{v}_{\mathbf{k}}|^2 + \omega_k |v_{\mathbf{k}}|^2 \text{ is minimized,}$$

which can be solved together with the other constraints to yield

$$v_{\mathbf{k}} = \sqrt{\frac{1}{2\omega_k}} e^{i\omega_k t}.$$

Because we take  $\omega_k$  to be positive, the mode functions  $v_{\mathbf{k}}$  are said to be negative frequency

$$\dot{v}_{\mathbf{k}} = i\omega_k v_{\mathbf{k}},$$

and  $v_{\mathbf{k}}^*$  are said to be positive frequency

$$\dot{v}_{\mathbf{k}}^* = -i\omega_k v_{\mathbf{k}}^*.$$

The positive and negative frequency modes are coefficients of respectively the annihilation and the creation operators. Note that you would get a similar decomposition for another inertial observer. For our purposes if you start with an action of the form (7.1.1) where coordinates are chosen such that  $ds^2 = -dt^2 + d\mathbf{x}^2$ , you can directly expand the field into creation and annihilation operators by use of the positive and negative frequency modes with respect to these coordinates. This defines a vacuum as the lowest energy eigenstate of the Hamiltonian according to an observer described by these coordinates. We will use

this fact in the next subsections when we go to curved spacetimes where we are able to rewrite the action in the form (7.1.1) by using an appropriate set of coordinates. In general for stationary spacetimes there exists a timelike Killing vector which makes it possible to define a global time coordinate resulting into well-defined positive and negative frequency modes with respect to that.

The total energy of the vacuum  $E_0 = \langle 0 | \hat{H} | 0 \rangle$  is divergent but since we neglect gravity we are only interested in energy differences between the states and therefore we renormalize it to zero. The Hamiltonian becomes

$$\hat{H}(t) = \int d^3k \omega_k \hat{a}_k^+ \hat{a}_{-k}^-,$$

furthermore one can define a momentum operator by using Noether's theorem for spatial translations:

$$P^i = - \int d^3x \pi \partial_i \phi \rightarrow \hat{P}^i = - \int \frac{d^3p}{(2\pi)^3} p a_p^+ a_p^-$$

It turns out that the excited states  $\hat{a}_k^+ |0\rangle$  have an energy of  $\omega_k$  and a momentum  $\mathbf{k}$  which exactly correspond to the energy-momentum relation of a particle. Therefore we say that the state  $\hat{a}_k^+ |0\rangle$  contains a particle with momentum  $\mathbf{k}$  (although it is not a localized particle). The Fock basis consists of the following states

$$|n_1, n_2, \dots\rangle = \frac{1}{\sqrt{n_1! n_2! \dots}} (\hat{a}_{\mathbf{k}_1}^+)^{n_1} (\hat{a}_{\mathbf{k}_2}^+)^{n_2} \dots |0\rangle,$$

which contain  $n_1$  particles of momentum  $\mathbf{k}_1$ ,  $n_2$  particles of momentum  $\mathbf{k}_2$  etcetera.

In order to emphasize the privileged position of the vacuum and particle states we consider how they behave under Poincaré transformations. Suppose we have another inertial observer described by the coordinates  $(t', \mathbf{x}')$  which are related to  $(t, \mathbf{x})$  by a Poincaré transformation. She would get the following expansion of the field operator in terms of its annihilation and creation operators  $\hat{b}_k^-$  and  $\hat{b}_k^+$

$$\hat{\phi}(t', \mathbf{x}') = \int \frac{d^3k}{(2\pi)^{3/2}} \frac{1}{\sqrt{2\omega}} \left[ e^{i\mathbf{k}\cdot\mathbf{x}' - i\omega t'} \hat{b}_k^- + e^{-i\mathbf{k}\cdot\mathbf{x}' + i\omega t'} \hat{b}_k^+ \right],$$

Now it turns out that the coefficient in front of  $\hat{a}_k^+$  given by  $\frac{1}{\sqrt{2\omega}} e^{-i\mathbf{k}\cdot\mathbf{x} + i\omega t}$  is proportional to  $\frac{1}{\sqrt{2\omega'}} e^{-i\mathbf{k}'\cdot\mathbf{x}' + i\omega' t'}$ , where the prime indicates the corresponding Poincaré transformed quantity with respect to the first inertial coordinate system. Therefore, according to the second observer  $\hat{a}_k^+$  corresponds to  $\hat{b}_{k'}^+$  and hence creates a particle with Poincaré transformed momentum  $\mathbf{k}'$  and energy  $\omega'$ . We will show this in case of a Lorentz boost of velocity  $\mathbf{v}$ , such that the coordinates of the two observers are related by

$$t = \gamma t' + \gamma \mathbf{v} \cdot \mathbf{x}', \quad \mathbf{x} = \gamma \mathbf{x}' + \gamma \mathbf{v} t',$$

and likewise the four-momenta are related by

$$\omega' = \gamma\omega - \gamma\mathbf{v} \cdot \mathbf{k}, \quad \mathbf{k}' = \gamma\mathbf{k} - \gamma\mathbf{v}\omega.$$

We can deduce:

$$\mathbf{k} \cdot \mathbf{x} - \omega t = \mathbf{k}' \cdot \mathbf{x}' - \omega' t',$$

which means that every positive (negative) frequency mode with respect to one observer corresponds to another positive (negative) frequency mode with respect to the other observer. Therefore, the excited states contain particles with Lorentz transformed four-momenta, but because the modes do not mix, all inertial observers agree on the number of particles in each state. Furthermore, all inertial observers agree on the vacuum state which explains the special status of the vacuum of QFT in flat spacetime. In general relativity however, there is in general no preferred coordinate system. If one observer defines particles with respect to a set of positive and negative frequency modes and another observer with respect to a second set, then they do in general not agree on the particle content of a state. Actually this phenomenon already manifests itself in the Unruh effect, where an accelerated observer in flat spacetime associates a thermal spectrum of particles in the vacuum state of an inertial observer, which we will see in section 7.3. Moreover, in general it is not possible to find plane wave solutions to the field equations of motion, which makes the idea of a particle even harder to grasp. Therefore in curved spacetime one could instead think about what a particle detector would detect and relate that to particles. To give an idea, a particle detector traverses some trajectory in spacetime with proper time as its time coordinate. This enables it to define positive and negative frequency modes which can be used to determine what kind of particles it detects in a certain state. Again this turns out only makes sense when the proper time of the detector is proportional to a Killing time.

We have seen that QFT in flat spacetime allows for an unambiguously defined vacuum state and particle states. In the next section we will use the groundwork we have just laid to more elaborately discuss the Unruh effect and later on we will generalize these results to curved spacetime. We will see that the vacuum state and particle states will fall off their pedestal in Schwarzschild spacetime and how this leads to particle creation.

## 7.2 Quantum Field Theory in Schwarzschild Spacetime

In this subsection, we will introduce quantum field theory on curved spacetime by considering the specific example of the Schwarzschild solution in two-dimensions.<sup>4</sup> We restrict

---

<sup>4</sup>This section is based on [1, Chapter 9], [111, Ch. 3] and [110, Ch. 5, 8, 9].

ourselves to two dimensions for the purpose of providing the reader with an understanding of the concepts that are important for defining the theory. We will follow the previous section closely to construct the theory on this background and will make the similarities and differences between QFT on flat and curved spacetime explicit. The section starts off with the introduction of different metrics that we have seen in previous chapters. By applying a coordinate change, we can go from one metric to another such that we can define a metric that describes the entire Schwarzschild spacetime. Moreover, as we will be able to write our action in the shape of equation (7.1.1), we can immediately use the field expansion (see equation (7.1.4)) as derived in the previous section. Next, we will define a general action for a massless scalar field in curved spacetime. From this action, we will determine the field equations using the different coordinate systems. These equations allow us to write a solution for the fields in terms of creation and annihilation operators. We will use these operators to define different vacua which we use to show that choosing a vacuum is not as unambiguous as one would think. We conclude the section by showing that what is perceived as a vacuum by one observer, is not necessarily perceived as a vacuum by another observer.

### 7.2.1 Review of Relevant Metrics

We start with the Schwarzschild metric, equation (2.1.1), for a nonrotating black hole without electric charge. We will consider the two-dimensional case so we neglect the angular part in the metric. We look at the two-dimensional case instead of the four-dimensional one for pedagogical reasons as our calculations will be more straightforward and comprehensible for the reader. Were we to treat the more realistic four-dimensional case, we would find that there is an extra contribution from the angles  $\theta$  and  $\phi$  to the mode functions we will retrieve later. However, because we are considering a symmetric black hole, we can renormalize to make these contributions disappear. In the section on Hawking radiation, the more realistic case of the collapsing black hole will be considered. We introduce the tortoise coordinates as seen in equation (2.1.3) so we can rewrite the metric

$$ds^2 = \left(1 - \frac{2M}{r(r^*)}\right) [dt^2 - dr^{*2}]. \quad (7.2.1)$$

The tortoise coordinate  $r^*$  is only defined for  $r > 2M$ . To simplify our metric, we will rewrite it in terms of the tortoise lightcone coordinates which were introduced in chapter

2 such that we find<sup>5</sup>

$$ds^2 = \left(1 - \frac{2M}{r(\tilde{u}, \tilde{v})}\right) d\tilde{u}d\tilde{v}. \quad (7.2.2)$$

Our first metric in Schwarzschild coordinates is singular at the black hole horizon  $r = 2M$ , and our metric in tortoise lightcone coordinates is only defined for  $r > 2M$ . These metrics thus only describe the exterior of the black hole.

We will now rewrite this metric in another coordinate system that allows us to describe the entire spacetime. Rewriting the relation for  $r^*$  and inserting  $\tilde{u}$  and  $\tilde{v}$  gives

$$1 - \frac{2M}{r} = \frac{2M}{r} \exp\left(1 - \frac{r}{2M}\right) \exp\left(\frac{\tilde{v} - \tilde{u}}{4M}\right), \quad (7.2.3)$$

leading to the following metric

$$ds^2 = \frac{2M}{r} \exp\left(1 - \frac{r}{2M}\right) \exp\left(\frac{\tilde{v} - \tilde{u}}{4M}\right) d\tilde{u}d\tilde{v}. \quad (7.2.4)$$

Finally, we will use the Kruskal-Szekeres lightcone coordinates of which a variation was seen in chapter 2,

$$u = -4M \exp\left(-\frac{\tilde{u}}{4M}\right), v = 4M \exp\left(\frac{\tilde{v}}{4M}\right) \quad (7.2.5)$$

to write

$$ds^2 = \frac{2M}{r(u, v)} \exp\left(1 - \frac{r(u, v)}{2M}\right) du dv. \quad (7.2.6)$$

This metric is regular at  $r = 2M$  in accordance with what we have seen for the Kruskal-Szekeres coordinates. The interval of the coordinates can be deduced from equation (7.2.5) and they are  $-\infty < u < 0$  and  $0 < v < +\infty$ . However, they can be analytically extended such that they have ranges  $-\infty < u < +\infty$  and  $-\infty < v < +\infty$ . We have thus managed to write down a metric that is well-defined over the entire Schwarzschild spacetime except at the true singularity of the black hole,  $r = 0$ .

## 7.2.2 Evaluation of Action

We will now consider the action of a scalar field in two-dimensions as in equation (6.2.2) where we will neglect the massive part. This action is conformally invariant. A conformal transformation looks like

$$g_{\alpha\beta} \rightarrow \tilde{g}_{\alpha\beta} = \Omega^2(x^\gamma) g_{\alpha\beta} \quad (7.2.7)$$

---

<sup>5</sup>Note here that in Chapter 2 they are written as  $u = t - r^*$  and  $v = t + r^*$ . In this chapter, we will denote these coordinates by  $\tilde{u} \equiv u$  and  $\tilde{v} \equiv v$ .

such that we find for the determinant and the contravariant metric

$$\sqrt{-g} \rightarrow \sqrt{-\tilde{g}} = \Omega^2 \sqrt{-g}, g^{\alpha\beta} \rightarrow \tilde{g}^{\alpha\beta} = \Omega^{-2} g^{\alpha\beta}.$$

Clearly, the  $\Omega^2$  factors cancel out when these two expressions are reinserted in the action. We have thus shown that our general action for a massless scalar field in two-dimensions for curved spacetime is conformally invariant. This invariance will reappear in later sections. Now a relevant question to ask is whether the results we derive using this two-dimensional specific invariance are still relevant for us in a four-dimensional case. The answer is yes. Upon taking the angles into consideration, we would still have that this invariance counts for part of the space, as long as we restrict ourselves to two coordinates. Moreover, as argued before, the contribution of the angles to the field  $\phi$  can be normalized out as we are dealing with a rotationally symmetric black hole.

This invariance has an important consequence as it means that all metrics that are conformally connected<sup>6</sup> give us the same equations of motion resulting from this action. Going back to our metrics, we see that the metrics expressed in tortoise lightcone coordinates in equation (7.2.2) and the metric in equation (7.2.6) of the Kruskal-Szekeres lightcone coordinates are indeed conformally connected and will thus yield field equations of the same form. We will make this statement explicit. Looking at the metric in equation (7.2.2) of the tortoise lightcone coordinates we see that we only have a non-zero term with  $g_{\tilde{u}\tilde{v}}$ . We find the following action

$$S[\phi] = \int d\tilde{u} d\tilde{v} \partial_{\tilde{u}}\phi \partial_{\tilde{v}}\phi, \quad (7.2.8)$$

such that its field equations are

$$\partial_{\tilde{u}}\partial_{\tilde{v}}\phi = 0. \quad (7.2.9)$$

If we now look at Kruskal-Szekeres lightcone metric in equation (7.2.6) we again find that  $g_{\mu\nu} \neq 0$  only if  $\mu \neq \nu$  such that the action and the field equations are

$$S[\phi] = \int du dv \partial_u\phi \partial_v\phi, \quad \text{and} \quad \partial_u\partial_v\phi = 0. \quad (7.2.10)$$

These field equations coincide with the equations of motion found in the previous section and have the same shape. This means that we can write the same field expansion as in equation (7.1.4). We can thus proceed in the same way as before by stating the solutions to these scalar field equations. We can write  $\phi$  in terms of the tortoise lightcone coordinates as

$$\phi = \tilde{A}(\tilde{u}) + \tilde{B}(\tilde{v}), \quad (7.2.11)$$

---

<sup>6</sup>This means that the metrics have coinciding coordinate dependence and only differ by a prefactor.

or, equivalently in Kruskal-Szekeres lightcone coordinates

$$\phi = A(u) + B(v). \quad (7.2.12)$$

The solution for  $\tilde{A}(\tilde{u})$  looks like

$$\phi \propto e^{-i\omega\tilde{u}} = e^{-i\omega(t-r^*)},$$

and describes a right-moving positive-frequency mode with respect to  $t$  which we will later on relate to particles propagating away from the black hole so from now on we will refer to them as outgoing modes. Likewise, for  $\tilde{B}(\tilde{v})$  we find

$$\phi \propto e^{-i\omega\tilde{v}} = e^{-i\omega(t+r^*)},$$

which then naturally describes the left-moving modes, or the ingoing modes. Upon realizing that  $u = u(\tilde{u})$  and that  $v = v(\tilde{v})$  and that the solutions of the wave equation are as in equations (7.2.11) and (7.2.12), we can conclude that the left- and right-moving modes do not affect each other and can be considered independently. One might wonder, why we expand our field in left- and right-moving modes for curved spacetime. The reasons for this will become apparent later on.

### 7.2.3 Solutions to Field Equations

We will now consider two cases. An observer far away from the black hole, described by the tortoise lightcone coordinates, and an observer in the vicinity of the horizon which is described by the Kruskal-Szekeres coordinates. For the first we find as we move far away from the black hole, *i.e.*  $r \rightarrow \infty$ , from equation (7.2.2) that

$$ds^2 \rightarrow d\tilde{u}d\tilde{v} = dt^2 - dr^{*2}$$

which implies that the proper time of an observer at rest located far away from the black hole coincides with  $t$ . We will now promote our field  $\phi$  to the operator  $\hat{\phi}$ . We expand equation (7.1.4) for two-dimensions in terms of ingoing and outgoing modes as follows

$$\begin{aligned} \hat{\phi} &= \int_{-\infty}^{+\infty} \frac{dk}{(2\pi)^{1/2}} \sqrt{\frac{1}{2\omega}} \left[ e^{-i\omega t + ik \cdot r^*} \hat{b}_k + e^{i\omega t - ik \cdot r^*} \hat{b}_k^\dagger \right] \\ &= \int_0^{+\infty} \frac{dk}{(2\pi)^{1/2}} \sqrt{\frac{1}{2\omega}} \left[ e^{-i\omega t + ik \cdot r^*} \hat{b}_k + e^{i\omega t - ik \cdot r^*} \hat{b}_k^\dagger \right] \\ &\quad + \int_{-\infty}^0 \frac{dk}{(2\pi)^{1/2}} \sqrt{\frac{1}{2\omega}} \left[ e^{-i\omega t + ik \cdot r^*} \hat{b}_k + e^{i\omega t - ik \cdot r^*} \hat{b}_k^\dagger \right] \end{aligned}$$

$$= \int_0^{+\infty} \frac{dk}{(2\pi)^{1/2}} \sqrt{\frac{1}{2\omega}} \left[ e^{-i\omega t + ik \cdot r^*} \hat{b}_k + e^{i\omega t - ik \cdot r^*} \hat{b}_k^\dagger + e^{-i\omega t - ik \cdot r^*} \hat{b}_{-k} + e^{i\omega t + ik \cdot r^*} \hat{b}_{-k}^\dagger \right].$$

We will now let  $(\omega, k) \rightarrow \Omega$  where we have constructed the integral such that  $\Omega$  is strictly positive. We can send  $k$  to  $\Omega$ , because  $\omega^2 = k^2 + m^2|_{m=0}$ , i.e.  $k = \omega$ , such that we find

$$\begin{aligned} \hat{\phi} &= \int_0^{+\infty} \frac{d\Omega}{(2\pi)^{1/2}} \frac{1}{\sqrt{2\Omega}} \left\{ \left[ e^{-i\Omega(t-r^*)} \hat{b}_\Omega + e^{i\Omega(t-r^*)} \hat{b}_\Omega^\dagger \right] + \left[ e^{-i\Omega(t+r^*)} \hat{b}_{-\Omega} + e^{i\Omega(t+r^*)} \hat{b}_{-\Omega}^\dagger \right] \right\} \\ &= \int_0^{+\infty} \frac{d\Omega}{(2\pi)^{1/2}} \frac{1}{\sqrt{2\Omega}} \left\{ \left[ e^{-i\Omega\tilde{u}} \hat{b}_\Omega + e^{i\Omega\tilde{u}} \hat{b}_\Omega^\dagger \right] + \left[ e^{-i\Omega\tilde{v}} \hat{b}_{-\Omega} + e^{i\Omega\tilde{v}} \hat{b}_{-\Omega}^\dagger \right] \right\}, \end{aligned} \quad (7.2.13)$$

where  $\hat{b}_\Omega^\dagger$  and  $\hat{b}_\Omega$  are the creation and annihilation operators respectively of the outgoing particle, and  $\hat{b}_{-\Omega}^\dagger$  and  $\hat{b}_{-\Omega}$  the creation and annihilation operator of the ingoing particles. These operators obey the relations in equation (7.1.5). In the previous section, the operator  $\hat{b}_k^\dagger$  created a particle with momentum  $k$  which could be either positive or negative. Now, we have split the expansion up in in- and outgoing modes, which means that we associate  $\hat{b}_\Omega^\dagger$  with the outgoing particle with momentum  $\Omega$  which is now strictly positive, and  $\hat{b}_{-\Omega}^\dagger$  with the ingoing particle with momentum  $-\Omega$  (where  $\Omega$  is still strictly positive). The reason for making the in- and outgoing modes explicit is because the observer at infinity can only measure the outgoing particles. Due to the horizon, all the ingoing particles will be absorbed by the black hole.

Following the preceding section on QFT in flat spacetime, we now proceed to defining the vacuum. We will see that the vacuum in curved spacetime is not as straightforwardly defined as in flat spacetime. We start by defining the eigenstate  $|0_B\rangle$

$$\hat{b}_\Omega |0_B\rangle = 0, \quad \forall \Omega > 0,$$

which is called the Boulware vacuum. This vacuum does not contain any particles from the point of view of the far away observer. However, the Boulware vacuum is singular on the black hole horizon as the tortoise lightcone coordinates only hold for  $r > 2M$ . One might ask the question at this point, why we include this vacuum in this section, if it is an unphysical state. We have included it with the main purpose of showing the reader, that one cannot just define any vacuum in curved spacetime. To find a vacuum, we need to be very careful to check that it is indeed a proper physical state.

We will now define a vacuum that is physical by considering the Kruskal-Szekeres which are well-defined on the horizon and cover the entire Schwarzschild spacetime except at its true singularity at  $r = 0$ . This makes these coordinates similar to the inertial coordinates in Minkowski spacetime. Near the horizon, when  $r \rightarrow 2M$ , we find for equation (7.2.5)

$$ds^2 \rightarrow dudv = dT^2 - dR^2.$$

In analogy with what we have seen before, we now say that an observer passing the horizon of the black hole associates particles with the positive-frequency modes with respect to the time  $T$ . Expanding the field now gives the following very similar operator expansion

$$\hat{\phi} = \int_0^\infty \frac{d\omega}{(2\pi)^{1/2}} \frac{1}{\sqrt{2\omega}} \left\{ [e^{-i\omega u} \hat{a}_\omega + e^{i\omega u} \hat{a}_\omega^\dagger] + [e^{-i\omega v} \hat{a}_{-\omega} + e^{i\omega v} \hat{a}_{-\omega}^\dagger] \right\}, \quad (7.2.14)$$

where  $\hat{a}_\omega^\dagger$  and  $\hat{a}_\omega$  are the creation and annihilation operators for the outgoing modes, and  $\hat{a}_{-\omega}^\dagger$  and  $\hat{a}_{-\omega}$  are the creation and annihilation operators of the ingoing modes. We can use these operators to define the Kruskal vacuum state, *i.e.*

$$\hat{a}_\omega |0_K\rangle = 0, \quad \forall \omega > 0.$$

Unlike the Boulware vacuum, this state is regular on the horizon, because the Kruskal-Szekeres coordinates are well defined everywhere except at the true singularity at  $r = 0$ . For this reason, we find a natural candidate in the Kruskal state  $|0_K\rangle$  for the true physical vacuum in the presence of a black hole.

### 7.2.4 Ambiguity of The Vacuum

We can relate the operators  $\hat{a}_\omega^\dagger$ ,  $\hat{a}_\omega$ ,  $\hat{b}_\Omega^\dagger$ , and  $\hat{b}_\Omega$  via the Bogolyobov transformations:

$$\hat{b}_\Omega = \int_0^\infty d\omega [\alpha_{\Omega\omega} \hat{a}_\omega - \beta_{\Omega\omega} \hat{a}_\omega^\dagger]. \quad (7.2.15)$$

As the tortoise lightcone coordinates only describe the exterior of the black hole and not the entire Schwarzschild spacetime, we cannot define the inverse Bogolyobov transformation. The transformation has the following normalization condition

$$\int_0^\infty (\alpha_{\Omega\omega} \alpha_{\Omega'\omega}^* - \beta_{\Omega\omega} \beta_{\Omega'\omega}^*) = \delta(\Omega - \Omega'). \quad (7.2.16)$$

We can use this Bogolyobov transformation to relate the two different vacua to each other.

We can now make an interesting observation namely that the observer far away detects particles in the Kruskal vacuum which seems counterintuitive. The Kruskal vacuum is a vacuum of *a*-particles so there can be *b*-particles in the vacuum. This can be seen by applying the *b*-outgoing particle number operator  $\hat{N}_\Omega = \hat{b}_\Omega^\dagger \hat{b}_\Omega$  to the Kruskal vacuum:

$$\begin{aligned} \langle 0_K | \hat{N}_\Omega | 0_K \rangle &= \langle 0_K | \hat{b}_\Omega^\dagger \hat{b}_\Omega | 0_K \rangle \\ &= \langle 0_K | \left( \int_0^\infty d\omega [\alpha_{\Omega\omega}^* \hat{a}_\omega^\dagger - \beta_{\Omega\omega}^* \hat{a}_\omega] \right) \end{aligned}$$

$$\begin{aligned}
& \times \left( \int_0^\infty d\omega' [\alpha_{\Omega\omega'} \hat{a}_{\omega'} - \beta_{\Omega\omega'} \hat{a}_{\omega'}^\dagger] \right) |0_K\rangle \\
&= \int d\omega d\omega' \beta_{\Omega\omega}^* \beta_{\Omega'\omega} \langle 0_K | \hat{a}_\omega \hat{a}_{\omega'}^\dagger | 0_K \rangle \\
&= \int d\omega d\omega' \beta_{\Omega\omega}^* \beta_{\Omega'\omega} \delta(\omega - \omega') \\
&= \int d\omega |\beta_{\Omega\omega}|^2,
\end{aligned} \tag{7.2.17}$$

which we interpret as the mean number of particles with frequency  $\Omega$  as seen by the far away observer.<sup>7</sup> Note that we have computed the particle number density for the outgoing particles only. We have thus seen that what is a vacuum to one observer, is not necessarily a vacuum to another observer. More specific examples of this will be seen for the consideration of the Unruh effect and Hawking radiation.

Before we end this subsection, we would like to discuss the notion of particles. The word has been used a couple times throughout the chapter and so far it has nowhere been made clear what this term actually means. It is important to realize that for Minkowski space (*i.e.* flat spacetime) there is not one uniquely defined vacuum, but that the vacuum introduced in the previous section is conventionally agreed upon to be the vacuum for all inertial measuring devices. This is so because this vacuum is Poincaré invariant just as the inertial observers in Minkowski space. For curved spacetime, it is not as straightforward. The fact that a vacuum for one observer is not necessarily a vacuum for another observer in curved spacetime is an indication that the "state of motion" of an observer measuring particles plays a significant role in the observation of particles as we will see in the next section [111, p. 48]. Therefore, the definition of a vacuum and thus a particle is highly non-trivial.

### 7.3 The Unruh Effect

In the previous section the idea of particles with positive energy being associated with positive frequencies was presented. With the necessary tools available we will now present the effect of positive and negative frequency mixing in flat spacetime due to acceleration. This is called the Unruh effect and it can be stated as follows: while a stationary observer in flat Minkowski space will measure the state of the fields to be a pure vacuum an accelerated one will measure particles with a thermal spectrum. To derive it without complications

---

<sup>7</sup>Just as a reminder, as we cannot invert the Bogolyobov transformation, we cannot calculate the mean number of particles as seen by the observer close to the black hole horizon.

we will consider a massless scalar field in 1+1 dimensional spacetime. It shall be studied in both Minkowski and Rindler coordinates.<sup>8</sup>

### 7.3.1 Rindler space Revisited

In Chapter two we presented the Rindler space. Here we will use the derived Rindler metric, equation (2.4.12), and bring it into its conformally flat form. Firstly by using a translation  $\xi \rightarrow \xi - \frac{1}{\alpha}$  we obtain:

$$ds^2 = -(\alpha\xi)^2 d\tau^2 + d\xi^2 \quad (7.3.1)$$

The Rindler horizon is now translated to  $\xi = 0$  and the observer with acceleration  $\alpha$  will be at the position  $\xi = \frac{1}{\alpha}$  for  $\tau = 0$ . This metric can be used for both Regions I and III of Fig.(2.21). This can be seen by putting a minus sign in front of the transformations (2.4.3), (2.4.4) and following the same procedure. As a result of the relative minus sign between the Minkowski time coordinate  $t$  and the Rindler one  $\tau$  the timelike Killing vector is  $-\partial_\tau$  in Region III. The final conformal form is obtained by the transformation

$$\xi \rightarrow \frac{e^{\alpha\xi}}{\alpha}, \quad (7.3.2)$$

yielding:

$$ds^2 = e^{2\alpha\xi^1} [-(d\xi^0)^2 + (d\xi^1)^2] \quad (7.3.3)$$

It is now convenient to shift to the lightcone coordinates in both Minkowski and Rindler space. This amounts to the following redefinition of the coordinates:

$$u = t - x, \quad \tilde{u} = \xi^0 - \xi^1, \quad (7.3.4)$$

$$v = t + x, \quad \tilde{v} = \xi^0 + \xi^1 \quad (7.3.5)$$

where  $u, v$  and  $\tilde{u}, \tilde{v}$  stand for Minkowski and Rindler lightcone coordinates respectively. As both metrics describe the same Minkowski spacetime in different coordinates we can equate the two line elements which gives:

$$ds^2 = -dudv = -e^{\alpha(\tilde{v}-\tilde{u})} d\tilde{u} d\tilde{v}. \quad (7.3.6)$$

To conclude we want to find the relations between these two coordinate systems hence find how  $u(\tilde{u}, \tilde{v})$  and  $v(\tilde{u}, \tilde{v})$  depend on the respective Rindler coordinates. Now we can see that each of the Minkowski coordinates will depend on only one of the two arguments. If this

---

<sup>8</sup>The derivation proceeds along the lines of Chapter 8 out of [110].

was not the case we would have  $d\tilde{u}^2$  and  $d\tilde{v}^2$  terms in the Rindler metric. Thus, without loss of generality, we choose

$$u = u(\tilde{u}), \quad v = v(\tilde{v}), \quad (7.3.7)$$

and we see from (7.3.6) that the following relations hold:

$$u = -\frac{e^{-\alpha\tilde{u}}}{\alpha}, \quad v = \frac{e^{\alpha\tilde{v}}}{\alpha}. \quad (7.3.8)$$

This concludes the necessary reformulation of the Rindler space formalism for the purposes of this chapter.

### 7.3.2 The Effect

Starting from a massless scalar field in 1+1 dimensions we will derive the mode expansions for the field in both Minkowski and Rindler spacetime. As seen in the previous subsection the fact that we work in 1+1 dimensional spacetime implies that the action is conformally invariant and hence we can discard the conformal factor of the Rindler metric. Now we consider the action (6.2.2) for a massless case. In Subsection 7.2.2 it was shown that a conformal transformations of the following form:

$$g_{\mu\nu} \rightarrow \Omega^2 g_{\mu\nu} \quad (7.3.9)$$

leaves the action invariant. Therefore the conformal factors will always cancel and we have the following form in Minkowski and Rindler space coordinates respectively:

$$S = \frac{1}{2} \int d^2x [-(\partial_t \phi)^2 + (\partial_x \phi)^2] \quad (7.3.10)$$

$$= \frac{1}{2} \int d^2x [-(\partial_{\xi^0} \phi)^2 + (\partial_{\xi^1} \phi)^2] \quad (7.3.11)$$

It is now convenient to rewrite the action in the lightcone coordinates

$$S = -2 \int du dv \partial_u \phi \partial_v \phi = -2 \int d\tilde{u} d\tilde{v} \partial_{\tilde{u}} \phi \partial_{\tilde{v}} \phi. \quad (7.3.12)$$

After applying the variational method to the actions we obtain the Klein-Gordon equation formulated in Lightcone coordinates in the two coordinate frames:

$$\partial_u \partial_v \phi = 0, \quad \partial_{\tilde{u}} \partial_{\tilde{v}} \phi = 0 \quad (7.3.13)$$

The Klein Gordon equations have well known solutions which in the Minkowski space are of the form

$$\phi \propto e^{-i\omega(t-x)} = e^{-i\omega u}, \quad \phi \propto e^{-i\omega(t+x)} = e^{-i\omega v}.$$

The first solution is the right moving positive frequency mode and the second is the left moving one. In the case of the Rindler coordinates we have to make a distinction between regions I and III. As stated before, the Killing vector in region III has an overall minus sign difference with respect to the Killing vector in region I implying that different modes have to be defined in each region. Thus a basis satisfying the KG-Gordon equation and this peculiarity will be of the following form:

$$\phi \propto e^{-i\omega(\xi^0 - \xi^1)} = e^{-i\omega\tilde{u}}, \quad \text{I}, \quad (7.3.14)$$

$$\phi \propto e^{-i\omega(-\xi^0 - \xi^1)} = e^{i\omega\tilde{v}}, \quad \text{III} \quad (7.3.15)$$

Each set forms a complete basis of their respective region but do not cover the entire Minkowski space. On the other hand when the two are combined they are complete and the lines

$$\xi^0 = \text{constant}$$

are Cauchy surfaces. This means that the modes can be analytically continued into the regions II and IV where  $\alpha$  is imaginary. Therefore this is as good a basis for the scalar field as the usual Minkowski modes.

After this intermezzo about Rindler modes we shall restrict the calculations to region I. In both spacetimes the derivation of the mode expansion precedes as presented in Section 7.1 and the result is the following:

$$\hat{\phi} = \int_0^\infty \frac{d\omega}{\sqrt{2\pi}} \frac{1}{\sqrt{2\omega}} [e^{-i\omega u} \hat{a}_\omega + e^{i\omega u} \hat{a}_\omega^\dagger + e^{-i\omega v} \hat{a}_{-\omega} + e^{i\omega v} \hat{a}_{-\omega}^\dagger] \quad (7.3.16)$$

$$= \int_0^\infty \frac{d\Omega}{\sqrt{2\pi}} \frac{1}{\sqrt{2\Omega}} [e^{-i\Omega\tilde{u}} \hat{b}_\Omega + e^{i\Omega\tilde{u}} \hat{b}_\Omega^\dagger + e^{-i\Omega\tilde{v}} \hat{b}_{-\Omega} + e^{i\Omega\tilde{v}} \hat{b}_{-\Omega}^\dagger]. \quad (7.3.17)$$

Here, following the procedure of semiclassical quantization, the coefficients associated with the modes have been uplifted to creation and annihilation operators satisfying the usual commutation relations

Associated with the annihilation and creation operator comes the notion of a vacuum. Here the Minkowski vacuum will be denoted by  $|0_M\rangle$  and the Rindler one by  $|0_R\rangle$  and the annihilation operators act as follows

$$\hat{a}_\omega |0_M\rangle = 0, \quad \hat{b}_\Omega |0_R\rangle = 0. \quad (7.3.18)$$

In contrast to the examples seen in the previous section these two vacua are not the same modulo a Lorentz transformation. This follows from the structure of the Rindler modes which are not analytic at the origin of the Minkowski spacetime ( $u = 0$  or  $v = 0$ ). Rindler modes in region I do not go over smoothly to modes in region III and vice versa

in contrast to the Minkowski modes which do [111, p. 115]. This implies that mixing of positive and negative frequencies must occur when one expresses the Rindler modes in terms of Minkowski modes as a superposition of positive Minkowski frequencies maintain their analyticity. Therefore a Rindler observer in the Minkowski vacuum will measure particles. This is the Unruh effect.

### 7.3.3 Unruh Temperature

To determine what an accelerating observer measures when the field is in the Minkowski vacuum, it is necessary to relate the Rindler creation and annihilation operators with the corresponding Minkowski operators. This can be done for the right and left moving modes separately. One can see that this is possible by looking at the mode expansion and remembering that  $u = u(\tilde{u})$  and  $v = v(\tilde{v})$  holds. Therefore from now on we will focus on the right moving modes as the derivation for the left moving modes proceeds in a similar way. In Section 7.1 we presented how we can relate operators in different bases through a Bogolyubov transformation. For our operators  $\hat{a}, \hat{b}$  the transformation takes the following form:

$$\hat{b}_\Omega = \int_0^\infty d\omega [\alpha_{\Omega\omega} \hat{a}_\omega - \beta_{\Omega\omega} \hat{a}_\omega^\dagger] \quad (7.3.19)$$

$$\hat{b}_\Omega^\dagger = \int_0^\infty d\omega [\alpha_{\Omega\omega}^* \hat{a}_\omega^\dagger - \beta_{\Omega\omega}^* \hat{a}_\omega] \quad (7.3.20)$$

with  $\alpha$  and  $\beta$  being complex coefficients. It is important to note that these transformations cannot be inverted due to the non analyticity of the Rindler modes. As usual the transformation coefficients are properly normalized according to

$$\int_0^\infty d\omega (\alpha_{\Omega\omega} \alpha_{\Omega'\omega}^* - \beta_{\Omega\omega} \beta_{\Omega'\omega}^*) = \delta(\Omega - \Omega') \quad (7.3.21)$$

It is now a matter of finding the corresponding coefficients. Substituting the Bogolyubov transformation (7.3.19) into the mode expansion yields

$$\frac{e^{-i\omega u}}{\sqrt{\omega}} = \int_0^\infty \frac{d\Omega'}{\sqrt{\Omega'}} (\alpha_{\Omega'\omega} e^{-i\Omega' \tilde{u}} - \beta_{\Omega'\omega}^* e^{i\Omega' \tilde{u}}). \quad (7.3.22)$$

Inverting this relation yields the coefficients and they have the form

$$\frac{\alpha_{\Omega\omega}}{\beta_{\Omega\omega}} = \int_{-\infty}^\infty e^{\mp i\omega u + i\Omega \tilde{u}} d\tilde{u} = \pm \frac{1}{2\pi} \sqrt{\frac{\Omega}{\omega}} \int_{-\infty}^0 (-\alpha u)^{-\frac{i\Omega}{\alpha} - 1} e^{\mp i\omega u} du \quad (7.3.23)$$

$$= \pm \frac{1}{2\pi\alpha} \sqrt{\frac{\Omega}{\omega}} e^{\pm \frac{\pi\Omega}{2\alpha}} e^{\frac{i\Omega}{\alpha} \ln \frac{\omega}{\alpha}} \Gamma(-\frac{i\Omega}{\alpha}) \quad (7.3.24)$$

To get this result we multiplied (7.3.22) with  $e^{\pm i\Omega\tilde{u}}$ , used the definition of the  $\delta$ -function and integrated over  $\tilde{u}$ . Finally in the second equality of (7.3.23) we used the relation between  $u$  and  $\tilde{u}$  as given in (7.3.8). Now it is clear that the following relationship between the two coefficients holds

$$|\alpha_{\Omega\omega}|^2 = e^{\frac{2\pi\Omega}{\alpha}} |\beta_{\Omega\omega}|^2 \quad (7.3.25)$$

As we can now express the Rindler creation and annihilation operators in the respective Minkowski ones we are able to compute the expectation value of the Rindler number operator when the field is in the Minkowski vacuum. Then, as foretold, it will become evident that the Minkowski vacuum contains particles from the point of view of the Rindler observer. The number operator is  $\hat{N}_\Omega = \hat{b}_\Omega^\dagger \hat{b}_\Omega$  and the resulting expectation value is

$$\langle \hat{N}_\Omega \rangle = \langle 0_M | \int_0^\infty d\omega [\alpha_{\Omega\omega}^* \hat{a}_\omega^\dagger - \beta_{\Omega\omega}^* \hat{a}_\omega] (\int_0^\infty d\omega [\alpha_{\Omega\omega} \hat{a}_\omega - \beta_{\Omega\omega} \hat{a}_\omega^\dagger]) | 0_M \rangle \quad (7.3.26)$$

$$= \int_0^\infty d\omega |\beta_{\Omega\omega}|^2 \quad (7.3.27)$$

Now rewriting the normalization condition (7.3.21) for  $\Omega' = \Omega$  and using the relation between the Bogolyubov coefficients, eq. (7.3.25), we have

$$\int_0^\infty d\omega (|\alpha_{\Omega\omega}|^2 - |\beta_{\Omega\omega}|^2) = \delta(0) \Rightarrow \int_0^\infty d\omega (\exp[\frac{2\pi\Omega}{\alpha}] - 1) |\beta_{\Omega\omega}|^2 = \delta(0) \quad (7.3.28)$$

Inserting this result in the expectation value of the number operator (7.3.26) yields the final result

$$\langle \hat{N}_\Omega \rangle = \int_0^\infty d\omega |\beta_{\Omega\omega}|^2 = [\exp(\frac{2\pi\Omega}{\alpha}) - 1]^{-1} \delta(0) \quad (7.3.29)$$

This shows our claim. The Minkowski vacuum is not devoid of particles from the point of view of a Rindler observer. It actually diverges. This divergence is a result of the use of plane wave basis modes which are non-square integrable. If we had used normalized wave packets we would not have encountered this. Another way of looking at this is seeing the divergence as a result of the infinite volume of the Rindler slice. If we had quantized our field in a box it would be equal to the volume. Hence it is more relevant to look at the mean particle density per frequency:

$$n_\Omega = \frac{\langle \hat{N}_\Omega \rangle}{V} = [\exp(\frac{2\pi\Omega}{\alpha}) - 1]^{-1} \quad (7.3.30)$$

Here the Unruh effect is shown in all its glory. If we uniformly accelerate a detector in the Minkowski vacuum it will result in particles being measured which obey the Bose-Einstein distribution with a temperature

$$T = \frac{\alpha}{2\pi} \quad (7.3.31)$$

called the Unruh temperature. Therefore it is shown that the acceleration of the detector exactly determines the temperature modulo a constant.

Having derived this result it is natural to consider its physical implications. A Minkowski observer describes the Minkowski vacuum state as a state of zero energy or in other words with a vanishing expectation value of the energy momentum tensor. This seems to contradict the measurement of the Rindler observer which measures positive energy particles. This can be explained by considering what must be done to keep an observer uniformly accelerating. It is necessary to do constant work on the Rindler observer hence energy is not conserved! This means that in the Rindler spacetime there exists a source of energy which couples to the quantum field and excites it in such a way that the detector is in a thermal bath with a temperature proportional to the acceleration. From the point of view of a Minkowski observer the detector emits and absorbs particle at a continuous rate as a result of the coupling which necessarily enters the action to facilitate the acceleration. So in the end it is clear that the energy measured by the Rindler observer is an artifact of the work done to keep it uniformly accelerating.[110, p. 108] [1, p. 412].

## 7.4 Hawking radiation

In this section, different ways to derive Hawking radiation are presented. Then some physical aspects of Hawking radiation are revealed.

### 7.4.1 The Unruh effect in extended Schwarzschild spacetime

There is also an Unruh effect in extended Schwarzschild spacetime. This effect is very analogous to the effect in Minkowski spacetime derived above. The derivation in this subsection follows Mukhanov's book [110, Sec. 9.1]. We consider a massless Klein-Gordon field in extended Schwarzschild spacetime. The equations of motion and how to quantize field in curved spacetime are introduced at the beginning of this chapter. Just like in the case of the Minkowski Unruh effect, we consider two different observers. One observer uses the tortoise coordinate system. The other observer uses the Kruskal coordinate system. We can now perform a mode expansion in terms of tortoise and in terms of Kruskal coordinates, and obtain two different vacua in this way. The vacuum obtained by doing the mode expansion with respect to the tortoise coordinates is called the Boulware vacuum and the vacuum obtained with the mode expansion for the Kruskal coordinates is the Hartle-

Rindler	Schwarzschild
Inertial observers: vacuum $ 0_M\rangle$	Free falling observers: vacuum $ 0_K\rangle$
Accelerated observers: $ 0_R\rangle$	Observers at constant radius: $ 0_T\rangle$
Proper acceleration $a$	Proper acceleration $(4M)^{-1}$

Table 7.1: Hawking Radiation

Hawking vacuum. If the annihilation operators for the Kruskal coordinates are denoted by  $\hat{a}_{\pm\omega}^-$  and the annihilation operators for the tortoise coordinates by  $\hat{b}_{\pm\omega}^-$ , where  $\omega$  denotes the frequency, the vacua are specified by:

$$\hat{a}_{\pm\omega}^- |0_K\rangle = 0; \quad \hat{b}_{\pm\omega}^- |0_T\rangle = 0. \quad (7.4.1)$$

We can compare the vacua obtained here to the case treated in the section on the Unruh effect. Rindler spacetime only covers part of Minkowski spacetime, so does Schwarzschild spacetime in tortoise coordinate to Schwarzschild spacetime in Kruskal coordinates. Therefore the Boulware vacuum corresponds to the Rindler vacuum and the Hartle-Hawking vacuum corresponds to the Minkowski vacuum. The derivation is analogous to the derivation of the Unruh effect in Minkowski spacetime, with the identification  $a = (4M)^{-1}$ . We note that this similarity only holds in extended Schwarzschild spacetime in  $1+1$  dimensions. An overview of the correspondence is shown in table 7.4.1 (table taken from [110]):

Using this similarity and recalling section on Unruh effect, we find that the remote observer must see particles with the thermal spectrum,

$$\langle \hat{N}_\Omega \rangle \equiv \langle 0_K | \hat{b}_\Omega^+ \hat{b}_\Omega^- | 0_K \rangle = [\exp(\frac{2\pi\Omega}{\kappa}) - 1]^{-1} \delta(0), \quad (7.4.2)$$

corresponding to the temperature

$$T_H = \frac{\kappa}{2\pi} = \frac{1}{8\pi M}. \quad (7.4.3)$$

Now that we know Hawking radiation temperature  $T$ , we can easily derive the Hawking-Bekenstein entropy. According to the first law of thermodynamics of black holes,  $dM = TdS$ , which leads to  $S = 4\pi M^2 = \frac{1}{4}A$ ,  $A$  is the area of event horizon. Upon reintroducing elementary constant, we obtain:

$$S_{BH} = \frac{k_B c^3}{4\pi\hbar G} A, \quad (7.4.4)$$

which verifies the entropy deduced in Chapter 5.

Note that the state  $|0_K\rangle$  contains not only outgoing (right-moving) particles, but also the incoming (left moving) particles with the same thermal spectrum. Only in this case the

Kruskal vacuum is non-singular on the past horizon ( $v = 0$ ) of the eternal Schwarzschild spacetime. Therefore, in the presence of quantum fields the picture of an eternal black hole is consistent only if the black hole is placed in a thermal reservoir with the temperature  $T_H$ . Because the black hole absorbs particles, it should also emit them to maintain the equilibrium. It then follows that the black hole placed in an empty space must evaporate by emitting thermal radiation with the temperature given above.

If we consider a black hole formed as a result of gravitational collapse, the past horizon at  $v = 0$  does not exist, and therefore there is no need to choose for the left-moving v-modes the Kruskal state annihilated simultaneously by the operators  $\hat{a}^-$  for both right- and left-moving modes. Instead, it is more natural to choose the state annihilated by the operators  $\hat{a}^-$  for the right-moving modes and by the operators  $\hat{b}^-$  for the left-moving modes. Because there is no past horizon, this state is also non-singular and does not contain incoming particles from the point of view of the remote observer. Hence this observer sees only thermal radiation coming from the black hole. The corresponding choice of the quantum state is justified by the consideration of the black hole formed as a result of a spherical shell collapse [112]. In the following section, we give a detailed treatment of Hawking radiation from a collapsing black hole.

### 7.4.2 The Hawking Effect for a Collapse to a Schwarzschild Black Hole

We now consider the case where matter undergoes a collapse to a Schwarzschild black hole of mass  $M$ . We will show that at sufficiently late times, the black hole emits Planckian radiation at temperature  $T = \frac{\kappa}{2\pi}$ , where  $\kappa$  is the surface gravity of the black hole, given by (5.1.12). The derivation given here follows the original paper by Hawking [77], but is clarified using aspects from the derivations in the books “General Relativity” [113] and “Quantum Field Theory in Curved Spacetime and Black Hole Thermodynamics” [114], both by Wald.

#### A scalar field in collapsing Schwarzschild geometry

Assume any geometry corresponding to matter collapsing to a Schwarzschild black hole.<sup>9</sup> Without essential loss of generality we can assume the matter to be spherically symmetric.

---

<sup>9</sup>Collapses to more general black holes are discussed at the end of this subsection.

We are interested in the behaviour at asymptotically late times, at which the black hole has settled down and the effects of the details of the collapse will be asymptotically small. Outside of the collapsing body, the spacetime is isomorphic to a part of extended Schwarzschild spacetime. A picture of the spacetime is shown in figure 7.1. We note that the spacetime is asymptotically static in the past and future outside the collapsing matter and black hole.

We will again consider a massless Klein-Gordon field. In this geometry, we make the following ansatz<sup>10</sup> for the solution outside the collapsing matter (*cf.* eqns. (6.2.5) - (6.2.7) or [111] eqns. (8.1)-(8.2))

$$\phi(t, r, \theta_1, \theta_2) = \int \sum_{l,m} d\omega \frac{e^{-i\omega t}}{r} R_{\omega,l}(r) Y_{l,m}(\theta_1, \theta_2), \quad (7.4.5)$$

$$\frac{d^2 R_{\omega,l}}{dr_*^2} + (\omega^2 - V_l(r)) R_{\omega,l} = 0, \quad (7.4.6)$$

$$r_* = r + 2M \ln \left| \frac{r}{2M} - 1 \right|, \quad (7.4.7)$$

$$V_l(r) = \left( \frac{l(l+1)}{r^2} + \frac{2M}{r^3} \right) \left( 1 - \frac{2M}{r} \right). \quad (7.4.8)$$

In the above equations, we labelled the spherical spatial coordinates  $r, \theta_1, \theta_2$  and time coordinate  $t$  and we used spherical harmonics  $Y_{l,m}$ .

## Semiclassical quantisation

We can define *in*-states by considering the Cauchy surface that coincides with the past infinity  $\mathcal{J}^-$  (marked in blue in figure 7.1) and constructing the Fock space in the manner described in previous sections. This leads to the following representation of  $\phi$  in terms of a complete family of orthonormal positive frequency solutions  $\{f_i\}_{i \in \mathbb{N}}$  and creation and annihilation operators  $\{\mathbf{a}_i^\dagger\}_{i \in \mathbb{N}}, \{\mathbf{a}_i\}_{i \in \mathbb{N}}$

$$\phi = \sum_i f_i \mathbf{a}_i + \bar{f}_i \mathbf{a}_i^\dagger. \quad (7.4.9)$$

Another Cauchy surface (marked in red)  $\Sigma$  is shown in the picture: it intersects the horizon outside the collapsing matter. The massless Klein-Gordon field satisfies the “asymptotic completeness” property in the sense that every incoming state propagates either out into future infinity or into the black hole and any state that enters either the black hole or

---

<sup>10</sup>This is essentially the same ansatz as in section 6.2

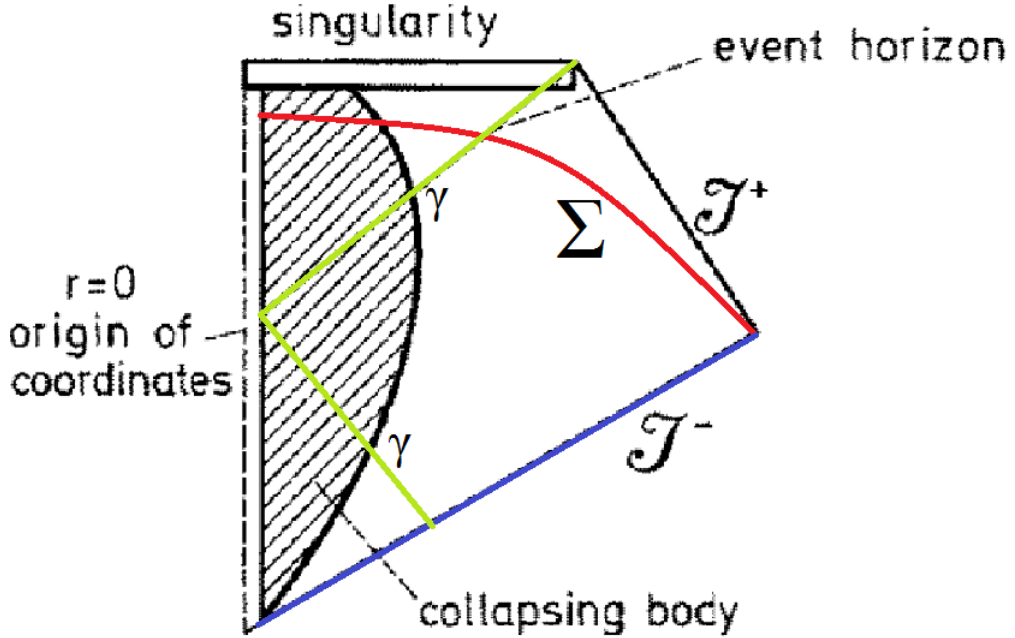


Figure 7.1: Collapse of spherical matter to form a Schwarzschild black hole. Picture edited from [77].

future infinity can be traced back to past infinity [115]. We can define the *late*-states by considering states that are only supported on the Cauchy surface  $\Sigma$  outside the event horizon and complete the description by adding *early*-states that are only supported on  $\Sigma$  inside the horizon. If we let  $\{p_i\}_{i \in \mathbb{N}}$  be a *late*-complete family of orthonormal positive frequency solutions and  $\{q_i\}_{i \in \mathbb{N}}$  an *early*-complete family of orthonormal solutions, then

$$\phi = \sum_i p_i \mathbf{b}_i + \bar{p}_i \mathbf{b}_i^\dagger + q_i \mathbf{c}_i + \bar{q}_i \mathbf{c}_i^\dagger, \quad (7.4.10)$$

where  $\{\mathbf{b}_i^\dagger\}_{i \in \mathbb{N}}, \{\mathbf{b}_i\}_{i \in \mathbb{N}}$  are creation and annihilation operators for the *late*-particles and no meaningful *particle* interpretation for  $\{\mathbf{c}_i^\dagger\}_{i \in \mathbb{N}}, \{\mathbf{c}_i\}_{i \in \mathbb{N}}$  is claimed [77, 114].

The two expressions for  $\phi$  should of course coincide, so the solutions and operators can be expressed as linear combinations of each other

$$p_i = \sum_j \alpha_{ij} f_j + \beta_{ij} \bar{f}_j, \quad (7.4.11)$$

$$q_i = \sum_j \gamma_{ij} f_j + \eta_{ij} \bar{f}_j, \quad (7.4.12)$$

$$\mathbf{b}_i = \sum_j \bar{\alpha}_{ij} \mathbf{a}_j - \bar{\beta}_{ij} \mathbf{a}_j^\dagger, \quad (7.4.13)$$

$$\mathbf{c}_i = \sum_j \bar{\gamma}_{ij} \mathbf{a}_j - \bar{\eta}_{ij} \mathbf{a}_j^\dagger. \quad (7.4.14)$$

We can immediately see <sup>11</sup> that the expectation value of the *late* number operator for the  $i$ th mode in the *in*-vacuum is given by

$$\langle 0_{in} | \hat{N}_i^{late} | 0_{in} \rangle = \sum_j |\beta_{ij}|^2. \quad (7.4.15)$$

Going to the continuum case, in which our Fourier components are no longer discrete, we write  $f_i = f_{\omega',l,m}$ , where  $\omega'$  is now a continuous frequency, and  $p_{\omega,l,m}$ , with another continuous frequency  $\omega$ . If we fix the radial indices  $l,m$ , and omit them from future notation, we obtain the following expression for  $p_\omega$

$$p_\omega = \int_0^\infty d\omega' \alpha_{\omega\omega'} f_{\omega'} + \beta_{\omega\omega'} \bar{f}_{\omega'}. \quad (7.4.16)$$

### Scattering by the black hole

In the following, we make use of Eddington-Finkelstein coordinates, given by (2.1.5) (incoming Eddington-Finkelstein coordinates are denoted by  $v$  and outgoing Finkelstein coordinates are denoted by  $u$ ). Let  $x$  be a point on the intersection of the event horizon with  $\Sigma$  and  $\gamma$  the null geodesic generator of the horizon that goes through  $x$ . We can continue  $\gamma$  into the past, and define  $v_0$  as the incoming Eddington-Finkelstein time at which  $\gamma$  intersects past infinity  $\mathcal{J}^-$ . In figure 7.1,  $\gamma$  is marked in green. We define  $\vec{n}^a$  as a (normalised [77]) future- and radially inward directed null vector at  $x$ .

We decompose  $p_\omega = p_\omega^{(1)} + p_\omega^{(2)}$ . The subscript (1) denotes the part of the wave that travels directly from past to future infinity. We will be interested in the part  $p_\omega^{(2)}$  that originated on  $\mathcal{J}^-$ , with  $v$  close to but smaller than  $v_0$  and that propagated through the collapsing matter, where it was scattered or reflected. We will use the geometric optics approximation <sup>12</sup>. We are interested in waves that propagated through space-time points “close” to the black hole horizon. Near the horizon the waves will have been blue-shifted, and their high wave numbers justify the geometric optics approximation. Because of asymptotic freedom and because  $p_\omega$  is purely outgoing, we assume that  $p_\omega \sim e^{-i\omega u}$  for observers at sufficiently late times. For more details and motivations for the definitions and approach above, please consult [77, 113].

<sup>11</sup>The derivation is completely analogous to that of (7.2.17) or (7.3.26).

<sup>12</sup>i.e. the wave will travel along a null surface, see [113, Sec. 4.3].

Let  $\epsilon$  be small and positive. Then the vector  $-\epsilon\vec{n}^a$  connects  $x$  to a null surface of constant  $u$  and hence of constant phase of the wave  $p_\omega^{(2)}$ . At late times the geometry outside the collapsing body is (almost) isomorphic to a portion of extended Schwarzschild spacetime, by Birkhoff's theorem (see Section 3.1) [114]. We will exploit this isomorphism by looking at the analogous situation in extended Schwarzschild spacetime. A picture of the embedding of our actual spacetime into extended Schwarzschild spacetime is shown in figure 7.2. In this picture, the collapsing matter is shown in brown, other coloured lines are the same as in 7.1 and black and white hole horizons are labeled with “ $r = 2GM$ ”.

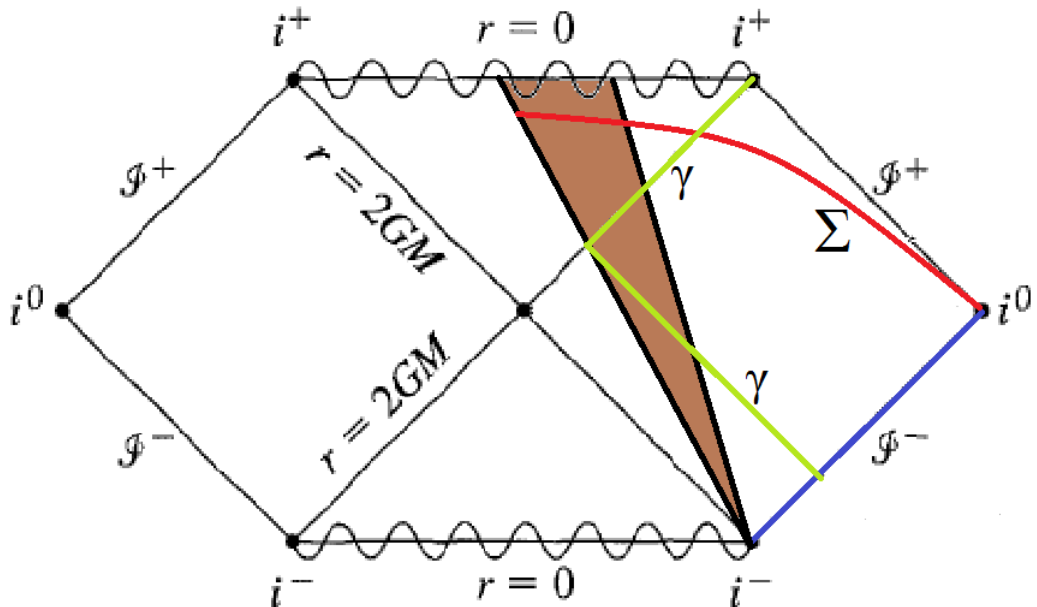


Figure 7.2: An embedding of 7.1 into extended Schwarzschild spacetime. Picture edited from 2.1.1.

We can parallelly transport the vector  $-\epsilon\vec{n}^a$  along the black hole horizon, until it lies along the white hole horizon. We note that  $-\epsilon\vec{n}^a$  will still connect a null surface of constant phase to the black hole horizon.

An affine parametrization of the white hole horizon is given by the Kruskal coordinate  $U = -e^{-\kappa u}$ . We can choose  $U$  to be zero at the intersection of black and white hole horizons. We now perform an affine re-parametrisation  $\lambda = CU$  (with  $C$  a positive constant), such that the length of  $\vec{n}^a$  with respect to  $\lambda$  is 1. We conclude that  $u = -\frac{\ln(\epsilon/C)}{\kappa}$ . It is clear that we now have that  $p_\omega \sim e^{i\left(\frac{\omega \ln(\epsilon/C)}{\kappa}\right)}$ . We conclude that  $-\epsilon\vec{n}^a$  connects the black hole horizon with the null surface of constant phase  $-\frac{\omega \ln(\epsilon/C)}{\kappa}$  of  $p_\omega^{(2)}$ .

We now return to the collapsing geometry, where the phase is still the same as above. We can parallelly transport the vector  $\vec{n}$  along  $\gamma$  until the begin of  $\gamma$  at  $v_0$ . It is clear that the vector  $\vec{n}^a$  will end up along  $\mathcal{J}^-$ . The affine parameter along the null geodesic generator of  $\mathcal{J}^-$  is in fact the incoming Eddington-Finkelstein coordinate  $v$ , so we can proceed as above to conclude that our null surface has constant phase

$$u\omega = -\frac{\omega \ln \left( \frac{v_0-v}{CD} \right)}{\kappa},$$

(with  $D$  a positive constant) for  $p_\omega^{(2)}$ , where  $v_0 - v$  is small and positive.

It follows<sup>13</sup> (see [77, 116]) from the above analysis, that for sufficiently large  $\omega'$  the following relation holds<sup>14</sup>

$$|\alpha_{\omega\omega'}^{(2)}| = \exp \left( \frac{\pi\omega}{\kappa} \right) |\beta_{\omega\omega'}^{(2)}|. \quad (7.4.17)$$

This is a situation that looks very much like the one encountered in the section on the Unruh effect.

### Derivation of black body radiation using wave packets

We demonstrate<sup>15</sup> how to use normalised wave packets to obtain that the Black hole radiates as a perfect black body at temperature  $\frac{\kappa}{2\pi}$ .

Define a wave packet  $p_{jn}$ , for positive integers  $j, n$  and  $0 < \epsilon \ll 1$ , by<sup>16</sup>

$$p_{jn} = \epsilon^{-\frac{1}{2}} \int_{j\epsilon}^{(j+1)\epsilon} e^{\frac{-2\pi i n \omega}{\epsilon}} p_\omega d\omega. \quad (7.4.18)$$

These wave packets have frequency  $\approx j\epsilon$ , width  $\approx \epsilon$  and are at outgoing Eddington-Finkelstein time  $u \approx 2\pi n \epsilon^{-1}$ . Expansion in terms of *in*-mode functions is straightforward:

$$p_{jn} = \int_0^\infty (\alpha_{j,n,\omega'} f_{\omega'} + \beta_{j,n,\omega'} \bar{f}_{\omega'}) d\omega', \quad (7.4.19)$$

where

$$\alpha_{j,n,\omega'} = \epsilon^{-\frac{1}{2}} \int_{j\epsilon}^{(j+1)\epsilon} e^{\frac{-2\pi i n \omega}{\epsilon}} \alpha_{\omega\omega'} d\omega \quad \text{etc.} \quad (7.4.20)$$

---

<sup>13</sup>We have to fill in our asymptotic approximation for  $p_\omega^{(2)}$  into (7.4.16) and then perform a computation analogous to the computation done for the Unruh effect, *cf.* (7.3.22), (7.3.23) and (7.3.25)

<sup>14</sup>In addition to this, asymptotic expressions (in the big  $\omega'$  limit) for  $\alpha_{\omega\omega'}^{(2)}$  and  $\beta_{\omega\omega'}^{(2)}$  can be given, *cf.* [77] eqns. (2.19) and (2.20). These expressions are analogous to (7.3.25).

<sup>15</sup>Following [77].

<sup>16</sup>This is in general a different  $\epsilon$  than the vector length above.

For sufficiently large  $n$  (*i.e.* at late outgoing Eddington-Finkelstein time) we can use the asymptotic expression for  $\alpha_{\omega,\omega'}^{(2)}$  to compute  $\alpha_{j,n,\omega'}$  (*cf.* [77], eqns. (2.19), (2.20) and (2.25)). In particular, we still have, for  $\omega := j\epsilon$

$$|\alpha_{j,n,\omega'}^{(2)}| = \exp\left(\frac{\pi\omega}{\kappa}\right) |\beta_{j,n,\omega'}^{(2)}|. \quad (7.4.21)$$

When we consider a *late* wave packet, we can trace it back into the past. The flux into the collapsing body will be given by

$$\Gamma_{jn} = \int_0^\infty (|\alpha_{j,n,\omega'}^{(2)}|^2 - |\beta_{j,n,\omega'}^{(2)}|^2) d\omega'. \quad (7.4.22)$$

The minus sign in front of  $|\beta_{j,n,\omega'}^{(2)}|^2$  appears because this term corresponds to a flux out of the collapsing matter. If we combine (7.4.21) and (7.4.22), we obtain

$$\begin{aligned} \Gamma_{jn} &= \int_0^\infty (|\alpha_{j,n,\omega'}^{(2)}|^2 - |\beta_{j,n,\omega'}^{(2)}|^2) d\omega' \\ &= \int_0^\infty (e^{\frac{2\pi\omega}{\kappa}} - 1) |\beta_{j,n,\omega'}^{(2)}|^2 d\omega' \\ &= (e^{\frac{2\pi\omega}{\kappa}} - 1) \int_0^\infty |\beta_{j,n,\omega'}^{(2)}|^2 d\omega' \end{aligned} \quad (7.4.23)$$

$$= (e^{\frac{2\pi\omega}{\kappa}} - 1) \langle 0_{in} | \hat{N}_{j,n}^{late(2)} | 0_{in} \rangle. \quad (7.4.24)$$

However, since there is no direct contribution from the *in*-vacuum to the *late* number operator expectation value, we have

$$\langle 0_{in} | \hat{N}_{j,n}^{late(2)} | 0_{in} \rangle = \langle 0_{in} | \hat{N}_{j,n}^{late} | 0_{in} \rangle.$$

Another observation is that the part of the *late* wave packet that enters the collapsing matter is almost the same as the part that would have entered the white hole in the extended Schwarzschild spacetime, which is the same as the part of an incoming wave packet that would enter the black hole (in extended Schwarzschild spacetime), by time reversal symmetry. This means that we can identify  $\Gamma_{jn}$  with the absorption cross section of the black hole, so, using (7.4.24), we obtain our conclusion: at asymptotically late times, the black hole emits Planckian radiation of temperature  $\frac{\kappa}{2\pi}$ .

### 7.4.3 The Hawking effect for a Collapse to a Kerr(-Newman) Black Hole

There is also a Hawking effect for collapses to black holes that have non-zero charge or angular momentum. The derivations are essentially the same [77]. The two main changes

in the results are that the surface gravity  $\kappa$  will be different (see appendix A.4 and section 5.1) and that the frequency  $\omega$  will be shifted. For (massless, scalar) fields that are *not charged*, we have to replace

$$\omega \rightarrow \omega - m\Omega,$$

in (7.4.24), where  $m$  is the axial quantum number and  $\Omega$  the black hole angular momentum. We note that the Hawking radiation will decrease the net angular momentum of the black hole, since for a fixed  $\omega$ , more particles will be emitted if  $m$  and  $\Omega$  carry the same sign, as opposed to if they carry a different sign. Conservation of angular momentum will now dictate that  $\Omega$  will go to 0. We also note that if  $\omega - m\Omega < 0$ , then  $(e^{\frac{2\pi}{\kappa}(\omega-m\Omega)} - 1) < 0$ . This is no cause for concern, since by the area theorem (see section 5.3), the absorption cross-section of the black hole will also be negative for modes like this. This classical effect is called ‘‘superradiant scattering’’ and was already encountered in section 2.4. Hence, even for  $\omega < m\Omega$ , the amount of particles observed far away remains positive [77].

If the fields are *charged*, we have to replace

$$\omega \rightarrow \omega - m\Omega - e\Phi,$$

in (7.4.24), where  $e$  is the charge of the wave packet and  $\Phi$  is the electrostatic potential of the black hole [77]. By the same arguments as above, the charge of the black hole will go to 0 and the area theorem guarantees that the far away observer will encounter a positive flux of particles.

#### 7.4.4 Physical aspects of Black hole emission

At first sight, black hole radiance seems paradoxical, for nothing can apparently escape from within the event horizon. However, inspection of the radiation spectrum shows that the average wavelength of the emitted quanta is  $\sim M$ , *i.e.*, comparable with the size of the hole. As it is not possible to localize a quantum to within one wavelength, it is therefore meaningless to trace the origin of the particles to any particular region near the horizon. The particle concept, which is basically global, is only useful near  $j^+$ . In the vicinity of the hole, the spacetime curvature is comparable with the radiation wavelength in the energy range of interest, and the concept of locally-defined particles breaks down.

Heuristically, one can envisage the emergent quanta as ‘tunnelling’ out through the event horizon. Alternatively, the continuous, spontaneous creation of virtual particle-antiparticle pairs around the black hole can be used to explain the Hawking radiation. Virtual particle

pairs created with wavelength  $\lambda$  separate temporarily to a distance  $\simeq \lambda$ . For  $\lambda \sim M$ , the size of the hole, strong tidal forces operate to prevent re-annihilation. One particle escapes to infinity with positive energy to contribute to the Hawking flux, while its corresponding antiparticle enters the black hole trapped by the deep gravitational potential well on a timelike path of negative energy relative to infinity. Thus the hole radiates quanta with wavelength  $\simeq M$ . For charged black hole, Schwinger-pair production was proposed to produce particles in a strong electric field.

In spite of the ill-defined nature of particles near the horizon, it is clear that the thermal emission will carry away energy to  $j^+$ , and the question arises as to what is the source of this energy. It can only come from the gravitational field itself, which must lose mass as a consequence. To study this steady depletion of mass-energy, we can investigate the stress-tensor expectation value,  $\langle T_{\mu\nu}(x) \rangle$ , in the vicinity of the hole. Unlike the particle concept, the stress-tensor is a local object, and hence may be used to probe the physics close to, and within, the black hole itself.

The collapsing process has already been treated in section 3.3. For simplicity,  $1 + 1$  dimension is considered. And the construction of stress-tensor basically follows Chapter 6 of Birrell and Davies's book [111]. Here we consider a freely-falling observer with two-velocity  $\bar{C}^{-\frac{1}{2}}(1, 0)$ .  $\bar{C}$  is the conformal factor in Kruskal coordinates and is given by

$$\bar{C} = 2Mr^{-1}e^{-r/2M}. \quad (7.4.25)$$

Using Kruskal coordinates to compute the energy density measured by the observer

$$\bar{C} \langle 0 | \hat{T}_{tt}(x) | 0 \rangle = \langle 0 | \hat{T}_{\bar{u}}^{\bar{v}} + \hat{T}_{\bar{v}}^{\bar{u}} + 2\hat{T}_{\bar{u}}^{\bar{u}} | 0 \rangle, \quad (7.4.26)$$

where

$$\langle 0 | \hat{T}_{\bar{u}}^{\bar{v}} | 0 \rangle = \frac{(24\pi)^{-1}(\bar{v})^2 e^{-r/2M}}{8Mr} \left( 1 + \frac{4M}{r} + \frac{12M^2}{r^2} \right), \quad (7.4.27)$$

$$\langle 0 | \hat{T}_{\bar{v}}^{\bar{u}} | 0 \rangle = \frac{(24\pi)^{-1} e^{r/2M}}{\bar{v}^2} \left( \frac{1}{r^2} - \frac{3M}{2r^3} \right), \quad (7.4.28)$$

$$\langle 0 | \hat{T}_{\bar{u}}^{\bar{u}} | 0 \rangle = -\frac{R}{48\pi} = -\frac{M}{12\pi r^3}. \quad (7.4.29)$$

It is clear that for a free-falling observer near the event horizon, the energy density is finite as  $\bar{u} \rightarrow \infty$ , because  $\bar{v}$  remains finite on the future horizon. Hence we conclude that an observer who crosses the event horizon along a constant Kruskal position line measures a finite energy density.

These considerations resolve an apparent paradox concerning the Hawking effect. The proper time for a freely-falling observer to reach the event horizon from a finite distance

is finite, yet the time as measured at infinity is infinite. Ignoring back-reaction, the black hole will emit an infinite amount of radiation during the time that the falling observer is seen, from a distance, to reach the event horizon. Hence it would appear, that in the falling frame, the observer should encounter an infinite amount of radiation in a finite time, and so be destroyed. On the other hand, the event horizon is a global construct, and has no local significance, so it is absurd to conclude that it acts as a physical barrier to the falling observer.

The paradox is resolved when a careful distinction is made between particle number and energy density. When the observer approaches the horizon, the notion of a well-defined particle number loses its meaning at the wavelengths of interest in the Hawking radiation since the observer is ‘inside’ the particles. We need not, therefore, worry about the observer encountering an infinite quantity of particles. On the other hand, energy does have a local significance. In this case, however, although the Hawking flux does diverge as the horizon is approached, so does the static vacuum polarization, and the latter is negative. The falling observer cannot distinguish operationally between the energy flux due to the oncoming Hawking radiation and that due to the fact that he is sweeping through the cloud of vacuum polarization. The net effect is to cancel the divergence on the event horizon, and yield a finite result.

The present analysis also solves the mystery of how the black hole can lose mass without matter crossing from the interior of the black hole into the outside universe. Inspection of  $\langle 0 | \hat{T}_{vv}(x) | 0 \rangle = -\frac{\kappa^2}{48\pi}$  at the event horizon shows that it is negative and equal to minus the Hawking flux at infinity. This is necessarily true because covariant conservation was built into the construction of  $\langle T_{\mu\nu} \rangle$ . As  $\langle T_{vv} \rangle$  represents a null flux crossing the event horizon, one can see that the steady loss of mass-energy by the Hawking flux is balanced by an equal negative energy flux crossing into the black hole from outside. The hole therefore loses mass, not by emitting quanta, but by absorbing negative energy.

In the above analysis, we have assumed that the quantum state is the conventional vacuum state in the in-region. One might wonder to what extent the presence of initial quanta will change the Hawking effect. The form of the outgoing modes in the out region is given by  $U = -e^{-\kappa u}$ , from which one readily sees that the effect of initial quanta fades out exponentially on the same timescale as any surface luminosity, and the black hole soon settles down to thermal equilibrium, having ‘forgotten’ the details of the initial state. We may therefore conclude that the Hawking effect is extremely general, and independent of any physically reasonable initial quantum state. This conclusion is consistent with the statement by Hawking that how a black hole collapses does not effect Hawking radiation.

The above discussion about black hole radiance persists in the full four-dimensional treatment. Now we go into evolution of black hole due to Hawking radiation, which might offer some observational effects.

### 7.4.5 Evolution of black holes

As already discussed in Chapter 5, Hawking radiation provides a strong connection between black holes and thermodynamics. We might ask how a black hole evolves in an ideal environment, that's to say, nothing surrounds the black hole. The following part presents some features of the evolution of a black hole as a thermodynamical object.

Since for Schwarzschild black holes with  $T \sim 1/M$ , they have a negative specific heat: they get hotter while radiating. As the black hole is evaporating, the back-reaction effect, which is ignored while deriving Hawking radiation, might become important and is not negligible. As a consequence of back-reaction, the horizon evolution equation is nonlinear, which makes it difficult to predict the final state of black hole evaporation.

In Chapter 5, it was proved that the surface gravity cannot become zero by Hawking radiation according to the third law of black hole dynamics. It has been conjectured that the end result of the Hawking evaporation process is an explosive disappearance, a naked singularity, or perhaps a Planck mass object. Whatever the outcome, the detailed behavior of the hole in the final stages will depend on the nature of subatomic particles at high energies. For example, if there are a small number of truly elementary particles, then the emission rate does not escalate as fast as if the number of particles species rises rapidly at high masses, suggested by Hagedorn [117]. These could affect the observational consequences. Thus a study of black hole evaporation could provide a unique opportunity for us to probe the physics of ultra-high energy particles.

Now we present some implications of Hawking radiation. During the final tenth of a second of its life, a black hole will emit in excess of  $10^{30}$  ergs, or the equivalent of  $10^6$  megaton thermonuclear bombs, a significant fraction of which will be in the form of  $\gamma$ -radiation. The fact that such bursts have not been detected with current equipment enables an upper limit to be placed on the black hole explosion rate of about  $10^{-5} \text{ pc}^{-3} \text{ yr}^{-1}$ .

Another interesting feature of black holes is that the quantum black hole enables some of the laws of particle physics to be transcended. In spite of the fact that a quantum black hole creates elementary particles and antiparticles in pairs, some of the subatomic

conservation laws are violated. For example, a hole that forms from the collapse of a star swallows up mainly baryons, but emits mainly neutrinos and photons, as for the greater part of its life its temperature is too low for massive particle emission. Thus, the law of baryon number conservation is transcended. Another example discussed by Hawking [118] is  $\mu^\pm \rightarrow \text{black hole} \rightarrow e^\pm + \gamma$ , which is otherwise forbidden by conservation of muon lepton number.

It is possible to develop a complete theory of black hole thermodynamics including features such as phase transitions, Carnot cycles, stability analysis, etc, and even extend the theory to non-equilibrium situations. Some problems remain, however: What is the relation between information loss due to the imploded star and the internal microstates of an eternal black hole, such as described by the Kruskal solution that is everywhere a vacuum solution of Einstein's equation? Can the notion of black hole entropy be extended to arbitrary gravitational fields? Will Hawking radiation always be precisely thermal, even in the presence of interactions and recoil of the hole? Does the Hawking process imply time-reversal symmetry violation in quantum gravity? Many of these questions are still under active investigation. The following part will treat one of the greatest mysteries of black holes.

## 7.5 Information Loss Paradox

### 7.5.1 The Paradox

We saw in 5.5 that we can treat black holes as thermodynamic systems and assign entropy to them. For convenience we reprint eq (7.4.4) here,

$$S_{BH} = \frac{k_B c^3}{4\hbar G} A. \quad (7.5.1)$$

Although this thermodynamic quantity is a little awkward to interpret, in 5.5.2 we chose to view it as a measure of the inaccessibility of information on the internal configuration. From the point of view of statistical mechanics it counts the number of (internal) microstates, but since these are hidden from us due to the lack of hair<sup>17</sup> on a black hole we assume entropy tells us how much information is unknown to us. The fact that this information is inaccessible to and that the nature of the underlying microstates is unknown to us does not, in principle, pose an insurmountable problem. However, a far worse problem appears when

---

<sup>17</sup>See Chapter 4 for more details.

we try to reconcile this notion of a black hole carrying information with the phenomenon of Hawking Radiation described earlier in this chapter.

Hawking's calculations show that the spectrum of particles radiated by a black hole is exactly thermal. This distribution of outgoing particles is insensitive to the internal state of the black hole or, more importantly, the initial state of whatever body that collapsed to form the hole. As the black hole evaporates its area will decrease and along with it the amount of information contained within, according to (7.5.1). If we wait long enough for the black hole to evaporate all that remains are thermal spectra, we have lost all information about the initial state of the collapsing body.

Information is constantly lost as entropy increases in the universe. Indeed, a gas that initially only occupies half of the volume of its container and expands to fill the entire container increases its entropy. So why should we be surprised that information is lost when a black hole evaporates?

The point is that information on the initial state of an expanding gas only lost *in practice*. If we were able to measure the microstate of the expanded gas to sufficient accuracy we could recover the initial state by applying Newton's laws backwards in time. Unlike the individual gas particles, thermal spectra radiated by a black hole do not carry any information about the initial state of the collapsing body and the information is lost *in principle*.

We can emphasize this point by stating the paradox more sharply. In our current understanding of quantum mechanics the time evolution operator  $\exp(i\hat{H}t/\hbar)$  is a unitary operator from the Hilbert space  $\mathcal{H}$  to itself. Unitarity of the time evolution operator implies that if we know the precise quantum state  $|\psi(t_0)\rangle$  at some time  $t_0$  then we know this state for all  $t$  by the appropriate time evolution.

We remind the reader that a general state can be described by a density matrix

$$\hat{\rho} = \sum_i c_i |\psi_i\rangle \langle \psi_i|, \quad \text{where } |\psi_i\rangle \in \mathcal{H}, c_i \in \mathbb{C} \text{ and } \text{Tr}(\hat{\rho}) = 1. \quad (7.5.2)$$

States described by these density matrices are pure if  $\hat{\rho}^2 = \hat{\rho}$  (or equivalently  $\text{Tr}(\hat{\rho}^2) = 1$ ) and are otherwise mixed<sup>18</sup> (then  $\text{Tr}(\hat{\rho}^2) < 1$ ). A density matrix describing a pure state can be written as  $\hat{\rho}_\phi = |\phi\rangle \langle \phi|$ , where  $|\phi\rangle$  is a vector in  $\mathcal{H}$ . The same is not possible for

---

<sup>18</sup>Mixed states differ subtly from a superposition of pure states; consider for example a two-state Hilbert space  $\mathcal{H} = \{|\psi_1\rangle, |\psi_2\rangle\}$  and the two density matrices  $\hat{\rho}_1 = \frac{1}{2}(|\psi_1\rangle \langle \psi_1| + |\psi_2\rangle \langle \psi_2|)$  and  $\hat{\rho}_2 = |\phi\rangle \langle \phi|$  for the superposition  $|\phi\rangle = \frac{1}{\sqrt{2}}(|\psi_1\rangle + |\psi_2\rangle)$ . We leave it as an exercise to the reader to show the first represents a mixed state while the second represents a pure state.

mixed states because a mixed state represents a statistical ensemble of quantum states in  $\mathcal{H}$ , which itself is not a state vector.

In the language of density matrices the paradox states that the initially pure state quantum of the collapsing has evolved into an mixed state of radiation with a thermal spectrum [119, 120], thereby leaving the Hilbert space  $\mathcal{H}$  entirely! This fact is impossible to reconcile with a time evolution operator that is unitary as such an operator will always evolve a pure state to a pure state.

In going from a pure state to a mixed state we have lost the ability to evolve back in time in the conventional manner, in a sense the mixed state does not contain all the information necessary to do so. The paradox invites us to explain where this information has gone or otherwise come up with a scheme that preserves unitarity. To date satisfying explanation has yet been found that can fully account for this, although many attempts have been made. If we stay within the framework of semiclassical quantization there are, roughly speaking, three responses to this paradox.

- The information did actually come out with the radiation.
- The information stays in the black hole.
- The information goes somewhere else, but is not lost.

We will give a brief overview of several attempts, as well as some of the problems they encounter, following the example of [121] for 7.5.2 through 7.5.4. We will be grossly oversimplifying matters as a thorough discussion is well beyond the scope of this chapter.

### 7.5.2 Information Comes Out With the Radiation

A pragmatic physicist might draw a comparison with setting fire to a book. The chemical reactions by which the book burns are governed by the laws of quantum mechanics under an appropriately complex Hamiltonian and so time evolution should be unitary. The initially pure state of the unburnt book will evolve to a ground state of smoke and ash, plus a thermal spectrum of radiation. The information contained in the book is not lost as the radiation state will be entangled with the states of the smoke and ash. This entanglement precisely encodes the information we are “missing” and ensures that the final state is still pure.

While it is prohibitively difficult to recover the contents of the book, by measuring the quantum state of the system at any point during or after the burning process to sufficient accuracy should in principle allow us to reconstruct the entire text. Why should things be any different when instead of setting the book on fire, we throw it into a black hole? If we suppose that the process of the book falling into a black hole and being radiated away is unitary, then we should be able to apply the same logic. We argue that, since Hawking radiation is all that remains once the black hole has evaporate, the information must be contained in entanglement between radiation quanta emitted at different times [121].

This means that particles emitted earlier during evaporation must be carry information about the internal state of the black hole in order for them to be entangled to particles emitted some time later. This goes against the no hair theorems from Chapter 4, which state that no information other than the black hole's mass, charge and angular momentum is accessible to outside observers.

However if no such information is carried by the earlier quanta then violation of causality is required to induce the desired correlations when the later quanta are emitted to transport the information.

Should we want to keep our no hair theorems and preserve causality we must conclude that no information ever entered the black hole in the first place. Some mechanism must erase the pages of the book before it reaches the horizon and somehow store this information outside the horizon before radiating it away [120]. Such a process seems unlikely as there is nothing special about the horizon locally.

### 7.5.3 Information Stays in the Black Hole

If a black hole does carry information and the view that it comes out with the emitted radiation is untenable, then perhaps the information simply stays in a black hole. Hawking's calculations tell us that the black hole must continue to evaporate within the semiclassical regime down to the Planck scale, at which point our understand of quantum theory breaks down. The idea proposed is that some quantum gravity effect could stop the black hole from evaporating, leaving behind a stable black hole remnant (with mass of order  $M_{Planck}$ ) that contains all the information about the collapsing body.

There is no upper limit to the size of the original body that collapsed to form the black hole. By eq. (7.5.1) it follows we must be able to store an arbitrary amount of information

in a black hole remnant. 't Hooft argues in [122] that we can construct such a Planck-scale, non-radiating remnant as a “particle” for which the density of states is infinite. However the contributions of such infinitely degenerate particles to the graviton propagator and scattering amplitudes become divergent.

Essentially, if the remnants couple to the gravitational field in the usual way, the theory admits creation of pairs of such remnants whenever a Planck-scale amount of energy is available [120]. Even if this probability is tiny the total rate will still diverge on account of the infinite density of states.

However it is perhaps presumptuous of us to treat such Planck-scale objects using our understanding of physics on a much larger scale and we should not dismiss the possibility of stable remnants out of hand. Yet since these objects will be governed by physics unknown to us at the present we cannot really know what will happen until such a theory is found.

#### 7.5.4 Information Goes Somewhere Else

It seems that neither putting the information in the radiation, nor hiding it in a stable black hole remnant can resolve the paradox. There is a third, rather poetic alternative that says that a collapsing body does not form a true singularity inside the black hole. Rather, much like a droplet falling on a flat surface of water causes a backjet to jump up, the collapse creates a closed “baby universe” separate from our own that carries away the collapsing matter and with it the information. For all intents and purposes the information is lost to observers in our universe as the baby universe is causally disconnected from ours, but in the context of a quantum mechanical multiverse the information is still available to a “superobserver” that has access to both universes [123, 124].

Yet this explanation is still not entirely satisfactory as we cannot hope to retrieve the information for ourselves, nor does it describe the mechanism by which this new universe nucleates and carries away the information. We would also be tasked with proving such baby universes exist, but this is impossible to do as they are unobservable to us. In the end this point of view amounts to little more than explaining away the problem and invites us to invoke Ockham’s razor as it adds very little to our understanding but presupposes much.

### 7.5.5 Outlook

Despite ongoing efforts to resolve the Information Loss Paradox, no satisfactory solution has yet been found. While a discussion of the more advanced attempts is beyond the scope of this work, we would like to point the interested reader towards Black Hole Complementarity, a solution proposed by Susskind et al [125] and 't Hooft [126].

This proposal spawned a further paradox known as the Firewall Paradox described by Almheiri et al [127]. The discussion is still ongoing with publications as recent as January 2014 by Hawking [128], where it is questioned whether true singularities and horizons occur at all.

Perhaps the paradox is simply a feature inherent to the semiclassical picture and is a sign that it does not provide a complete description of physics involved. It has been suggested that to fully resolve the paradox we must quantize gravity as well.

This is a task easier said than done as there are many obstacles that have so far prevented a successful quantum theory of gravity from emerging.

To highlight some of the difficulties involved, consider a quantization scheme where we start by promoting the metric  $g_{\mu\nu}$  to an operator  $\hat{g}_{\mu\nu}$  and in first instance require that

$$[\hat{g}_{\mu\nu}(x), \hat{g}_{\rho\sigma}(x')] = 0, \quad (7.5.3)$$

for  $x$  and  $x'$  spacelike related, in analogy to the procedure that we apply to quantize ordinary fields. However, the interpretation of this quantization requirement remains obscure. We cannot say which points are spacelike related prior to measuring  $g$ , yet at the same time (7.5.3) is an operator equation that should hold regardless of the state or distribution of the metric [113]. The notion of causality loses its meaning if we treat the metric nonclassically and it is not obvious how to apply a proper quantization procedure.

Alternatively we might try to treat quantization perturbatively by writing

$$g_{\mu\nu} = \eta_{\mu\nu} + \gamma_{\mu\nu}, \quad (7.5.4)$$

where  $\eta_{\mu\nu}$  is the Minkowski spacetime metric (treated classically) and  $\gamma_{\mu\nu}$  is a quantum correction that encodes interaction of a spin-2 field of gravitons. In this scheme it is possible to obtain formal power series expansions for physical observables. Unfortunately, Feynman diagrams associated with the interaction of two or more gravitons will diverge. The degree of divergence increases as the order of perturbation goes up, meaning a perturbative theory of quantum gravity is non-renormalizable.

It is clear that the information paradox remains a difficult problem to tackle. As black holes are some of the more extreme objects in the universe it is not surprising that it is a hard problem. The difficulty is compounded by our obvious lack of experimental capabilities, restricting all work to the theoretical domain. Whatever new ideas will eventually resolve the paradox, the road to reaching a satisfying conclusion is already paved with interesting new physics and is bound to produce even more.

# Appendix A

## A.1 Varying the Einstein-Hilbert Action

The Einstein equation can be derived from the Euler-Lagrange equation of the Einstein-Hilbert action. The convention used for the cosmological constant in the Einstein-Hilbert action restricts ergo the convention of the cosmological constant in the Einstein equation. Choose the cosmological constant factor such that the Einstein-Hilbert action reads

$$S_{\text{EH}} := \int \sqrt{-g}(R - \Lambda) \quad (\text{A.1.1})$$

with  $g$  the determinant of the metric tensor,  $R$  the Ricci scalar and  $\Lambda$  the cosmological constant. What is the corresponding Euler-Lagrange equation? Coupling this action to matter<sup>1</sup> and varying the action gives

$$0 = \delta S_{\text{matter}} + \frac{1}{2} \delta S_{\text{EH}} = \delta S_{\text{matter}} + \frac{1}{2} \int ((R - \Lambda)\delta\sqrt{-g} + \sqrt{-g}\delta R) \quad (\text{A.1.2})$$

Remember that

$$\delta\sqrt{-g} = -\frac{1}{2}\sqrt{-g}g_{\mu\nu}\delta g^{\mu\nu} \quad (\text{A.1.3})$$

$$\delta R = \delta(R_{\mu\nu}g^{\mu\nu}) = R_{\mu\nu}\delta g^{\mu\nu} + \text{some total derivative term} \quad (\text{A.1.4})$$

$$T_{\mu\nu} = -\frac{2}{\sqrt{-g}}\frac{\delta S_m}{\delta g^{\mu\nu}} \quad (\text{A.1.5})$$

Putting the identities together and setting the variation at the boundary to zero, we find that

$$0 = \delta S_{\text{matter}} + \delta S_{\text{EH}} = \frac{1}{2} \int \sqrt{-g} \left( -T_{\mu\nu} + R_{\mu\nu} - \frac{1}{2}(R - \Lambda)g_{\mu\nu} \right) \delta g^{\mu\nu} \quad (\text{A.1.6})$$

---

<sup>1</sup>In literature the coupling factor is often chosen to be  $\frac{1}{16\pi}$  instead of  $\frac{1}{2}$ . In this book we chose  $\frac{1}{2}$  to drop the  $8\pi$  factor from the Einstein equation for simplicity.

We conclude that the corresponding Euler-Lagrange equation reads

$$R_{\mu\nu} - \frac{1}{2}Rg_{\mu\nu} + \frac{1}{2}\Lambda g_{\mu\nu} = T_{\mu\nu}. \quad (\text{A.1.7})$$

This will be our convention for the Einstein equation throughout the book.

## A.2 Properties of the Metric Tensor in Asymptotically Flat Black Hole Exterior.

We have chosen a coordinate system where the time component of any asymptotic flat metric which admits a black hole solution becomes  $g_{00} = -1$  at spacial infinity. This  $g_{00}$  is the square of the Killing vector responsible for time translations in our static geometry. Should no singularities be present then the invariant  $g_{00}$  is continuous in the black hole exterior. This value will never become positive at any given point of the exterior.

Assume that a surface that allows the sign change from negative to positive in the exterior exists. This would allow for the existence of a surface which admits  $g_{00} = 0$ . It cannot extend itself to infinity (where  $g_{00} = -1$ ) so it must either close in on itself surrounding a region exterior to the horizon, or it will intersect with the horizon and close in on itself outside of it, or close about the horizon. It cannot remain an open surface because of the opposite signs of  $g_{00}$  on either side.

A proof exists that states that any  $g_{00} = 0$  surface of a static metric is always null [129]. This means our surface is null. In addition it is non-singular by hypothesis so it corresponds to the horizon or at the very least part of it. It is then clear that  $g_{00} < 0$  in the exterior except for a possible isolated surface which has  $g_{00}$  negative on either side and zero somewhere in between (so that it could be an open surface). In any case  $g_{00} \leq 0$  on and outside the horizon. When  $g_{00} \leq 0$  a static coordinate system such as ours is realizable with test particles or photons, and so the spatial distance  $dl$  between two given points separated by the coordinate interval  $dx^i$  is well defined as

$$dl^2 = g_{ij}dx^i dx^j.$$

It's quite clear that  $g_{ij}$  is a positive definite matrix except on the horizon, since it is a null there according to

$$g_{ij}dS^i dS^j = 0,$$

and therefore it is positive semi-definite only. So for an arbitrary real number  $\lambda$  and real  $b^i$  and  $dS^i$ ,

$$g_{ij}(dS^i + \lambda b^i)(dS^j + \lambda b^j) \geq 0.$$

Should we pick  $\lambda = -g_{ij}dS^i b^j / (g_{ij}b^i b^j)$  (providing that the denominator does not vanish), we arrive at the Schwarz inequality:

$$(g_{ij}dS^i b^j)^2 \leq (g_{ij}dS^i dS^j)(g_{nm}b^n b^m).$$

### A.3 Tetrads and Spinors in Curved Spacetime

As it is known, a (Pseudo)Riemannian manifold  $\mathcal{M}$  is *locally* Euclidean. We can exploit this property and define a family of inertial observers at each point of the space time. Each one of them will be carrying their own coordinate system. Mathematically, we postulate a coordinate chart independent orthogonal basis of vector  $e^a(x)$  of  $T_{P(x)}\mathcal{M}$ .

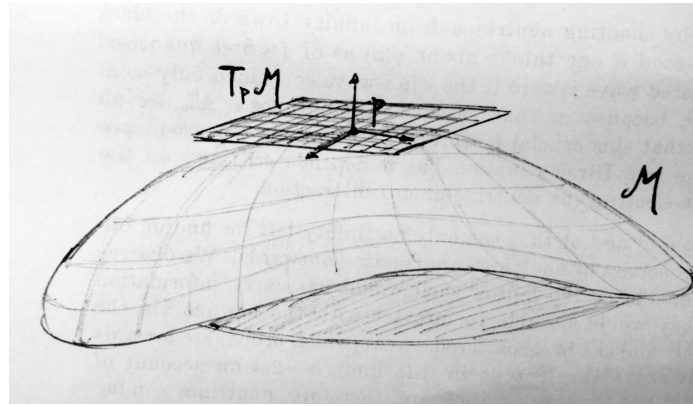


Figure A.1: Picture used with the kind courtesy of Bruno Rodrigues.

In a local frame  $\{x^\mu\}$  point of view, we have of course  $e^a(x) = e_\mu^a(x)dx^\mu$  where the coefficients are called **tetrads**, **vierbeins** or **frame fields**.

Orthogonality is meant in the Minkowski sense. Namely,

$$e_\mu^a(x)g^{\mu\nu}(x)e_\nu^b(x) = \eta^{ab} \quad (\text{A.3.1})$$

It's natural to interpret the Latin indices as Local Lorentz or "flat" while the Greek ones label the general spacetime coordinates. Assuming inversability<sup>2</sup> for the  $d \times d$  matrices

---

<sup>2</sup>This simply amounts to  $\det g \neq 0$ .

$e_\mu^a(x)$ , namely  $e_\mu^a e_\nu^\mu = \delta_\nu^a$  and  $e_\mu^\mu e_\nu^a = \delta_\nu^a$ , we invert (A.3.1)

$$g_{\mu\nu}(x) = e_\mu^a(x) \eta_{ab} e_\nu^b(x). \quad (\text{A.3.2})$$

This relation is the cornerstone of the following discussion. First of all, it denotes the conversion from a local Minkowski spacetime to a curved one and vice versa with the use of the frame fields. The index structure of  $e_\mu^a$  is further justified by its transformation laws:

- Under a general coordinate transformation(GCT),  $g'_{\mu\nu}(x') = \frac{\partial x^\lambda}{\partial x'^\mu} \frac{\partial x^\rho}{\partial x'^\nu} g_{\lambda\rho}(x)$  induces

$$e'_\mu^a(x') = \frac{\partial x^\nu}{\partial x'^\mu} e_\nu^a(x).$$

Therefore the Greek indices stand for  $GL[d, \mathbb{R}]$  transformations as usual.

- The freedom to jump from one local Lorentz observer to the other encloses a Local Lorentz Symmetry

$$e'_\mu^a(x) = (\Lambda^{-1})_b^a(x) e_\mu^b(x).$$

Note that(A.3.2) stays invariant under the above *Local Lorentz Transformation*(LLT).

So the Latin indices correspond to  $SO(d - 1, 1)$  gauge transformations.

These new “toys” we just defined can help us transform from general coordinate system to local ones. More explicitly, an arbitrary vector  $V$  can be expressed in the tetrad basis as  $V = V_a(x)e^a = V_a(x)e_\mu^a(x)dx^\mu$  while in coordinate basis  $V = V_\mu(x)dx^\mu$ , thus yielding the law  $V_\mu(x) = e_\mu^a(x)V_a(x)$  and its inverse  $V_a(x) = e_\mu^a(x)V_\mu(x)$ . In addition, we can also construct GCT and LLT scalars by contracting the proper indices of the quantities at hand.

It is accustomed to say that from (A.3.2) the frame fields are the “square root” of the metric. That’s true since after diagonalisation we can solve for  $e_\mu^a$  in terms of  $g_{\mu\nu}$ . We are inevitably tempted to ask if the inverse is possible. Can we build the spacetime from the frame fields? The answer is yes with a subtlety regarding the degrees of freedom. In particular, the metric has  $\frac{d(d+1)}{2}$  components whereas  $e_\mu^a(x)$  has  $d^2$  which after the help of the  $SO(d - 1, 1)$  internal symmetry agrees with the metric. This establishes the Cartan formalism of General Relativity.

From now on the Local Lorentz Symmetry should be carried in every calculation. We will not get into full detail of how we can construct formally this gauge theory but will mention the basic elements.<sup>3</sup>

---

<sup>3</sup>A physicist-friendly presentation can be found in *Supergravity* by Freedman and Van Proeyen.

As it is always the case with having a gauge symmetry, we have to introduce a connection to remedy the non-local Lorentz invariance of the exterior derivative  $dX^a$ . we define an enhanced exterior derivative

$$DX^a = dX^a + \omega_b^a \wedge X^b.$$

The new object  $\omega^{ab}$  is a 2-form called **Spin Connection**. In a coordinate basis this is translated to

$$D_\mu X^a = \partial_\mu X^a + \omega_{\mu b}^a X^b.$$

Demanding the new 1-form to transform as a LLT vector we deduce the transformation law for the spin connection

$$\omega'_b^a = (\Lambda^{-1})_d^a \omega_c^d \Lambda_b^c - \Lambda_b^c (d\Lambda^{-1})_c^a. \quad (\text{A.3.3})$$

The resemblance of  $\omega_b^a$  to a gauge field is most compelling now<sup>4</sup>.

Now we turn on the general coordinate indices. Once again, diffeomorphism invariance asks for an affine connection  $\Gamma$ . The induced covariant derivative  $\nabla$  acts as

$$\nabla_\mu X^\nu = \partial_\mu X^\nu + \Gamma_{\mu\rho}^\nu X^\rho.$$

This is an LLT scalar so it can only be obtained as

$$\begin{aligned} \nabla_\mu X^\nu &\equiv e_a^\nu D_\mu X^a = e_a^\nu [\partial_\mu X^a + \omega_{\mu b}^a X^b] \\ &= e_a^\nu \partial_\mu X^a + e_a^\nu \omega_{\mu b}^a X^b \\ &= e_a^\nu \partial_\mu (e_\lambda^a X^\lambda) + e_a^\nu \omega_{\mu b}^a e_\lambda^b X^\lambda \\ &= e_a^\nu e_\lambda^a \partial_\mu X^\lambda + e_a^\nu (\partial_\mu e_\lambda^a) X^\lambda + e_a^\nu \omega_{\mu b}^a e_\lambda^b X^\lambda \\ &= \partial_\mu X^\nu + e_a^\nu (\partial_\mu e_\lambda^a + \omega_{\mu b}^a e_\lambda^b) X^\lambda \end{aligned}$$

But on the other hand,  $\nabla_\mu X^\nu = \partial_\mu X^\nu + \Gamma_{\mu\lambda}^\nu X^\lambda$ . We just discovered a relation between the affine and spin connection

$$\Gamma_{\mu\lambda}^\nu = e_a^\nu (\partial_\mu e_\lambda^a + \omega_{\mu b}^a e_\lambda^b)$$

or written differently as

$$\partial_\mu e_\nu^a + \omega_{\mu b}^a e_\nu^b - \Gamma_{\mu\nu}^\sigma e_\sigma^a = 0$$

This is called the **Vielbein Postulate** and it means basically that  $\nabla_\mu e_\nu^a = 0$ . We can extend the covariant derivative to act also on d-forms with general coordinate dependence. For instance,

$$\nabla_\mu X_\nu^{ab} = e_\nu^C D_\mu X_c^{ab} = e_\nu^c (\partial_\mu X_c^{ab} + \omega_{\mu d}^a X_c^{db} + \omega_{\mu d}^b X_c^{ad} - \omega_{\mu c}^d X_d^{ab}) =$$

---

<sup>4</sup>The analysis can be paved almost in the same lines as in the Yang-Mills theories.

$$\begin{aligned}
&= \partial_\mu X_\nu^{ab} - X_c^{ab} \partial_\mu e_\nu^c + e_\nu^c (\omega_{\mu d}^a X_c^{db} + \omega_{\mu d}^b X_c^{ad} - \omega_{\mu c}^d X_d^{ab}) = \\
&= \partial_\mu X_\nu^{ab} - X_c^{ab} [-\omega_{\mu d}^c e_\nu^d + \Gamma_{\mu\nu}^\sigma e_\sigma^c] + e_\nu^c (\omega_{\mu d}^a X_c^{db} + \omega_{\mu d}^b X_c^{ad} - \omega_{\mu c}^d X_d^{ab}) = \\
&= \partial_\mu X_\nu^{ab} + \Gamma_{\mu\nu}^\sigma X_\sigma^{ab} + \omega_{\mu d}^a X_\nu^{db} + \omega_{\mu d}^b X_\nu^{ad}
\end{aligned}$$

where we used a partial differentiation and the vielbein postulate.

From standard General Relativity we know that we can fully determine the affine connection if it is metric compatible and torsion-free. Let us impose the former

$$\begin{aligned}
\nabla_\rho g_{\mu\nu} = 0 &\implies \nabla_\mu (e_\nu^a e_\rho^b \eta_{ab}) = 0 \\
&\implies e_\nu^a e_\rho^b D_\mu \eta_{ab} = 0 \\
&\implies e_\nu^a e_\rho^b [-\omega_{\mu a}^c \eta_{cb} - \omega_{\mu b}^c \eta_{ac}] = 0 \\
&\implies e_\nu^a e_\rho^b [-\omega_{\mu ba} - \omega_{\mu ab}] = 0 \\
&\implies \omega_\mu^{ab} = -\omega_\mu^{ba}
\end{aligned}$$

Therefore, antisymmetry of the spin connection ensures metric compatibility and metric preservation along parallel transport.

Ultimately, for a given frame field  $e_\mu^a(x)$  we can solve for a spin connection  $\omega_\mu^{ab}$ , antisymmetric in  $[ab]$ . The unique solution is the following

$$\begin{aligned}
\omega_{\mu[\nu\rho]} &= \omega_{\mu[\nu\rho]}(e) + K_{\mu[\nu\rho]} \\
\omega_{\mu[\nu\rho]}(e) &\equiv \omega_{\mu ab} e_\nu^a e_\rho^b = \frac{1}{2} [\Omega_{[\mu\nu]\rho} - \Omega_{[\nu\rho]\mu} + \Omega_{[\rho\mu]\nu}] \\
\omega_\mu^{ab}(e) &= 2e^{\nu[a} \partial_{[\mu} e_{\nu]}^{b]} - e^{\nu[a} e^{b]\sigma} e_{\mu c} \partial_\nu e_\sigma^c \\
K_{\mu[\nu\rho]} &= -\frac{1}{2} [T_{[\mu\nu]\rho} - T_{[\nu\rho]\mu} + T_{[\rho\mu]\nu}] \\
T_{[\mu\nu]\rho} &= \Omega_{[\mu\nu]\rho} + \omega_{\mu[\rho\nu]} - \omega_{\nu[\rho\mu]} \\
\Omega_{[\mu\nu]\rho} &= (\partial_\mu e_\nu^a - \partial_\nu e_\mu^a) e_{a\rho}
\end{aligned}$$

where  $\omega_\mu^{ab}(e)$  is the torsion-free spin connection while  $K_{\mu\nu}^\rho = -K_{\nu\mu}^\rho$  is related to the torsion of the spacetime. Substituting the above knowledge to the definition of  $\Gamma_{\mu\nu}^\rho$  we get

$$\Gamma_{\mu\nu}^\rho = \Gamma_{\mu\nu}^\rho[g] - K_{\mu\nu}^\rho$$

where  $\Gamma_{\mu\nu}^\rho[g] = \frac{1}{2} g^{\rho\sigma} [\partial_\mu g_{\sigma\nu} + \partial_\nu g_{\mu\sigma} - \partial_\sigma g_{\mu\nu}]$  are the familiar Christoffel symbols. At last, we managed to suggest the equivalence below

$$(e_\mu^a(x), \omega_\mu^{ab}(x)) \rightarrow (g_{\mu\nu}(x), \Gamma_{\mu\nu}^\rho(x)) .$$

We should also note that throughout the discussion the connection is torsion-free.

The orthonormal group  $SO(d - 1, 1)$  possesses two distinct representations, the tensorial and the spinor one with the former being trivially generalized to the larger group  $GL(d, \mathbb{R})$  while the latter needs special care.

We only know how a spinor behaves in a D-dimensional flat spacetime. It has  $2^{[\frac{D}{2}]}$  components and the generators of the Lorentz transformations are  $\Sigma^{ab} = \frac{1}{4}\gamma^{ab} \equiv \frac{1}{4}[\gamma^a, \gamma^b]$  where the gamma matrices satisfy the Clifford algebra

$$\{\gamma^a, \gamma^b\} = 2\eta^{ab}\mathbf{I}. \quad (\text{A.3.4})$$

The first step to covariantize the Dirac equation  $(\gamma^a \partial_a - m)\psi(x) = 0$  is to promote (A.3.4) to

$$\{\gamma^\mu(x), \gamma^\nu(x)\} = 2g^{\mu\nu}(x)\mathbf{I}$$

which can be solved for  $\gamma^\mu(x) = e_a^\mu(x)\gamma^a$  which transforms as a general coordinate vector. Next, the covariant derivative on the spinor is defined

$$\nabla_\mu\psi(x) = D_\mu\psi(x) \equiv [\partial_\mu + \Gamma_\mu]\psi(x) = [\partial_\mu + \frac{1}{4}\omega_\mu^{ab}(x)\gamma_{ab}]\psi(x) \quad (\text{A.3.5})$$

with  $\omega_\mu^{ab}(x) = e^\nu_a(x)[\partial_\mu e_\nu^b(x) - \Gamma_{\mu\nu}^\sigma(x)e_\sigma^b(x)]$  from the vielbein postulate.  $\nabla_\mu\psi$  transforms as a general coordinate vector and also as a Local Lorentz vector.

A proof of this is in order. Under a Local Lorentz transformation  $x'^\mu = \Lambda(\lambda)_\rho^\mu x^\rho$  with  $\lambda^{ab}(x)$  denoting the parameters of the transformation,

$$\begin{aligned} \nabla'_\mu\psi'(x) &= (\partial_\mu + \frac{1}{4}\omega'_\mu{}^{ab}\gamma_{ab})L(\lambda)^{-1}\psi = \\ &= L^{-1}\partial_\mu\psi + \partial_\mu L^{-1}\psi + \frac{1}{4}\omega'_\mu{}^{ab}\gamma_{ab}L^{-1}\psi \end{aligned} \quad (\text{A.3.6})$$

where  $L(\lambda)^{-1}$  is the spin- $\frac{1}{2}$  representation of the transformation. Using the standard property  $L\gamma^\rho L^{-1} = \gamma^\sigma\Lambda_\sigma^\rho$ , we manipulate the third term to pass  $L^{-1}$  to the left,

$$\gamma_a\gamma_b L^{-1} = \gamma_a L^{-1} \Lambda_b^e \gamma_e = L^{-1} \Lambda_a^s \Lambda_b^e \gamma_s \gamma_e$$

so

$$\begin{aligned} \gamma_{ab}L^{-1} &= [\gamma_a, \gamma_b]L^{-1} = L^{-1}(\Lambda_a^s \Lambda_b^e \gamma_s \gamma_e - \Lambda_b^s \Lambda_a^e \gamma_s \gamma_e) = L^{-1} \Lambda_a^s \Lambda_b^e [\gamma_s \gamma_e - \gamma_e \gamma_s] \\ &= L^{-1} \Lambda_a^s \Lambda_b^e \gamma_{se}. \end{aligned}$$

Substituting this into (A.3.6) we have

$$\nabla'_\mu\psi' = L^{-1}\partial_\mu\psi + \partial_\mu L^{-1}\psi + \frac{1}{4}L^{-1}\omega'^a b_\mu \Lambda_a^s \Lambda_b^e \gamma_{se}\psi.$$

Next step is to use (A.3.3)

$$\begin{aligned}\omega'_\mu{}^{ab} \Lambda_a^s \Lambda_b^e &= (\Lambda^{-1}_c{}^a \partial_\mu \Lambda^{cb} + \Lambda^{-1}_d \omega_\mu{}^d_c \Lambda^{cb}) \Lambda_a^s \Lambda_b^e = \\ &= (-\Lambda^{cb} (\partial_\mu \Lambda^{-1})_c{}^a + \Lambda^{-1}_d \omega_\mu{}^d_c \Lambda^{cb}) \Lambda_a^s \Lambda_b^e = \\ &= -(\partial_\mu \Lambda^{-1})^{ae} \Lambda_a^s + \omega_\mu{}^{se}.\end{aligned}$$

Finally we get,

$$\begin{aligned}\nabla'_\mu \psi' &= L^{-1} \left( \partial_\mu + \frac{1}{4} \omega_\mu{}^{se} \gamma_{se} \right) \psi + \left( \partial_\mu L^{-1} - \frac{1}{4} L^{-1} \partial_\mu \Lambda^{-1}{}^{ae} \Lambda_a^s \gamma_{se} \right) \psi = \\ &= L^{-1} \nabla_\mu \psi + \left( \partial_\mu L^{-1} - \frac{1}{4} L^{-1} (\partial_\mu \Lambda^{-1})^{ae} \Lambda_a^s \gamma_{se} \right) \psi\end{aligned}$$

The last unwanted term can be easily shown to be zero for infinitesimal transformations. This suffices to claim that

$$\nabla'_\mu \psi' = L(\lambda)^{-1}(x) \nabla_\mu \psi.$$

Equipped with a covariant derivative for spinors, we arrive to the minimally coupled to gravity Dirac field action

$$S_{matter} = \int d^4x \sqrt{-g} \bar{\psi}(x) (\gamma^\mu D_\mu - m) \psi(x).$$

## A.4 Surface Gravity of the Reissner-Nordström and Kerr Solutions

### A.4.1 Reissner-Nordström Solution

By defining:

$$\Delta = r^2 - 2Mr + Q^2 = (r - r_+)(r - r_-),$$

we can write the Reissner-Nordström line element as:

$$ds^2 = -\frac{\Delta}{r^2} dt^2 + \frac{r^2}{\Delta} dr^2 + r^2 d\Omega^2.$$

Our calculation will follow the same steps that we did for Schwarzschild solution. In this case we will focus on the  $M > |Q|$  case since this is the most stable physical solution out of all 3 cases [1].

For this we will use once again the incoming Eddington-Finkenstein coordinates  $(v, r, \theta, \phi)$  where:

$$v = t + r_* ,$$

and

$$r_* = r + \frac{r_+^2}{(r_+ - r_-)} \ln \left( \frac{|r - r_+|}{r_+} \right) + \frac{r_-^2}{(r_- - r_+)} \ln \left( \frac{|r - r_-|}{r_-} \right) .$$

In these coordinates the line element is given by:

$$ds^2 = -\frac{\Delta}{r^2} dv^2 + 2dvdr + r^2 d\Omega^2 ,$$

and the inverse metric is given by:

$$g^{\mu\nu} = \begin{bmatrix} 0 & 1 & 0 & 0 \\ 1 & \frac{\Delta}{r^2} & 0 & 0 \\ 0 & 0 & \frac{1}{r} & 0 \\ 0 & 0 & 0 & \frac{1}{r^2 \sin^2 \theta} \end{bmatrix} .$$

We are interested in hypersurfaces of the form  $S(x) = r = \text{const}$ . Now we proceed to calculate the normal vector for such hypersurfaces, by means of equation (5.1.2):

$$l = N(x) g^{\mu r} \partial_\mu = N(x) [g^{rr} \partial_r + g^{vr} \partial_v] = N(x) \left[ \frac{\Delta}{r^2} \partial_r + \partial_v \right] .$$

Now we will look for null-hypersurfaces:

$$0 = l^2 = N^2(x) g_{\mu\nu} (g^{\mu\sigma} \partial_\sigma S) (g^{\nu\rho} \partial_\rho S) = g_{\mu\nu} g^{\mu r} g^{\nu r} N^2(x) = N^2(x) g^{rr} = N^2(x) \frac{\Delta}{r^2} .$$

Therefore the hypersurfaces defined by  $r = r_\pm$ , the event horizons of the Reissner-Nordström solution, will be null-hypersurfaces.

Due to the fact that the components of the metric are independent on time, we have that  $\xi = \partial_t$  will be a Killing vector. In the incoming Eddington-Finkenstein coordinates this translates into the fact that:

$$\xi = \frac{\partial}{\partial t} = \frac{dv}{dt} \frac{\partial}{\partial v} = \partial_v .$$

Comparing this result with our result for  $l$  we see that at the Killing horizon  $\xi \propto l$  since  $\Delta = 0$  there.

Now we proceed to calculate the surface gravity using equation (5.1.6):

$$\begin{aligned} \xi^\alpha \nabla_\alpha \xi^v |_{r=r_\pm} &= \xi^\mu \Gamma_{\mu\sigma}^\nu \xi^\sigma |_{r=r_\pm} = \Gamma_{vv}^v |_{r=r_\pm} = \frac{1}{2} g^{v\lambda} (\partial_v g_{v\lambda} + \partial_\lambda g_{vv} - \partial_\lambda g_{vv}) |_{r=r_\pm} \\ &= \frac{1}{2} \left[ \frac{\partial_r \Delta}{r^2} - 2 \frac{\Delta}{r^3} \right] \Big|_{r=r_\pm} = \frac{(r - r_-)(r - r_+)}{2r_\pm^2} \Big|_{r=r_\pm} = \frac{(r_\pm - r_\mp)}{2r_\pm^2} \xi^v , \end{aligned}$$

where we used the fact that  $\xi^v = 1$ . Comparing this equation with equation (5.1.6) we find the following expression for the surface gravity:

$$\kappa_{\pm} = \frac{r_{\pm} - r_{\mp}}{2r_{\pm}^2}, \quad (\text{A.4.1})$$

where the subindex in  $\kappa_{\pm}$  corresponds to the surface gravity at  $r = r_{\pm}$  respectively.

### A.4.2 Kerr Solution

We now proceed to calculate the surface gravity for the Kerr solution satisfying  $M > a$ , since this is the case of more physical interest. For this we will start by introducing the so called ‘‘Kerr coordinates’’  $(v, r, \theta, \chi)$ :

$$dv = dt + \frac{(r^2 - a^2)}{\Delta} dr \quad , \quad d\chi = d\phi + \frac{a}{\Delta} dr .$$

Using this coordinates the line element looks like [64]:

$$ds^2 = -\frac{(\Delta - a^2 \sin^2 \theta)}{\rho^2} dv^2 + 2dvdr - \frac{2a \sin^2 \theta (r^2 + a^2 - \Delta)}{\rho^2} dv d\chi \\ - 2a \sin^2 \theta d\chi dr + \frac{[(r^2 + a^2)^2 - \Delta a^2 \sin^2 \theta]}{\rho^2} \sin^2 \theta d\chi^2 + \rho^2 d\theta^2 ,$$

where we recall that  $\Delta = (r - r_+)(r - r_-)$ .

Just as we did before, we will consider hypersurfaces of the type  $S(x) = r = \text{Const}$ . From equation (5.1.2) we have that normal vectors can be written as:

$$l = N(x) g^{\mu r} \partial_{\mu} = N(x) g^{\mu r} \partial_{\mu} = N(x) [g^{rr} \partial_r + g^{vr} \partial_v + g^{xr} \partial_x] \\ = N(x) \left[ \frac{2(a^2 + r^2)}{a^2 + 2r^2 + a^2 \cos(2\theta)} \partial_v + \frac{\Delta}{\rho^2} \partial_r + \frac{2a}{a^2 + 2r^2 + a^2 \cos(2\theta)} \partial_x \right] .$$

We see that at  $r = r_{\pm}$  this reduces to:

$$l|_{r=r_{\pm}} = N(x) \frac{(a^2 + r_{\pm}^2)}{r_{\pm}^2 + a^2 \cos^2(\theta)} \left[ \partial_v + \frac{a}{a^2 + r_{\pm}^2} \partial_x \right] .$$

We will now look for null-hypersurfaces. We have that the norm of the normal vector is given by:

$$l^2 = N^2(x) g^{\mu r} g^{\nu r} g_{\mu\nu} = N^2(X) g^{rr} = N^2(x) \frac{\Delta}{\rho^2} .$$

From this it is clear that  $l^2$  vanishes when  $\Delta$  vanishes, therefore the hypersurfaces defined by  $r = r_{\pm}$  are null.

Now we proceed to construct the Killing vectors for this coordinates. As was mentioned before we have that  $\xi = \partial_t + \Omega_H \partial_\phi$ . In order to specify completely our Killing vector we will calculate  $\Omega_H$  by using coordinates  $(t, r, \theta, \phi)$ :

$$\begin{aligned} 0 &= \xi^2|_{r=r_\pm} = \xi^\mu \xi^\nu g_{\mu\nu}|_{r=r_\pm} = [g_{tt} + 2\Omega_H g_{t\phi} + \Omega_H^2 g_{\phi\phi}]|_{r=r_\pm} \\ &= -\left(1 - \frac{2mr_\pm}{r_\pm^2 + a^2 \cos^2 \theta}\right) - \left(\frac{4mar_\pm \sin^2 \theta}{r_\pm^2 + a^2 \cos^2 \theta}\right) \Omega_H \\ &\quad + \Omega_H^2 \left(r_\pm^2 + a^2 + \frac{2ma^2 r_\pm \sin^2 \theta}{r_\pm^2 + a^2 \cos^2 \theta}\right) \sin^2 \theta \\ &= a^2 - 4mar_\pm \Omega_H + \Omega_H^2 (r_\pm^2 + a^2)^2. \end{aligned}$$

Solving this equation for  $\Omega_H$  one finds that:

$$\Omega_H = \frac{a}{r_\pm^2 + a^2}.$$

In “Kerr coordinates”  $(v, r, \theta, \chi)$  the Killing vector becomes:

$$\xi = \frac{dv}{dt} \partial_v + \Omega_H \frac{d\chi}{d\phi} \partial_\chi = \partial_v + \Omega_H \partial_\chi.$$

From the equation for  $\Omega_H$  and our result for  $l|_{r=r_\pm}$  we see that  $\xi$  and  $l$  are indeed proportional at the horizon.

Now we sketch the calculation of the surface gravity, for this we start from equation (5.1.6):

$$\xi^\sigma \nabla_\sigma \xi^\mu|_{r=r_\pm} = \xi^\sigma \Gamma_{vv}^\mu + 2\Gamma_{v\chi}^\mu \Omega_H + \Gamma_{\chi\chi}^\mu \Omega_H^2.$$

We are interested in the components  $\mu = v$  and  $\mu = \chi$ . As we see in the equation above, it is necessary to calculate the inverse Kerr metric in “Kerr coordinates” and then calculate the Christoffel symbols that are needed. Clearly this is a lengthy task for this metric and we won’t get into the details. However, using a computer one can show that:

$$\kappa_\pm = \frac{r_\pm - r_\mp}{2(r_\pm^2 + a^2)}, \tag{A.4.2}$$

where  $\kappa_+$  ( $\kappa_-$ ) corresponds to the surface gravity at  $r = r_+$  ( $r = r_-$ ).

## A.5 Euclidean Gravity: Kerr Solution

In this appendix we calculate the temperature of the Kerr black hole using the Euclidean gravity approach, as was done in Section 5.6 for the Schwarzschild and Reissner-Nordström solutions. Here we closely follow [130].

We start with the Kerr metric (2.3.4), which we write in the form

$$\begin{aligned} ds^2 = & -\frac{\Delta - a^2 \sin^2 \theta}{\rho^2} dt^2 - \frac{2a \sin^2 \theta (r^2 + a^2 - \Delta)}{\rho^2} d\phi dt + \frac{\rho^2}{\Delta} dr^2 \\ & + \rho^2 d\theta^2 + \left( r^2 + a^2 + \frac{(r^2 + a^2)^2 - \Delta a^2 \sin^2 \theta}{\rho^2} \right) \sin^2 \theta d\phi^2, \end{aligned} \quad (\text{A.5.1})$$

where  $a = J/M$ ,  $\rho^2 = r^2 + a^2 \cos^2 \theta$  and  $\Delta = r^2 - 2Mr + a^2$ . Unlike the metric tensors we considered in Section 5.6, the Kerr metric is not diagonal. If we now perform a Wick rotation to imaginary time  $\tau = it$ , we see that the off-diagonal component  $g_{t\phi}$  becomes imaginary. The way to fix this is to simultaneously introduce the complex angular momentum per unit mass  $\alpha = ia$ . When all calculations are done, we can perform analytic continuation back to a real-valued  $a$ . The Euclidean metric then reads

$$\begin{aligned} ds^2 = & \frac{\Delta + \alpha^2 \sin^2 \theta}{\rho^2} d\tau^2 + \frac{2\alpha \sin^2 \theta (r^2 - \alpha^2 - \Delta)}{\rho^2} d\phi dt + \frac{\rho^2}{\Delta} dr^2 \\ & + \rho^2 d\theta^2 + \left( r^2 - \alpha^2 + \frac{(r^2 - \alpha^2)^2 + \Delta \alpha^2 \sin^2 \theta}{\rho^2} \right) \sin^2 \theta d\phi^2, \end{aligned} \quad (\text{A.5.2})$$

where now  $\rho^2 = r^2 - \alpha^2 \cos^2 \theta$  and  $\Delta = r^2 - 2Mr - \alpha^2$ .

Next, we introduce the following one-forms:

$$\omega = \frac{r^2 - \alpha^2}{\rho^2} (d\tau - \alpha \sin^2 \theta d\phi) \quad (\text{A.5.3})$$

$$\tilde{\omega} = \frac{r^2 - \alpha^2}{\rho^2} \left( d\phi + \frac{\alpha}{r^2 - \alpha^2} d\tau \right). \quad (\text{A.5.4})$$

The reason for introducing these one-forms is that they are precisely the dual forms to the orthogonal Killing vectors  $\xi = \partial_\tau - \frac{\alpha}{r^2 - \alpha^2} \partial_\phi$  and  $\tilde{\xi} = \alpha \sin^2 \theta \partial_\tau + \partial_\phi$  of the Kerr solution. Compare this to the case of the Schwarzschild metric. There, the one-forms  $dt$  and  $d\phi$  are the dual forms to the Killing vectors  $\partial_\tau$  and  $\partial_\phi$ , so we express the Schwarzschild metric in  $\{t, r, \phi, \theta\}$  coordinates. Similarly, we can write the Kerr metric using dual forms  $\omega$  and  $\tilde{\omega}$  as

$$ds^2 = \frac{\Delta \rho^2}{(r^2 - \alpha^2)^2} \omega^2 + \frac{\rho^2}{\Delta} dr^2 + \rho^2 (d\theta^2 + \sin^2 \theta \tilde{\omega}^2). \quad (\text{A.5.5})$$

Using the abovementioned similarity between  $dt$  and  $\omega$  and between  $d\phi$  and  $\tilde{\omega}$ , one could think that we have diagonalized the Kerr metric here. However, we did not: unlike  $dt$  and  $d\phi$ , the one-forms  $\omega$  and  $\tilde{\omega}$  are not exact, which means that we cannot write them as differentials of some coordinate function.

In Section 2.3, it was shown that the Kerr black hole has event horizons at  $r_{\pm} = M \pm \sqrt{M^2 + \alpha^2}$ . We now introduce the coordinate  $\xi = r - r_+$  such that  $\xi \downarrow 0$  as we approach the black hole from the outside. Noting that  $\Delta = (r - r_+)(r - r_-)$ , it is an easy task to expand the metric tensor components around the outer event horizon. To lowest orders in  $\xi$  this yields

$$ds^2 \approx \frac{(r_+ - r_-)\rho^2}{(r_+^2 - \alpha^2)^2} \xi \omega^2 + \frac{\rho^2}{(r_+ - r_-)\xi} d\xi^2 + \rho^2(d\theta^2 + \sin^2 \theta \tilde{\omega}^2), \quad (\text{A.5.6})$$

where  $\rho$ ,  $\omega$  and  $\tilde{\omega}$  are now evaluated at the outer horizon  $r_+$ .

As in Chapter 5, the last two terms in (A.5.6) are just a two-sphere. To see this, note that as  $\tilde{\omega}$  is now being evaluated at  $r_+$ , it *can* be written as a differential. Indeed, we can write  $\tilde{\omega} = d\psi$ , where  $\psi = \frac{r_+^2 - \alpha^2}{\rho^2} \left( \phi + \frac{\alpha}{r_+^2 - \alpha^2} \tau \right)$ . Then last two terms of the above metric read  $\rho^2(d\theta^2 + \sin^2 \theta d\psi^2)$ , which is indeed just a two-sphere. To avoid singularities at the points  $\theta = 0$  and  $\theta = \pi$ , we must have  $\psi \in [0, 2\pi]/\sim$ .<sup>5</sup>

Introducing  $\chi = \tau - \alpha \sin^2 \theta \phi$ , such that  $\omega = \frac{r_+^2 - \alpha^2}{\rho^2} d\chi$ , we can write the metric (A.5.6) as

$$ds^2 = \frac{(r_+ - r_-)\xi}{\rho^2} d\chi^2 + \frac{\rho^2}{(r_+ - r_-)\xi} d\xi^2 \quad (\text{A.5.7})$$

where we ignored the  $S^2$  part of the metric. Now define the coordinate  $\zeta$  by  $\zeta^2 = \frac{4\rho^2\xi}{r_+ - r_-}$ . In terms of this new coordinate, the metric reads

$$ds^2 = \frac{(r_+ - r_-)\zeta^2}{4\rho^4} d\chi^2 + d\zeta^2. \quad (\text{A.5.8})$$

Using the same argument as in section 5.6, we see that in order to avoid a conical singularity we must demand that  $\chi \in [0, \frac{4\pi\rho^2}{r_+ - r_-}]/\sim$ . However, notice that in this case  $\rho$  depends on the angle  $\theta$ . In order for the required periodicity of  $\chi$  to hold for all  $\theta$ , we must require that points  $(\tau, \phi)$  are identified with the points  $\left(\tau + \frac{4\pi(r_+^2 - \alpha^2)}{r_+ - r_-}, \phi - \frac{4\pi\alpha}{r_+ - r_-}\right)$ . Note that with this identification  $\psi$  is still a well-defined coordinate, i.e. identified points have the same value of  $\psi$ . As usual, the inverse temperature is equal to the period of the  $\tau$  coordinate. Therefore we find

$$T = \frac{r_+ - r_-}{4\pi(r_+^2 - \alpha^2)} = \frac{\kappa}{2\pi}. \quad (\text{A.5.9})$$

where we used equation (A.4.2) for the surface gravity of the Kerr black hole. Thus, we indeed find that the Hawking temperature also holds for the Kerr black hole. In terms of

---

<sup>5</sup>The argument here is similar to the argument used in Section 5.6 concerning the conical singularities. In this case, if  $\psi$  is not periodic in  $2\pi$ , the resulting topological space will look like a rugby ball rather than a cone, since we have two conical singularities.

the mass  $M$  and the angular momentum  $J$  of the black hole, the temperature reads

$$T = \frac{\sqrt{M^4 - J^2}}{4\pi M (M^2 + \sqrt{M^4 - J^2})}, \quad (\text{A.5.10})$$

which indeed reduces to the temperature of the Schwarzschild black hole when  $J = 0$ .

## A.6 The Reason for Quantum Field Theory

It is good to remind ourselves why we formulate relativistic quantum mechanics in terms of fields using the second quantization scheme. To this end we will follow the structure of [131, Ch. 2].

To quantize relativity, or to relativistically extend quantum mechanics, one might start by considering the mass-shell identity

$$E^2 = \mathbf{p}^2 + m^2 \quad (\text{A.6.1})$$

and try to apply the familiar correspondence principle

$$\begin{aligned} E &\rightarrow i\frac{\partial}{\partial t} \\ \mathbf{p} &\rightarrow -i\nabla. \end{aligned} \quad (\text{A.6.2})$$

This will lead us directly to the Klein-Gordon equation

$$\left( \frac{\partial^2}{\partial t^2} - \nabla^2 + m^2 \right) \psi(t, \mathbf{x}) = 0, \quad (\text{A.6.3})$$

which was Schrödinger's first attempt to find an equation that describes a relativistic particle. We might naively write down plane wave solutions to this equation as

$$\psi(t, \mathbf{x}) = e^{-iEt+i\mathbf{p}\cdot\mathbf{x}} \qquad E = \pm\sqrt{\mathbf{p}^2 + m^2}. \quad (\text{A.6.4})$$

But now something strange happens. To form a complete basis of the Hilbert space of solutions must include both positive- and negative-energy solutions to equation (A.6.3). The energy spectrum of the theory is therefore unbounded from below, which will lead to all sorts of complications – the least of which is the absence of a ground state.

If we were to couple this theory to the electromagnetic field, any state of the relativistic particle described by the Klein-Gordon equation (A.6.3) is unstable, as nothing prevents

decay of any particular state to a lower-energy state by emission of a photon. In particular, positive energy particles cannot exist as stable solutions to (A.6.3), which seems to contradict our notions of reality.

This problem can be at least heuristically tackled in the case of the Dirac equation, which describes spin- $\frac{1}{2}$  particles. Dirac argued that, since fermions obey the Pauli exclusion principle, we could construct the ground state vacuum of the system as the state in which all negative-energy states are occupied – an interpretation called the Dirac Sea. In this picture a sufficiently energetic photon can excite a particle to a positive-energy state, which we interpret as an electron, leaving behind a ‘hole’ in the vacuum that can be interpreted as a positron; a process that indeed occurs in semiconductors.

However this explanation is not entirely satisfactory, as it would require that the ‘bare’ vacuum has an infinity positive charge to compensate and runs into other problems, most notably Klein’s Paradox<sup>[132]</sup><sup>6</sup>.

What this issue tells us is that it is quintessentially wrong to interpret the Dirac equation as a single-particle equation. Indeed, the famous  $E = mc^2$  in fact *demands* that in order to marry relativity and quantum mechanics we should set up a formalism that is equipped from the very beginning with the tools to describe multiparticle systems.

Another hint towards this comes from relativistic considerations. In ordinary quantum mechanics we consider the object  $|\psi(t, \mathbf{x})|^2$  to describe a probability amplitude in space. This view is unfortunately untenable in a relativistic context as the conservation of probability is not a covariant equation.

Lastly, in quantum mechanics we describe observables as self-adjointt operators acting on some Hilbert space. These operators are, at worst, dependent on time in the Heisenberg picture. However relativity tells us that no information can travel faster than the speed of light and we should truly consider a measurement of an observable to be localized in space as well as in time. Causality then requires that two spacelike separated measurements cannot affect one another, hence the observables  $\mathcal{O}_1$  and  $\mathcal{O}_2$  that describe two measurements should satisfy

$$[\mathcal{O}_1(x_1), \mathcal{O}_2(x_2)] = 0 \quad (x_1 - x_2)^2 > 0. \quad (\text{A.6.5})$$

In a relativistic quantum theory, operators in the Heisenberg picture must also depend on the space-time position  $x_\mu$ . This view demotes the position  $\mathbf{x}$  to a label similar to time, rather than an observable in and of itself.

---

<sup>6</sup>For more pedagogical reviews refer to [133], [134] and [135].

In light of these considerations it is very natural to turn to the second quantization formalism.

## A.7 Evaluation of Action in Curved Spacetime

We have included this appendix to provide the reader with tools of how to find and work with an action in curved spacetime. To construct a general action, we will use the action defined in equation (7.1.1) and apply the following set of rules that describe how to transform an action on flat spacetime to one on curved spacetime:

- i. replace the metric for flat spacetime  $\eta^{\mu\nu}$  for that for curved spacetime,  $g^{\mu\nu}$ ;
- ii. write covariant derivatives instead of ordinary derivatives<sup>7</sup>;
- iii. instead of using the usual volume element  $d\mathbf{x}dt$ , insert the covariant volume element  $d^4x\sqrt{-g}$ , with  $g \equiv \det(g_{\mu\nu})$ .

These rules allow us to rewrite the action of equation (7.1.1) in the familiar form:<sup>8</sup>

$$S_{\text{matter}}[\phi] = \frac{1}{2} \int d^4x \sqrt{-g} (g^{\mu\nu} \partial_\mu \phi \partial_\nu \phi + m\phi^2). \quad (\text{A.7.1})$$

This action is the matter part of the Hilbert-Einstein action mentioned in chapter 1. We can add extra terms to this action such as for example the generalized Maxwell action to curved spacetime

$$S_{\text{Maxwell}}[A] = -\frac{1}{4} \int d^4x \sqrt{-g} (g^{\mu\rho} g^{\nu\sigma} F_{\mu\nu} F_{\rho\sigma}),$$

where  $F_{\mu\nu} = \partial_\mu A_\nu - \partial_\nu A_\mu$  describes the familiar electromagnetic field tensor with  $A_\mu$  the electromagnetic field vector.<sup>9</sup> Another example is the coupling of the field  $\phi$  to the curvature scalar  $R$

$$S_{\text{curvature}}[\phi] = - \int d^4x \sqrt{-g} \xi R \phi^2,$$

where  $\xi$  is the coupling constant.<sup>10</sup> It is important to realize here that whereas an action for flat spacetime must be Poincaré invariant to preserve translational and Lorentz invariance,

<sup>7</sup>Remember here that the first covariant derivative coincides with an ordinary derivative because  $\phi$  is a scalar.

<sup>8</sup>Notice here that we went back to four-dimensions, because we want to provide the reader with a general explanation. Later on we will return to our two-dimensional example.

<sup>9</sup>For more information on the origin of this action [110, Ch. 5].

<sup>10</sup>For more information, see [1, Ch. 9].

the presence of gravity takes away this condition for the action in curved spacetime. However, the action in an arbitrarily chosen curved spacetime does have to be invariant under general coordinate transformations as to ensure coordinate independence of the physical properties. Moreover, the conservation of charges is related to presence of internal symmetries such that the action must also obey these symmetries. We have thus promoted the action we had for flat spacetime to curved spacetime and seen some examples of extra terms that can be added to the action that describe different physics.



# Bibliography

- [1] S. M. Carroll, *Spacetime and geometry. An introduction to general relativity*, vol. 1. 2004.
- [2] “Falling into a Black Hole.” <http://cosmic-horizons.blogspot.nl/2012/04/falling-into-black-hole.html>, 2012. Visited January 2014.
- [3] J. Hartong, “On problems in de Sitter spacetime physics,” 2004.
- [4] S. W. Hawking and G. F. R. Ellis, *The large scale structure of space-time*, vol. 1. Cambridge university press, 1973.
- [5] V. di Carlo, “Conformal compactification and anti-de Sitter space,” *Master Thesis*, 2007.
- [6] K. Schleich and D. M. Witt, “A simple proof of Birkhoff’s theorem for cosmological constant,” *Journal of Mathematical Physics*, vol. 51, p. 112502, 2010.
- [7] Z. Stuchlík and S. Hledík, “Some properties of the Schwarzschild–de Sitter and Schwarzschild–anti-de Sitter spacetimes,” *Physical Review D*, vol. 60, no. 4, p. 044006, 1999.
- [8] N. Cruz, M. Olivares, and J. R. Villanueva, “The geodesic structure of the Schwarzschild anti-de Sitter black hole,” *Classical and Quantum Gravity*, vol. 22, no. 6, p. 1167, 2005.
- [9] Z. Stuchlík and S. Hledík, “Properties of the Reissner-Nordström Spacetimes with a Nonzero Cosmological Constant,” *arXiv preprint arXiv:0803.2685*, 2008.
- [10] R. P. Kerr, “Gravitational field of a spinning mass as an example of algebraically special metrics,” *Phys. Rev. Letters*, vol. 11, 1963.
- [11] E. T. Newman and A. Janis, “Note on the Kerr Spinning-Particle Metric,” *Journal of Mathematical Physics*, vol. 6, p. 915, 1965.

- [12] R. Penrose and R. Floyd, “Extraction of rotational energy from a black hole,” *Nature*, vol. 229, no. 6, pp. 177–179, 1971.
- [13] G. t. Hooft, “Introduction to general relativity.” <http://www.staff.science.uu.nl/~hooft101/lectures/>, 2012.
- [14] C. Semay, “Penrose diagram for an uniformly accelerated observer,” tech. rep., 2006.
- [15] J. Maldacena, “The large-N limit of superconformal field theories and supergravity,” *International journal of theoretical physics*, vol. 38, no. 4, pp. 1113–1133, 1999.
- [16] S. A. Hartnoll, “Lectures on holographic methods for condensed matter physics,” *Classical and Quantum Gravity*, vol. 26, no. 22, p. 224002, 2009.
- [17] B. Sprenger, “On Lifshitz rotating black holes and black branes in light of AdS/CFT,” Master’s thesis, Universiteit Utrecht, the Netherlands, 2012.
- [18] R. Emparan, “AdS/CFT duals of topological black holes and the entropy of zero-energy states,” *Journal of High Energy Physics*, vol. 1999, no. 06, p. 036, 1999.
- [19] R. C. Tolman, “Effect of inhomogeneity on cosmological models,” *Proceedings of the national academy of sciences of the United States of America*, vol. 20, no. 3, p. 169, 1934.
- [20] R. C. Tolman, “Static solutions of Einstein’s field equations for spheres of fluid,” *Physical Review*, vol. 55, no. 4, p. 364, 1939.
- [21] J. R. Oppenheimer and G. M. Volkoff, “On massive neutron cores,” *Physical Review*, vol. 55, no. 4, p. 374, 1939.
- [22] O. Pols, “Stellar structure and evolution.” [https://www.astro.ru.nl/~onnop/education/stev\\_utrecht\\_notes/](https://www.astro.ru.nl/~onnop/education/stev_utrecht_notes/), 2011. Visited January 2014.
- [23] S. Chandrasekhar, “The highly collapsed configurations of a stellar mass,” *Monthly Notices of the Royal Astronomical Society*, vol. 91, pp. 456–466, 1931.
- [24] W. A. Hiscock, “General relativistic fluid spheres with nonzero vacuum energy density,” *Journal of mathematical physics*, vol. 29, p. 443, 1988.
- [25] C. W. Misner and J. A. Wheeler, *Gravitation: Charles W. Misner, Kip S. Thorne, John Archibald Wheeler*. Macmillan, 1973.
- [26] V. Kalogera and G. Baym, “The maximum mass of a neutron star,” *The Astrophysical Journal Letters*, vol. 470, no. 1, p. L61, 1996.

- [27] R. Tiwari, J. Rao, and R. Kanakamedala, “Electromagnetic mass models in general relativity,” *Physical Review D*, vol. 30, no. 2, p. 489, 1984.
- [28] S. Ray, A. L. Espindola, M. Malheiro, J. P. Lemos, and V. T. Zanchin, “Electrically charged compact stars and formation of charged black holes,” *Physical Review D*, vol. 68, no. 8, p. 084004, 2003.
- [29] S. Bonazzola and J. Schneider, “An exact study of rigidly and rapidly rotating stars in general relativity with application to the crab pulsar,” *The Astrophysical Journal*, vol. 191, pp. 273–290, 1974.
- [30] T. W. Baumgarte, S. L. Shapiro, and M. Shibata, “On the maximum mass of differentially rotating neutron stars,” *The Astrophysical Journal Letters*, vol. 528, no. 1, p. L29, 2000.
- [31] J. R. Oppenheimer and H. Snyder, “On continued gravitational contraction,” *Physical Review*, vol. 56, no. 5, p. 455, 1939.
- [32] R. H. Price, “Nonspherical perturbations of relativistic gravitational collapse. I. Scalar and gravitational perturbations,” *Physical Review D*, vol. 5, no. 10, p. 2419, 1972.
- [33] R. H. Price, “Nonspherical perturbations of relativistic gravitational collapse. I. Scalar and gravitational perturbations,” *Physical Review D*, vol. 5, no. 10, p. 2419, 1972.
- [34] R. H. Price, “Nonspherical perturbations of relativistic gravitational collapse. II. Integer-spin, zero-rest-mass fields,” *Physical Review D*, vol. 5, no. 10, p. 2439, 1972.
- [35] J. M. Senovilla, “Singularity Theorems in General Relativity: Achievements and Open Questions,” in *Einstein and the Changing Worldviews of Physics*, pp. 305–316, Springer, 2012.
- [36] S. W. Hawking, R. Penrose, and M. Atiyah, *The nature of space and time*, vol. 59. Princeton University Press Princeton, 1996.
- [37] D. Christodoulou, “Violation of cosmic censorship in the gravitational collapse of a dust cloud,” *Communications in Mathematical Physics*, vol. 93, no. 2, pp. 171–195, 1984.
- [38] A. Ori and T. Piran, “Naked singularities and other features of self-similar general-relativistic gravitational collapse,” *Physical Review D*, vol. 42, no. 4, p. 1068, 1990.

- [39] R. Ruffini and J. A. Wheeler, “Introducing the Black Hole.,” *Physics Today*, 1971.
- [40] W. Israel, “Event horizons in static vacuum space-times,” *Physical review*, vol. 164, no. 5, p. 1776, 1967.
- [41] B. Carter, “Black hole equilibrium states,” *Black holes*, pp. 57–214, 1973.
- [42] J. D. Bekenstein, “Nonexistence of baryon number for static black holes,” *Physical Review D*, vol. 5, no. 6, p. 1239, 1972.
- [43] E. Ayón-Beato, “Improving the” No-Hair” Theorem for the Proca Field,” *arXiv preprint gr-qc/0210001*, 2002.
- [44] E. Fischbach, “Long range forces and neutrino mass,” *arXiv preprint hep-ph/9603396*, 1996.
- [45] M. E. Rose, “Relativistic electron theory,” *American Journal of Physics*, vol. 29, pp. 866–866, 1961.
- [46] J. B. Hartle, “Long-range neutrino forces exerted by Kerr black holes,” *Physical Review D*, vol. 3, pp. 2938–2940, 1971.
- [47] M. S. Volkov and D. V. Gal'tsov *JETP Lett.*, vol. 50, no. 312, 1989.
- [48] P. Bizon *Phys. Rev. Lett.*, vol. 64, no. 2844, 1990.
- [49] S. Droz, M. Heussler, and N. Straumann *Phys. Lett. B*, vol. 268, no. 371, 1991.
- [50] K. Y. Lee, V. P. Nair, and E. Weinberg *Phys. Rev. Lett.*, vol. 68, no. 1100, 1992.
- [51] B. R. Greene, S. D. Mathur, and C. M. O'Neill *Phys. Rev. D*, vol. 47, no. 2242, 1993.
- [52] T. Torii and K. Maeda *Phys. Rev. D*, vol. 48, no. 1643, 1993.
- [53] M. Heusler, S. Droz, and N. Straumann, “Linear stability of Einstein-Skyrme black holes,” *Physics Letters B*, vol. 285, no. 1, pp. 21–26, 1992.
- [54] H. Watabe and T. Torii, “Perturbations of global monopoles as a black hole’s hair,” *Journal of Cosmology and Astroparticle Physics*, vol. 2004, no. 02, p. 001, 2004.
- [55] N. Bocharova, K. Bronnikov, and V. Melnikov *Vestn. Mosk. Univ. Fiz. Astron.*, vol. 6, no. 706, 1970.
- [56] L. Parker, “Conformal Energy-Momentum Tensor in Riemannian Space-Time,” *Physical Review D*, vol. 7, no. 4, p. 976, 1973.

- [57] K. Bronnikov and Y. N. Kireyev, “Instability of black holes with scalar charge,” *Physics Letters A*, vol. 67, no. 2, pp. 95–96, 1978.
- [58] A. Achucarro, R. Gregory, and K. Kuijken, “Abelian Higgs hair for black holes,” *Phys. Rev. D*, vol. 52, no. 5729, 1995.
- [59] D. M. Eardley, G. T. Horowitz, D. A. Kastor, and J. Traschen, “Breaking cosmic strings without monopoles,” *Physical review letters*, vol. 75, no. 19, p. 3390, 1995.
- [60] T. Torii, K. Maeda, and M. Narita, “Scalar hair on the black hole in asymptotically anti-de Sitter spacetime,” *Physical Review D*, vol. 64, no. 4, p. 044007, 2001.
- [61] P. A. Gonzales, E. Papantonopoulos, J. Saavedra, and Y. Vasques, “Four-Dimensional Asymptotically AdS Black Holes with Scalar Hair,” *JHEP*, vol. 1312, no. 021.
- [62] C. Martínez, R. Troncoso, and J. Zanelli, “Exact black hole solution with a minimally coupled scalar field,” *Physical Review D*, vol. 70, no. 8, p. 084035, 2004.
- [63] S. Bhattacharya and A. Lahiri, “Black-hole no-hair theorems for a positive cosmological constant,” *Physical review letters*, vol. 99, no. 20, p. 201101, 2007.
- [64] P. K. Townsend, “Black holes,” *arXiv preprint gr-qc/9707012*, 1997.
- [65] F. Dowker, “Black holes: lecture notes.” <https://dl.dropboxusercontent.com/u/9717190/bh.pdf>, 2012. Visited January 2014.
- [66] B. Carter, “Axisymmetric black hole has only two degrees of freedom,” *Physical Review Letters*, vol. 26, no. 6, pp. 331–333, 1971.
- [67] R. M. Wald, “Final states of gravitational collapse,” *Physical Review Letters*, vol. 26, no. 26, p. 1653, 1971.
- [68] J. M. Bardeen, B. Carter, and S. W. Hawking, “The four laws of black hole mechanics,” *Communications in Mathematical Physics*, vol. 31, no. 2, pp. 161–170, 1973.
- [69] G. J. Galloway, “Maximum principles for null hypersurfaces and null splitting theorems,” in *Annales Henri Poincaré*, vol. 1, pp. 543–567, Springer, 2000.
- [70] J. L. Jaramillo and E. Gourgoulhon, “Mass and angular momentum in general relativity,” in *Mass and Motion in General Relativity*, pp. 87–124, Springer, 2011.
- [71] R. Penrose, “Battelle Rencontres: 1967 Lectures in Mathematics and Physics,” *Editors CM de Witt and JA Wheeler, Benjamin*, p. 121, 1968.

- [72] R. M. Wald and V. Iyer, “Trapped surfaces in the Schwarzschild geometry and cosmic censorship,” *Physical Review D*, vol. 44, no. 12, p. R3719, 1991.
- [73] S. W. Hawking, “Gravitational radiation from colliding black holes,” *Physical Review Letters*, vol. 26, pp. 1344–1346, 1971.
- [74] W. Israel, “Third law of black-hole dynamics-A formulation and proof,” *Physical review letters*, vol. 57, pp. 397–399, 1986.
- [75] M. C. Cheng, “The Thermodynamics of Reissner-Nordstrom Black Holes and the Extreme Limit,” Master’s thesis, Universiteit Utrecht, 2003.
- [76] J. D. Bekenstein, “Black holes and entropy,” *Physical Review D*, vol. 7, no. 8, p. 2333, 1973.
- [77] S. W. Hawking, “Particle creation by black holes,” *Communications in mathematical physics*, vol. 43, no. 3, pp. 199–220, 1975.
- [78] G. Gibbons and M. Perry, “Black holes and thermal Green functions,” *Proceedings of the Royal Society of London. A. Mathematical and Physical Sciences*, vol. 358, no. 1695, pp. 467–494, 1978.
- [79] H.-P. Nollert, “Quasinormal modes: the characteristic sound of black holes and neutron stars,” *Classical and Quantum Gravity*, vol. 16, no. 12, p. R159, 1999.
- [80] F. J. Zerilli, “Tensor harmonics in canonical form for gravitational radiation and other applications,” *Journal of mathematical Physics*, vol. 11, p. 2203, 1970.
- [81] T. Regge and J. A. Wheeler, “Stability of a Schwarzschild singularity,” *Physical Review*, vol. 108, no. 4, pp. 1063–1069, 1957.
- [82] R. Konoplya and A. Zhidenko, “Quasinormal modes of black holes: from astrophysics to string theory,” *Reviews of Modern Physics*, vol. 83, no. 3, p. 793, 2011.
- [83] H.-J. Blome and B. Mashhoon, “Quasi-normal oscillations of a schwarzschild black hole,” *Physics Letters A*, vol. 100, no. 5, pp. 231–234, 1984.
- [84] R. H. Price and J. Pullin, “Colliding black holes: The Close limit,” *Physical Review Letters*, vol. 72, no. 21, p. 3297, 1994.
- [85] K. D. Kokkotas and B. G. Schmidt, “Quasi-normal modes of stars and black holes,” *Living Rev. Rel.*, vol. 2, no. 2, p. 262, 1999.

- [86] E. Berti, V. Cardoso, and A. O. Starinets, “Quasinormal modes of black holes and black branes,” *Classical and Quantum Gravity*, vol. 26, no. 16, p. 163001, 2009.
- [87] C. Burgess and C. Lütken, “Propagators and effective potentials in anti-de Sitter space,” *Physics Letters B*, vol. 153, no. 3, pp. 137–141, 1985.
- [88] V. Cardoso and J. P. Lemos, “Quasinormal modes of Schwarzschild–anti-de Sitter black holes: Electromagnetic and gravitational perturbations,” *Physical Review D*, vol. 64, no. 8, p. 084017, 2001.
- [89] G. T. Horowitz and V. E. Hubeny, “Quasinormal modes of AdS black holes and the approach to thermal equilibrium,” *Physical Review D*, vol. 62, no. 2, p. 024027, 2000.
- [90] D. Birmingham, I. Sachs, and S. N. Solodukhin, “Conformal field theory interpretation of black hole quasinormal modes,” *Physical review letters*, vol. 88, no. 15, p. 151301, 2002.
- [91] P. Breitenlohner and D. Z. Freedman, “Positive energy in anti-de Sitter backgrounds and gauged extended supergravity,” *Physics Letters B*, vol. 115, no. 3, pp. 197–201, 1982.
- [92] P. Breitenlohner and D. Z. Freedman, “Stability in gauged extended supergravity,” *Annals of Physics*, vol. 144, no. 2, pp. 249–281, 1982.
- [93] S. Avis, C. Isham, and D. Storey, “Quantum field theory in anti-de Sitter space-time,” *Physical Review D*, vol. 18, pp. 3565–3576, 1978.
- [94] “Lecture notes, Massachusetts Institute of Technology.” <http://ocw.mit.edu/courses/physics/8-821-string-theory-fall-2008/lecture-notes/>, 2008. In particular see the homework solution <http://ocw.mit.edu/courses/physics/8-821-string-theory-fall-2008/assignments/soln04.pdf> Visited January 2014.
- [95] H.-W. Hammer and R. Higa, “A model study of discrete scale invariance and long-range interactions,” *The European Physical Journal A*, vol. 37, no. 2, pp. 193–200, 2008.
- [96] K. Case, “Singular potentials,” *Physical Review*, vol. 80, no. 5, p. 797, 1950.
- [97] S. Moroz, “Below the Breitenlohner-Freedman bound in the nonrelativistic AdS/CFT correspondence,” *Physical Review D*, vol. 81, no. 6, p. 066002, 2010.

- [98] F. Olver and L. Maximon, “Digital Library of Mathematical Functions.” <http://dlmf.nist.gov/10>, 2013. Visited January 2014.
- [99] L. Mezincescu and P. Townsend, “Stability at a local maximum in higher dimensional anti-deSitter space and applications to supergravity,” *Annals of Physics*, vol. 160, no. 2, pp. 406–419, 1985.
- [100] P. Minces and V. O. Rivelles, “Energy and the AdS/CFT correspondence,” *Journal of High Energy Physics*, vol. 2001, no. 12, p. 010, 2001.
- [101] I. R. Klebanov and E. Witten, “AdS/CFT correspondence and symmetry breaking,” *Nuclear Physics B*, vol. 556, no. 1, pp. 89–114, 1999.
- [102] R. Narayan, “Black holes in astrophysics,” *New Journal of Physics*, vol. 7, no. 1, p. 199, 2005.
- [103] E. Berti and V. Cardoso, “Supermassive black holes or boson stars? Hair counting with gravitational wave detectors,” *International Journal of Modern Physics D*, vol. 15, no. 12, pp. 2209–2216, 2006.
- [104] S. Waldman, “The Advanced LIGO gravitational wave detector,” *arXiv preprint arXiv:1103.2728*, 2011.
- [105] D. A. Shaddock, “An Overview of the Laser Interferometer Space Antenna,” *Publications of the Astronomical Society of Australia*, vol. 26, no. 2, pp. 128–132, 2009.
- [106] E. E. Flanagan and S. A. Hughes, “Measuring gravitational waves from binary black hole coalescences. I. Signal to noise for inspiral, merger, and ringdown,” *Physical Review D*, vol. 57, no. 8, p. 4535, 1998.
- [107] E. Berti, V. Cardoso, and C. M. Will, “Gravitational-wave spectroscopy of massive black holes with the space interferometer LISA,” *Physical Review D*, vol. 73, no. 6, p. 064030, 2006.
- [108] E. Berti, J. Cardoso, V. Cardoso, and M. Cavaglia, “Matched filtering and parameter estimation of ringdown waveforms,” *Physical Review D*, vol. 76, no. 10, p. 104044, 2007.
- [109] F. D. Ryan, “Spinning boson stars with large self-interaction,” *Physical Review D*, vol. 55, no. 10, p. 6081, 1997.
- [110] V. Mukhanov and S. Winitzki, *Introduction to quantum effects in gravity*. Cambridge University Press, 2007.

- [111] N. D. Birrell and P. C. W. Davies, *Quantum fields in curved space*. No. 7, Cambridge university press, 1984.
- [112] W. G. Unruh, “Notes on black-hole evaporation,” *Physical Review D*, vol. 14, no. 4, p. 870, 1976.
- [113] R. M. Wald, “General relativity,” 1984.
- [114] R. M. Wald, *Quantum field theory in curved spacetime and black hole thermodynamics*. University of Chicago Press, 1994.
- [115] J. Dimock, “Scattering for the wave equation on the Schwarzschild metric,” *General relativity and gravitation*, vol. 17, no. 4, pp. 353–369, 1985.
- [116] R. M. Wald, “On particle creation by black holes,” *Communications in Mathematical Physics*, vol. 45, no. 1, pp. 9–34, 1975.
- [117] E. Hagedorn and J. Ranft, “Statistical Thermodynamics of Strong Interactions at High Energies.,” 1966.
- [118] S. W. Hawking, “Acausal Propagation in Quantum Gravity,” in *Quantum Gravity II* (C. J. Isham, R. Penrose, and D. W. Sciama, eds.), p. 393, 1981.
- [119] D. N. Page, “Information in black hole radiation,” *Physical review letters*, vol. 71, no. 23, p. 3743, 1993.
- [120] L. Susskind and L. Thorlacius, “Hawking radiation and back-reaction,” *Nuclear Physics B*, vol. 382, no. 1, pp. 123–147, 1992.
- [121] J. Preskill, “Do black holes destroy information?,” *arXiv preprint hep-th/9209058*, 1992.
- [122] G. t Hooft, “On the quantum structure of a black hole,” *Nuclear Physics B*, vol. 256, pp. 727–745, 1985.
- [123] S. W. Hawking, “Wormholes in spacetime,” *Physical Review D*, vol. 37, no. 4, p. 904, 1988.
- [124] S. W. Hawking and R. Laflamme, “Baby universes and the non-renormalizability of gravity,” *Physics Letters B*, vol. 209, no. 1, pp. 39–41, 1988.
- [125] L. Susskind, L. Thorlacius, and J. Uglum, “The stretched horizon and black hole complementarity,” *Physical Review D*, vol. 48, no. 8, p. 3743, 1993.

- [126] G. t Hooft, “The black hole interpretation of string theory,” *Nuclear Physics B*, vol. 335, no. 1, pp. 138–154, 1990.
- [127] A. Almheiri, D. Marolf, J. Polchinski, and J. Sully, “Black holes: complementarity or firewalls?,” *Journal of High Energy Physics*, vol. 2013, no. 2, pp. 1–20, 2013.
- [128] S. Hawking, “Information Preservation and Weather Forecasting for Black Holes,” *arXiv preprint arXiv:1401.5761*, 2014.
- [129] C. Vishveshwara, “Generalization of the“Schwarzschild Surface”to Arbitrary Static and Stationary Metrics,” *Journal of Mathematical Physics*, vol. 9, p. 1319, 1968.
- [130] R. B. Mann and S. N. Solodukhin, “Conical geometry and quantum entropy of a charged Kerr black hole,” *Physical Review D*, vol. 54, no. 6, p. 3932, 1996.
- [131] L. Alvarez-Gaume and M. A. Vazquez-Mozo, “Introductory lectures on quantum field theory,” *arXiv preprint hep-th/0510040*, 2005.
- [132] O. Klein, “Die Reflexion von Elektronen an einem Potentialsprung nach der relativistischen Dynamik von Dirac,” *Zeitschrift für Physik*, vol. 53, no. 3-4, pp. 157–165, 1929.
- [133] B. R. Holstein, “Kleins paradox,” *American Journal of Physics*, vol. 66, no. 6, pp. 507–512, 1998.
- [134] N. Dombey and A. Calogeracos, “Seventy years of the Klein paradox,” *Physics Reports*, vol. 315, no. 1, pp. 41–58, 1999.
- [135] A. Calogeracos and N. Dombey, “History and physics of the Klein paradox,” *Contemporary physics*, vol. 40, no. 5, pp. 313–321, 1999.